DOCTOR OF PHILOSOPHY

Partitioning of stable isotopes between scallop shell calcite and sea water and factors influencing shell growth and microgrowth patterns.

Owen, Richard John

Award date:
1998

Awarding institution:
Bangor University

Partitioning of stable isotopes between scallop shell calcite and sea water and factors influencing shell growth and microgrowth patterns

Richard John Owen

(BSc. University of Wales Bangor)

A thesis in partial fulfilment of the requirements of the University of Wales for the degree of Doctor of Philosophy

University of Wales, Bangor
School of Ocean Sciences,
Menai Bridge
Anglesey LL59 5EY
United Kingdom

ifysgol Cymru SUMMARY OF THESIS University of Wales

This summary sheet should be completed by the candidate after having read the notes overleaf. The completed sheet should be submitted by the candidate to his Head of Department together with two copies of the thesis, two copies of Section 1 of the combined Notice of Candidature/Report and Result form and either a certificate regarding financial obligations or the required fee.

andidate's Surname ....OWEN.....

andidate's Forenames ..RICHARD JOHN.....

Institution at which study pursued:
BANGOR (OCEAN SCIENCES)

andidate for the Degree of ....PhD..... (MPhil *or* PhD *or* Doctor by Examination and Thesis *or* Eng D)

ull title of thesis .....PARTITIONING OF STABLE ISOTOPES BETWEEN SCALLOP SHELL CALCITE.....
.....AND SEAWATER AND FACTORS INFLUENCING SHELL GROWTH.....
.....AND MICROGROWTH PATTERNS.....

ummary:

There is great potential for establishing historical records of water temperature / the oxygen isotopic composition of sea water ($\delta^{18}O$ - H_2O) and the carbon isotopic composition of dissolved inorganic carbon ($\delta^{13}C$ - ΣCO_2) from oxygen and carbon isotopic records in scallop shell calcite ($\delta^{18}O$ and $\delta^{13}C$). Variations in $\delta^{13}C$ - ΣCO_2 in oceanic environments often reflect productivity cycles which may potentially be recorded within shell $\delta^{13}C$ records. The establishment of such records is based upon two fundamental assumptions. These are that precipitation of shell calcite occurs in isotopic equilibrium with sea water and that growth occurs over an entire annual cycle. Important information may also be gained from microgrowth patterns on the scallop shell surface ('striae') once factors governing their deposition are understood.

The above assumptions were tested for the scallop (*Pecten maximus*) by controlled experiment and in a year - long field study. During periods of slow growth shell oxygen isotopes were found to be precipitated in isotopic equilibrium with sea water. Shell carbon isotopes were found to be depleted with respect to isotopic equilibrium. This was interpreted as resulting from a metabolic effect, probably reflecting incorporation of respiratory CO_2 into the growing shell. At higher shell growth rates depletions / further depletions in $\delta^{18}O$ / $\delta^{13}C$ with respect to isotopic equilibrium occurred, interpreted as reflecting kinetic effects. Shell growth exhibited distinct seasonality, with growth cessation during the Winter months (below 8- 9°C) and maximal growth rates in the Summer. Stria deposition was found to be strongly related to shell growth rate. The combined effects of growth cessation and precipitation of shell isotopes out of isotopic equilibrium with sea water precluded accurate determination of mean and annual ranges of water temperature / $\delta^{18}O$ - H_2O and $\delta^{13}C$ - ΣCO_2 from the shell isotopic record. Shell $\delta^{18}O$ / $\delta^{13}C$ and striae abundance records for *Pecten maximus* collected from an offshore site were interpreted in the context of the calibration work undertaken.

Acknowledgements

Anyone who has worked within the stable isotope field will appreciate that the research is by its nature expensive and often slow, requiring a high level of continuous supervisory support. It is in this context that I would like to thank my supervisors Dr Chris Richardson and Dr Hilary Kennedy, whose support has been total at every level. I would like to thank Dr Gideon Middleton and Paul Kennedy, with whom I worked closely over the years and who taught me many of the techniques in the vac.lab. and the intricacies of our mass spec. I would also like to thank Paul Dennis at U.E.A., Norwich, in particular for his help with the $\delta^{18}O$-H_2O methodology, but more generally for his advice and comments on many aspects of the work. I am indebted to Su Utting and Peter Millican at C.E.F.A.S., Conwy for a continuous supply of healthy scallops and Peter Dare for supplying archive material for analysis.I have had to call upon the expertise of many colleagues within the School of Ocean Sciences at Menai Bridge; Dave Gill and his team in the workshop, who were instrumental both in the experimental and field studies and spent many hours with arms submerged in icy waters attaching heavy boxes to the raft; Dave Roberts in the Photography department; our Marine Chemistry Technicians Viv and Sandy; Dr Andy Neal for his advice and comments. I would also like to thank all my other colleagues within the Graduate and Lecturing community at Menai Bridge who made the research environment enjoyable, motivating and frequently entertaining. Finally I would like to thank my wife Terry for her immeasurable support and encouragement.

This research was funded by N.E.R.C., Grant No. GT4 / 93 / 261 / A

Contents

Abstract

Detailed investigations into the partitioning of stable oxygen and carbon isotopes between biogenic calcite (scallop shell) and sea water and the factors governing deposition of microgrowth patterns (striae) found on the scallop shell surface were undertaken. The scallop shell may be considered as a time series of biologically-precipitated calcite. The oxygen isotopic composition (^{18}O:^{16}O) of a precipitating calcite ($\delta^{18}O$) is governed by the oxygen isotopic composition of sea water ($\delta^{18}O$-H_2O) and water temperature, with isotopic partitioning between calcite and sea water occurring as result of temperature - dependent equilibrium isotope effects. Such partitioning results in differences in calcite oxygen isotope ratios relative to those of water i.e. isotopic fractionation. The fractionation factor and associated temperature coefficient for calcite-water oxygen isotope exchange (embodied within the palaeotemperature equation) may be used along with profiles of $\delta^{18}O$ taken along the axis of shell growth to establish historical records of water temperature / $\delta^{18}O$-H_2O. This is the basis of the many palaeotemperature determination studies using fossil carbonates that followed the early work of Urey, Epstein and McCrea in the 1940's and 1950's. Similarly, since the carbon isotopic composition of carbonates ($\delta^{13}C$) is governed by the isotopic composition of dissolved inorganic carbon ($\delta^{13}C$-ΣCO_2) and water temperature it should be possible to establish historical records of $\delta^{13}C$-ΣCO_2 from shell $\delta^{13}C$. In open ocean systems a major factor influencing $\delta^{13}C$-ΣCO_2 is biological productivity / remineralisation and the shell carbon isotope record may therefore be potentially used to establish historical records of primary production.

Other important environmental information may be obtained from shell microgrowth patterns once the factors governing their deposition are known. The scallop contains well-defined striae on its shell surface and this fact, in addition to its widespread occurrence throughout the geological record make this epifaunal bivalve a suitable case organism for study. Two fundamental, yet frequently untested assumptions underlie the use of stable isotopic profiles to establish historical records of water temperature / $\delta^{18}O$-H_2O and $\delta^{13}C$-ΣCO_2. These are firstly that the carbonate is precipitated in isotopic equilibrium with sea water over the range of organismal growth rates, and secondly that precipitation occurs over a complete annual cycle.

In addition to determining the factors governing striae deposition, the research represented a calibration exercise to test these fundamental assumptions for the scallop *Pecten maximus* and, on the basis of the results, allow interpretation of stable isotopic and microgrowth pattern profiles from oceanic scallops.

Prior to the main experimental and field work, some of the underlying methodologies central to the research were evaluated in a series of experiments. It was shown that organic components of the shell matrix caused erroneous enrichments of shell $\delta^{18}O$ and $\delta^{13}C$ and must be removed prior to sealed vessel acidification for accurate isotopic determinations. Additionally, the sealed vessel method was found to result in both imprecise and inaccurate $\delta^{18}O$ and $\delta^{13}C$ data at sample weights below 1mg. The hypothesis that *Pecten* shell isotopes are precipitated in isotopic equilibrium with sea water was tested in a controlled experiment in which partitioning of isotopes between juvenile scallop shell calcite and sea water was determined at various temperatures. The observed inverse relationship between *Pecten* shell $\delta^{18}O$ and water temperature agreed with expressions for inorganic calcite-water isotopic partitioning at isotopic equilibrium, implying that *Pecten* shell oxygen isotopes were precipitated in isotopic equilibrium with sea water. Variability in shell $\delta^{18}O$ was examined and found to be largely of an analytical nature. Shell $\delta^{13}C$ was found to be depleted relative to $\delta^{13}C$ of calcite precipitated in isotopic equilibrium with dissolved inorganic carbon by approximately -2 °/oo. Such depletions with respect to isotopic equilibrium were explained as resulting from a metabolic effect due to incorporation of isotopically depleted respiratory CO_2 into the precipitating shell. The data were in agreement with a model of isotopic disequilibrium postulated by McConnaughey (1989b) where metabolic effects result in depletions in skeletal $\delta^{13}C$ with respect to isotopic equilibrium but do not result in simultaneous depletions in skeletal $\delta^{18}O$. Partitioning of isotopes between *Pecten* shell calcite and sea water was further investigated during a year - long time series field study. In the study, shell $\delta^{18}O$ and $\delta^{13}C$ data were obtained from juvenile scallops placed in the field for monthly periods over the year, and for the entire annual period. Shell isotopic data were compared to predicted data for calcite precipitated in isotopic equilibrium with sea water, the latter calculated from water samples collected at fortnightly intervals over the year.

In addition, seasonal changes in shell growth rate and microgrowth patterns were investigated, related to environmental factors (water temperature, concentrations of chlorophyll and P.O.C., P.O.N.), and the influence of growth rate upon shell isotopic data considered.

Shell growth rate was found to exhibit distinct seasonality, with minimum growth rates in the winter / spring (when shell growth ceased) and maximum growth rates in the summer. Striae deposition was found to be strongly related to shell growth rate, with higher number of striae deposited per day, higher stria width and lower striae abundances (striae per mm shell) at higher growth rates. Shell growth rate was also found to influence partitioning of isotopes between *Pecten* shell calcite and sea water. At low shell growth rates, oxygen isotopes were precipitated in isotopic equilibrium with sea water and shell $\delta^{13}C$ was found to be depleted with respect to isotopic equilibrium of the order of -1 to -2 °/oo, confirming the experimental findings. At the higher shell growth rates displayed during the summer depletions / further depletions in shell $\delta^{18}O$ / $\delta^{13}C$ with respect to isotopic equilibrium occurred, of the order of -0.45 °/oo and -0.36 °/oo respectively. These simultaneous isotopic depletions at higher growth rates with respect to isotopic equilibrium were interpreted as resulting from a kinetic effect, supporting the model postulated by McConnaughey (1989b). The curvilinear relationships between striae abundance / striae width and shell growth rate precluded the identification of areas of the shell associated with kinetic effects. The results of isotopic and microgrowth pattern profiles for *Pecten maximus* collected at an offshore, seasonally-stratifying site were interpreted in the light of the results of the experimental and field work.

Pecten shell isotopes are considered unsuitable for establishing accurate historical records of water temperature / $\delta^{18}O$-H_2O and $\delta^{13}C$-ΣCO_2. This is due firstly to the fact that it cannot be assumed that shell growth occurs over a complete annual cycle and secondly that precipitation of shell isotopes occurs out of isotopic equilibrium with sea water. These combined effects result in erroneous shell-derived values for both the annual mean and range of these parameters.

Chapter 1 Introduction

1.1. Overview

Naturally - occurring stable isotopes of oxygen (^{16}O, ^{17}O and ^{18}O) comprise 99.76%, 0.04% and 0.20% of the total atmospheric oxygen (Nier, 1950). Similarly, the naturally-occurring stable isotopes of carbon (^{13}C and ^{12}C) comprise approximately 98.9% and 1.1% of total carbon (Nier, 1950). In general the heavier isotope of an element is the rarer form; for example the absolute ratio of ^{18}O : ^{16}O in CO_2 liberated from a carbonate upon acidification is 415.1×10^{-5} : 1 (Craig, 1957). Despite the fact that stable isotopic species of an element differ only in the addition of one or more neutrons this may have a profound influence on the physico - chemical behaviour of that species e.g. reaction rates. The ratios of ^{18}O : ^{16}O and ^{13}C : ^{12}C in both inorganic and organic oxygen and carbon - containing compounds can therefore frequently change as a result of physico-chemical and biological processes.

Following the original discovery by Urey *et al.* (1932) of the isotopes of hydrogen, differences in the chemical behaviour of the light isotopes, including those of carbon and oxygen, have been both calculated by statistical mechanics and determined empirically by experiment. The earliest theoretical studies (Bigeleisen and Mayer (1947), Urey (1947)) showed that the ^{18}O : ^{16}O ratio of carbonates ($\delta^{18}O$) precipitated in sea water should vary, purely on thermodynamic grounds, as a function of water temperature and the oxygen isotopic composition of the water itself ($\delta^{18}O$-H_2O). Urey foresaw the potential for using stable oxygen isotopic ratios in limestones to reconstruct historical records of water temperature (in this early paper the oxygen isotopic composition of sea water was assumed to be constant over geological time). This theoretical paper initiated a large body of experimental work in the following decades (McCrea, 1950, Epstein *et al.* 1953, Craig, 1965, O'Neil *et al.* 1969, Tarutani *et al.* 1969, Horibe and Oba, 1972 , Grossman and Ku, 1986) quantifying the relationship between the oxygen isotopic compositions of inorganic and biogenic calcites / aragonites and water temperature and testing the assumption that the isotopic composition of sea water was indeed constant.

In addition, many studies from that time (beginning with a study by Urey *et al.* 1951) have analysed contemporary and fossil carbonates of many genera (principally molluscs, foraminifera, brachiopods and corals) with the aim of reconstructing historical records of water temperature for both contemporary and palaeo-oceans.

Similarly, changes in $^{13}C:^{12}C$ ratios of carbonates ($\delta^{13}C$) precipitated in sea water, based purely upon thermodynamic considerations, have been shown to vary as a function of the carbon isotopic composition of dissolved inorganic carbon (ΣCO_2) and water temperature (Emrich *et al.* 1970, Romanek *et al.* 1992). A major factor influencing the carbon isotopic composition of dissolved inorganic carbon ($\delta^{13}C$-ΣCO_2) in open ocean systems has been found to be the biologically - mediated processes of inorganic carbon uptake and enzymatic fixation by phytoplankton and bacterial remineralisation (as well as carbonate precipitation and dissolution) (Kroopnick, 1985).

If one considers a molluscan shell to be a time series of biologically-precipitated carbonate there exists a great potential for establishing high resolution records of both water temperature / $\delta^{18}O$-H_2O and seasonal cycles of production and remineralisation from oxygen and carbon isotopic profiles taken along the shell. Such records may be established for both contemporary oceans (where continuous data may be sparse) and palaeo-oceans. An additional advantage of analysing molluscan shells is the wealth of information that may be obtained from macro and micro growth patterns observed within the sectioned surfaces, and on the surface itself, of the shell, once the factors governing the deposition of these growth patterns are known (Richardson , 1991, 1996).

The use of shell stable isotopic profiles to reconstruct historical records of water temperature / $\delta^{18}O$-H_2O and $\delta^{13}C$-ΣCO_2 is based upon two fundamental assumptions ; firstly that partitioning of isotopes between the precipitating carbonate and oxygen / dissolved inorganic carbon in sea water is complete at a given temperature (when precipitation is said to be in isotopic equilibrium with sea water) and secondly that shell is deposited over the whole range of water temperatures / values of $\delta^{18}O$-H_2O and $\delta^{13}C$-ΣCO_2 in any given annual cycle.

Whilst both assumptions were identified in some of the earliest work in the field (Urey *et al.* 1951, Epstein and Lowenstam, 1953), and despite the large volume of work which has made inferences from isotopic data in biogenic carbonates, these fundamental assumptions remain frequently untested for the species under investigation.

The research undertaken within this thesis represents an attempt to rigorously test these assumptions for the scallop *Pecten maximus* as well as investigating the factors that influence microgrowth patterns found on the surface of the shell. As a case organism for study the scallop, an epifaunal bivalve, is a suitable candidate because of its widespread occurrence within the sedimentary record, e.g. Quaternary deposits in Scotland, within early Pleistocene deposits in the Antarctic (Barrerra *et al.* 1990), Arctic Paleocene deposits (Bice *et al.* 1996) and clastic deposits covering the Tertiary period in low latitudes (Smith, 1991). The surface of the scallop shell contains well-defined micro and macro growth patterns. As mentioned above, such growth patterns in molluscan shells can be a useful source of environmental information once the factors governing their deposition are known. The present work also builds upon existing stable isotope and microgrowth pattern studies undertaken by Gruffydd (1981), Dare and Deith (1989) and Dare (1991).

The approach has been to investigate the partitioning of stable isotopes between *Pecten* shell calcite and sea water and factors influencing microgrowth patterns a) by carefully controlled laboratory experiment and b) in a year long field study. Additional experimental work assessing some of the underlying methodologies central to the research has also been undertaken. Finally, based upon this calibration work, an analysis of *Pecten* shell stable isotopic profiles and microgrowth patterns from individuals collected from offshore, seasonally-stratifying waters has been undertaken in order to establish whether annual cycles of $\delta^{13}C$-ΣCO_2 and water temperature / $\delta^{18}O$-H_2O in bottom waters associated with establishment and breakdown of seasonal stratification are recorded within the shell.

1.2. Underlying Theory

1.2.1. Isotope effects

Isotope effects are differences in physical properties (such as diffusion) and chemical properties of an element arising from differences in atomic mass of that element. Differences in chemical properties arise as a result of quantum mechanical effects and may be explained in terms of differences in zero point energies of isotopic species in molecules with the same molecular formula. Molecules containing the heavier isotope have a lower zero point energy (the energy possessed by a molecule in the ground state, at absolute zero temperature) than molecules containing the lighter isotope and consequently form stronger bonds i.e. in general molecules containing the lighter isotope will react slightly more readily than those containing the heavier isotope.

Such isotope effects lead to a partitioning of isotopes between two or more compounds within a reaction pathway, a phenomenon known as fractionation. Two main processes result in fractionations ;

a) isotope exchange reactions, in which isotopic distribution between two or more compounds or phases occurs (resulting in fractionation of isotopes between these compounds or phases) until the lowest energy state of the system is reached at any given temperature. This does not result in any chemical changes but only isotopic distribution, based upon thermodynamic grounds. Once the lowest energy state of the system has been attained, a state of isotopic equilibrium is said to have been reached.

b) kinetic isotope effects, dependent upon differences in reaction rates of molecules containing the heavier or lighter isotopes i.e. the rate of a chemical reaction is sensitive to atomic mass at a particular position within the reaction pathway.

As an illustration of an isotope exchange reaction, if one considers isotopic exchange between a precipitating carbonate and water, this exchange may be written as;

$$H_2{}^{18}O + {}^1/_3\, CaC^{16}O_3 \text{ <-----> } H_2{}^{16}O + {}^1/_3\, CaC^{18}O_3 \quad \ldots\ldots\ldots\ldots\ldots\ldots \quad (1)$$

This exchange, once isotopic equilibrium has been established, is quantitatively described by the equilibrium constant for the exchange, K , at any given temperature. Another equilibrium isotope effect, this time between phases, is that of a vapour pressure isotope effect, where the species containing the heavier isotope tends to be less volatile than that containing the lighter isotope. For example, during the process of condensation, there is enrichment of the heavier oxygen isotope in the condensate, with the remaining vapour being depleted in the heavier isotope.

$$H_2{}^{16}O_{(condensate)} + H_2{}^{18}O_{(vapour)} \text{<-----> } H_2{}^{18}O_{(condensate)} + H_2{}^{16}O_{(vapour)}$$

and this again is quantitatively described by the equilibrium constant for the exchange, K, at any given temperature.

For any given isotope exchange reaction of the form ;

$$aA_1 + bB_2 \text{ <-----> } aA_2 + bB_1$$

(where the subscripts indicate that compounds A and B contain either the lighter isotope (1) or the heavier isotope (2)) , the equilibrium constant;

$$K = (A_2 / A_1)^a \; / \; (B_2 / B_1)^b$$

may, by statistical mechanics, be expressed in terms of partition ratios (Q);

$$K = (QA_2 / QA_1) \; / \; (QB_2 / QB_1)$$

The equilibrium constant is therefore the product of the two partition function ratios. Q is defined in terms of ;

$$Q = \Sigma_i \, (g_i \exp (-E_i / KT) \ldots\ldots\ldots\ldots\ldots\ldots (2)$$

where the summation is over all allowed energy levels of the molecules (E_i). In fact the partition function may be separated into each energy type - translational, vibrational and rotational. Differences in both rotational and translational energy are similar on both sides of the exchange reaction, and this leaves vibrational energy as the source of the isotope effect. The most important factor contributing to the vibrational energy of a molecule is related to the zero point energy. Important to note is the dependence of the equilbrium constant K upon temperature (Equation 2 above).

During any equilibrium isotope exchange process, the partitioning or fractionation of isotopes between two compounds or phases may be described by the fractionation factor α.

i.e. α = ratio $_{(A)}$ / ratio $_{(B)}$ .....(3)

where α is related to the equilibrium constant K by the relationship $\alpha = K^{(1/n)}$ and n is the number of atoms exchanged (Friedman and O'Neil, 1977). For simplicity, isotope exchange reactions are written such that only one atom is exchanged, as in Equation 1 above, and the equilibrium constant equals the fractionation factor.
i.e. for the isotope exchange reaction shown in Equation 1;

$$\alpha = \frac{^{18}O / ^{16}O\ CaCO_3}{^{18}O / ^{16}O\ H_2O} = 1.031 \text{ at } 25^{\circ}C \qquad \text{(Friedman and O'Neil, 1977)}$$

Three important points should be noted;
i) isotopic fractionations are only observed if the reaction is not quantitative i.e.does not go to completion (Hayes, 1982). This is particularly important where kinetic isotope effects may occur but at completion the isotopic composition of the pooled product must match that of the starting reactant and there is no overall fractionation (Figure 1.1a). Similarly, during the reaction of carbonate with excess phosphoric acid to produce CO_2, a fractionation with respect to oxygen isotopes might be observed since resultant H_3PO_4 and CO_2 are both present in a closed system and may exchange. However, no fractionation is likely to be observed for carbon isotopes since all resulting carbon is in the form CO_2.

Although the first formed CO_2 may be depleted and carbonate enriched with respect to carbon either due to exchange or kinetic effects, as the reaction progresses both carbonate and CO_2 become progressively enriched and at completion the pooled product (CO_2) will have the same isotopic composition as the initial reactant (CO_3^{2-}), yield being 100%.

Figure 1.1a

Isotopic fractionations in a closed system as a reaction proceeds to completion. R = isotopic composition of residual reactant, P' that of instantaneously formed product, P that of pooled product (from Hayes, 1982)

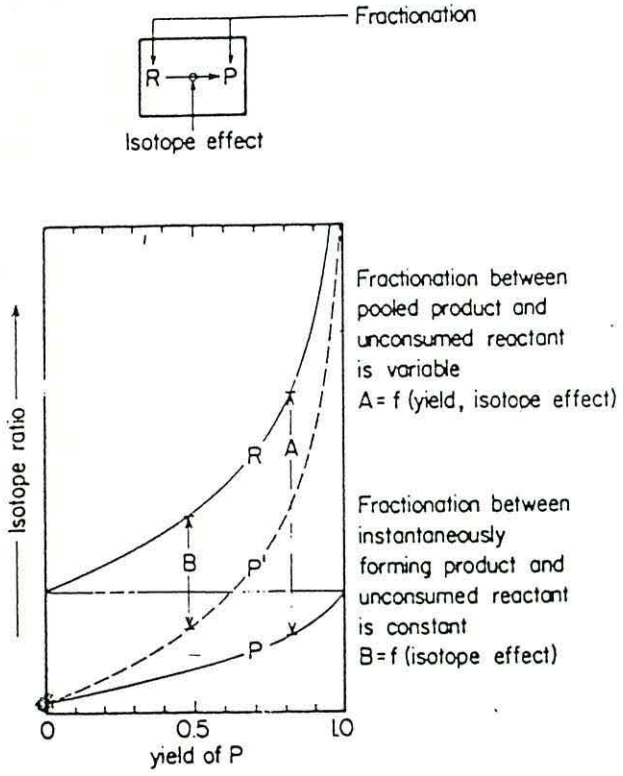

Figure 1.1b

^{18}O of cloud vapour and a condensate as a function of remaining vapour in the cloud. Open system where the condensate is removed as precipitation. (from Rye and Sommer, 1980, after Dansgaard, 1964)

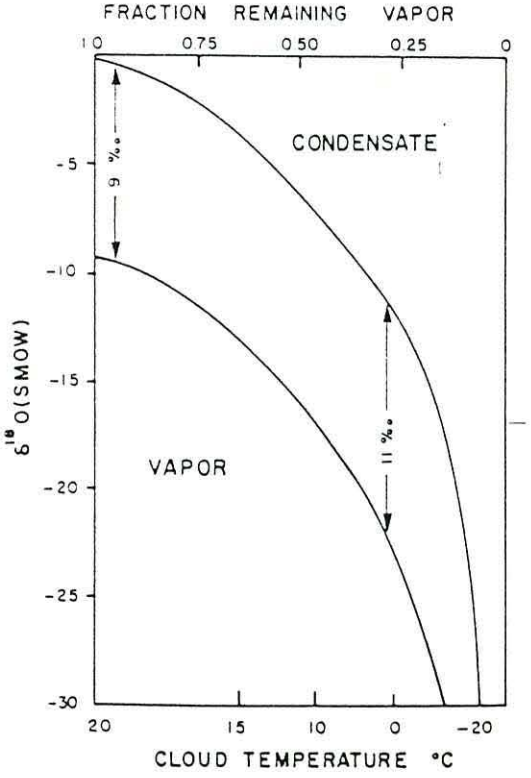

ii) there is a distinction between open and closed systems.

Condensation, due to vapour pressure isotope effects, results in an enriched condensate and depleted vapour with respect to oxygen isotopes.

However the condensate is removed as precipitation i.e. an open system, and the next formed condensate from the same air mass will be further enriched and the residual vapour further depleted (Dansgaard, 1964) (Figure 1.1b). These so-called Rayleigh distillations are the basis of latitudinal changes in the isotopic composition of precipitation which have such a critical bearing on palaeotemperature determinations (see Section 1.5 below).
iii) as in all equilibria, the fractionation factor is temperature dependent.

1.2.2. Notation

The isotopic ratio of a sample is expressed as the deviation relative to that of a standard

$$\text{i.e. } \delta\,{}^{o}/_{oo} = \frac{[R_{(sample)} - R_{(standard)}] * 1000}{R_{(standard)}} \quad \ldots\ldots\ldots\ldots (4)$$

to give a delta value in per mil ($^{o}/_{oo}$) i.e. if the fractionation factor for an exchange between two compounds is 1 + 0.001a the fractionation is a $^{o}/_{oo}$. This per mil notation was formally defined as above by McKinney *et al.* (1950) since changes occur at the third significant figure of the isotope ratio level. They also introduced the δ notation, indicating that the term above is a *relative* value, relative to a standard. The conventional notation is then $\delta\,{}^{o}/_{oo}$. Due to the requirement of highly precise analytical techniques for measurement of changes in isotopic ratios in, e.g CO_2, it has been found that comparing values between the sample and a reference (i.e. relative values) is more convenient than obtaining absolute values, allowing for day to day instrument - based differences in measured sample ratios since such errors will be accounted for by referencing to the reference sample (Hayes, 1982).

In terms of quantities measured in the laboratory the fractionation factor defined in Equation 3 above, after substitution of the term in Equation 4, becomes

$$\alpha = \{1 + \delta\,(A) / 1000\} / \{1 + \delta\,(B) / 1000\}$$

$$\text{or, } \alpha = \{\delta\,(A) + 1000\} / \{\delta\,(B) + 1000\} \quad \ldots\ldots\ldots\ldots (5)$$

A frequently used term is the enrichment factor ε, which is defined as

$\varepsilon_{B}A = (\alpha - 1)*1000 = \delta(A) - \delta(B)$.

For small values of ε, this is equivalent to $1000 \ln\alpha$, another frequently used term.

1.2.3. Partitioning of oxygen isotopes between precipitating carbonates and sea water and the historical development of the palaeotemperature equation.

As indicated previously, it was Urey (1947) and Bigeleisen and Mayer (1947) who first investigated, using purely thermodynamic approaches, the partitioning of oxygen isotopes between carbonates and water and the temperature dependence of this partitioning. Bigeleisen and Mayer (1947) calculated that, for carbonate - water oxygen isotope exchange, $\ln\alpha$ varies with $1/T^2$ and $1/T$ for temperatures above and below 300K

i.e. above 300K $\ln\alpha = A' + B'/T^2$, A' and B' being constants.

i.e. from Equation (3) above

$\ln\alpha = \ln\{1 + \delta(A)/1000\} - \ln\{1 + \delta(B)/1000\}$

which, for small values of δ approximates to $\{\delta(A) - \delta(B)\}/1000$

i.e. $\{\delta(A) - \delta(B)\}/1000 = A' + B'/T^2$

For small temperature ranges Craig (1965) showed that this equation approximates to

$t^{o}c = a + b\{\delta(A) - \delta(B)\} + c\{\delta(A) - \delta(B)\}^2$

This is the generalised form of the palaeotemperature equation. Any pair of exchanging compounds A and B that are in isotopic equilibrium may act as a geothermometer.

Urey (1947) suggested that the carbonate - water oxygen isotope exchange reaction would prove most useful since the fractionation per unit temperature was large for this exchange and oxygen was a conservative element which formed relatively stable compounds which were less prone to diagenesis (unlike, for example, carbon). In 1947 he published theoretical fractionation factors for carbonate - water oxygen isotope exchange and calculated the temperature dependence of the fractionation factor.

The precipitation of calcium carbonate is determined by the chemical exchange reactions

$CO_{2(g)}$ <-------> $CO_{2(aq)}$

$CO_{2(aq)} + H_2O$ <-------> $H^+ + HCO_3^-$

HCO_3^- <-------> $CO_3^{2-}{}_{(aq)} + H^+$

$CO_3^{2-}{}_{(aq)} + Ca^{2+}$<-------> $CaCO_{3\ (mineral)}$

For oxygen there are exchanging steps between the precipitating mineral and $CO_3^{2-}{}_{(aq)}$, between HCO_3^- and $CO_3^{2-}{}_{(aq)}$, between HCO_3^- and $CO_{2(aq)}$ / H_2O and between $CO_{2(aq)}$ and $CO_{2(g)}$. Under equilibrium conditions the fractionations at each exchange step are purely temperature dependent. Water represents such an enormous oxygen pool when compared to all the other oxygen species and remains isotopically constant with regard to isotopic exchange with bicarbonate and $CO_{2(aq)}$. Under equilibrium conditions, the fractionation between H_2O (isotopically constant), $CO_{2(aq)}$ and bicarbonate and that between bicarbonate and $CO_3^{2-}{}_{(aq)}$ and between $CO_3^{2-}{}_{(aq)}$ and $CaCO_{3\ (mineral)}$ (i.e. the overall fractionation $CaCO_3$ - H_2O) will be purely dependent on temperature and the isotopic composition of the water itself (oxygen isotopic composition of $CO_{2(g)}$ having negligible effect). At the time of publication Urey considered sea water to be isotopically constant throughout geological time.

Following these initial, theoretical studies McCrea (1950) considered the temperature dependence of the carbonate - water oxygen isotope fractionation factor by experiment.

He first extended Urey's theoretical calculations to include the fractionation between solid carbonate and $CO_3^{2-}{}_{(aq)}$ and then precipitated calcite samples from sea water at various temperatures by addition of excess 3M calcium chloride. His empirically - derived temperature equation for slowly-precipitated calcites was;

$$t^{\circ}C = 16.0 - 5.17\ \Delta O^{18} + 0.092(\Delta O^{18})^2$$

where ΔO^{18} is the °/oo difference between the ratio of masses 46 to 44 of the sample CO_2 to the reference CO_2 i.e. $^{12}C^{18}O^{16}O$ / $^{12}C^{16}O^{16}O$ (see below for the distinction between this and the so-called 'Craig corrected' $^{18}O/^{16}O$ ratio). The temperature coefficient for this relationship is -0.175 °/oo per °C which compares well to the theoretical value of -0.183 °/oo per °C. Whilst the temperature coefficient is independent of the water oxygen isotopic composition and referencing standard used, the expression above actually refers explicitly to the isotopic composition of CO_2 when referenced to his standard CO_2 and assumes the isotopic composition of CO_2 in equilibrium with water is zero °/oo compared to his standard CO_2. It applies to calcite, since aragonite has a slightly different temperature coefficient (see below.)

Following this study, Epstein *et al.* (1951, 1953) published a carbonate-water temperature scale based on biologically - precipitated carbonates. In their modified 1953 study they conducted a constrained experiment in which the shells of a number of species were notched and the organisms subsequently maintained at 19, 21.5 and 29.5°C in the laboratory. The regenerated shell was then analysed. Other data points between 7°C and 21.5°C were obtained using a variety of species from locations where the seasonal temperature variation was known; successive growth layers were ground from the shell and the average ^{18}O / ^{16}O maxima and minima matched to the average recorded maxima and minima. A water oxygen isotope value was reported for each laboratory tank or location and this was used to correct the carbonate value. This followed the earlier suggestion by McCrea (1950) that the isotopic composition of water may not be constant and must be accounted for. A discussion of the constancy of water isotopic values may be found below (see section 1.5. below)

The Epstein *et al.* (1953) palaeotemperature equation is;

$$t^{o}C = 16.5 - 4.3\,(\delta'_{c} - \delta'_{w}) + 0.14\,(\delta'_{c} - \delta'_{w})^{2}$$

where δ'_{c} is the ratio of mass 46/44 for sample CO_2 relative to the reference CO_2, and δ'_{w} is the ratio of mass 46/44 for CO_2 in equilibrium with the water sample relative to the reference CO_2. This form of the equation applies to PDB as the reference carbonate, to which all subsequent work has by convention (Craig, 1957) been referenced (see below, Isotopic Standards). When the difference in isotopic composition of the waters was accounted for between the Epstein *et al.* (1953) study and that of McCrea (1950), the palaeotemperature equations agreed reasonably well, suggesting that biogenic carbonates were precipitated in isotopic equilibrium with seawater as proposed by theory.

Rye and Sommer (1980) have highlighted some of the errors inherent in the derivation of the palaeotemperature scale within the Epstein *et al.* (1953) study. The temperature coefficient for aragonite - water and calcite- water oxygen isotope exchange have been found to differ (Tarutani *et al.* 1969, Grossman and Ku, 1986). Rye and Sommer (1980) argue that the organisms used within the Epstein *et al.* (1953) study were largely of calcitic mineralogy and the carbonate - water palaeotemperature scale so described should be more appropriately described as a calcite - water palaeotemperature scale. The Epstein equation was modified by Craig (1965), who made so-called Craig corrections (see below) and corrected for the isotopic composition of the CO_2 before equilibration with the water sample;

$$t^{o}C = 16.9 - 4.2\,(\delta_{c} - \delta_{w}) + 0.13\,(\delta_{c} - \delta_{w})^{2}$$

where δ values are as for the Epstein *et al.* (1953) expression i.e. relative to PDB-CO_2, but Craig corrected. A fuller discussion of the exact meaning of δ_{c} and δ_{w} may be found below (see 'Isotopic Standards').

This form of the calcite palaeotemperature equation has been used in most subsequent work as the expression for oxygen isotope exchange between calcite and sea water.

Whilst it is in broad agreement with the equation for inorganic calcite precipitated under conditions where isotopic equilibrium had been established (McCrea, 1950), if any one of the species in fact exhibited any degree of precipitation where isotopic equilibrium had not been established at one or more temperatures this introduces a level of error. For specimens taken from the field it also assumes that growth occurred at all recorded temperatures and it assumes that there is no variability in water isotope composition from the recorded value. To this end the equation determined by O'Neil *et al.* (1969) under carefully constrained experimental conditions for inorganic calcite, whilst in broad agreement with the above expressions, is a more accurate expression for calcite - water oxygen isotope partitioning at isotopic equilibrium;

$$t^{o}C = 16.9 - 4.38\,(\delta_{c} - \delta_{w}) + 0.10\,(\delta_{c} - \delta_{w})^{2}$$

1.2.4. Isotopic Standards

As discussed, all carbonate oxygen and carbon isotopic ratios are reported as °/oo deviations relative to a standard carbonate and corrected as by Craig (1957), the latter being referred to as Craig corrections (various isotopic species in CO_2 have the same mass e.g. mass 45 consists of 93.67% $^{13}C^{16}O^{16}O$ and 0.0748% $^{12}C^{16}O^{17}O$. Craig (1957) calculated correction factors for conversion of molecular mass ratio differences such as 45/44 into specific isotope ratio differences $^{13}C/^{12}C$).

The original carbonate standard, the working standard used at the University of Chicago during the 1950's at the time of the development of the palaeotemperature equation, was a sample of Belemnite Guard from the Peedee Formation in N.Carolina (PDB). This was first described and defined by Urey *et al.* (1951). This standard was exhausted and secondary standards produced by the National Bureau of Standards in the U.S. are now used e.g. NBS19.

In the laboratory, Craig - corrected isotope ratios of sample gas are expressed as °/oo deviations relative to a working reference gas (i.e. an internal standard), and are then reported relative to PDB - CO_2, (i.e.the term δ_{c}), knowing the $CO_{2(\text{reference -NBS19})}$ and $CO_{2(\text{NBS19-PDB})}$ offsets and employing the following equation for both carbon and oxygen;

$\delta CO_{2(sample\text{-}PDB)}$ {i.e. δ_c} = $\delta CO_{2(sample\text{-}ref)}$ + $\delta CO_{2(ref\text{-}PDB)}$ + 10^{-3} ($\delta CO_{2(ref\text{-}PDB)}$ * $\delta CO_{2(sample\text{-}ref)}$) (Craig, 1957)

The offsets for both carbon and oxygen are determined using values for δCO_2 (NBS19-PDB) (known) and δCO_2 (NBS19- working reference gas) (as calculated by running replicate NBS19 standards against the working reference gas in the mass spectrometer) and employing the form of the equation above. The overall δCO_2 (PDB- working reference gas) offset is strictly speaking that applying to mass 46/44 and 45/44 ratios of the gases. Craig - corrected $\delta CO_{2(sample\text{-}PDB)}$ {i.e. δ_c} data are then converted to $\delta^{18}O_{(sample\text{-}PDB)}$ data (i.e. °/oo deviations of the calcite mineral relative to PDB mineral), employing the the CO_3^{2-} - CO_2 fractionation factor associated with sealed - vessel acidification. This fractionation is associated with the liberation of CO_2 from the calcite sample in an evacuated reaction vessel using phosphoric acid.

If the reaction between calcite and phosphoric acid is considered,

$$CaCO_3 + H_3PO_4 = CaHPO_4 + CO_2 + H_2O$$

it can be seen that all three products contain oxygen and there is potential exchange of oxygen isotopes between CO_2 and both the PO_4^{3-} group and H_2O. Since acid is added to excess there is also potential for exchange between CO_2 and the PO_4^{3-} group in the acid. Since carbon is completely converted to CO_2 there is no associated fractionation of carbon isotopes during acidification (this was demonstrated by Swart *et al.* 1991). The sealed vessel CO_3^{2-}- CO_2 fractionation factor was determined experimentally by Sharma and Clayton (1965) and later corrected by Friedman and O'Neil (1977) who reported a value of 1.01025. The fractionation factor is dependent upon carbonate mineralogy , varies both with temperature of acidification (Sharma and Sharma, 1969, Swart *et al.* 1991) and with technique (an alternative to sealed vessel acidification is the common acid bath technique, Swart *et al.* 1991). Walters *et al.* (1972) found that during the course of the acidification CO_2 evolved was initially depleted in ^{18}O with subsequent progressive isotopic enrichment. This effect decreased with increasing particle size and was suggested as being a fractionation associated with diffusion away from the particle surface and therefore dependent upon surface area i.e. a kinetic isotope effect.

This emphasises the need for the reaction to go to completion. For calcite of crystal size < 74μm the reaction is complete within 2 hours; in practice samples are left in the water bath for at least 12 hours to ensure complete reaction over the particle size range. Acid viscosity may also affect the CO_3^{2-} - CO_2 fractionation factor (Swart *et al.* 1991). Phosphoric acids of different specific gravity will have different proportions of orthophosphate, pyrophosphate and triphosphate. The O-bearing phosphate polymers may be in isotopic equilibrium with each other but have unknown associated fractionation factors, influencing any isotopic exchange between acid and CO_2. In their study Sharma and Clayton (1965) used acid of specific gravity 1.88, identical to that used by McCrea (1950) and since it is Sharma and Clayton's modified value of the fractionation factor that is employed, acid of this specific gravity should be used.

The $\delta^{18}O$ term therefore refers to the $^{18}O/^{16}O$ °/oo deviation of sample calcite relative to PDB calcite and implies that the CO_3^{2-}-CO_2 fractionation factor of 1.01025 has been employed, the reaction effected using the sealed acid method with acid of specific gravity 1.88 at 25°C for >12hours.

Water oxygen isotope ratios are expressed relative to SMOW (Standard Mean Ocean Water, (Craig, 1961)). This term is referred to as $\delta^{18}O$ - H_2O. Determination of the oxygen isotopic composition of water involves the equilibration of the water with CO_2 within an evacuated reaction vessel at 25°C and subsequent analysis of the CO_2 (see Chapter 2, Methods), data being referenced to CO_2 in isotopic equilibrium with SMOW. The oxygen isotopic compostion of the water sample itself relative to SMOW (i.e. $\delta^{18}O$ - H_2O) is then determined using the CO_2 - H_2O fractionation factor at 25°C (reported by Friedman and O'Neil, 1977 as 1.0412). It should be noted that, within the palaeotemperature equation, the term δ_w refers to the oxygen isotopic composition of CO_2 in equilibrium with the water sample, but referenced to CO_2 liberated from PDB. CO_2 prepared by acidification at 25°C from PDB is +0.22 °/oo relative to the CO_2 equilibrated with SMOW at 25°C i.e. a fractionation factor of 1.00022 (Craig, 1961). Knowing the fractionation factors for CO_3^{2-} - CO_2 (1.01025) and CO_2 - H_2O (1.0412) at 25°C it is possible to relate $\delta^{18}O$, $\delta^{18}O$ - H_2O and δ_w. This is summarised in Figure 1.2. below and described by the equations;

$$\delta_w = 0.99978\ \delta^{18}O\text{-}H_2O - 0.22$$

$\delta^{18}O = 0.97006\ \delta^{18}O\text{-}H_2O - 29.94$

$\delta^{18}O\text{-}H_2O = 1.03086\ \delta^{18}O + 30.86$

Figure 1.2. Relationship between PDB, PDB - CO_2, SMOW and SMOW - CO_2 (From Rye and Sommer, 1980 after Friedman and O'Neil, 1977)

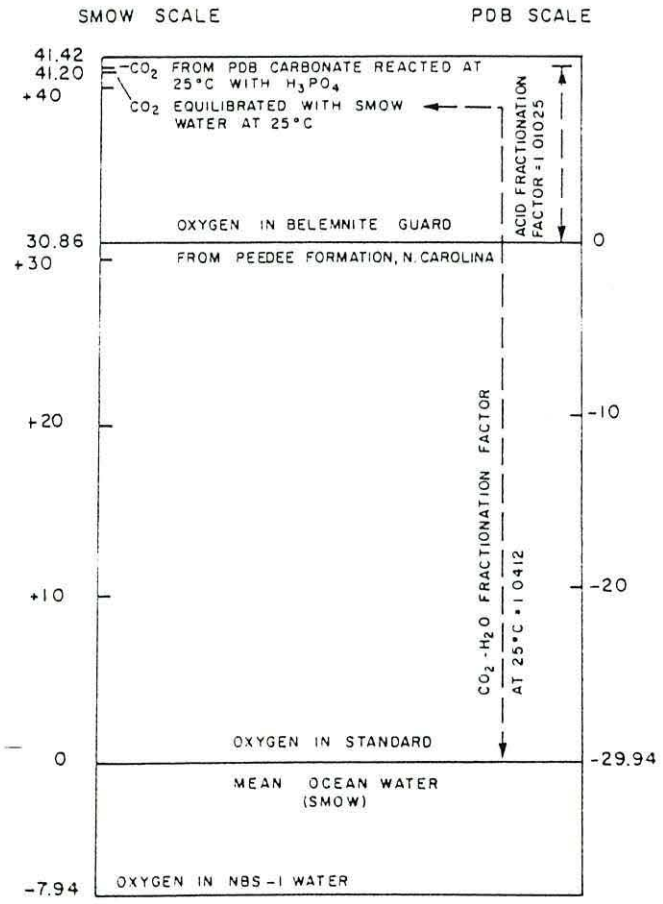

It should be also noted that whilst the paleotemperature equation refers to sample CO_2 referenced to PDB-CO_2, this is numerically the same as isotopic deviations of the sample calcite relative to PDB calcite (since the fractionation factor is applied to both sample and reference gases) i.e. $\delta_c = \delta^{18}O$ and the data do not require modification as in the δ_w - $\delta^{18}O\text{-}H_2O$ relationship above.

1.2.5. Partitioning of carbon isotopes within Dissolved Inorganic Carbon (ΣCO_2) and between precipitating carbonates and ΣCO_2.

The carbon isotopic composition of a carbonate precipitating in isotopic equilibrium with dissolved inorganic carbon is set by the isotopic compositions of the various aqueous carbon species that constitute dissolved inorganic carbon at a given temperature.

Considering the various exchange equilibria between a precipitating carbonate and the aqueous carbon species that in total constitute dissolved inorganic carbon it can be seen that there are fractionations associated with each of the partitioning steps 1. to 4. below.

$$CO_{2\,(g)} \quad \overset{1.}{<\text{-------}\ \text{-------}>} \quad CO_{2\,(aq)}$$

$$CO_{2\,(aq)} + H_2O \quad \overset{2.}{<\text{-------}\ \text{-------}>} \quad HCO_3^- + H^+$$

$$+ OH^- \qquad\qquad\qquad\qquad HCO_3^-$$

$$HCO_3^- \quad \overset{3.}{<\text{-------}\ \text{-------}>} \quad CO_3^{2-}{}_{(aq)}$$

$$CO_3^{2-}{}_{(aq)} \quad \overset{4.}{<\text{-------}\ \text{-------}>} \quad CO_3^{2-}{}_{(mineral)}$$

The carbon isotopic composition of the precipitating (mineral) carbonate, $\delta^{13}C$, is readily calculated by determining the isotopic composition of HCO_3^- (δ_b) and employing the equilibrium enrichment factor between HCO_3^- and $CO_3^{2-}{}_{(mineral)}$ i.e. steps 3. and 4. above (refer to Chapter 3.) δ_b is in turn calculated by rearrangement of a standard mass balance relationship describing partitioning of isotopes within dissolved inorganic carbon (i.e. steps 1. to 3.)

$$\delta_\Sigma = (\delta_a * f_a) + (\delta_b * f_b) + (\delta_c * f_c)$$

where δ_Σ = the carbon isotopic composition of ΣCO_2

δ_a = the carbon isotopic composition of $CO_{2\,(aq)}$

δ_b = the carbon isotopic composition of HCO_3^-

δ_c = the carbon isotopic composition of $CO_3^{2-}{}_{(aq)}$

f_a = the fraction $CO_{2\,(aq)}$ comprises of the ΣCO_2 pool

f_b = the fraction HCO_3^- comprises of the ΣCO_2 pool

f_c = the fraction $CO_3^{2-}{}_{(aq)}$ comprises of the ΣCO_2 pool

As will be shown in Chapter 3, the determination of δ_b is based upon two data set requirements. Firstly, the proportion that each of the aqueous carbon species contributes to the ΣCO_2 pool must be known (i.e. f_a, f_b and f_c above). This is readily determined from pH, temperature and salinity measurements. Secondly, the enrichment factors between $CO_{2(aq)}$ - $CO_{2(g)}$, HCO_3^- - $CO_{2(g)}$ and $CO_3^{2-}{}_{(aq)}$ - $CO_{2(g)}$ must be known at the temperature of precipitation i.e. partitioning of carbon isotopes within ΣCO_2 relative to atmospheric CO_2, ($CO_{2(g)}$).

Isotopic enrichment factors for the ΣCO_2 / mineral carbonate system.

The isotopic enrichment factors calculated by various workers for the ΣCO_2 / mineral carbonate system are shown in Table 1.1. and reviewed below. A full explanation of notation is given in section 1.2.2.

1. ε $CO_{2(aq)}$ - $CO_{2\,(g)}$ {$\varepsilon_{\,g\,a}$}

In the earliest closed vessel equilibration experiments, Deuser and Degens (1967) equilibrated gaseous CO_2 with a) $CO_{2(aq)}$, by adjusting the pH such that all the dissolved inorganic carbon was in the form $CO_{2(aq)}$, with subsequent separation of gaseous and aqueous phases, and b) with $CO_{2(aq)}$ + HCO_3^-, again by pH adjustment. δ_a was determined directly in the former case and indirectly, accounting for the HCO_3^- - $CO_{2\,(g)}$ fractionation, in the latter case . These workers found no significant difference between the isotopic compositions of $CO_{2\,(aq)}$ and $CO_{2\,(g)}$.

Table 1.1. A summary of the published isotopic enrichment factors for the ΣCO_2 / mineral carbonate system.

Enrichment Factor	°/oo @ t°C / temperature dependence	Matrix of aqueous medium	Author	Notes
$\varepsilon_g a$	-1.18 °/oo + 0.0041 t°C -1.31 °/oo + 0.0049 t°C	Demineralised water DDW / ($NaHCO_3$ / Na_2CO_3)	Vogel *et al.* (1970) Zhang *et al.* (1995)	
$\varepsilon_g b$	+9.2 °/oo @ 0°C +6.8 °/oo @ 30°C	DDW / ($NaHCO_3$ / Na_2CO_3)	Deuser and Degens (1967)	
$\varepsilon_g b$ $\varepsilon_a b$	+9.483(1000/T) - 23.89 °/oo +9.87 (1000/T) - 24.12 °/oo	DDW / $NaHCO_3$ Determined indirectly	Mook *et al.* (1974)	Using Vogel et al. (1970) $\varepsilon_g a$ and Thode et al. (1965) $\varepsilon_g c$ to correct.
$\varepsilon_g b$	+8.38 °/oo @ 20°C	DDW / $NaHCO_3$	Emrich *et al.* (1970)	
$\varepsilon_g b$	+ 8.21 °/oo @ 25°C + 6.71 °/oo @ 40°C	DDW / $NaHCO_3$	Lesniak and Sakai (1989)	
$\varepsilon_g b$	+ 10.78 °/oo - 0.114t°C	DDW / $NaHCO_3$	Zhang *et al.* (1995)	
$\varepsilon_g c$	+ 7.5 °/oo @ 25°C	Theoretical	Thode *et al.* (1965)	
$\varepsilon_g c$	+ 8.38 °/oo @ 25°C + 6.62 °/oo @ 40°C	DDW / ($NaHCO_3$ / Na_2CO_3)	Lesniak and Sakai (1989)	
$\varepsilon_g c$	+ 7.22 °/oo - 0.052t°C	DDW / $NaHCO_3$	Zhang *et al.* (1995)	
$\varepsilon_g c$ mineral	+10.17 °/oo @ 20°C (-0.063 °/oo °C^{-1})	DDW / ($NaHCO_3$ / Na_2CO_3)	Emrich *et al.* (1970)	Calcite / aragonite mixture
ε_g calcite ε_g aragonite	+11.98 - 0.12t°C +13.88 - 0.13t°C	DDW / ($NaHCO_3$ / Na_2CO_3)	Romanek *et al.* (1992)	
$\varepsilon_b c$ mineral	+1.85 °/oo @ 20°C (0.035°/oo °C^{-1})	DDW / ($NaHCO_3$ / Na_2CO_3)	Emrich *et al.* (1970)	Calcite / aragonite mixture
ε_b calcite ε_b aragonite	+ 1.0 °/oo (no sig. temp dependence) + 2.7 °/oo (no sig. temp dependence)	DDW / ($NaHCO_3$ / Na_2CO_3)	Romanek *et al.* (1992)	

This approach of closed vessel equilibration of $CO_{2\,(g)}$ with demineralised water containing $CO_{2\,(aq)}$ (with <1% HCO_3^-) and subsequent, quantitative separation of gaseous and aqueous phases was also adopted by Vogel *et al.* (1970). In contrast to the earlier experiments these investigators determined ε_g a as being;

$\varepsilon_g a = -1.18 + 0.0041\ t^oC$

which was in agreement with their theoretical predictions. This enrichment factor is in agreement with the most recent experimental determinations of Zhang *et al.* (1995);

$\varepsilon_g a = -1.31 + 0.0049\ t^oC$

2. ε HCO_3^- - $CO_{2(g)}$ {ε_g b}

It has long been recognised that atmospheric CO_2 is isotopically depleted relative to dissolved inorganic carbon (which is predominantly HCO_3^- at sea water pH). Craig (1953) found $CO_{2\,(g)}$ to be depleted by 7°/oo relative to oceanic bicarbonate. Abelson and Hoering (1961) determined a $CO_{2\,(g)}$ - HCO_3^- fractionation factor of 1.0083 at 25°C and until the work of Deuser and Degens (1967) this was the only value determined by laboratory experiment. These workers, in equilibration experiments at controlled pH, determined the enrichment factor ε_g b as being +9.2°/oo at 0°C and +6.8 °/oo at 30°C.

In similar equilibration experiments Mook *et al.* (1974) determined the enrichment factor over a temperature range 5 to 25°C as ;

$\varepsilon_g b = +9.483\ (1000/T) - 23.89$ °/oo (where T is in °K)

They used the Vogel *et al.* (1970) ε_g a temperature relationship and a similar relationship for ε_g c derived theoretically by Thode *et al.* (1965) (see below) to make the necessary corrections for the isotopic compositions of $CO_{2\,(aq)}$ and $CO_3^{2-}{}_{(aq)}$ in their equilibration vessel.

It should be noted that uncertainties in the value of ε_g b in a sea water matrix may introduce a level of error into the above relationship (see below).

Based on their experimentally - derived $\varepsilon_g b$ expression, and using the Vogel *et al.* (1970) $\varepsilon_g a$ expression above Mook *et al.* (1974) then derived a relationship for the enrichment between HCO_3^- and $CO_{2\,(aq)}$ ($\varepsilon_a b$) as;

$\varepsilon_a b = +9.87\,(1000/T) - 24.12\ ^o/oo$

Similar studies have since been conducted by Emrich *et al.* (1970) (who calculated $\varepsilon_g b$ as +8.38°/oo at 20°C , but did not account for the isotopic composition of $CO_3^{2-}{}_{(aq)}$ (δ_c) in their calculations), and by Lesniak and Sakai (1989) (who determined $\varepsilon_g b$ as +8.21°/oo at 25°C).

In the most recent study, Zhang *et al.* (1995) have determined $\varepsilon_g b$ as being ;

$\varepsilon_g b = -0.114t^oC + 10.78^oC.$

which is in agreement with the data presented by Mook *et al.* (1974) and Lesniak and Sakai (1989).

3. $\varepsilon\ CO_3^{2-}{}_{(aq)} - CO_{2\,(g)}$ $\{\varepsilon_g c\}$

In contrast to the above enrichment factors $\varepsilon_g a$ and $\varepsilon_g b$, the values for which there is largely agreement within the literature, studies determining $\varepsilon_g c$ have been associated with considerable variation. Determinations of $\varepsilon_g c$ are difficult due to the problems of extracting sufficient quantities of CO_2 in the presence of $CO_3^{2-}{}_{(aq)}$. In the earliest experiments of Thode *et al.* (1965) in which CO_2 was equilibrated in a closed system at high pH, such that all the dissolved inorganic carbon was largely $CO_3^{2-}{}_{(aq)}$, reproducibility was poor, as was agreement with a theoretically derived value of $\varepsilon_g c$ (+7.5°/oo at 25°C).

Lesniak and Sakai (1989) circumvented the experimental problems by performing equilibrations in an open system in which CO_2 was bubbled through the chamber at the same pCO_2 as that in the solution at medium and high pH.

They calculated $\varepsilon_g c$ as +8.38°/oo at 25°C and +6.62°/oo at 40°C, in agreement with the theoretical data presented by Thode *et al.* (1965). Zhang *et al.* (1995) have more recently determined $\varepsilon_g c$ as being ;

$\varepsilon_g c = +7.22 - 0.052\ t°C$

which is offset from the Thode *et al.* (1965) and Lesniak and Sakai (1989) data by some 2-3°/oo.

4. $\varepsilon\ CO_3^{2-}{}_{mineral} - CO_{2\ (g)}$ {$\varepsilon_g c$ mineral}

In a series of slow precipitation experiments, and including data from an earlier study by Baertschi (1957), Emrich *et al.* (1970) calculated $\varepsilon_g c$ mineral as + 10.17°/oo at 20°C, with a temperature dependence of -0.063°/oo per °C. However, carbonate precipitates were not of a single mineralogy, being a mixture of calcite and aragonite, for which different enrichment factors apply (see below). Romanek *et al.* (1992) performed the first well-constrained experiments in which precipitation rate and mineralogy were carefully controlled and determined the relationships;

ε_g calcite $= +11.98 - 0.12t°C$

ε_g aragonite $= +13.88 - 0.13t°C$

Emrich *et al.* (1970) also reported values for $\varepsilon_b c$ mineral as + 1.85°/oo at 20°C, with a temperature dependence of 0.035°/oo per °C but again this was for calcite / aragonite mixtures.

Romanek *et al.* (1992) calculated the following relationships;

ε_b calcite $= +1.0$ °/oo

ε_b aragonite $= +2.7$ °/oo

with no significant temperature effects for these enrichment factors.

In addition to the uncertainties in $\varepsilon_g c$ highlighted above, Zhang *et al.* (1995) have questioned the appropriateness of using the above values for these enrichment factors within a sea water matrix. The data for the enrichment factors shown in Table 1.1 were determined using a matrix of (distilled water + $NaHCO_3$ + Na_2CO_3). Sea water is clearly a far more complex matrix and contains a high proportion of additional inorganic carbon species (notably mineral $MgCO_3$ and $CaCO_3$, which account for up to 70% of the total carbonate in sea water, (Stumm and Morgan , 1981)). Zhang *et al.* (1995) measured the enrichment factor between dissolved inorganic carbon and $CO_{2(g)}$ ($\varepsilon_g \Sigma CO_2$) directly in sea water samples at different temperature and pH. They found a discrepancy between measured $\varepsilon_g \Sigma CO_2$ and $\varepsilon_g \Sigma CO_2$ calculated using the enrichment factors $\varepsilon_g a$, $\varepsilon_g b$ and $\varepsilon_g c$ above (as determined in the distilled water matrix). pH had a noticable effect on the discrepancy between measured and calculated $\varepsilon_g \Sigma CO_2$, increasing as the proportion of carbonate increased.

This observation suggested to the authors that carbonate complexes in sea water such as $MgCO_3$ and $CaCO_3$ might significantly influence the fractionation between ΣCO_3^{2-} i.e. ($CO_3^{2-}{}_{(mineral)} + CO_3^{2-}{}_{(aq)}$) and gas, $\varepsilon_g \Sigma c$. Similar influences on $\varepsilon_g b$ might occur due to the presence of $MgHCO_3$ as a major bicarbonate species in addition to free HCO_3^-. Such complexes might account for the above discrepancies in $\varepsilon_g \Sigma CO_2$ noted by these authors and there is a clear need to determine the above enrichment factors in a sea water matrix.

The establishment of historical records of water temperature / $\delta^{18}O$ - H_2O and $\delta^{13}C$ - ΣCO_2 from $\delta^{18}O$ and $\delta^{13}C$ records in biogenic carbonates implicitly implies;

a) that the carbonate is continuously precipitated throughout the time period for which the record is being established and

b) both oxygen and carbon isotopes are precipitated in isotopic equilibrium with sea water over the range of growth rates exhibited by the organism in question.

1.3. Implications of changes in organismal accretion rate to establishing historical records of water temperature / $\delta^{18}O - H_2O$ and $\delta^{13}C$-ΣCO_2.

The establishment of historical records of water temperature / $\delta^{18}O - H_2O$ and $\delta^{13}C - \Sigma CO_2$ from $\delta^{18}O$ and $\delta^{13}C$ records in biogenic carbonates is determined by the method of isotopic profiling along the shell i.e. drilling consecutive samples along the shell midline axis. Isotopic profiling may be undertaken along the shell midline axis i) on the shell surface (Krantz *et al.* 1984, Tan *et al.* 1988, Dare and Deith, 1989, Dare, 1991) or ii) on the surface of a shell embedded in epoxy resin and sectioned along the midline axis (Jones *et al.* 1983, Margosian *et al.* 1987, Weidman *et al.* 1994). Under a given isotopic sampling protocol, e.g. drilling consecutive samples along the shell midline axis of 1 mm drill hole width, any change in accretion rate will lead to changes in time resolution i.e. the amount of time integrated by each sample of shell and the amount of time between samples. This will also change with size of hole drilled e.g. drilling consecutive 1mm or 5mm width drill holes.

The rate of carbonate accretion by an organism can potentially change both with season and age, accretion possibly ceasing completely. Richardson *et al.* (1982), for example found that both age and season had effects on the shell growth of the Queen Scallop, *Chlamys opercularis*. Growth was reduced both in the winter at a particular age and with age for a particular season, such that by the third year of life winter growth was negligible. Similarly, Mason (1957a) found a distinct seasonal pattern to shell growth in *Pecten maximus*, shell growth commencing in the spring, reaching a maximum in the summer and then decreasing in the autumn to reach a minimum in February. Clearly, such changes in shell growth rate would potentially lead to large variations in the amount of time integrated per carbonate sample during isotopic analysis. This will have implications as to the resolution with which changes in water temperature / $\delta^{18}O - H_2O$ and $\delta^{13}C - \Sigma CO_2$ can be tracked within the shell isotopic record. This is of particular importance if these parameters are changing rapidly with time and growth is relatively slow at certain periods, or if overall shell growth by the organism is slow.

Additionally, cessation of shell growth may influence the absolute range and mean values of these parameters as determined from the shell record, if for example shell cessation occurs during the coldest water temperatures.

Epstein and Lowenstam (1953) first considered the implications of seasonal changes in growth rate to temperature derivations from the carbonate isotope record. Successive thin layers of carbonate were ground parallel to the growth lines in the shells of two species from the waters of Bermuda. In the case of the conch *Strombus gigas,* accounting for deviations in $\delta^{18}O$ - H_2O and microenvironmental deviations in temperature, both of which were small, the range of the recorded and shell-derived temperatures were equal and it was deduced that, for this species, deposition of shell continued throughout the year, including the cooler winter months. Similar findings were reported for the mussel *Modiolus modiolus* from the waters of Nova Scotia by Margosian *et al.* (1987). However, for the clam *Chama macerophylla*, Epstein and Lowenstam (1953) reported that shell-derived winter temperatures were absent and it was concluded that shell deposition was confined to the warmer months of the year. Clearly, the latter species used alone would give erroneous values of both mean annual temperature and the annual temperature range. Other studies have examined the implications of seasonal growth variation upon isotopically - derived mean and annual temperature ranges. Krantz *et al.* (1987), found that individuals of the surf clam *Spissula solidissima* sampled from the New Jersey Shelf did not record the heaviest isotopic values and it was suggested that this species ceased shell calcification when water temperatures fell below 10°C, confirming earlier studies for this species by Jones *et al.* (1983) and Arthur *et al.* (1983). The lightest summer isotopic values were found to be recorded in shells in all three studies. Jones *et al.* (1986), found however that the ^{18}O values for warmer parts of the year were lost after the Giant Clam *Tridacna maxima* reached sexual maturity and energy was diverted from shell growth to gametogenesis and spawning, highlighting the need to sample carbonate deposited before the onset of maturity. It should be noted that, when calculating mean annual temperatures, the midpoint (median value) between the maximum and minimum $\delta^{18}O$ values should be used. Early studies (e.g. Keith and Parker, 1965) analysed carbonate homogenised from the whole shell to obtain an average temperature of growth; this would potentially bias values toward summer temperatures due to potential time averaging. As a general rule, fast growing, massive species taken from the middle of their geographic range and sampled in their first years of growth will give best time resolution. For species exhibiting logistic growth years of maximal growth following slow initial growth should be sampled.

There is a clear need to determine the growth function for the studied organism and to investigate seasonal changes in, and factors controlling shell growth in order to calibrate the extent of time averaging in the species concerned under a given sampling protocol before derivation of mean annual water temperature / $\delta^{18}O$ - H_2O and $\delta^{13}C$-ΣCO_2 and their respective annual ranges.

1.4. Biological calcification and the assumption of carbonate precipitation in isotopic equilibrium with sea water.

1.4.1. Concepts.

Biomineralisation in bivalves is an extracellular, cell - mediated process. Precipitation of shell carbonate in bivalves occurs within the extrapallial fluid (E.P.F.) This is the fluid confined within the extrapallial cavity, which is located between the mantle epithelial cells and the precipitating shell. The isotopic composition of skeletal carbonate is determined by the isotopic composition of the E.P.F.

In general, precipitation of carbonates out of isotopic equilibrium with sea water may occur by two mechanisms (McConnaughey, 1989a,b), namely *metabolic* and *kinetic* effects. Within the literature these have been frequently grouped together under a term first coined by Urey *et al.* (1951) as *'vital effects'*, which has been subsequently adopted by many authors (Weber and Woodhead, 1970, Kahn ,1979, Kahn and Williams, 1981).

a) A *metabolic effect* occurs when the H_2O / ΣCO_2 pool within the E.P.F. becomes isotopically altered with respect to oxygen / carbon relative to sea water H_2O / ΣCO_2. (see Figure 1.3). This may occur by the addition of respiratory CO_2 to the mantle epithelial ΣCO_2 pool or uptake of CO_2 from this pool by symbiont - associated photosynthesis. As discussed below, preferential uptake of ^{12}C during photosynthesis by symbiotic algae may result in the addition of isotopically enriched CO_2 from the mantle epithelium ΣCO_2 pool to the E.P.F. ΣCO_2 pool, resulting in enrichment of this pool with ^{13}C relative to the surrounding seawater (Vogel *et al.* 1970.) Conversely, respiration may add isotopically depleted CO_2 to the E.P.F. ΣCO_2 pool which becomes isotopically depleted relative to the surrounding sea water ΣCO_2 pool.

As discussed below, such a metabolic effect is confined to carbon isotopes and results in measured enrichments / depletions in carbon isotopic ratios in carbonates, relative to values when precipitation occurs in isotopic equilibrium with surrounding sea water.

b) A *kinetic effect* occurs as a result of incomplete partitioning of isotopes at some point during the precipitation pathway. This is most likely to occur within the E.P.F. and will affect both carbon *and* oxygen isotopes, resulting in measured depletions in carbon and oxygen isotopic ratios in carbonates relative to values when precipitation occurs in isotopic equilibrium with sea water.

1.4.2. The potential for precipitation of biological carbonates out of isotopic equilibrium with seawater.

To understand the mechanisms underlying metabolic and kinetic effects during biological carbonate precipitation it is necessary to understand the mechanisms of biological carbonate precipitation itself. The fractionation factors for carbonate - sea water oxygen and carbon isotope exchange are those associated with slow precipitation in which isotopic equilibration between carbon species and between oxygen species is complete. During this process, changes in the oxygen isotopic composition of water or the carbon isotopic composition of any species within the dissolved inorganic carbon system are reflected within a precipitated inorganic (i.e. abiological) carbonate by equilibrium exchange processes and modified by temperature as predicted by the temperature coefficients for the various fractionation factors. Biological calcification differs from this slow precipitation model. It is more rapid, confined within semi - permeable membranes and uses trans - membrane diffusive CO_2 as an important raw material in addition to HCO_3^- supplied by fluid transport (see below). This has important consequences which may be manifested as a kinetic disequilibrium effect. This kinetic effect may in turn be modulated by metabolic effect.

Simkiss (1976), McConnaughey (1988, 1989(b)), Watabe and Kingsley (1989) and Wheeler (1992) provide comprehensive reviews of the physiology of calcification and only a brief overview is presented here. Wheeler (1992) has identified several major compartments relating to molluscan biomineralisation (see Figure 1.3).

Figure 1.3 Inorganic carbon and oxygen pools involved in biological calcification
After McConnaughey (1989a,b), Wheeler (1992), McConnaughey *et al.* (1997)

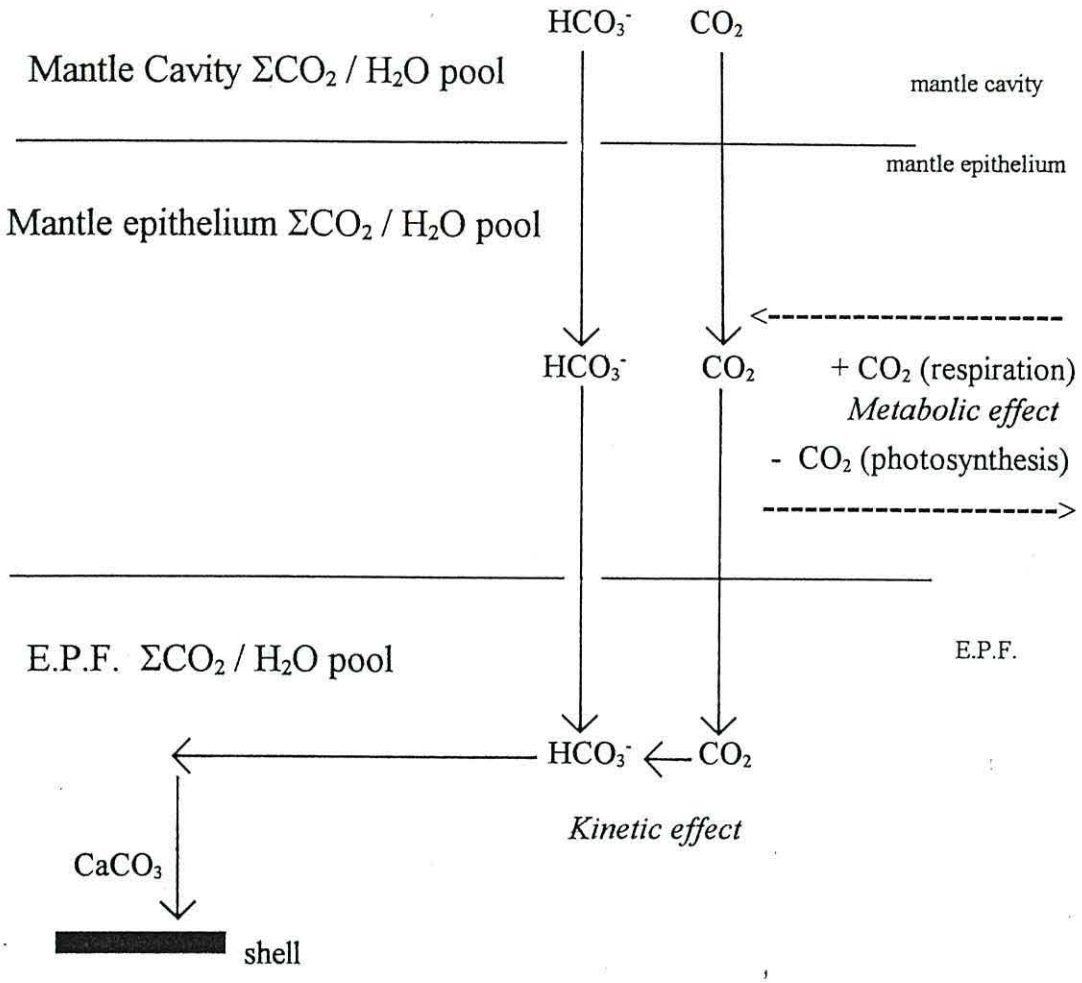

Effect	Response of stable isotopes	
Metabolic effect	*skeletal $\delta^{13}C$ depleted* with respect to carbonate precipitated in isotopic equilibrium with sea water.	*skeletal $\delta^{18}O$ same* as carbonate precipitated in isotopic equilibrium with sea water.
Kinetic effect	*skeletal $\delta^{13}C$ depleted* with respect to carbonate precipitated in isotopic equilibrium with sea water.	*skeletal $\delta^{18}O$ depleted* with respect to carbonate precipitated in isotopic equilibrium with sea water.
Metabolic + Kinetic effect	*additional depletion in skeletal $\delta^{13}C$* to that associated with kinetic effect alone.	*skeletal $\delta^{18}O$ depleted* as for kinetic effect.

The mantle epithelial layer is adjacent to the extrapallial cavity externally and mantle cavity internally. Evidence has been reviewed by Wheeler (1992) supporting the fact that the mantle epithelium is the primary shell-forming tissue and is responsible for both shell thickening and lengthening at the mantle edge. The extrapallial cavity (between the mantle epithelial layer and precipitating shell) contains the extrapallial fluid (E.P.F.) from which the shell precipitates. The mantle cavity contains essentially the same medium as the sea water medium bathing the entire organism (although this may be modified upon shell closure.) Shell precipitation occurs extracellularly within the E.P.F. and mantle cavity ΣCO_2 / H_2O, mantle epithelial (i.e.cellular) ΣCO_2 / H_2O and E.P.F. ΣCO_2 / H_2O therefore form three distinct carbon / oxygen pools separated by semi - permeable membranes (Figure 1.3). Carbonates are precipitated from E.P.F. HCO_3^- derived from two sources : i) CO_2 which diffuses across the mantle epithelial layer from the mantle cavity ΣCO_2 pool and then forms HCO_3^- in the E.P.F. by CO_2 hydration / hydroxylation (reactions 1 and 2, below) The proportion of HCO_3^- formed by hydration and hydroxylation is pH dependent. ii) HCO_3^- which may also enter the E.P.F. from the mantle cavity ΣCO_2 pool directly via fluid transport across the mantle epithelium.

McConnaughey (1989b) has postulated that membrane Ca ATP*ase* catalyses exchange of Ca^{2+} for H^+, raising the pH in the E.P.F. The concentration of $CO_3^{2-}{}_{(aq)}$ in equilibrium with a particular CO_2 level is inversely proportional to the square of the hydrogen ion concentration . Therefore, the pH gradient set up across the skeletogenic (epithelial) membrane will concentrate HCO_3^- and $CO_3^{2-}{}_{(aq)}$ in the E.P.F, drawing CO_2 across the membrane. The exchange of H^+ for Ca^{2+} by Ca ATP*ase* both raises the pH and the Ca^{2+} / $CO_3^{2-}{}_{(aq)}$ concentrations in the E.P.F. The epithelial membrane, whilst permeable to CO_2, is impermeable to $CO_3^{2-}{}_{(aq)}$ and HCO_3^-. This anion impermeability maintains the supersaturated state of the E.P.F. and, by raising the $[Ca^{2+}]$ $[CO_3^{2-}]$ ion activity product in the E.P.F, results in rapid precipitation. This is summarised in Figure 1.4. Wheeler (1992) has postulated a slightly different model in which Ca^{2+} access to the E.P.F. across the mantle epithelium is by passive, paracellular pathways. In this model CO_2 hydration / hydroxylation occurs within the epithelial cells rather than the E.P.F. and the resulting HCO_3^- is supplied to the E.P.F.

Figure 1.4. A model describing potential chemical pathways associated with the biological precipitation of calcium carbonate. Modified from McConnaughey (1988, 1989b).

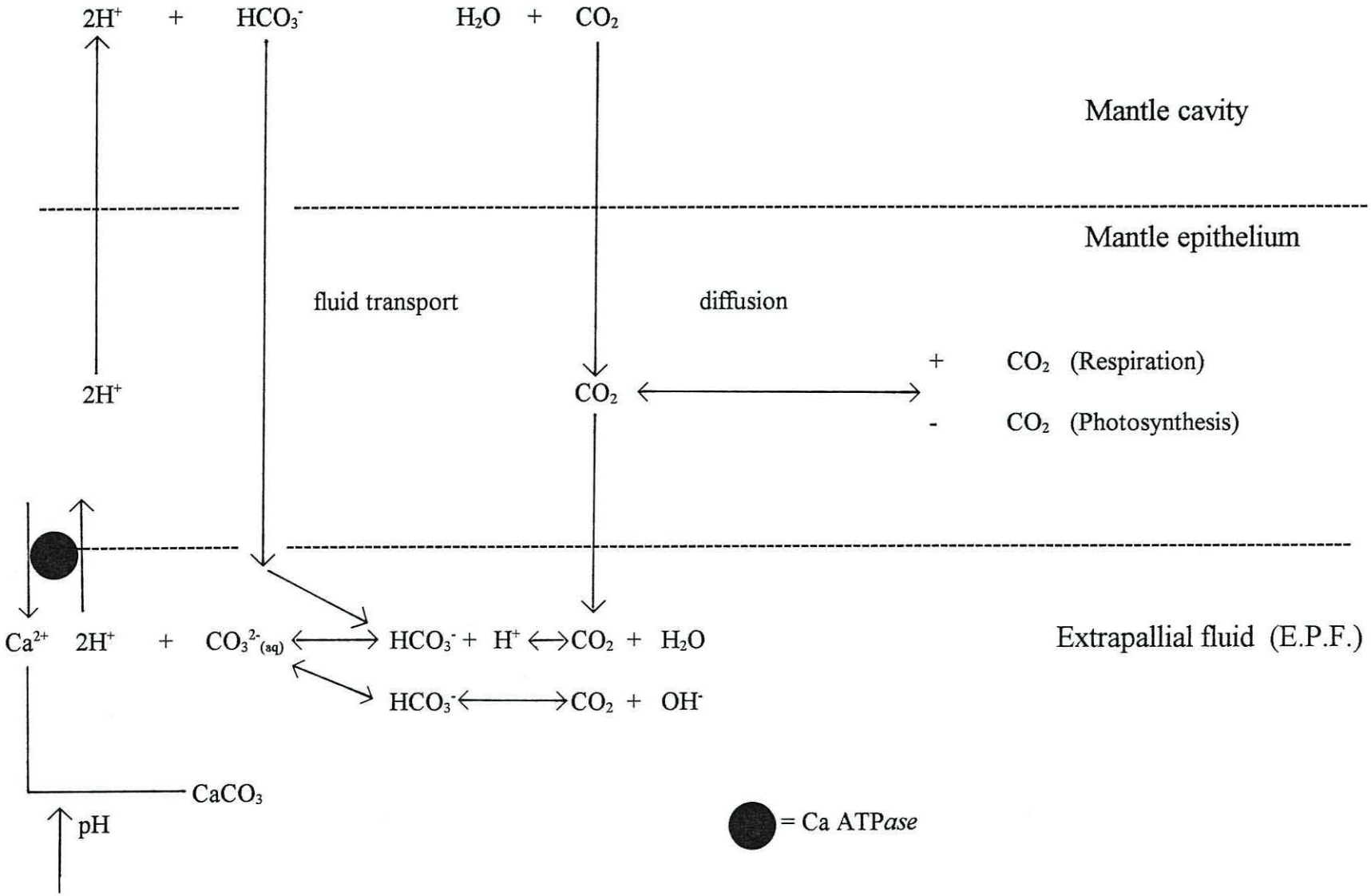

The H^+ ion produced during $CaCO_3$ deposition may then be removed by a reaction with additional E.P.F. bicarbonate which then forms CO_2 , catalysed by plasma membrane - bound carbonic anhydr*ase*. This CO_2 may then diffuse out of the E.P.F. into the epithelial cells where it may be eliminated into the mantle cavity or recycled for mineralisation. Importantly, from an isotopic viewpoint, both of these models are associated with two sources of inorganic carbon supply to the E.P.F. (CO_2 and HCO_3^-).

Precipitation of oxygen isotopes out of isotopic equilibrium with sea water can only result from either a change in the oxygen isotopic composition of the water within the E.P.F. (relative to sea water) i.e. a metabolic effect, or incomplete partitioning of oxygen isotopes between the carbonate and water i.e. a kinetic effect.

Alteration of the oxygen isotopic composition of the water in the E.P.F. is unlikely since fluxes of water between sea water and the E.P.F. are large compared to fluxes of metabolic CO_2 to the E.P.F. Additionally, calcareous organisms contain abundant carbonic anhydrase (Simkiss, 1976), which is found in particular within mantle epithelial cells. This enzyme catalyses ^{18}O exchange between (respiratory) CO_2 and (mantle epithelium) H_2O (Silverman ,1973). This will tend to equilibrate oxygen isotopes with mantle cavity / sea water H_2O and CO_2 entering the E.P.F is likely to be in isotopic equilibrium with sea water with respect to oxygen isotopes. The precipitation of mineral carbonate from $CO_3^{2-}{}_{(aq)}$ occurs at the same rate as oxygen isotope exchange between the crystal and aqueous ion ($CO_3^{2-}{}_{(s)}$ - $CO_3^{2-}{}_{(aq)}$) so that the growing crystal surface will equilibrate isotopically with $CO_3^{2-}{}_{(aq)}$. The equilibration between $CO_3^{2}{}_{(aq)}$ and HCO_3^- is almost instantaneous.

However the following reactions are associated with much slower exchange equilibria:

$CO_2 + H_2O$ ----------> $H^+ + HCO_3^-$ (CO_2 hydration).....reaction 1

$CO_2 + OH^-$ ----------> HCO_3^- (CO_2 hydroxylation).....reaction 2

When HCO_3^- precipitates rapidly from the E.P.F., this may occur before isotopic equilibration between HCO_3^- and CO_2 / H_2O / OH^- is complete, resulting in a kinetic effect.

Raising the pH has the effect of both increasing the rate of precipitation and increasing the time for isotopic equilibration since the balance between CO_2 hydration / hydroxylation changes with pH and the two reactions (1. and 2. above) are associated with different rate constants and therefore kinetic isotope effects.

McConnaughey (1989b) and Wheeler (1992) have postulated that the raw materials for biological carbonate precipitation are trans - epithelial membrane diffusive CO_2 and HCO_3^- supplied by fluid transport, both derived from the mantle cavity ΣCO_2 pool. HCO_3^- supply to the E.P.F. adds bicarbonate in isotopic equilibrium with mantle cavity / sea water ΣCO_2. This is not subject to kinetic isotope effect as above and tends to isotopically equilibrate the E.P.F.bicarbonate pool with mantle cavity / sea water HCO_3^- with respect to oxygen. As the rate of precipitation increases the proportion of precipitating HCO_3^- derived from trans - membrane CO_2 diffusion increases. i.e. the kinetic effect increases.

The above kinetic hydration / hydroxylation mechanism of isotopic fractionation also applies to the behaviour of carbon isotopes during precipitation within the E.P.F. and therefore *simultaneous* depletions in skeletal $\delta^{18}O$ and $\delta^{13}C$ will reflect a kinetic effect. This model of a kinetic effect during biological precipitation was used by McConnaughey (1989b), to explain correlations between $\delta^{18}O$ and $\delta^{13}C$ observed in non-photosynthetic corals where such simultaneous depletions in $\delta^{18}O$ and $\delta^{13}C$ were correlated with skeletal extension rate (i.e. calcification rate). As extension rate decreased the carbonate isotopic ratios approached those calculated for precipitation in isotopic equilibrium at ambient water temperatures. Similar observations of isotopic depletions with calcification rate have been reported in corals by Land *et al.* (1975), Erez (1977), (1978) and Weil *et al.* (1981). Vinot-Bertouille and Duplessey (1973) reported large disequilibria in large, rapidly - growing benthic foraminifera. There is therefore a distinct possibilty that precipitation of oxygen and carbon isotopes may occur out of isotopic equilibrium with sea water as a result of a kinetic effect, particularly at high precipitation rates. As discussed above, respiratory CO_2 reaching the E.P.F. is likely to be in oxygen isotopic equilibrium with mantle cavity / sea water H_2O.

However, the absence of an enzyme catalysing carbon isotope exchange between the CO_2 and ΣCO_2, (c.f. carbonic anhydr*ase*), and the relatively low fluxes ($\Sigma CO_{2\ seawater}$ - $\Sigma CO_{2\ E.P.F.}$) compared with water, may result in incomplete carbon isotopic equilibration between respiratory CO_2 within the mantle epithelium and seawater ΣCO_2. Potential addition of isotopically depleted respiratory CO_2 to the E.P.F. ΣCO_2 pool may then result in isotopic depletions in skeletal $\delta^{13}C$, not accompanied by isotopic depletions in skeletal $\delta^{18}O$. Conversely, preferential removal of ^{12}C during symbiont - associated photosynthesis may isotopically enrich the E.P.F. ΣCO_2 pool and result in isotopically enriched skeletal $\delta^{13}C$. Such potential metabolic modulations of $\delta^{13}C$ ratios may be superimposed upon any kinetic isotope effects and may explain the differences in $\delta^{13}C$ between photosynthetic and non-photosynthetic corals observed by McConnaughey *et al.* (1989a).Other studies have reported elevations in $\delta^{13}C$ in photosynthetic corals (Weber and Woodhead, 1970, Goreau, 1977, Swart, 1983) and foraminifera (Kahn and Williams, 1981, Erez and Honjo, 1981).

In summary, a kinetic isotope effect during biological calcification appears to be a consequence of the compartmentalisation of calcification within semi - permeable membranes and the use of diffusive CO_2 as an important raw material in addition to HCO_3^- obtained by fluid transport across the skeletogenic (mantle epithelial) membrane. Such a kinetic isotope effect is manifested as simultaneous depletions in skeletal $\delta^{13}C$ / $\delta^{18}O$ with respect to isotopic equilibrium. A metabolic effect results in depletions or enrichments in skeletal $\delta^{13}C$ with respect to isotopic equilibrium (but with no modulations in skeletal $\delta^{18}O$). This may occur as a result of the inclusion of respiratory CO_2 to the E.P.F. or uptake of CO_2 by symbiont-associated photosynthesis and associated carbon isotopic fractionation during carbon fixation.

1.5. Variations in $\delta^{18}O$ - H_2O and its implications to water temperature derivations from skeletal $\delta^{18}O$ data.

The isotopic composition of carbonates is governed by water temperature and $\delta^{18}O$ - H_2O i.e. the establishment of historical records of water temperatures from carbonate $\delta^{18}O$ data assumes that $\delta^{18}O$ - H_2O is known.

In his original paper Urey (1947) assumed that $\delta^{18}O$ - H_2O was a constant term. Subsequent work undertaken from the 1950's onwards has shown that this is far from the case. Both spatial and temporal variability in $\delta^{18}O$ - H_2O over a range of timescales may occur. Fresh water is characteristically isotopically lighter than sea water, reflecting isotopic partitioning during distillation (see Section 1.2.1. above); mixing of fresh water with sea water causes covariations in salinity and $\delta^{18}O$ -H_2O. Epstein and Mayeda (1953) explored the spatial variability in the oxygen isotopic composition of natural waters and found latitudinal changes in the isotopic composition of fresh water, which has been subsequently reported by other workers (e.g. Fairbanks, 1982). Epstein and Mayeda (1953) explained the underlying mechanism as a multiple stage (Rayleigh) distillation process in an open system where there is a progressive isotopic lightening of meteoric waters with increasing latitude, as shown in Figure 1.5 below. Waters at low latitudes are characteristic of a single distillation and have distillate of relatively heavy $\delta^{18}O$ -H_2O. As an air mass moves northward and cools additional rain results in depletion of ^{18}O in the remaining vapour, further depleted by any evaporation.

Figure 1.5. Isotopic composition of meteoric waters across North America (From Fairbanks, 1982. $\delta^{18}O$ -H_2O data in °/oo.

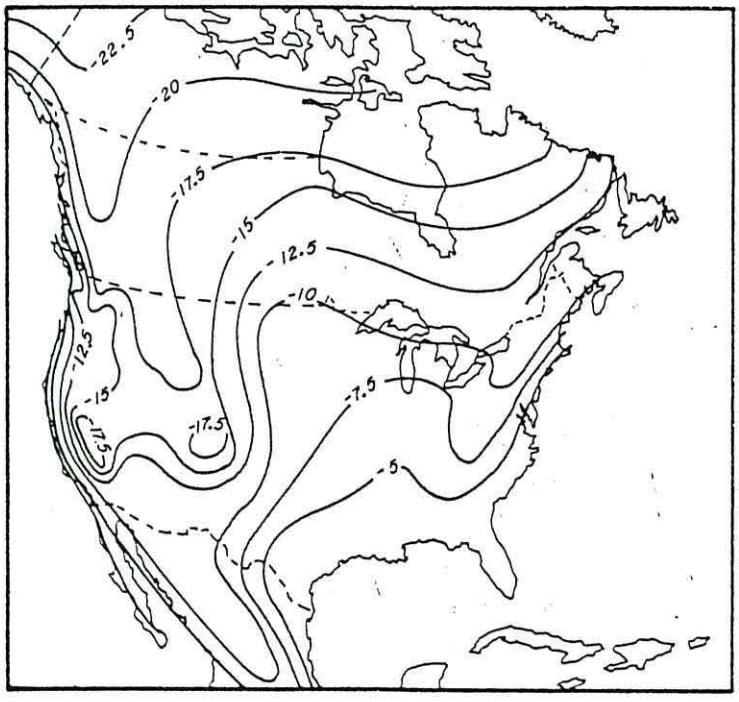

The effect of altitude is to cause further cooling and additional rainfall, explaining the isotopic lightening of meteoric waters with altitude seen over the Rocky Mountains in Figure 1.5 i.e. orographic effects. The formation of ice and snow at high latitudes removes the lighter distillate and maintains the ^{18}O enrichment of surface oceanic waters. A consequence of this process is that, for a given salinity, $\delta^{18}O\text{-}H_2O$ will vary as a function of latitude and the altitude of the watershed contributing fresh water to the water mass and this influences the relationship between salinity and $\delta^{18}O\text{-}H_2O$ for different water masses. Superimposed upon this will be any seasonal effects such as evaporation in the oceanic surface mixed layer associated with seasonal stratification.

In addition to spatial and temporal variations, changes in $\delta^{18}O\text{-}H_2O$ over geological time scales may occur, related to changes in global ice volume (the enrichment of the surface oceanic waters maintained by the permanent ice fields changing between glacial / non-glacial periods at a given latitude). For example, the enrichments during the Pleistocene glaciation have been estimated as 0.4°/oo (Emiliani, 1955), 1°/oo (Craig, 1965) and 1.4°/oo (Shackleton, 1967).

Determination of the $\delta^{18}O\text{-}H_2O$ term in palaeotemperature equation calculations has been done in three ways a) taking actual water samples in the region (Margosian *et al.* 1987, Dare and Deith 1991 b) use of a $\delta^{18}O\text{-}H_2O$-salinity relationship (Arthur *et al.* 1983, Krantz *et al.* 1987) where this relationship is known or may be reasonably estimated, and historic salinity data are available or may be reasonably estimated. c) estimation - this is commonly made for palaeooceanographic work since neither $\delta^{18}O\text{-}H_2O$ nor salinity data are available.

For palaeo work ,whilst it may be possible to estimate the latitude at which a fossil lived and the likely $\delta^{18}O\text{-}H_2O$ - salinity relationship using the present day model of change in ^{18}O of meteoric waters and a known temperature gradient between the Poles and Equator at that time several fundamental sources of error exist. Firstly, it is very difficult to determine the depth at which the animal lived and therefore proximity to the fresh water input. This may be accounted for to some degree if shell form changes with depth (Krantz *et al.* 1987). Secondly, the spatial and short-term (annual) temporal variations in $\delta^{18}O\text{-}H_2O$ outlined above are difficult to account for (even fully oceanic water is associated with variability in $\delta^{118}O\text{-}H_2O$). Thirdly, it is difficult to estimate altitude of the water shed supplying fresh water. Finally changes over geological time scales are difficult to account for.

It should be noted that in some cases, in particular in low latitudes where annual water temperature variation may be small, $\delta^{18}O\text{-}H_2O$ may be the dominant factor governing changes in $\delta^{18}O$.

1.6. Shell growth patterns in Pectinids.

Shell macro and microgrowth patterns may potentially provide useful environmental information once the factors governing their deposition are known (Richardson, 1991, 1996). The shell surfaces of many scallop species contain macroscopic rings and concentric fine ridges variously termed lamellae or striae which are visible on the scrubbed external surface under the binocular microscope at x20 - 50 magnification. Such striae have been reported for *Pecten diegensis* (Clark, 1968, 1975), *Chlamys opercularis* (Broom and Mason, 1978), *Pecten maximus* (Antoine, 1978, Gruffydd, 1981), and juvenile *Placopecten magellanicus* (Parsons *et al.* 1993).

External rings, originally thought to be of annual periodicity (Mason, 1957a) and traditionally used to age scallops (Merrill *et al.* 1965) have been shown from isotopic profiles to be deposited with a non-annual periodicity in some geographical locations (Dare and Deith, 1989).

There have been two schools of thought within the literature regarding factors governing the production of striae in scallops, with striae production being thought to be either a periodic phenomenon or deposited as a function of shell growth rate. Parsons *et al.* (1993) found striae production to be of daily periodicity (i.e. one per day) for *Placopecten magellanicus* up to 15 -20 mm height. Clark (1968, 1975) reported a daily periodicity of stria production in *Pecten diegensis* and *Argopecten gibbus*, although occasionally more or less than one stria per day were deposited. Broom and Mason (1978) reported that whilst *Chlamys opercularis* produced 1 stria per day during May and June, either side of this period frequency of ridge production decreased. The hypothesis of a daily rhythmicity of stria formation in *Pecten maximus* was refuted by experiment by Gruffydd (1981) who maintained scallops in the laboratory and found that the illumination regime (number of hours light and dark) had no effect on the number of striae produced, the number deposited never being one per day.

Gruffydd (1981) found that both striae number and width (i.e. the increment of shell between consecutive striae) increased with growth rate, striae number and width increasing with both water temperature and initial size for scallops in the 25 - 30mm height range which had been marked and kept for 53 days in the laboratory. He also found that the striae number and width varied with position on the shell valve with maximum striae number and width at the shell dorsoventral midline (where shell growth rates were maximal). Previous reports of a daily periodicity of striae deposition appeared to be coincidental. Since stria width has been shown to decrease with growth rate this results in higher striae abundance (number of striae per mm) during periods of lower shell growth. Dare (1991) used isotopic analysis to show that periods of higher striae abundance were associated with decreases in shell growth rate during the winter for *Pecten maximus* in U.K waters.

Chapter 2. Methods.

The determination of the carbon / oxygen isotopic composition of carbonates, dissolved inorganic carbon and waters involves either the quantitative conversion of the carbon / oxygen into CO_2 (carbonates, dissolved inorganic carbon) or a CO_2 equilibration method (waters), with subsequent analysis of the CO_2 using a dual inlet isotope ratio mass spectrometer (V.G.SIRA2).

2.1. Determination of the oxygen and carbon isotopic composition of carbonates ($\delta^{18}O$, $\delta^{13}C$).

Determination of $\delta^{18}O$ and $\delta^{13}C$ is based upon the sealed vessel (S.V.) method developed by McCrea (1950). This involves the reaction of the carbonate with anhydrous phosphoric acid, H_3PO_4, (S.G. 1.88) at constant temperature (25°C) within a reaction vessel evacuated prior to closure. The CO_2 evolved is subsequently cleaned up (isolating it from H_2O / H_3PO_4 vapour and N_2) before mass spectrometric analysis.

The carbonate sample to be analysed is placed into a glass Durham tube (BDH). Each Durham tube is loaded into a pear-shaped glass reaction vessel containing $2cm^3$ of anhydrous H_3PO_4. The latter is made by addition of 700g of P_2O_5 to 1 dm^3 of orthophosphoric acid heated to 90°C and continously stirred within a Pyrex beaker. Each reaction vessel is evacuated to high vacuum ($< 2x10^{-4}$ mbar) before closure. Evacuation is undertaken for 12 hours to ensure outgassing is complete. The carbonate is then reacted with the acid for 12 hours in a water bath set at 25°C. The evolved CO_2 is subsequently 'cleaned-up' before mass spectrometric analysis. Clean-up of CO_2 is carried out using a ten place vacuum line consisting of five individual units, each of which has ports for two reaction vessels. An individual unit of the ten place line is shown in Plate 2.1. The reaction vessel is placed on the upper arm of the unit via an Ultratorr fitting and pumped to high vacuum via the manifold. The manifold is common to all five units of the line and opens to valves allowing either roughing to a two stage rotary pump or evacuation to high vacuum via an Edwards vapour pump which is backed out through the rotary pump.

Plate 2.1 Individual unit of Ten Place Line for clean up of CO_2 evolved from carbonates and equilibrated with waters.

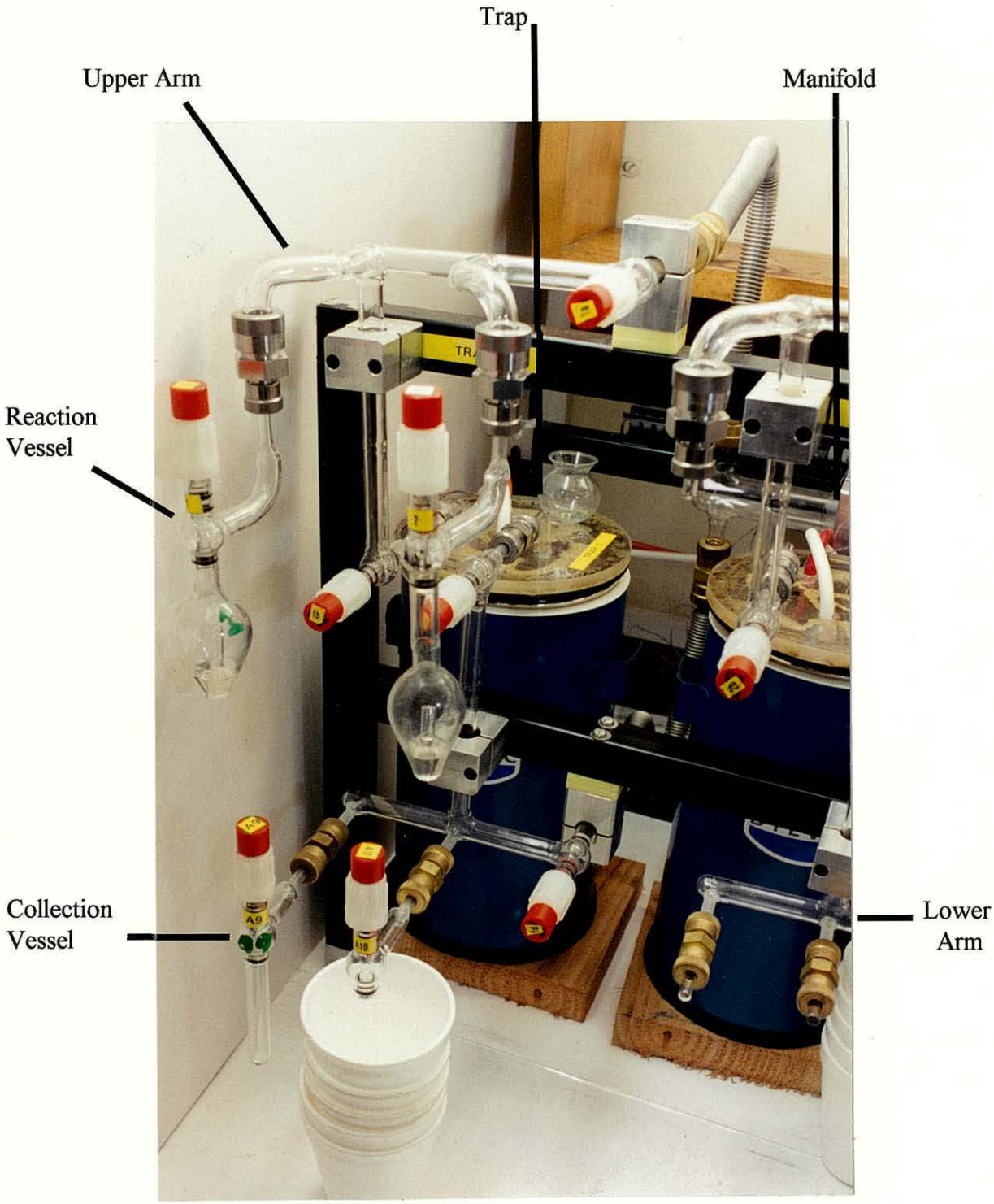

The remainder of the unit consists of a W shaped glass trap housed within a dewar which opens via Lowers Hapert taps to both the upper arm of the unit and the lower arm, the latter containing ports for the attachment of collection vessels. The glass trap is enclosed within a brass casing containing copper filings and which has a small tray at its base.The trap is thermostatically regulated to operator-set temperatures by the combined action of bubbling up of liquid nitrogen from a reservoir within the dewar into the casing tray and the action of a heating unit. After evacuation of the system to high vacuum the gas from the reaction vessel is expanded into the trap for ten minutes. The trap temperature is set at -85°C for cryogenic removal of water and acid vapour. The gas is then expanded into a collection vessel on the bottom arm of the unit and the CO_2 frozen into the reaction vessel over ten minutes by gradual addition of liquid nitrogen into a polystyrene cup placed around the collection vessel. Non - condensible gases are then pumped from the bottom arm of the unit after this has been isolated from the trap. The collection vessel is then shut for analysis on the mass spectrometer. Methodological accuracy and precision were monitored by running one internal standard (marble chips) with every four samples.The $\delta^{18}O$ and $\delta^{13}C$ values of this internal standard were checked against values based on long term calibrations directly against NBS19. Precision associated with the method was 1 σ = 0.08°/oo for $\delta^{18}O$ determination and 1 σ = 0.02°/oo for $\delta^{13}C$ determination for carbonate samples of 5mg weight.

2.2. Stable Isotopic determination of CO_2 using the Dual Inlet Isotope Ratio Mass Spectrometer.

Analysis of CO_2 within the mass spectrometer commences with ionisation of the gas by electrons emitted from a filament within an evacuated source and then, by the application of a high voltage, acceleration of the ionised gas through a semi-circular flight tube maintained under vacuum to three ion collectors. Stable isotopic CO_2 species are focussed into separate ion beams by the application of a magnetic field between the source and collectors. This may be summarised by the following equation;

$$M / Z = (B^2 R^2) / 2V$$

where M and Z are the mass and charge of the CO_2 species respectively upon ionisation, B the strength of the magnetic field, R the radius of travel of the molecule and V the voltage applied to accelerate the ion beam. When B,V and Z are fixed the radius of travel of the molecule is purely a function of mass. Therefore ion beams corresponding to the CO_2 stable isotopic species $^{12}C^{18}O^{16}O$ (mass 46), $^{13}C^{16}O^{16}O$ (mass 45) and $^{12}C^{16}O^{16}O$ (mass 44) are focussed into three separate ion beams onto the three collectors. $^{12}C^{16}O^{16}O$ is the most abundant CO_2 species and the beam associated with this species is consequently known as the major beam. The ratio of the amplified output voltages from the collectors corresponding to the mass 46 and mass 44 ion beams constitute the isotopic ratio $^{18}O/^{16}O$ (after some necessary corrections, see Chapter 1, Isotopic Standards.) Similarly, the ratio of the amplified output voltages from the collectors corresponding to the mass 45 and mass 44 ion beams constitute the isotopic ratio $^{13}C/^{12}C$.

Advances in natural abundance stable isotope mass spectrometry followed the development of the high precision dual inlet isotope ratio mass spectrometer by Nier (1947) and McKinney *et al.* (1950) with modifications by workers such as Shackleton (1965). The basic design of the dual inlet mass spectrometer has, in essence, been little changed since the early pioneering work. A schematic diagram of a triple collector, dual inlet isotope ratio mass spectrometer is shown in Figure 2.1. Within the source a thoria filament generates electrons which traverse a helical path through the gas to create a positively charged ion beam. The beam is focussed onto three Faraday collectors which collect and amplify the resolved ion beams. The simultaneous collection of the three resolved beams is one key feature that permits high precision measurements by the dual inlet mass spectrometer to be made. The other key feature of the instrument is the fact that sample gas is analysed in tandem with a reference gas of known isotopic composition using a changeover valve located immediately before the inlet probe entering the source. Sample and reference gases are admitted through capillary tubing from fixed volumes within the sample and reference inlet system into the source via the change over valve. This valve toggles between sample and reference sides such that reference gas then sample gas is admitted in turn into the source. A minimum of three reference/sample toggles (and typically six) are made for each sample run. The stable isotopic composition of the gas is then determined *relative* to the (calibrated) reference gas.

It is important that the pressure of both the reference and sample gases within the fixed volumes on the reference and sample inlet sides are identical during each analysis. This is because it is essential that the gases deplete from the fixed volumes into the analyser, housing the source, at the same rate. Heavier isotopic species diffuse at slower rates than the lighter species and this fractionates the gas within each of the reference and sample fixed inlet volumes during a run. The fractionation will be effectively the same for both reference and sample gases provided the gases deplete at the same rate. Gases within the reference and sample fixed inlet volumes are pressure equalised by changing the magnitude of the fixed inlet volume on the reference and sample sides, by the action of a variable volume bellows. Therefore if the sample of gas is small the sample inlet bellows is ramped up or the reference bellows ramped down. In practice this procedure involves equalising (or balancing) the reference and sample gas major beams at the beginning of each sample analysis. When the gas is not being admitted into the source during a run, the toggling action of the change over valve allows the gas to continue depleting at the same rate to the vacuum pump.

Figure 2.1 Schematic diagram of an isotope ratio mass spectrometer (from Boutton, 1991)

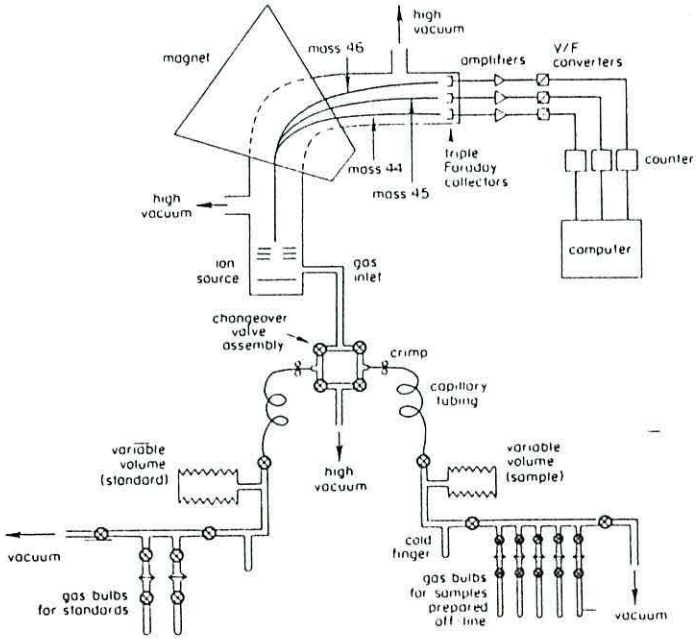

2.3. The effects of pretreating biological carbonates to remove organic components upon stable isotopic data

The pretreatment of biogenic carbonates to remove organic material prior to isotopic analysis has become common practice since the initial findings of Epstein *et al.* (1951, 1953). In their original study Epstein *et al.* (1951), heated powdered biogenic (shell) carbonate at 400°C for 60 minutes in a slow stream of helium to sweep volatile decomposition products of heated organic compounds away from the carbonate and found that carbonate ^{18}O was depleted after pretreatment. Inorganic carbonates analysed with and without heat treatment did not show changes in isotopic composition i.e. biogenic carbonates alone were affected by heat treatment, although an underlying mechanism could not be offered. This early study was however associated with experimental problems.The helium used in the purification process was purified from organic compounds by passing it over CuO heated to 700°C. Oxygen originating from the CuO and from back diffusion through the furnace opening was believed to contaminate the helium, oxidising the organic material in the shell to form CO_2 which in turn they suggested exchanged with the carbonate. They believed that CO_2 formed from atmospheric O_2 (-20°/oo relative to CO_2 produced upon acidification of shell carbonate) exchanged with shell carbonate to cause isotopic depletion. The process for organic matter purification was modified. Roasting again resulted in depletion in carbonate ^{18}O, by varying amounts for different organisms (see Table 2.1.)

Since this early work, other studies have used a number of pretreatment techniques to remove organic material from biogenic carbonates ; roasting in He at 470°C (Mook, 1971, Weidman *et al.* 1994), vacuum roasting (Erez and Honjo, 1981, Grossman *et al.* 1986, Kalish, 1991, Klein *et al.* 1996 a,b), treatment with 5% sodium hypochlorite solution (Fritz and Poplawski, 1974) and oxidation in a low temperature oxygen plasma (Swart, 1981). Indeed the pretreatment process has become standard practice in stable isotope analyses of biogenic carbonates and is considered essential in obtaining accurate isotopic data. Plasma ashing has the advantage in that heating can cause inversion of aragonite to calcite at temperatures as low as 150°C (Gaffey *et al.* 1991). In these studies similar depletions in isotopic ratios on pretreatment have also been reported and are summarised in Table 2.1.

Table 2.1. Summary of previous studies in which pretreatment of biogenic carbonates from a range of genera were undertaken to remove organic material prior to isotopic analysis.

Organism	**Pretreatment Method**	**^{18}O change on pretreatment °/oo**	**^{13}C change on pretreatment °/oo**	**Authors**
Snail *(Kelletia)*	Roasting in He for 1hr at 470°C	-1.10	not reported	Epstein *et al.* (1953)
Abalone (*Haliotis*)		-0.55	not reported	
Calcareous worms		-0.90	not reported	
Snail (*Strombus*)		-0.15	not reported	
Mussels	Roasting in He for 15 mins at 475°C	-0.55	-0.18	Mook (1971)
	Roasting *in vacuo*	-0.56	-0.22	
Pteropods	Vacuum roasting at 470°C	-0.40	no change	Grossman *et al.* (1986)
	Crushing in sodium hypochlorite	no change	no change	Grossman and Ku (1986)
Corals	Roasting in He	up to -1.5		Weber *et al.* (1976)
Globigerinoides ruber (foraminiferan)	Vacuum roasting at 470°C, 2hrs	-0.38	-0.10	Erez and Honjo (1981)
	Plasma ashing for 1 hr	-0.57	-0.25	
G.sacculifer (foraminiferan)	Vacuum roasting at 470°C, 2hrs	0.01	-0.19	
	Plasma ashing for 1 hr	-0.62	-0.45	
G.dutertrei (foraminiferan)	Vacuum roasting at 470°C, 2hrs	-0.23	-0.06	
	Plasma ashing for 1 hr	-0.70	-0.61	

The magnitude of isotopic depletion on pretreatment reported within these studies is far from constant and exhibits considerable interspecies variability. Due to this, a series of experiments were performed during this study to examine the effects of pretreatment on *Pecten* shell isotopic data. In experiment A, samples of homogenised *Pecten* shell were pretreated by plasma ashing for 4.5 hours. Organic removal is complete after 3 hours of ashing and an extra 90 minutes was built in to be absolutely sure ashing was complete. Ashed shell samples were then prepared for stable isotopic analysis by standard methods (sealed vessel acidification with phosphoric acid , S.G.1.88 for 12hours (McCrea, 1950)). Untreated shell samples were similarly prepared. The results of this this experiment are shown in Table 2.2.

In a separate time trial experiment (experiment B) homogenised *Pecten* shell was ashed for 0, 4.5 and 9 hours and subsequently prepared for isotopic analysis. Data for the time trial experiment are shown in Figure 2.2. and summarised in Table 2.3.

In both experiments significant depletions in both the ^{18}O and ^{13}C of scallop calcite occurred upon pretreatment for 4.5hrs, in agreement with the general findings outlined in Table 2.1. There was no additional depletion in either $\delta^{18}O$ or $\delta^{13}C$ at 9hrs. The depletion in $\delta^{18}O$ ($\Delta_{\text{non ashed - ashed}}$) was of the order of -0.90 °/oo and -0.38°/oo in experiments A and B respectively whilst depletion in $\delta^{13}C$ was of the order of -0.25 °/oo and -0.09 °/oo in experiments A and B respectively.

Depletion in $\delta^{13}C$ was therefore consistently of lower magnitude compared to depletion in $\delta^{18}O$, again in agreement with the trend of the data observed in the previous studies. Homogenised shell was obtained from separate individuals in each of the two experiments above. The observed difference in isotopic depletion on pretreatment ($\Delta_{\text{non ashed - ashed}}$) between the two experiments may reflect differing levels of organic material. This may also account for differences observed in the different studies documented in Table 2.1.

It is important to establish that the observed isotopic depletions arising from pretreatment are due to the removal of organic material from the shell and are not artefacts of the pretreatment process itself. This is of particular importance since precipitation of biogenic carbonates out of isotopic equilibrium with sea water (either as a result of kinetic effect or introduction of metabolic CO_2) results in depletions in carbonate isotopic ratios (see Chapter 1, section 1.4).

Table 2.2. Summary of the effects of plasma ashing for 4.5hours upon homogenised *Pecten maximus* shell calcite isotopic ratios (Experiment A).

Sample	n	mean / median (*) °/oo	s.d. °/oo	test	p	Difference (Δ ashed - non ashed) °/oo
Non-ashed shell $\delta^{18}O$	7	1.52 (*)	N.A	mood	<0.01	-0.90
Ashed shell $\delta^{18}O$	7	0.62 (*)	N.A			
Non-ashed shell $\delta^{13}C$	7	1.05	0.02	pooled t test	<0.01	-0.25
Ashed shell $\delta^{13}C$	7	0.80	0.05			

Median data are reported where data displayed non-normal distribution.
N.A. = not applicable

Table 2.3. The effects of ashing time upon homogenised *Pecten maximus* shell carbonate isotopic ratios (number of samples = 6 at each time interval) (Experiment B).

	Time in plasma asher		
Sample	0hrs	4.5hrs	9hrs
Mean Shell $\delta^{18}O$ (s.d) °/oo	0.79 (0.08)	0.41 (0.11)	0.37 (0.12)
Mean Shell $\delta^{13}C$ (s.d) °/oo	0.65 (0.05)	0.56 (0.01)	0.54 (0.02)

Figure 2.2. The effects of ashing time upon homogenised *Pecten maximus* shell carbonate isotopic ratios. (number of samples = 6 at each time interval) . (Experiment B).

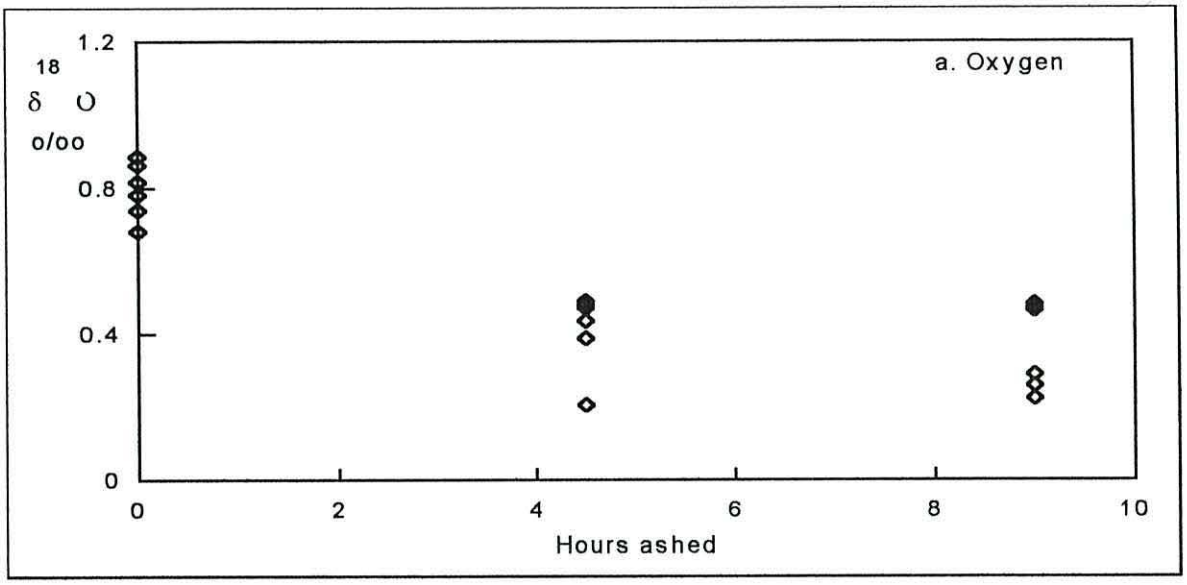

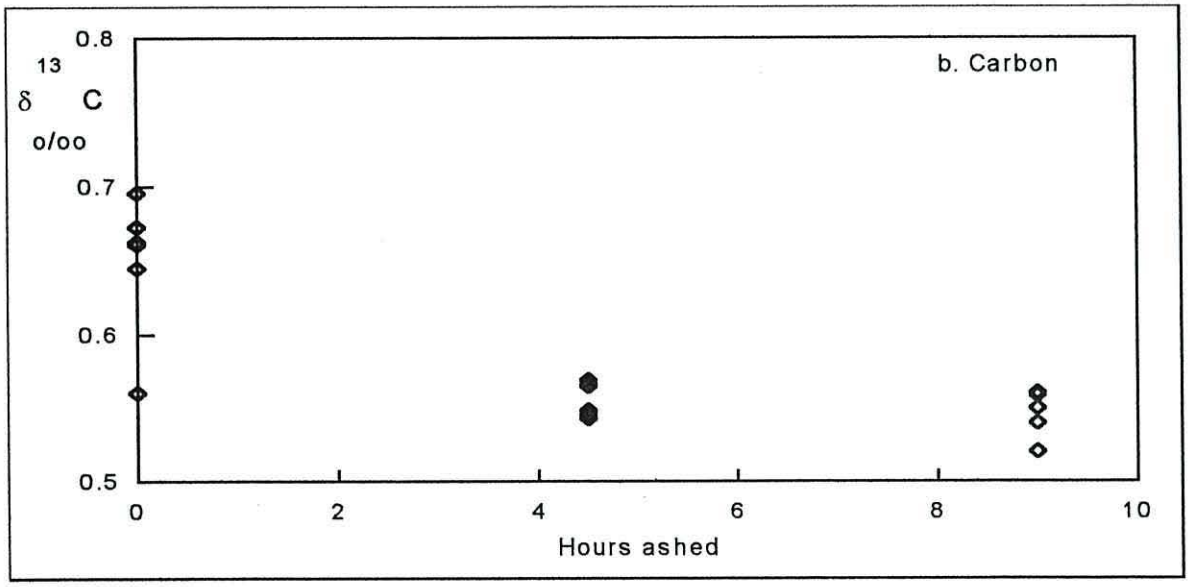

The process of plasma ashing involves the use of a low temperature reactive oxygen plasma to oxidise organic material. This presents the opportunity for a) isotopic exchange between the reactive oxygen and oxygen within the carbonate and b) isotopic exchange between CO_2 or other oxidation products derived from the oxidation of shell organic matter and carbon / oxygen within the carbonate. An experiment (experiment C) was undertaken to address these possibilities. Pyrex boats containing inorganic marble chips were plasma ashed for 4.5hrs immediately next to boats containing homogenised shell and the inorganic marble chips subsequently analysed for $\delta^{18}O$ / $\delta^{13}C$. Table 2.4. shows that the marble chips were isotopically indistinct from marble chips which had not been ashed with respect to both oxygen and carbon. This suggests that isotopic exchange does not occur in the plasma asher by either of the processes above.

In experiments designed to examine the possibility of isotopic exchange during pretreatment Epstein *et al.* (1953) heated shell material in an atmosphere of isotopically enriched CO_2 (+100°/oo) at temperatures that facilitated isotopic exchange between organic material and the CO_2 without oxidising the organic components. Some isotopic exchange was found to have occurred between the enriched CO_2 and the carbonate (as shown by data for CO_2 evolved from shell first pretreated to remove organic material and then exposed to the isotopically enriched carbon dioxide). However, CO_2 produced from untreated shell which was exposed to the enriched CO_2 showed a relatively greater isotopic enrichment. The authors concluded that this indicated that shell organic components must either directly or indirectly affect the isotopic composition of CO_2 extracted from untreated shell upon acidification. From the experiments conducted in the present study, the observed depletions in shell isotopic ratios shown in Table 2.2. and Table 2.3. appear to be a result of organic removal rather than an artefact of ashing itself, e.g. an isotopic exchange process.

It may be inferred that some (organic) constituent within the shell material a) contributes to masses 44-46 either directly, or as a result of cracking on the source filament, or b) exchanges isotopically with carbonate-derived CO_2 upon acidification within the reaction vessel. Both $\delta^{18}O$ and $\delta^{13}C$ ratios were found to be higher for untreated shell when compared to ashed shell. Shell organic constituents are extremely depleted in ^{13}C (Cobabe and Pratt, 1995) i.e. CO_2 produced directly from shell organic material will be depleted in ^{13}C.

Table 2.4. Isotopic ratios of inorganic marble chips ashed in close vicinity to homogenised *Pecten* shell as compared to non-ashed marble chips (Experiment C).

Sample	n	mean °/oo	s.d. °/oo	test	p
Non-ashed chips $\delta^{18}O$	6	-2.14	0.06	pooled t test	N.S
Ashed chips $\delta^{18}O$	6	-2.11	0.04		
Non-ashed chips $\delta^{13}C$	6	2.05	0.01	pooled t test	N.S.
Ashed chips $\delta^{13}C$	6	2.02	0.03		

Table 2.5. Effect of alanine additions to marble chips upon carbonate isotopic ratios. (Experiment D)

	0% alanine	5% alanine	20% alanine	50% alanine
$\delta^{18}O$ °/oo (s.d)	-2.00 (0.08)	-2.10 (0.04)	-2.08 (0.07)	-2.09 (0.08)
$\delta^{13}C$ °/oo (s.d)	2.02 (0.03)	1.99 (0.02)	2.04 (0.03)	2.05 (0.02)

This would result in depleted isotopic ratios for unashed shell (either by direct contribution to the CO_2 pool in the reaction vessel or isotopic exchange) compared to ashed shell where organic material is removed prior to acidification. In fact the opposite effect was observed (Tables 2.2. and Table 2.3.) N_2O would also increase the mass 44 ion beam and again produce depleted rather than enriched isotopic ratios in untreated shell.

In an attempt to investigate the effect of organic material on carbonate isotopic ratios, an experiment was conducted (experiment D) in which marble chips ($\delta^{13}C = 2.02$ °/oo, $\delta^{18}O = -2.06$ °/oo) were mixed with varying amounts of alanine ($\delta^{13}C = -23.2$ °/oo). Alanine is an important molluscan shell constituent amino acid (Qian *et al.* 1995). Carbonate - alanine mixtures were then acidified with phosphoric acid.

Table 2.5 shows that there was no difference in marble chips $\delta^{18}O$ or $\delta^{13}C$ over a range of weight alanine : weight marble chips ratios of 5 : 95, 20 : 80 and 50 : 50.

Although an important constituent of shell organic material, alanine is only one of many shell organic components. Based on the data from experiments A and B it is concluded that, whilst organic components result in erroneously enriched carbonate isotopic data (see Tables 2.2 and 2.3), an underlying mechanism cannot be offered here. Indeed the arguments presented above suggest that organic components should in fact produce erroneously isotopically depleted data. It can only be speculated that a shell organic constituent (other than alanine), produced upon acidification, interferes with the 44 - 46 ion beams in the mass spectrometer and that this unknown constituent a) affects only masses 45 and 46 or b) affects all masses 44 - 46, but, (as suggested by Weber *et al.* 1976), since the mass 44 ion beam is larger than the 45 and 46 ion beams only beams 45 and 46 are significantly affected to produce the observed isotopic ratio enrichments.

In summary therefore, the organic components of *Pecten* shell calcite have a significant effect upon calcite isotopic data, although an underlying mechanism is presently unknown. In agreement with previous studies involving biogenic carbonates, organic components in *Pecten* calcite result in erroneously enriched isotopic data and must therefore be removed before accurate $\delta^{18}O$ and $\delta^{13}C$ determinations can be made.

2.4. The effects of sample size upon $\delta^{18}O$ and $\delta^{13}C$ data.

It is clearly desirable, in order to maximise time resolution, to obtain detailed $\delta^{18}O$ and $\delta^{13}C$ data when sampling along the axis of accretionary growth. This allows accurate determination of maximum / minimum shell isotopic data as well as tracking changes in $\delta^{18}O$ and $\delta^{13}C$ with fine resolution. In some instances, e.g. where the organism's growth is rapid or changes in $\delta^{18}O$ / $\delta^{13}C$ with time are slow, sample size can be large without significantly losing resolution. This enables the total number of samples analysed from a shell to be kept to a minimum, important for considerations of running time and finance. In other cases, e.g. where the organism is slow growing or where changes in $\delta^{18}O$ and $\delta^{13}C$ occur rapidly with time, carbonate samples should (optimally) be infinitely small. A particularly relevant example of this lies in the case of sampling along the *Pecten* shell axis. Accretionary growth becomes extremely slow during the winter, stopping altogether during periods associated with the coldest water temperatures (see Chapter 4).

An investigation was therefore conducted to investigate whether carbonate sample size affected the precision and accuracy associated with $\delta^{18}O$ and $\delta^{13}C$ data. Replicate inorganic carbonate samples of NBS-19 standard were weighed at 5mg, 0.5mg and 0.2mg and prepared for isotopic analysis as outlined in section 2.1 above. Table 2.6. shows the results of these analyses. The experiment was again repeated with a greater weight range (1-10mg) of replicate standards, the results of which are shown in Table 2.7. The isotopic standard deviation data and Δ data (i.e. the difference between the mean isotopic composition at a given weight and the mean at 5mg) as shown in Tables 2.6. and 2.7. are shown graphically in Figure 2.3.

The data shown in Tables 2.6 and 2.7 and Figure 2.3 show that the sealed vessel method is associated with acceptable accuracy and precision for carbonate sample weights above a threshold value between 0.5mg and 1mg. Below this threshold $\delta^{18}O$ data become both increasingly inaccurate, deviating toward erroneously depleted values and also become increasingly imprecise. $\delta^{13}C$ data also become increasingly inaccurate below this threshold, but the magnitude of erroneous isotopic depletion is less than that for oxygen by a factor of between 3.3 - 5.6 . Unlike oxygen, precision is not compromised by decreasing sample weight below the 0.5 -1mg threshold.

Table 2.6. Effect of carbonate sample size on isotopic analyses.
Standard = NBS19 ($\delta^{18}O$ = -2.20 °/oo , $\delta^{13}C$ = +1.95 °/oo.)
Δ = difference between mean isotopic composition at that weight and mean at 5mg .C.F. = cold finger used. See text for explanation of chopping in the mass spectrometer.

	Weight of NBS-19 standard		
	5mg (n=8)	0.5mg (n=7) C.F. , Chops no. = 2	0.2mg (n=6) C.F. , Chops no. = 1
Mean $\delta^{18}O$ °/oo	-2.25	-2.51 (Δ = –0.26)	-2.98 (Δ = –0.73)
S.D °/oo	0.07	0.33	0.42
Mean $\delta^{13}C$ °/oo	1.94	1.86 (Δ = –0.08)	1.81 (Δ = –0.13)
S.D. °/oo	0.01	0.01	0.02

Table 2.7. Effect of carbonate sample size on isotopic analyses.
Standard = marble chips (internal standard, $\delta^{18}O$ = -2.12 °/oo , $\delta^{13}C$ = +2.06 °/oo).
Δ = difference between mean isotopic composition at a given weight and mean at 5mg. C.F. = cold finger used.

	Weight of standard			
	10mg (n=7)	5mg (n=7)	3mg (n=7)	1mg (n=8) C.F.,Chops no.= 3
Mean $\delta^{18}O$ °/oo	-2.13 (Δ = –0.01)	-2.12	-2.14 (Δ = –0.02)	-2.10 (Δ = +0.02)
S.D °/oo	0.02	0.04	0.05	0.10
Mean $\delta^{13}C$ °/oo	2.08 (Δ = +0.02)	2.06	2.06 (Δ = 0.00)	2.06 (Δ = 0.00)
S.D °/oo	0.01	0.01	0.01	0.03

Table 2.8. Mean isotopic data and associated errors obtained during manifold backfill CO_2 runs.

	Bellows Run (no chops)	Cold finger Run (3 chops)
Mean $\delta^{18}O$ CO_2 °/oo	8.45	8.48
S.D °/oo	0.03	0.02
Mean $\delta^{13}C$ CO_2 °/oo	2.12	2.06
S.D °/oo	0.02	<0.01

Figure 2.3. Isotopic standard deviation and Δ data (the difference between the mean isotopic composition at a given weight and the mean at 5mg) associated with increasing carbonate sample size.

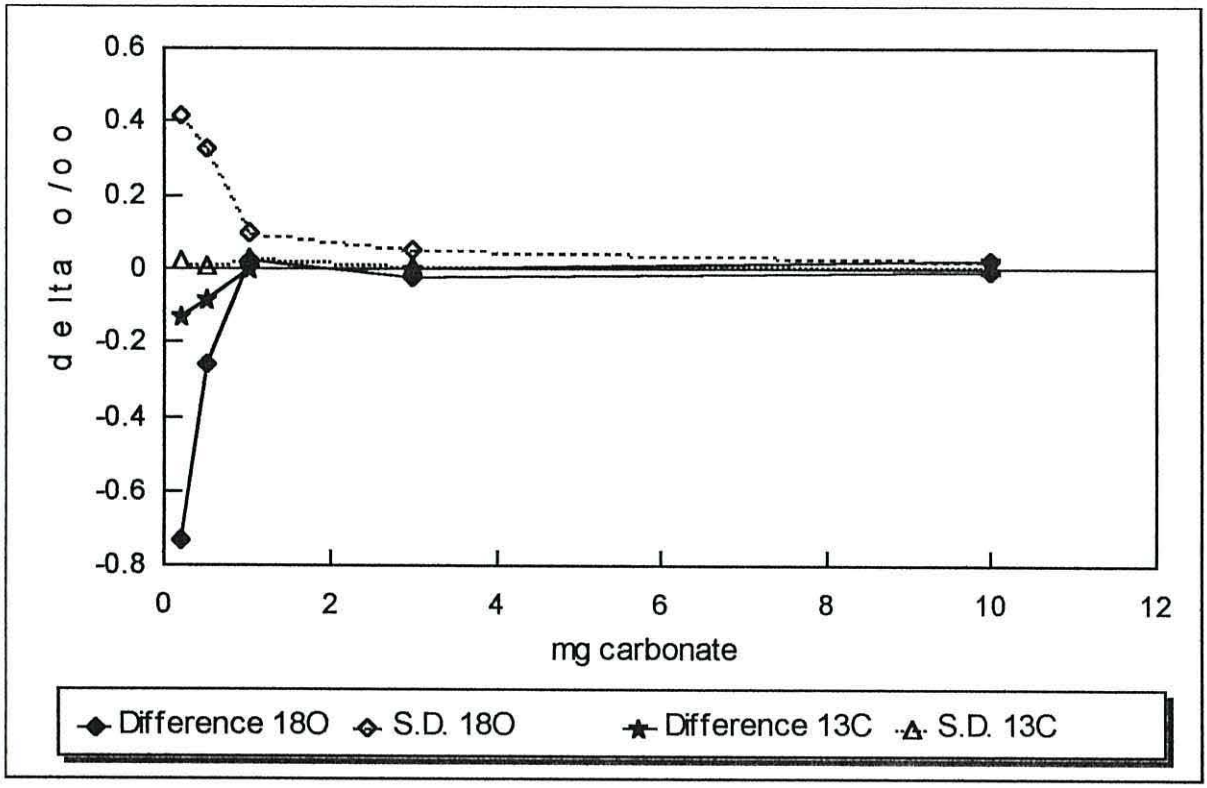

Table 2.9 Effect of reduction in acid volume upon precision and accuracy of carbonate isotopic data. Volume of phosphoric acid = 0.25 - 0.5cm^3.

	Sample Weight		
	5mg	0.5mg	0.2mg
mean $\delta^{13}C$ ‰	2.06	1.94	1.97
1σ $\delta^{13}C$ ‰	0.02	0.03	0.02
mean $\delta^{18}O$ ‰	-2.12	-2.04	-2.00
1σ $\delta^{18}O$ ‰	0.04	0.04	0.08

There are two areas within the analytical pathway where sample size -related effects may potentially arise.

a) *instrument - based.*

The analysis of small quantities of CO_2 involves the manipulation of the gas within the mass spectrometer. In general, beam sizes of reference and sample gas are equalised after expansion of the sample gas from the collection vessel manifold into the inlet system and isolation there within a fixed volume. Equalisation (to a target beam size) is achieved by the use of a variable volume bellows located within the reference and sample inlet systems before the change over valve (see Figure 2.1) The smallest number of moles of CO_2 that can be analysed in the sample inlet fixed volume (i.e. with the sample inlet bellows fully ramped up) is set by the minimum major beam size of the reference gas (i.e with the reference bellows fully ramped down). If the sample major beam size is below this value it is not possible to balance the reference and sample beam sizes, essential for isotopic ratio determination. In the case of large samples, only an aliquot of gas is analysed i.e. the inlet fixed volume is isolated from the manifold after expansion and equilibration of the gas from the manifold. If the sample major beam size is below that of the minimum reference major beam size, the remaining gas (within the manifold) is frozen into a cold finger volume within the sample inlet system and then expanded into the inlet volume after this has been isolated from the manifold.The mass spectrometer is tuned to be linear over a range of major beam sizes. On expansion of the gas from the cold finger volume , if the sample major beam size is now above this range of linearity, then the gas is expanded into an expansion volume and an aliquot pumped away after re-isolation of the inlet fixed volume. Such 'chopping' of the gas continues until the sample major beam size is within the range of instrument linearity. Clearly, the smaller the quantity of gas, the fewer the number of chops that are executed. The possibility exists that CO_2 manipulation in this way may be responsible for the observed errors. To check this a simple exercise was conducted whereby the sample inlet manifold was backfilled with CO_2 at a pressure corresponding to the threshold between a bellows run and a cold finger run with three chops. Due to the slight differences in volume of the manifold ports, 6 samples ran as cold finger runs and 4 samples ran as bellows runs. Mean isotopic data and errors obtained are shown in Table 2.8.

The data in Table 2.8. clearly show that increased gas manipulation in the mass spectrometer does not influence either precision or accuracy of $\delta^{18}O$ / $\delta^{13}C$ determination.

b) method -based.

The other area where errors may potentially arise is at the acidification step of the method. In a recent study, Ball *et al.* (1996) reported similar trends in precision and accuracy to those noted in this study, when analysing CO_2 yield and isotopic composition of standard calcite across a weight range 0.05mg - 6.5mg. At sample weights below 0.5mg progressive shifts to more negative isotopic values occurred with simultaneous decreases in the actual : expected CO_2 yield on recovery and increases in % blank contribution. The data in the present study are in agreement with the data of Ball *et al.* (1996), as are the conclusions; namely that the sealed vessel method as outlined in Section 2.1. is unreliable for sample weights below between 0.5mg and 1mg.

Ball *et al.* (1996) suggested two possible mechanisms associated with the acidification step that might explain these shifts. One possible mechanism is the retention of calcite-liberated CO_2 within the phosphoric acid (i.e. as dissolved CO_2) during cryogenic clean - up of the gases as outlined in Section 2.1. above ; this would explain the observed decreases in actual : expected yields as the ratio of the proportion of CO_2 retained : CO_2 collected increased. Possible fractionation between dissolved and gaseous CO_2 was also considered as a potential contributing factor. The other possible mechanism suggested was contamination through the 'O' rings of the reaction vessel by atmospheric CO_2. Again, as the number of moles of calcite - liberated CO_2 decreased with sample size, this would have had an increasingly significant effect. However, it was noted that whilst atmospheric contamination ($\delta^{13}C$ of approximately -11°/oo, $\delta^{18}O$ of approximately +6.5°/oo) would result in the observed negative deviations in $\delta^{13}C$, it would produce enriched $\delta^{18}O$ values. The investigators concluded therefore that CO_2 retention may be a significant factor in explaining the observed changes in precision and accuracy observed in their study. These investigators found that reduction in the volume of phosphoric acid used for acidification significantly improved the precision and accuracy of isotopic data.

Tests were also conducted within this study in which the volume of acid was reduced to 0.25 - 0.5cm^3. Reaction vessels were modified from the original design (where the calcite sample is placed within a Durham tube which is subsequently placed into the pear - shaped reaction vessel). The sample was instead placed into the cut tip of a Durham tube which was subsequently placed into one arm of a two-armed reaction vessel. The other arm was loaded with 0.25 - 0.5cm^3 of phosphoric acid. After evacuation of the reaction vessel the acid was tipped into the sample arm for sample acidification. Replicate analyses of calcite samples gave considerably improved precisions and accuracies (see Table 2.9), in agreement with the findings of Ball *et al.* (1996).

2.5. Determination of the oxygen isotopic composition of sea water relative to SMOW ($\delta^{18}O\text{-}H_2O$)

Determination of $\delta^{18}O\text{-}H_2O$ is based upon isotopic equilibration of the water sample with (cylinder) CO_2 of known isotopic composition within a closed reaction vessel (i.e. a closed system) at known temperature (Epstein and Mayeda, 1953). The equilibration is undertaken in a shaking water bath to increase the rate at which isotopic equilibrium is reached.
At isotopic equilibrium the system is described by the mass balance relationship;

$$\delta^{18}O_{(system)} = \frac{a \,.\, \delta^{18}O\text{-}H_2O_{(i)} + b \,.\, \delta^{18}O\text{-}CO_{2(i)}}{a + b} = \frac{a \,.\, \delta^{18}O\text{-}H_2O_{(e)} + b \,.\, \delta^{18}O\text{-}CO_{2(e)}}{a + b} \quad \text{.... (Equation1)}$$

where:
a = no. moles oxygen in water sample
b = no. moles oxygen in CO_2
i = initial state
e = equilibrium state

The above expression may be rearranged to solve for $\delta^{18}O\text{-}H_2O_{(i)}$;

$$\delta^{18}O\text{-}H_2O_{(i)} = b/a \,(\, \delta^{18}O\text{-}CO_{2(e)} - \delta^{18}O\text{-}CO_{2(i)} \,) + \delta^{18}O\text{-}H_2O_{(e)} \quad \text{.....(Equation 2)}$$

$\delta^{18}O\text{-}H_2O_{(e)}$ may be expressed in terms of the CO_2 - H_2O equilibrium fractionation factor;

$$\alpha = \frac{1000 + \delta^{18}O\text{-}CO_{2(e)}}{1000 + \delta^{18}O\text{-}H_2O_{(e)}} \quad \text{..... (Equation 3)}$$

Equation 3 may then be rearranged in terms of $\delta^{18}O\text{-}H_2O_{(e)}$ and substituted into Equation 2 ;

$$\delta^{18}O\text{-}H_2O_{(i)} = b/a\ (\delta^{18}O\text{-}CO_{2(e)} - \delta^{18}O\text{-}CO_{2(i)}) + \frac{(1000 + \delta^{18}O\text{-}CO_{2(e)})}{\alpha} - 1000 \quad \text{..... (Equation 4)}$$

Both $\delta^{18}O\text{-}CO_{2(e)}$ and $\delta^{18}O\text{-}CO_{2(i)}$ are measured directly on the mass spectrometer. At 25°C the CO_2 - H_2O equilibrium fractionation factor α is 1.0412 (Friedman and O'Neil, 1977). a, the number of moles of oxygen in the water sample is determined by division of the sample volume by the molar volume of water ($18cm^3$) and b, the number of moles of CO_2, is determined using the gas law multiplied by 2 to account for the two oxygen atoms in CO_2 per atom of oxygen in H_2O.

i.e. $b = (PV /RT) * 2$ where R is the gas constant in $J\ K^{-1}\ mol^{-1}$.

P, the pressure of CO_2 in the reaction vessel in Pa, is measured manometrically during sample preparation. V, the volume of gas in M^3 is determined by subtracting the sample volume from the reaction vessel volume (the latter is determined by subtracting the weight of the reaction vessel when filled with water from the weight of the empty reaction vessel.) T is the absolute temperature at which the equilibration is carried out (298.15°K, 25°C) .

Each of the variables P,V,T, $\delta^{18}O\text{-}CO_{2(e)}$, $\delta^{18}O\text{-}CO_{2(i)}$ has an associated error. P. Dennis (unpublished data) has shown that the overall precision associated with the determination of $\delta^{18}O\text{-}H_2O_{(i)}$ by the standard equilibration method is of the order of $^{+}/-$ 0.386 °/oo. This constitutes a high level of analytical error (equivalent to $^{+}/-$ 1.7°C) . The major source of this error is associated with changes in temperature during sample clean-up in the laboratory after equilibration in the shaking water bath. The methodology implicitly assumes that isotopic equilibrium is established *at 25°C* and therefore the fractionation factor at this temperature (1.0412) is applicable. During sample clean-up deviations in the temperature of the closed system at equilibrium away from 25°C may occur if the laboratory temperature is not itself at 25°C.

This drift in temperature, which will be dependent upon the ambient laboratory temperature, contributes error i) in the determination of b and ii) in the determination of $\delta^{18}O\text{-}H_2O_{(e)}$ due to erroneous use of the fractionation factor for 25°C.

In the present study the method presented by Frew *et al.* (1995) was adopted in which precision in the determination of $\delta^{18}O\text{-}H_2O$ was shown to be greatly improved. Batches of five water samples were run at the same time. Within each batch of five, three were samples, one was a standard of known isotopic composition, and the remaining one was a second standard of known isotopic composition which was run to check the accuracy of the run. All five dry reaction vessels within the batch were charged with 2.5cm^3 of sample or standard using an Eppendorf pipette. After the water samples were frozen within the vessels on the line using liquid nitrogen, non-condensible gases were pumped from the reaction vessels and the vessels closed off and allowed to thaw. Scrubbed CO_2 was backfilled into the line on to which the reaction vessels were attached and after a period of equilibration in the line, admitted into the reaction vessels, which therefore had identical pCO_2 and were closed off and placed in the shaking water bath for 48hrs. The batch of five reaction vessels was cleaned up simultaneously and therefore each member of the batch experienced the same temperature history. $\delta^{18}O\text{-}H_2O_{(i)}$ values for each sample or standard were determined using equation 4 and substituting $\alpha = 1.0412$. This accounts for the small volume correction term (b) necessary to correct for differences in reaction vessel volume. Each sample $\delta^{18}O\text{-}H_2O_{(i)}$ and that of the second standard was then normalised to that of the first standard of known isotopic composition. Since the temperature history of all members of the batch was identical temperature effects on α were removed. Indeed it is not important that the equilibration takes place at 25°C ; nor is it necessary to know $\delta^{18}O\text{-}CO_{2(i)}$, since this is constant for both standard and samples. P.Dennis (unpublished data) has shown that the above normalisation procedure improves the overall methodological precision to $^{+}/-$ 0.017°/oo.

All $\delta^{18}O\text{-}H_2O$ values were normalised to SMOW (standard mean ocean water, taken as 0 °/oo on the SMOW scale). SMOW is supplied by N.I.S.T. and I.A.E.A. (Vienna) as VSMOW in limited quantities of 30cm^3 every 3 years and therefore an internal standard is used for normalisation.

A sample of North Sea Water (NSW) was supplied by P.Dennis at the University of East Anglia (U.E.A.), Norwich. NSW has a value quoted as +0.197°/oo. A sample of Norwich Tap Water (NTW) was also supplied by P.Dennis as a secondary standard with a value of -6.836°/oo.

Both standards were calibrated prior to use in the laboratory directly against VSMOW supplied by N.I.S.T. NSW was determined as having a value of +0.175 °/oo and NTW a value of -6.863 °/oo on the VSMOW scale. These values were in agreement with the values quoted for these standards by U.E.A. A further three sea water samples were sent by P.Dennis for inter laboratory comparison. Appendix 1 shows the values quoted for the samples by U.E.A.and the values determined in our laboratory, for which there was good interlaboratory agreement. Precisions of $1\sigma = 0.02$°/oo and 0.05°/oo were obtained for standards run in two batches of five samples (i.e. using the ten reaction vessels available) which is equivalent to temperature errors of 0.09°C and 0.22°C). However a more realistic assessment of methodological error is obtained by considering the error associated with long-term determination of NTW by normalisation on NSW from numerous sample runs. This was calculated as being $1\sigma =$ 0.04 °/oo (n=21) i.e. equivalent to a temperature error of 0.18°C .

2.6. Determination of the carbon isotopic composition and concentration of dissolved inorganic carbon in seawater ($\delta^{13}C$- ΣCO_2 , $[\Sigma CO_2]$).

a) water sampling and storage

Water was siphoned into a glass - stoppered bottle, poisoned with saturated $HgCl_2$ at 1µl cm^{-3} to halt biological activity and cold - stored in the dark (Kroopnick, 1980). Within 2 hrs a 10cm^3 sub-sample was filtered from this bottle through a 0.4µm Nucleopore filter (to remove any mineral carbonate) into a numbered, pre-weighed, nitrogen - flushed glass ampoule (Adelphi Tubes, U.K.) and flame - sealed for extended storage after re-weighing.

b) extraction of CO_2 from the sub-sample in the ampoule for determination of $\delta^{13}C$- ΣCO_2 and $[\Sigma CO_2]$

CO_2 extraction was performed employing an adaptation of the procedures outlined in Kroopnick (1974), McCorkle (1987) and Middleton (1997).

The glass ampoule containing the sea water sample was cracked under vacuum within a glass stripper containing 1 cm^3 H_3PO_4. The evolved CO_2 was subsequently flushed using CO_2- free nitrogen as a carrier gas through first a condenser and then a liquid nitrogen / methanol trap at -100°C (i.e. a water trap) to scrub water and then through two liquid nitrogen spiral traps at -180°C to trap the CO_2. The carrier gas and any other remaining non-condensible gases were slowly pumped from the spiral traps which were then isolated from the water trap. Subsequently the CO_2 was warmed to room temperature within the isolated spiral traps to release any traces of crystal-bound water before being scrubbed for a second period to remove any such water traces by placing the dewar containing the liquid nitrogen / methanol slush at -100°C around one of the spiral traps. The CO_2 was then frozen into an on-line manometer of known volume for pCO_2 measurement (and thereby determination of the number of moles of CO_2) before being frozen into a collection vessel for mass spectrometric measurement in the dual inlet mass spectrometer. [ΣCO_2] was determined knowing the weight of sample within the ampoule (see a) above).

The precision associated with the method, determined from replicate ampoules of an internal standard run with every 5-6 samples, was 1 σ = 0.03 °/oo for $\delta^{13}C$- ΣCO_2 and 1 σ = 17.5 μmol kg^{-1} for [ΣCO_2]. Determination of the accuracy associated with $\delta^{13}C$- ΣCO_2 and [ΣCO_2] analysis is hindered by the lack of an accredited standard (i.e. one that is equivalent to NBS-19 and VSMOW). The method therefore implicitly assumes that recovery yields of extracted CO_2 from the sea water sample are quantitative. Comparison of [ΣCO_2] data determined manometrically during the extraction procedure with data for the same samples determined independently by coulometer have previously shown recovery yields to be of the order of 99.5% (Middleton, 1997).

2.7. Biogeochemical parameters measured within the Field Study.

2.7.1. Chlorophyll and Phaeopigment concentration.

Water was filtered, using a filter rig attached to a diaphragm pump, onto a 47mm GFC filter which was placed onto a petri slide and covered before being frozen for extended storage.

A policy of filtering to set colour was employed. Analysis was according to the procedures outlined in Parsons *et al.* (1984). Each filter was defrosted and pigments extracted overnight in a sealed plastic centrifuge tube to which had been dispensed 10cm^3 of 90% acetone (i.e. 1 part distilled deionised water and 9 parts Analar grade acetone neutralised with sodium bicarbonate.) Extraction was done in a refrigerator in darkness to avoid pigment breakdown.Each centifuge tube was shaken for 5 minutes after extraction, centrifuged at 3500 r.p.m., re-shaken and centrifuged again to ensure that all pigments were brought into solution. A calibrated Turner Design Model 10 Fluorimeter was used to measure the fluorescence of the sample before and after addition of 2 drops of approximately 8% concentrated HCl by volume. The Fluorimeter cuvette was washed twice with 90% acetone between each sample to avoid cross contamination. Acetone blank readings were made before and after acidification at each sensitivity setting on the Turner Fluorimeter.

Pigment concentrations were calculated according to the following equations;

$[Chl] = K_f (f_o - f_a) * E / V$ ($\mu g\ dm^{-3}$) $\qquad$ $[Phaeo] = K_f (H_f * f_a - f_o) * E / V$ ($\mu g\ dm^{-3}$)

where f_o and f_a are the blank-corrected sample Fluorimeter readings before and after acidification, E and V are the extracted and sample volumes, and K_f and H_f are constants for the Fluorimeter calculated using a spectrophotometric method. Analysis of replicate seawater samples gave standard deviation at $1\sigma =$ 0.17 $\mu g\ dm^{-3}$ for chlorophyll concentration and $1\sigma =$ 0.06 $\mu g\ dm^{-3}$ for phaeopigment concentration.

2.7.2. a) Dissolved Nitrite and Nitrate concentrations.

The aspirator filtrate (i.e. filtered through GFC / GFF filter) was used to fill two 120 cm^3 polyethylene bottles for each of the above parameters, which were frozen for subsequent analysis. Determination of dissolved nitrite in sea water was according to the colorimetric procedure outlined in Parsons *et al.* (1984). In this procedure nitrite is reacted with an aromatic amine (sulphanilamide hydrochloride) to form a diazonium compound which couples with a second aromatic amine (n-(1-naphthyl) - ethylenediamine dihydrochloride) to form an azo dye.

The extinction of the azo dye at 543nm is measured and is proportional to the nitrite concentration over the range 0 -10μM. A calibration curve was established over the range 0.1 to 1.0μM (the expected environmental range). Standard nitrite solutions were made up in distilled deionised water as there are no sea water matrix effects. Analysis of replicate filtered seawater samples gave standard deviation at $1\sigma = 0.006$ μM.

Nitrate determination was according to the colorimetric procedure outlined in Parsons *et al.* (1984). The procedure involves the quantitative reduction (97-99% efficiency) of nitrate to nitrite by running the sample through a column containing copper - coated cadmium which has been activated with a high nitrate concentration spike. The quantity of nitrite is determined as above. Nitrate concentrations are then corrected for initial nitrite present in the sample by subtraction. A calibration curve was established over the range 1 to 15μM (the expected environmental range of nitrate concentration for the Menai Strait (Ewins and Spencer, 1967)). Standard nitrate solutions were made up in synthetic sea water due to known sea water matrix effects. Analysis of replicate filtered sea water samples gave standard deviation at $1\sigma = 0.18$ μM.

b) Dissolved Silicate Concentration

The aspirator filtrate (i.e. filtered through GFC / GFF filter) was used to fill a 120 cm^3 polyethylene bottle which was frozen for storage. Silicate determination was according to the colorimetric procedure outlined in Parsons *et al.* (1984).The samples were allowed to thaw prior to analysis, following the thawing times outlined in Macdonald *et al.* (1986). The samples were reacted with molybdate in acidic solution to form molybdosilicic acids. A reducing solution (containing metol and oxalic acid) reduced the silicomolybdate complexes to form a blue colour, the extinction of which was measured at 810nm. A calibration curve was established over the range 1 to 15μM (the expected environmental range of silicate concentration for the Menai Strait (Ewins and Spencer, 1967)). Standard silicate solutions were made up in synthetic sea water due to known sea water matrix effects (Parsons *et al.* 1984). Analysis of replicate filtered seawater samples gave standard deviation at $1\sigma = 0.25$μM.

c) Dissolved Phosphate Concentration

The aspirator filtrate (i.e. filtered through GFC / GFF filter) was used to fill a 120 cm^3 polyethylene bottle which was frozen for storage. Phosphate determination was according to the colorimetric procedure outlined in Parsons *et al.* (1984). In this procedure the sample reacts with a mixed reagent (containing molybdic acid, ascorbic acid and trivalent antimony) to form a complex which is reduced to form a blue solution. The extinction of this solution is measured at 885nm. A calibration curve was established over the range 0 to1.5μM (the expected environmental range of phosphate concentration for the Menai Strait (Ewins and Spencer, 1967)). Standard phosphate solutions were made up in distilled deionised water as there are no sea water matrix effects, (Parsons *et al.* 1984). Analysis of replicate filtered sea water samples gave standard deviation at $1\sigma = 0.02$ μM.

2.7.3. Particulate Organic Carbon and Nitrogen Concentrations.

Water was filtered onto a 25mm GFF filter which had been precombusted for 3 hours at 500°C. A policy of filtering to set colour was employed. The filter was placed onto a petri slide and covered before being frozen for extended storage. P.O.C. / P.O.N. determination involved the use of a Roboprep C/N Elemental Analyser. Scrunched aluminium balls containing the filters are combusted at 1020°C to form CO_2 and N oxides. A stream of helium sweeps the gases through a reduction furnace at 600°C where N oxides are reduced to dinitrogen gas.The gases are further swept through a water trap and a packed column G.C. at 105°C where gas separation occurs and finally on to a T.C.D. detector. Peak areas associated with the resolved CO_2 and N_2 peaks are integrated and output to a computer. The elemental analyser is calibrated with acetanilide of known weight (and therefore known values of μg C and μg N) with calibration curves established on each day of use before and after sample analysis.

Analysis of replicate sea water samples gave standard deviations at $1\sigma_{(POC)} = 79.75\mu gC\ dm^{-3}$ and $1\sigma_{(PON)} = 13.08\mu gN\ dm^{-3}$.

Chapter 3. Experimental investigation into the partitioning of stable oxygen and carbon isotopes between *Pecten maximus* calcite and sea water

3.1. Background and experimental aims

The determination of historical records of water temperature / $\delta^{18}O$ - H_2O and $\delta^{13}C$ - ΣCO_2 from oxygen and carbon stable isotopic ratios in biogenic carbonates implicitly assumes that isotopic equilibrium was established at the time of precipitation of the carbonate.A large number of studies have made inferences from stable isotopic ratios in contemporary and fossil biogenic carbonates (Tourtelot and Rye, 1969, Popp *et al.* 1986) and bivalves in particular (Killingley and Berger, 1979, Donner and Nord, 1986, Krantz *et al.* 1987, Muhs and Kyser, 1987, Krantz, 1990, Bice *et al.* 1996). Despite this few have tested the assumption that oxygen and carbon isotopes are precipitated in isotopic equilibrium with sea water for the species in question. This question is of particular importance given the potential firstly for incomplete isotopic partitioning (a kinetic effect), yielding depleted oxygen and carbon ratios, and secondly the introduction of isotopically - depleted respiratory CO_2 into the extrapallial fluid (E.P.F.) from which the calcite precipitates i.e. a metabolic effect (McConnaughey, 1989 b, McConnaughey *et al.* 1997).

Laboratory studies examining partitioning of oxygen isotopes between biogenic carbonates and water have been restricted to the early studies of Epstein *et al.* (1953), Horibe and Oba (1972) and Erez and Luz (1983) , who studied molluscs, pelecypods and foraminifera respectively. To date laboratory studies which have examined partitioning of carbon isotopes between biogenic carbonates and dissolved inorganic carbon have been restricted to the one study of Fritz and Poplawski (1974), involving fresh water molluscs. This chapter presents data from a laboratory study testing the assumption that oxygen and carbon isotopes in *Pecten maximus* calcite are precipitated in isotopic equilibrium with sea water.

3.2. Experimental apparatus and methods

An experimental recirculating tank system was constructed allowing animals to be grown simultaneously at 4 different, constantly - maintained temperatures (see Plates 3.1a and 3.1b). The system consisted of 4 individual units, one for each set temperature, each unit being continuously and slowly replenished with sea water. An individual unit is shown diagrammatically in Appendix 2. Within each unit, animals were held in 2 upper experimental tanks, each one receiving water through pipes from a reservoir tank positioned directly below, via a submersible pump seated within the reservoir tank. All tanks and pipes were insulated, with lids over the tanks to provide additional insulation. Water returned from each experimental tank via a return pipe to the reservoir tank. Within the reservoir tank a constant water temperature was maintained by a thermostatically - controlled, 1KW side-mounted submersible heater fighting a cooling system. The latter consisted of mains-supplied refrigerated glycol circulated through a submersed stainless steel coil mounted above the heater within the reservoir tank. A small flux of mains seawater was maintained in and out of the reservoir tank to replenish the recirculating system. Juvenile *Pecten maximus* individuals (15-20mm) were supplied by C.E.F.A.S., Conwy from spat collected by the Sea Fisheries Authority, Ardtoe, Scotland during 1993. All animals were individuals of one cohort and were approximately 8 months old. Juvenile animals were specifically chosen since it is the initial rapid shell growth that is analysed from animals taken in the field, as discussed in Chapter 1. Animals were acclimated from the ambient water temperature to the set experimental temperature by raising or lowering the temperature at a rate of 1°C every 2 days. Tank temperatures were maintained at 9.9°C, 12.8°C, 14.8°C and 16.9°C i.e. spanning the range 9.9 -16.9°C. This temperature range was chosen since it represents the natural seasonal range experienced by this species in U.K. waters and it has been suggested that *Pecten maximus* ceases shell growth below 9°C (Dare and Deith, 1991). Scallops were carefully marked along the shell valve margin using an indelible pen before being grown at the four temperatures. Each day scallops within each tank were fed 5dm^3 of mixed algal culture, predominately *Pavlova lutherii* and *Skeletonema costatum*. The water within each experimental tank was sampled periodically (every 3-4 days) during the experimental period for the following parameters:

Plate 3.1a Plan view of one of the experimental tanks holding juvenile *Pecten maximus*

Plate 3.1b The four units of the experimental tank system

a) Water temperature

Water temperature within the experimental tanks was measured at each sampling point by a hand held digital thermometer. Additionally, a tank - mounted data logger (Tiny Talk Temperature Logger, Orion Components, Chichester) was rotated every 7 days between the tanks to assess temperature stability and the thermistor probe attached to a Rostrak Chart recorder mounted in one tank for the duration of the experiment to assess the long term stability of tank water temperature.

b) Isotopic composition of seawater relative to VSMOW ($\delta^{18}O\text{-}H_2O$)

At each sampling point water samples were siphoned via Nalgene tubing from an experimental tank at each temperature into 150cm^3 glass Winchester bottles with screw - top lids containing rubber inserts to prevent evaporation / condensation. These were cold - stored in the dark. The standard equilibration method developed by Epstein and Mayeda (1953) as adapted by Frew *et al.* (1995) was employed. A summary of the theory underlying the methodology, and the methodological details are given in Chapter 2.

c) Isotopic composition and concentration of dissolved inorganic carbon
($\delta^{13}C\text{-}\Sigma CO_2$,[$\Sigma CO_2$])

At each sampling point water was siphoned from an experimental tank at each temperature via Nalgene tubing into a glass - stoppered bottle. This was poisoned with saturated $HgCl_2$ at 1µl cm^{-3} to halt biological activity and cold - stored in the dark (Kroopnick, 1980). Within 2 hrs a 10cm^3 sub-sample was filtered from each bottle through a 0.4µm Nucleopore filter into a numbered, pre-weighed, nitrogen - flushed glass ampoule (Adelphi Tubes, U.K.) and flame - sealed for extended storage after re-weighing. Extraction of CO_2 from the sub-sample in the ampoule for determination of $\delta^{13}C\text{-}\Sigma CO_2$ and [ΣCO_2] was performed by an adaptation of the procedures outlined in Kroopnick (1974), McCorkle (1987) and Middleton (1997).

d) Salinity

At each sampling point water samples were siphoned from an experimental tank at each temperature into standard salinity bottles and analysed on an AutoSal 8400A Autosalinometer calibrated with I.A.P.S.O. standard sea water.

e) Concentration of aqueous carbon species in sea water [$CO_{2\,(aq)}$], [HCO_3^-], [$CO_3^{2-}{}_{(aq)}$]

At each sampling point a 10cm spectrophotometer cell was flushed through with water siphoned from an experimental tank at each temperature, then filled and stoppered, excluding air bubbles. 150µl of creatine phosphate dye were injected into the cell and the extinction at 436 nm, 578 nm and 730nm simultaneously measured in a Hewlett Packard diode array spectrophotometer. Temperature was measured immediately before extinction measurements. This allowed determination of pH in the cell at the time of measurement (Middleton, 1997). Following the protocol employed by Middleton (1997), [ΣCO_2] measured in c) above , pH, salinity and temperature data were used to determine total alkalinity in the cell. Unlike pH, total alkalinity is temperature independent. Total alkalinity , salinity , [ΣCO_2] and tank water temperature data were then used to determine the concentration of the various carbon species in the sea water within each tank.

Pecten shell $\delta^{18}O$ and $\delta^{13}C$

After one month the experimental *Pecten* individuals were taken from the experimental tanks, the soft tissues removed and the upper shell valves removed, cleaned and dried. Each upper valve was examined under a binocular microscope and the increment of shell precipitated by each individual (between the valve margin and the indelible mark associated with the beginning of the experiment) removed by use of a dentist drill. In all cases a clear disturbance mark was visible in the shell associated with the beginning of the experiment. Shell material from each individual was collected into a glass Durham tube and pretreated to remove organic material by oxidation in a low temperature oxygen plasma for 4.5 hours.

A full discussion, with associated experiments, concerning the removal of organic material from biogenic carbonates and its effects upon carbonate isotopic ratios is presented in Chapter 2. Shell calcite samples were analysed according to standard methods (McCrea, 1950), as outlined in Chapter 2.

3.3. Results

3.3.1. Partitioning of oxygen isotopes between *Pecten* shell calcite and sea water

a) Predicted ^{18}O data for calcite precipitated in isotopic equilibrium with sea water during the experiment ($\delta_{c\text{-equilib}}$)

The O'Neil *et al.* (1969) palaeotemperature equation for calcite precipitated in isotopic equilibrium with sea water may be rearranged as :

$$\delta_{c\text{ - equilib}} = \delta_w + (21.90 - 3.162 (31.06 + t^{\circ}C)^{0.5})$$

where;
δ_c is the Craig - corrected $^{18}O/^{16}O$ ratio of calcite CO_2 relative to that of CO_2 from PDB.
δ_w is the $^{18}O/^{16}O$ ratio of CO_2 equilibrated with the water relative to that of CO_2 from PDB.

Predicted ^{18}O data for calcite precipitated in isotopic equilibrium with sea water ($\delta_{c\text{ - equilib}}$) were calculated for each tank as above using temperature and $\delta^{18}O\text{-}H_2O$ data collected from the four experimental tanks at sampling points over the experiment. Temperature and $\delta^{18}O\text{-}H_2O$ data were averaged for each tank. Temperatures were determined as 9.89°C ($1\sigma = 0.08$°C) , 12.88°C ($1\sigma = 0.08$), 14.74°C ($1\sigma = 0.09$°C) and 16.89°C ($1\sigma = 0.06$°C). Both the data recorded by the Rustrak temperature recorder and from the Tinytalk temperature Logger rotated around the four tanks during the experiment showed that the temperature within the tank system remained stable during the experiment (see Tinytalk output, Appendix 3).

$\delta^{18}O\text{-}H_2O$ data for the experiment are plotted in Figure 3.1 and tabulated in Appendix 4. The data show that $\delta^{18}O\text{-}H_2O$ remained stable within each experimental tank for the duration of the experiment; the variability in $\delta^{18}O\text{-}H_2O$ within each tank (1σ = 0.05 - 0.06 °/oo) was of the same order as that of the analytical error associated with determination of $\delta^{18}O\text{-}H_2O$ (1σ = 0.04 °/oo). Analysis of variance showed there was no significant difference in $\delta^{18}O\text{-}H_2O$ between the four tanks ($p = 0.391$, d.f. = 19, data normal and variance homogeneous.) Salinity data over the duration of the experiment period are tabulated in Appendix 4 and plotted in Figure 3.1. The variability in salinity over the experimental period within each tank (1σ = 0.07S) was considerably greater than the analytical error . The latter, determined by analysis of replicate bottles of sea water, gave precision of 1σ = 0.0004 S (n = 10.) This is a reflection of the very low instrument - associated error rather than reflecting large variability in salinity within each tank over the experiment. Analysis of variance showed there to be no significant differences in the mean salinity between tanks for the experimental period ($p = 0.621$. d.f. = 31, data normal and variance homogeneous). Whilst Figure 3.1 shows clear and synchronous changes in salinity in all four tanks over the duration of the experiment (associated with natural salinity fluctuations in the external mains sea water supply) the overall variability in salinity was low. Using a salinity - $\delta^{18}O\text{-}H_2O$ relationship established within this work for Menai Strait waters (see Chapter 4) where $\delta^{18}O\text{-}H_2O = -7.419 + 0.220S$ the expected variability in $\delta^{18}O\text{-}H_2O$ is of the order of $1\sigma = 0.016$°/oo. This variability is smaller than the analytical error associated with determination of $\delta^{18}O\text{-}H_2O$ ($1\sigma = 0.04$°/oo) and therefore small salinity -correlated changes in $\delta^{18}O\text{-}H_2O$ that might be expected to have occurred during the course of the experiment are masked by analytical error. The salinity data confirm that the variability in $\delta^{18}O\text{-}H_2O$ over the experiment was low and within the analytical error.

The O'Neil *et al.* (1969) relationship for calcite precipitated in isotopic equilibrium with sea water expresses the isotopic composition of sea water in terms of δ_w (the $^{18}O/^{16}O$ ratio of CO_2 equilibrated with the water relative to that of CO_2 from PDB). Therefore $\delta^{18}O\text{-}H_2O$ data (referenced to VSMOW) were converted to δ_w data using the relationship

$\delta_w = 0.99978\ \delta^{18}O\text{-}H_2O - 0.22$ (Friedman and O'Neil, 1977)

Figure 3.1. Salinity and $\delta^{18}O$-H_2O variation during the experiment.

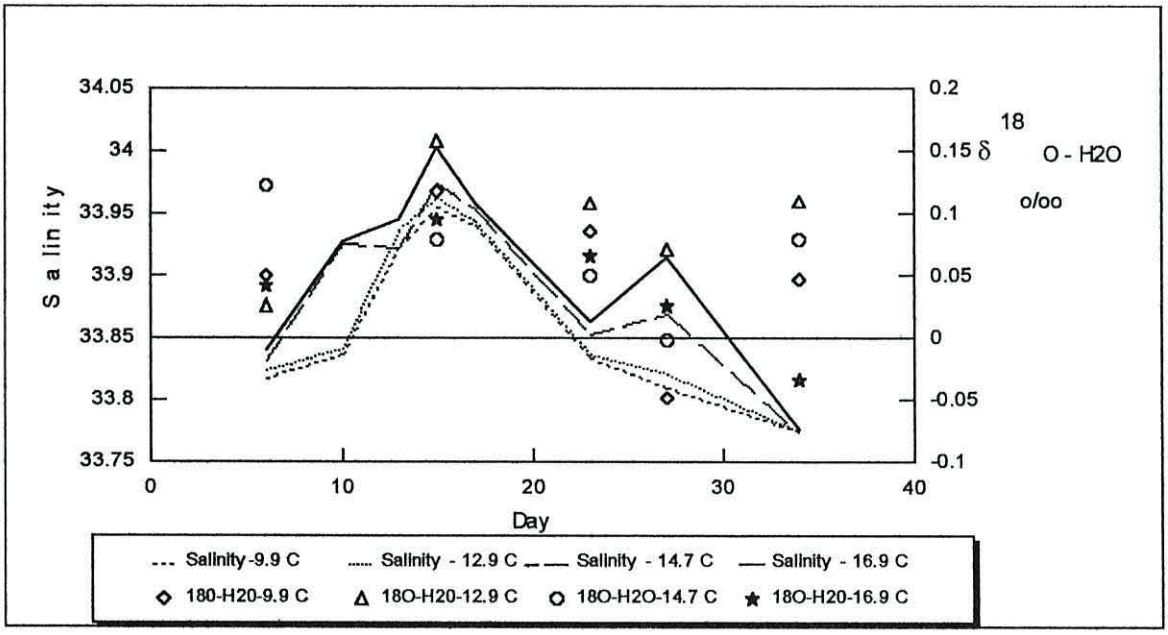

Predicted ($\delta_{c\text{ - equilib}}$) data for each tank were then calculated using temperature and δ_w data using the rearranged O'Neil *et al.* (1969) expression as above. These data are shown in Appendix 5 .

b) *Pecten* ^{18}O data ($\delta_{c\text{ - }Pecten}$)

$\delta_{c\text{ - }Pecten}$ data are tabulated in Appendix 5 along with predicted ($\delta_{c\text{ - equilib}}$) data. Each $\delta_{c\text{ - }Pecten}$ data point corresponds to the isotopic composition of the increment of shell secreted by an individual scallop during the course of the experiment. The O'Neil *et al.* (1969) relationship for calcite precipitated in isotopic equilibrium with sea water is expressed in terms of δ_c (the Craig - corrected $^{18}O/^{16}O$ ratio of calcite CO_2 relative to that of CO_2 from PDB).This is numerically the same as the $^{18}O/^{16}O$ ratio of calcite relative to PDB carbonate (i.e. calcite $\delta^{18}O = \delta_c$) and *Pecten* $\delta^{18}O$ data therefore require no modification.

Figure 3.2 shows a plot of $\delta_{c\text{ - }Pecten}$ and predicted ($\delta_{c\text{ - equilib}}$) data against temperature. A conventional plot of a regression of $\delta_{c\text{ -}Pecten} - \delta_w$ against temperature is plotted in Figure 3.3. This generalised form of the relationship allows for the necessary δ_w correction term. Included in Figure 3.3. are $\delta_c - \delta_w$ plots for the O'Neil *et al.* (1969) expression for calcite precipitated in isotopic equilibrium with sea water{$\delta_c - \delta_w = 21.90 - 3.162 (31.06 + t^oC)^{0.5}$} and the Epstein *et al.* (1953) expression derived from a number of molluscs of largely calcitic mineralogy {$\delta_c - \delta_w = 15.36 - 2.673 (16.52 + t^oC)^{0.5}$ }.

A linear model describes well the relationship between $\delta_{c\text{ - }Pecten}$ and temperature with slope of -0.227 °/oo per °C ($R^2 = 0.90$, $F = 258.98$ $p = <0.01$, $n = 31$, data normal and variance homogeneous). This compares well with the predicted slope of -0.239 °/oo per °C (O'Neil *et al.* 1969). To compare $\delta_{c\text{ - equilib}}$ and $\delta_{c\text{ - }Pecten}$ data using analysis of covariance requires both data sets. The experimental (raw) isotopic data are not included in the O'Neil *et al.* (1969) paper. It is therefore not possible to compare predicted data (i.e. data calculated from the rearranged O'Neil *et al.* equation) and $\delta_{c\text{ - }Pecten}$ data using analysis of covariance since only one actual data set is available.Therefore a significance test (one sample t test) of the regression coefficient for the $\delta_{c\text{ - }Pecten}$ data against the regression coefficient of the O'Neil *et al.* (1969) expression was performed and found to be not significant ($p = 0.147$, d.f. = 28).

Figure 3.2. The relationship between $\delta_{c\text{-}Pecten}$ and predicted ($\delta_{c\text{-}equilib}$) with temperature.

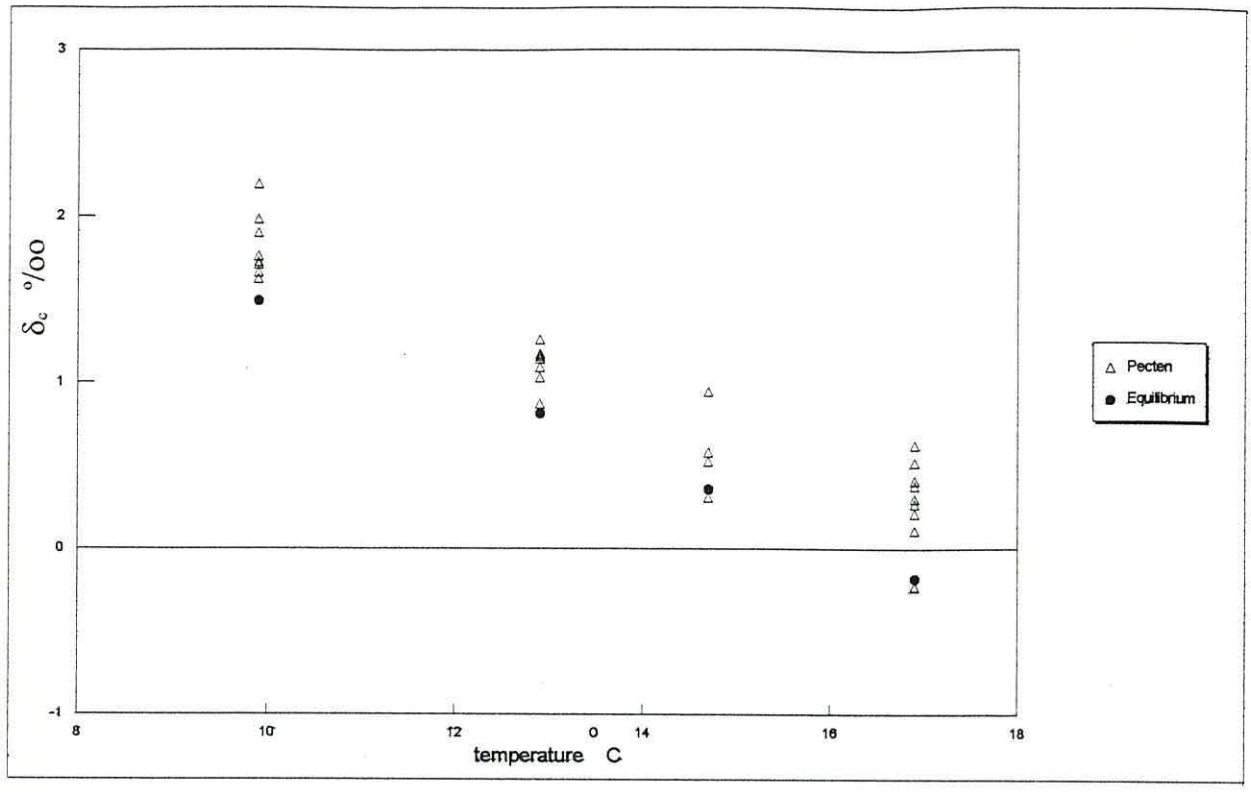

Figure 3.3. Plots of $\delta_c - \delta_w$ against temperature.

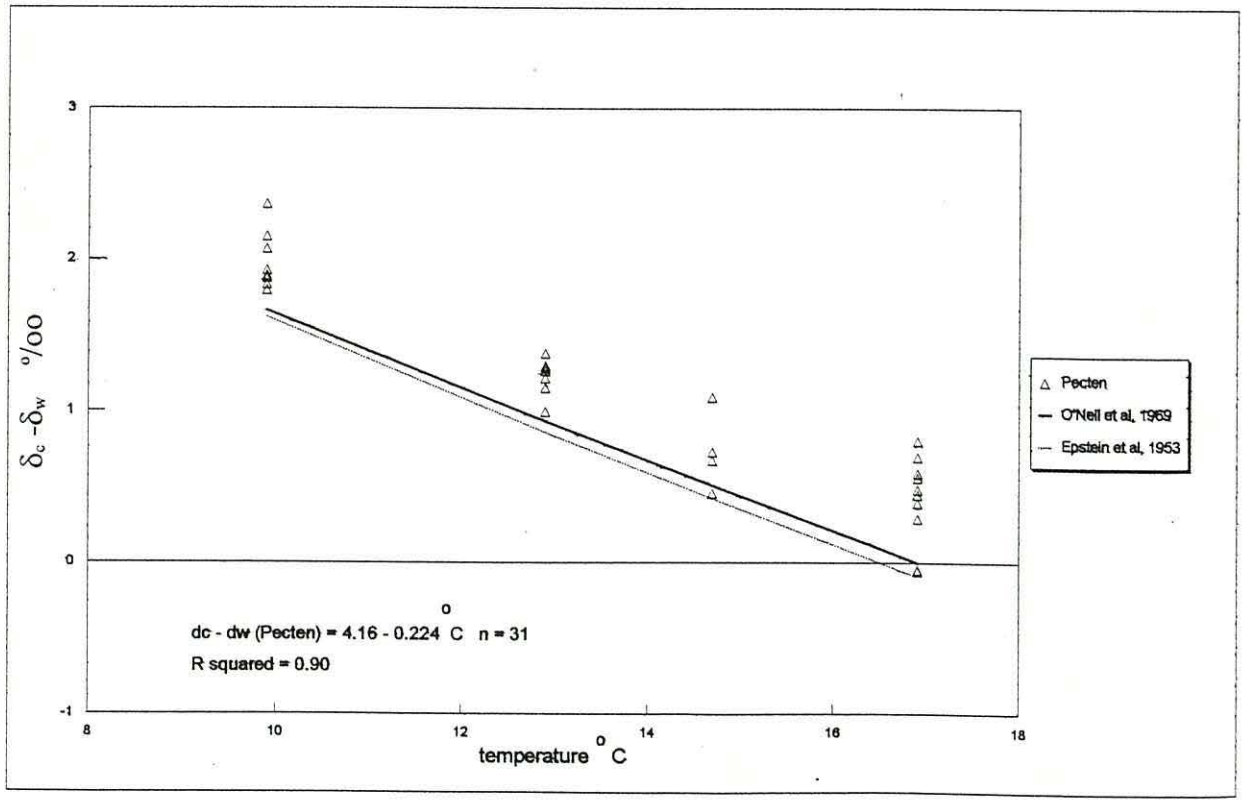

Similarly, a significance test (one sample t test) of the intercept of the $\delta_{c\text{ - }Pecten}$ data against the intercept of the O'Neil *et al.* (1969) expression was not significant ($p = 0.357$, d.f. = 28). The $\delta_{c\text{ - }Pecten}$ data are not significantly different from the predicted ($\delta_{c\text{ - equilib}}$) data, implying that, during the experiment, oxygen isotopes in *Pecten* calcite were precipitated in isotopic equilibrium with sea water. The generalised expression for the partitioning of oxygen isotopes between *Pecten* calcite and sea water shown in Figure 3.3. is well described by the linear relationship;

$$\delta_{c\ Pecten} - \delta_w = 4.16 - 0.224°C \quad (R^2 = 0.90, F = 244.55, p = <0.01, n = 31.)$$

Due to the slow growth exhibited by some individual scallops during the experiment, some of the calcite samples obtained during drilling were less than 1mg in weight. The methodological development work undertaken in Chapter 2 had shown that both accuracy and precision of oxygen isotopic data become significantly compromised below a threshold weight of between 0.5mg and 1mg. Removing experimental $\delta_{c\ Pecten} - \delta_w$ data below 1mg gave the following relationship;

$$\delta_{c\ Pecten} - \delta_w = 4.20 - 0.228°C \quad (R^2 = 0.91, F = 146.6, p = <0.01, n = 17.)$$

This is in agreement with the relationship based on the full data set above.

Accounting for the effects of sample size, the variability associated with $\delta_{c\ Pecten}$ data at any one temperature is of the order $1\ \sigma = 0.11 - 0.22$ °/oo i.e. an average of 0.17°/oo.This is equivalent to a temperature error of 0.76°C. Propagating errors for each tank associated with δ_c determination by the sealed vessel method (calcite weight >1mg ($1\ \sigma = 0.08$°/oo), variability in experimental $\delta^{18}O - H_2O$ ($1\ \sigma = 0.05$°/oo) and temperature ($1\ \sigma = 0.1$°C or 0.02°/oo)), expected variability associated with $\delta_{c\ Pecten}$ data is of the order $1\ \sigma = 0.10$ °/oo. This implies that variability associated with $\delta_{c\ Pecten}$ data at any one temperature is only marginally larger than the expected variability.

Since the experimental $\delta^{18}O$ - H_2O variability was smaller than that associated with $\delta^{18}O$ - H_2O determination itself, the majority component of expected variability at any one temperature is of a methodological nature i.e. analytical. This implies that the majority component of $\delta_{c\ Pecten}$ data variability is also of an analytical nature.

3.3.2. Partitioning of carbon isotopes between *Pecten* shell calcite and sea water

a) Predicted $\delta^{13}C$ data ($\delta^{13}C_{equilib}$) for calcite precipitated in isotopic equilibrium with dissolved inorganic carbon.

The distribution of carbon isotopes between dissolved inorganic carbon species in the ΣCO_2 pool ($CO_{2\,(aq)}$, HCO_3^-, $CO_3^{2-}{}_{(aq)}$) may be described by the following mass balance equation;

$$\delta_\Sigma = (\delta_a * f_a) + (\delta_b * f_b) + (\delta_c * f_c) \quad \text{..... equation 1.}$$

where δ_Σ = the carbon isotopic composition of ΣCO_2.

δ_a = the carbon isotopic composition of $CO_{2\,(aq)}$

δ_b = the carbon isotopic composition of HCO_3^-

δ_c = the carbon isotopic composition of $CO_3^{2-}{}_{(aq)}$

f_a = the fraction $CO_{2\,(aq)}$ constitutes of the ΣCO_2 pool

f_b = the fraction HCO_3^- constitutes of the ΣCO_2 pool

f_c = the fraction $CO_3^{2-}{}_{(aq)}$ constitutes of the ΣCO_2 pool

δ_b and δ_c may be described in terms of the enrichment factors between HCO_3^- / $CO_3^{2-}{}_{(aq)}$ and $CO_{2\,(aq)}$ (i.e. $\varepsilon_b a$ / $\varepsilon_c a$).

$$\delta_b = \delta_a - (\delta_a - \delta_b) = \delta_a - \varepsilon_b a \quad \text{..... equation 2.}$$

and

$$\delta_c = \delta_a - (\delta_a - \delta_c) = \delta_a - \varepsilon_c a \quad \text{..... equation 3.}$$

where $\varepsilon_b a = \delta_a - \delta_b$ = the enrichment factor between HCO_3^- and $CO_{2\,(aq)}$.

$\varepsilon_c a = \delta_a - \delta_c$ = the enrichment factor between $CO_3^{2-}{}_{(aq)}$ and $CO_{2\,(aq)}$.

and equation 1. becomes;

$$\delta_\Sigma = (\delta_a * f_a) + (\{\delta_a - \varepsilon_b a\} * f_b) + (\{\delta_a - \varepsilon_c a\} * f_c)$$

or, expanding bracketed terms;

$$\delta_\Sigma = (\delta_a * f_a) + (\delta_a * f_b - \varepsilon_b a * f_b) + (\delta_a * f_c - \varepsilon_c a * f_c) \quad \text{..... equation 4.}$$

Equation 4. may be rearranged to solve for δ_a;

$$\delta_\Sigma + (\varepsilon_b a * f_b) + (\varepsilon_c a * f_c) = \delta_a * (f_a + f_b + f_c)$$

And since $(f_a + f_b + f_c) = 1$

$$\delta_a = \delta_\Sigma + (\varepsilon_b a * f_b) + (\varepsilon_c a * f_c) \quad \text{..... equation 5.}$$

If enrichment factors are now defined between between $CO_3^{2-}{}_{(aq)}$ / HCO_3^- and atmospheric CO_2, $CO_{2\,(g)}$ (i.e. $\varepsilon_c g$, $\varepsilon_b g$) and between $CO_{2\,(g)}$ and $CO_{2\,(aq)}$ (i.e. $\varepsilon_g a$) as:

$\varepsilon_c g = \delta_g - \delta_c$ .....(i)

$\varepsilon_b g = \delta_g - \delta_b$ .....(ii)

$\varepsilon_g a = \delta_a - \delta_g$ .....(iii)

Then the terms $\varepsilon_b a$ and $\varepsilon_c a$ in equation 5 may be described in terms of the above enrichment factors (i), (ii) and (iii).

$\varepsilon_b a = (\delta_a - \delta_b) = (iii) + (ii) = (\varepsilon_g a + \varepsilon_b g)$ ..... equation 6.

$\varepsilon_c a = (\delta_a - \delta_c) = (iii) + (i) = (\varepsilon_g a + \varepsilon_c g)$ ..... equation 7.

Therefore substituting equations 6. and 7. into equation 5. gives the solution for δ_a ;

$$\delta_a = \delta_\Sigma + (\{\varepsilon_g a + \varepsilon_b g\} * f_b) + (\{\varepsilon_g a + \varepsilon_c g\} * f_c) \quad \text{..... equation 8.}$$

Substituting equations 6. and 7. into equations 2. and 3. gives solutions for δ_b and δ_c ;

$$\delta_b = \delta_a - (\varepsilon_b g + \varepsilon_g a) \quad \text{..... equation 9.}$$

$$\delta_c = \delta_a - (\varepsilon_g a + \varepsilon_c g) \quad \text{..... equation 10.}$$

The isotopic compositions of the dissolved inorganic carbon species $CO_{2\,(aq)}$, HCO_3^-, $CO_3^{2-}{}_{(aq)}$ i.e. δ_a, δ_b and δ_c are calculated according to the solutions in equations 8 -10. The terms f_a , f_b and f_c were determined as in 3.2 (e), above.

Values for the enrichment factors $\varepsilon_g a$ and $\varepsilon_b g$ used in the above determinations are as reported by Zhang *et al.* (1995) (data in agreement with earlier studies, see Chapter 1) There is however disagreement between authors on the enrichment factor $\varepsilon_c g$, as well as questions of the appropriateness of using $\varepsilon_c g$ as determined in a demineralised water matrix within sea water (see Chapter 1) Due to this, three separate determinations were employed to calculate $\delta^{13}C_{equilib}$.

1. Using values for $\varepsilon_g a$, $\varepsilon_b g$ and $\varepsilon_c g$ as reported in Zhang *et al.* (1995) (the most recent experimental work).

2. Using values for $\varepsilon_g a$, $\varepsilon_b g$ as reported in Zhang *et al.* (1995), and theoretical values of $\varepsilon_c g$ as reported in Thode *et al.* (1965).

Both of the above determinations utilise enrichment factors determined in a demineralised water matrix.

3. Using values for $\varepsilon_g a$, $\varepsilon_b g$ as reported in Zhang *et al.* (1995) and computed values for $\varepsilon_{\Sigma_c} g$ {where $\varepsilon_{\Sigma_c} g = 0.3\ (\varepsilon_c g)$ as reported in Zhang *et al.* (1995) + $0.7\ (\varepsilon_{c\ min} g)$ assuming mineral carbonate in sea water may be approximated as 50% $CaCO_3$ as calcite and 50% $CaCO_3$ as aragonite, and using mineral - $CO_{2\,(g)}$ enrichment factors as determined by Romanek *et al.* (1992)}. This crudely corrects for the fact that sea water contains mineral carbonate which may account for up to 70% of the total carbonate pool (Stumm and Morgan, 1981).

Using these enrichment factors Zhang *et al.* (1995) adequately accounted for the discrepancies between measured ε_g ΣCO_2 and ε_g ΣCO_2 calculated using enrichment factors that they determined in demineralised water matrix (1. above).

It should be noted that the above calculations assume that the various dissolved carbon species are in isotopic equilibrium with one another and with atmospheric CO_2.

The calcite- bicarbonate enrichment factor, ε_b calcite, for calcite precipitated in isotopic equilibrium with dissolved inorganic carbon has been shown to be + 1°/oo and shows no significant temperature dependence (Romanek *et al.* 1992).

i.e. $\delta^{13}C_{(equilib)} = \delta_b + 1$

This relationship has been used to determine the carbon isotopic composition of calcite precipitated in isotopic equilibrium with dissolved inorganic carbon.
Data for $\delta^{13}C$- ΣCO_2, $[\Sigma CO_2]$, $[CO_{2(aq)}]$, $[HCO_3^-]$, $[CO_3^{2-}{}_{(aq)}]$, pH, δ_a, δ_b and δ_c for each temperature during the course of the experiment are tabulated in Appendix 6.

b) *Pecten* $\delta^{13}C$ data ($\delta^{13}C_{Pecten}$)

$\delta^{13}C_{Pecten}$ data are tabulated together with $\delta^{13}C$- ΣCO_2 and $\delta^{13}C_{(equilib)}$ data in Appendix 7 and presented graphically in Figure 3.4. Mean $\delta^{13}C_{Pecten}$ data and 95% confidence intervals have been calculated from data corresponding to increments of shell secreted by individual scallops during the course of the experiment.

It is apparent that $\delta^{13}C$- ΣCO_2 did not remain constant during the course of the experiment at any of the four experimental temperatures. In the case of tanks 1 and 2, corresponding to temperatures 9.9°C and 12.9°C (Figure 3.4 A and B), $\delta^{13}C$- ΣCO_2 was relatively stable after an initial period of highly isotopically depleted ratios up to day 10 of the experiment. In the case of tanks 3 and 4, corresponding to temperatures 14.7°C and 16.9°C (Figure 3.4C and D), two distinct periods involving excursions to highly isotopically depleted ratios occurred during the course of the experiment.

Figure 3.4. Variation in experimental $\delta^{13}C_{Pecten}$, $\delta^{13}C$- ΣCO_2 and $\delta^{13}C_{(equilib)}$.

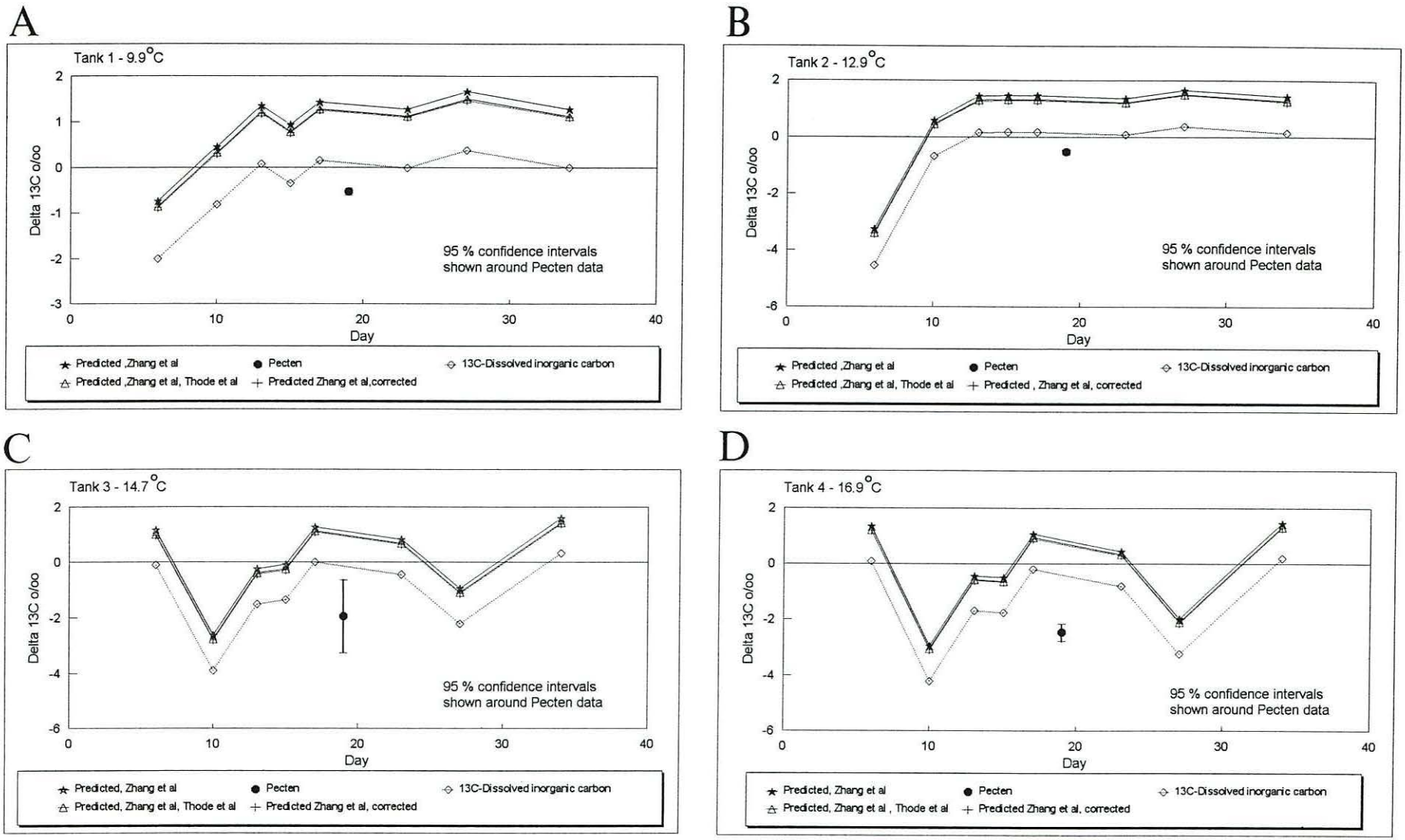

Mains -supplied sea water pumped from the Menai Strait at the time of the experiment (during late June to late July, post *Phaeocystis pouchetti* bloom) has a $\delta^{13}C$- ΣCO_2 value of +0.52°/oo,1 σ = 0.13°/oo (refer to Chapter 4). This is similar to the $\delta^{13}C$- ΣCO_2 ratio of tank sea water after the initially depleted ratios at 9.9°C and 12.9°C and at the start and end of the experiment at 14.7°C and 16.9°C. The time profile of $\delta^{13}C$- ΣCO_2 at 9.9°C was almost identical to that at 12.9°C. Similarly, the time profile of $\delta^{13}C$- ΣCO_2 at 14.7°C was almost identical to that at 16.9°C, with excursions to depleted $\delta^{13}C$- ΣCO_2 ratios occurring at the same time, and being of similar magnitude in both tanks. Mains sea water was ventilated through each reservoir tank via an inflow and outflow pipe (see Appendix 2), being piped from a common manifold via a T piece to the inflow pipes of tanks 1 (9.9°C) and 2 (12.9°C). Similarly, sea water was piped via a T piece to tanks 3 (14.7°C) and 4 (16.9°C) from a common supply pipe. Unavoidable variations in mains sea water supply pressure common to tanks 1 and 2 (and in particular common to tanks 3 and 4) were noted, with accumulation of sediment within the T pieces and associated piping. Since each pair of reservoir tanks had a common supply, it follows that common variations in supply would have resulted in synchronous changes in water residence time in tanks 1 and 2, or tanks 3 and 4. It is quite possible that a continous efflux of respiratory CO_2 from the growing scallops together with such common variations in water supply could have been responsible for the observed synchronous excursions to depleted isotopic ratios during times of higher water residence time (i.e. lower sea water flux through the tanks).

$\delta^{13}C_{(equilib)}$ data mirror changes in $\delta^{13}C$- ΣCO_2 at each temperature and are consequently equally variable. $\delta^{13}C_{Pecten}$ data were well constrained at 9.9°C (1 σ = 0.10 °/oo) and 12.9°C (1 σ = 0.12°/oo) . $\delta^{13}C_{Pecten}$ data were more variable at 14.7°C (1 σ = 0.95°/oo) and 16.9°C (1 σ = 0.40 °/oo), possibly indicating that some individuals did not grow continuously throughout the experiment at the two higher temperatures.

Table 3.1. shows the results of two sample significance tests undertaken between $\delta^{13}C_{(equilib)}$ and $\delta^{13}C_{Pecten}$ data sets at each temperature. At all temperatures, despite the noted variability above, $\delta^{13}C_{Pecten}$ data were significantly different to $\delta^{13}C_{(equilib)}$, being isotopically depleted in all cases.

Table 3.1. A summary of significance tests between experimental $\delta^{13}C_{(equilib)}$ and $\delta^{13}C_{Pecten}$ data sets.

	Experimental Temperature			
	9.9°C (Tank 1)	12.9°C (Tank 2)	14.7°C (Tank 3)	16.9°C (Tank 4)
Test	Mood (data non-normal and heterogeneous)	Mood (data non normal and heterogeneous)	Pooled t (data normal and homogeneous)	Non-pooled t (data normal and heterogeneous)
Significance	1.*significant at $p_{0.95} = < 0.01$ 2.*significant at $p_{0.95} = < 0.01$ 3.*significant at $p_{0.95} = < 0.01$	1.*significant at $p_{0.95} = < 0.01$ 2.*significant at $p_{0.95} = < 0.01$ 3.*significant at $p_{0.95} = < 0.01$	1.*significant at $p_{0.95} = 0.03$ 2.*significant at $p_{0.95} = 0.035$ 3.*significant at $p_{0.95} = 0.037$	1.*significant at $p_{0.95} = < 0.01$ 2.*significant at $p_{0.95} = < 0.01$ 3.*significant at $p_{0.95} = < 0.01$
$\Delta\ \delta^{13}C_{(equilib)} - \delta^{13}C_{Pecten}$ *(mean* / median*)*	1.*-1.80 °/oo 2.*-1.65 °/oo 3.*-1.62 °/oo	1.*-1.95°/oo 2.*-1.80 °/oo 3.*-1.77 °/oo	1.*-*2.07°/oo* 2.*-*1.92°/oo* 3.*-*1.89°/oo*	1.*-*2.27°/oo* 2.*-*2.14°/oo* 3.*-*2.11°/oo*

Note 1.* Using enrichment factors as reported in Zhang *et al.* (1995)
2.* Using enrichment factors ε_g a , ε_b g as reported in Zhang *et al.* (1995), and theoretical values of ε_c g as reported in Thode *et al.* (1965).
3.* Using enrichment factors as reported in Zhang *et al.* (1995) but with mineral correction for ε_c g.

Deviations of *Pecten* shell calcite carbon isotopes from isotopic equilibrium were of the order of -2.02°/oo (1σ = 0.20 °/oo) , -1.88 °/oo (1σ = 0.21°/oo) and -1.85 °/oo (1σ = 0.21°/oo) depending upon the values used for the enrichment factors employed in the determination of $\delta^{13}C_{(equilib)}$ as calculated above and shown in Appendix 7.

3.4 Discussion

The experimental data show that, during the experiment, oxygen isotopes in *Pecten* shell calcite were precipitated in isotopic equilibrium with sea water. After considerations of sample size, variability associated with *Pecten* shell oxygen isotopic data at any one temperature was found to be of the order 1σ = 0.17 °/oo (i.e. approximately equivalent to 0.75°C), which is marginally higher than the analytical variability (1σ = 0.10 °/oo). The experimental work therefore shows that *Pecten* shell calcite oxygen isotopes are both accurate and precise recorders of sea water temperature / $\delta^{18}O$-H_2O under laboratory conditions.

The calculation of $\delta^{13}C_{(equilib)}$ is complicated by uncertainties in the enrichment factor ε_c g and its applicability within a sea water matrix (see Chapter 1 for a full discussion). In all three $\delta^{13}C_{(equilib)}$ determination methods employed (one of which crudely corrects for this matrix effect), $\delta^{13}C_{(Pecten)}$ was significantly depleted with respect to $\delta^{13}C_{(equilib)}$ i.e. carbon isotopes in *Pecten* shell calcite were precipitated out of isotopic equilibrium with dissolved inorganic carbon. Deviations from isotopic equilibrium were of the order -1.85 °/oo to -2.02°/oo (1σ = 0.21°/oo). A model where a) oxygen isotopes are precipitated in isotopic equilibrium with sea water and b) carbon isotopes are precipitated out of isotopic equilibrium with sea water, exhibiting negative deviations from isotopic equilibrium, is in agreement with the general findings of Wefer and Berger (1991) in a review of the stable isotopic compositions of a large number of different taxa. These conclusions were based largely upon field studies.

Partitioning of oxygen isotopes between biogenic carbonates and sea water was examined by Epstein *et al.* (1953) in a similar experimental study involving a number of different molluscan species, mostly of calcitic mineralogy, grown at various temperatures. The species in this study appeared to precipitate oxygen isotopes in isotopic equilibrium with sea water (see Figure 3.3.).

In a well-constrained experimental study Erez and Luz (1983) also found that the planktonic foraminiferan *Globigerinoides sacculifer* precipitated oxygen isotopes in isotopic equilibrium with sea water. In the only previous laboratory study of its kind, Fritz and Poplawski (1974) grew several fresh water species of molluscs in tanks where $\delta^{13}C\text{-}\Sigma CO_2$ was artificially controlled. They concluded that shell carbonate was deposited in near isotopic equilibrium with dissolved inorganic carbon although they suggested that vital effects may have had some influence. Their data show that when $\delta^{13}C\text{-}\Sigma CO_2$ was set at high values (+5°/oo), shell carbonate was somewhat depleted with respect to $\delta^{13}C\text{-}\Sigma CO_2$. It should also be noted that at isotopic equilibrium shell calcite is approximately 1.3°/oo enriched with respect to $\delta^{13}C\text{-}\Sigma CO_2$ (see earlier). When $\delta^{13}C\text{-}\Sigma CO_2$ was set at extremely isotopically depleted values (-35.5°/oo) shell carbonate was somewhat isotopically enriched with respect to $\delta^{13}C\text{-}\Sigma CO_2$. This is suggestive of a contribution of metabolic CO_2 to shell carbonate (respiratory CO_2 being of approximately -20°/oo, (Tanaka *et al.* 1986). Field studies (Margosian *et al.* 1987, Klein *et al.* 1996 a,b) involving a number of molluscan species (*Modiolus modiolus, Mytilus trossulus*) have found shell oxygen isotopes to be precipitated in isotopic equilibrium with sea water, in agreement with the experimental work presented here for *Pecten maximus*. In a field study involving *Mytilus trossulus*, Klein *et al.* (1996 a,b) reported that whilst shell $\delta^{18}O$ were found to be in isotopic equilibrium with sea water, shell $\delta^{13}C$ were depleted with respect to estimated isotopic equilibrium by approximately -2°/oo (no actual $\delta^{13}C\text{-}\Sigma CO_2$ data were available). These findings are also in agreement with the results of this study. It should be noted that a few studies have presented evidence for precipitation of oxygen isotopes out of isotopic equilibrium in bivalves (e.g. Fastovsky *et al.* 1993). These authors reported results of a field study in which they found that shell oxygen isotopes of the fresh water unionid bivalve *Elliptio complanata* were depleted by approximately 2 to 2.5°/oo with respect to isotopic equilibrium.

Since kinetic effect is manifested as negative deviations from isotopic equilibrium for both skeletal carbon and oxygen isotopes it may be concluded by inference that a metabolic effect is responsible for the experimental observations.

McConnaughey (1989b) suggests hypotheses by which introduction of metabolic CO_2 may result in deviations from isotopic equilibrium toward depleted values for shell carbon isotopes whilst shell oxygen isotopes are not associated with similar depletions, but are precipitated in isotopic equilibrium. (see Chapter 1.) The most plausible explanation is one where (isotopically depleted) respiratory CO_2 may have been introduced into the skeleton during shell precipitation.

A review of the literature shows that incorporation of respiratory CO_2 into the growing skeleton occurs in numerous instances. In *Mytilus edulis*, whilst the E.P.F. is chemically similar to sea water (Crenshaw, 1972) its total carbon content is approximately 70% higher, suggesting additional internal (respiratory) CO_2 contributions to the E.P.F (Wheeler, 1992). In trials in which corals were fed ^{14}C - label, Pierce (1970) found that the label subsequently appeared within the coral skeleton, providing evidence for incorporation of metabolic CO_2. Wilbur (1964) has calculated that the activity of the mantle alone can account for more than enough CO_2 to supply the necessary inorganic carbon for shell formation in the oyster *Crassostrea virginica.* Dillaman and Ford (1982) reported that a significant proportion of shell carbonate was derived from respiratory sources for the clam *Mercenaria mercenaria.* Wheeler *et al.* (1975) concluded that, for the scallop *Argopecten irradians,* since the molar ratio of ^{45}Ca to ^{14}C bicarbonate deposited within shell during radioisotope incorporation experiments was not significantly different from unity, shell carbonate was primarily derived from the medium dissolved inorganic carbon. However, these authors also pointed out that if there was rapid turnover in CO_2 fixation within the mantle then bicarbonate from the medium could not be distinguished from that originating from respiratory CO_2. In the absence of CO_2 turnover rate data the authors concluded that the relative contribution of metabolic carbon to shell carbonate could not be determined from their experiments. Calculations presented later in Chapter 4 and reported by McConnaughey *et al.* (1997) show that contribution of metabolic CO_2 to molluscan shell carbon is probably small (3-5% for *Pecten maximus*), but this can account for the observed 1-2 °/oo deviations in shell $\delta^{13}C$ from isotopic equilibrium.

It should be noted that skeletal growth rates of the experimental scallops were low during the experiment, of the order < 0.1 mm day^{-1}. Field work undertaken as part of this research in the Menai Strait has shown that a kinetic effect is not likely to occur in *Pecten maximus* until higher growth rates (typically 0.125 mm day^{-1}) (see Chapter 4.)

An implicit assumption for the conclusions made above is that calcification was continuous throughout the duration of the experiment. Intermittent or partial growth would have little bearing on the conclusions made concerning partitioning of oxygen isotopes, since conditions (namely temperature and $\delta^{18}O$ -H_2O) were constant throughout the course of the experiment . However, the temporal variation in $\delta^{13}C$- ΣCO_2 (and therefore $\delta^{13}C_{(equilib)}$) was such that if growth occurred over only part of the duration of the experiment (coinciding with only depleted, or only enriched $\delta^{13}C$- ΣCO_2 ratios) very different conclusions would be drawn. The large variability in $\delta^{13}C_{(Pecten)}$ at the higher two temperatures appears to indicate that for some of the individuals growth was not constant. The conclusions made concerning partitioning of carbon isotopes in *Pecten* calcite therefore require further substantiation.

Chapter 4 Partitioning of stable isotopes between *Pecten maximus* shell calcite and sea water and factors influencing shell growth and microgrowth patterns : a field study.

4.1. Overview of study

A detailed field study was conducted covering the period October 1994 to October 1995, during which time scallops, *Pecten maximus*, were placed in the Menai Strait a) for periods of one month and b) for the entire year. Shell isotopic data were compared to predicted data for calcite precipitated in isotopic equilibrium with sea water as determined from water samples collected from the Menai Strait every 1-2 weeks. Other biogeochemical parameters were also measured at each sampling point in order to investigate factors influencing shell accretionary growth and shell surface microgrowth patterns (striae).

4.2. Background and objectives of the study

The objectives of the study were:

a) To further investigate whether changes in sea water temperature / $\delta^{18}O\text{-}H_2O$ and $\delta^{13}C$ - ΣCO_2 may be accurately and precisely tracked within *Pecten* shell $\delta^{18}O$ and $\delta^{13}C$. The study follows on from the experimental work undertaken in Chapter 3 and examines whether *Pecten* shell isotopes are precipitated in isotopic equilibrium with sea water over a range of shell accretionary growth rates.

The experimental work in Chapter 3 had shown that *Pecten* shell oxygen isotopes were precipitated in isotopic equilibrium with sea water, but that this was not the case for shell carbon isotopes. Deviations from isotopic equilibrium over the experimental temperature range for *Pecten* $\delta^{13}C$ were of the order of -2°/oo. It was inferred from the experimental data that a component of respiratory CO_2 was incorporated into the shell upon precipitation i.e. a metabolic effect.

Shell growth rates during the laboratory experiment were noted to be low (typically of the order of 0.05mm day^{-1}). Growth rates achieved in the field are likely to be much higher. For example, Mason (1957a) found growth rates for *Pecten maximus* of the order of 0.12 mm day^{-1} during periods of maximum growth in the summer. There exists the distinct possibility, at these high growth rates, of i) variation in the incorporation of respiratory CO_2 into the shell (i.e. a variable metabolic effect) resulting in variation in negative $\delta^{13}C$ deviations from isotopic equilibrium and / or ii) kinetic effects, resulting in further negative deviations from isotopic equilibrium for $\delta^{13}C$ and simultaneous depletions in shell $\delta^{18}O$ (McConnaughey, 1989b).

The field study aimed to test the hypothesis that shell oxygen and carbon isotopes are precipitated in isotopic equilibrium with sea water over the range of shell growth rates experienced in the natural environment.

The annual range in temperature in the Menai Strait is of the order of 13°C (6°C -19°C) , with low aperiodic variations in salinity (Ewins and Spencer, 1967). This temperature range i) is therefore associated with large range in predicted $\delta^{18}O$ ii) is larger than the environmental temperatures experienced by scallops in U.K. waters iii) should produce large changes in shell growth rate during the annual cycle.

The seasonal cycle of algal succession in the Menai Strait is characterised by low algal abundance in the winter, followed by a diatom bloom which is rapidly succeeded by an intense and short-lived bloom (several weeks duration) of *Phaeocystis pouchetti* (Ewins and Spencer, 1967, Blight *et al.* 1995, Middleton, 1997). This predictable succession is associated with large changes in $\delta^{13}C$ - ΣCO_2 and other biogeochemical parameters (Middleton, 1997). A year long field study in the Menai Strait therefore presented an ideal opportunity to test the above hypotheses, with large annual ranges in predicted $\delta^{18}O$ and $\delta^{13}C$ during an annual cycle and associated large predicted changes in shell growth rate.

b) To investigate changes in shell accretionary rate in the field, identify factors influencing shell growth rate and assess changes in the time integrated per sample drilled from the shell with growth rate.

Establishing historical records of sea water temperature / $\delta^{18}O\text{-}H_2O$ and $\delta^{13}C$ - ΣCO_2 from shell calcite is achieved by analysing carbonate samples taken sequentially along the axis of maximum growth (along the length of the shell from the umbo to the valve margin) i.e. isotopic profiling (refer to Chapter 1.) Establishing the absolute environmental range and median values of these parameters depends upon continuous accretionary growth over their whole annual range. For many organisms this is not the case in some or all environmental conditions (refer to Chapter 1.) The annual cycle in the Menai Strait is associated with a wide range in the potential factors influencing accretionary growth (temperature, algal abundance, particulate organic matter concentrations). This presented an opportunity to investigate the relative importance of these parameters in influencing shell growth in *Pecten maximus.*

The study also presented an opportunity to quantify the time integrated for a given shell sampling protocol (e.g. samples taken every 1.5mm along the shell axis) associated with such seasonal changes in accretionary rate. This allows i) parameter limits to be defined, between which the range and median values of shell-derived water temperature and $\delta^{13}C$ - ΣCO_2 may be accurately determined from the shell isotopic record under this sampling protocol and ii) quantification of the level of resolution that changes in environmental water temperature and $\delta^{13}C$ - ΣCO_2 may be tracked in the shell isotopic record over the annual growth cycle.

c) To investigate factors influencing striae abundance / width and the deposition of growth rings i.e. *Pecten* shell surface micro and macro growth patterns.

The surface of the *Pecten* upper shell valve contains macro and micro growth patterns (concentric growth rings and striae). There has been some discussion within the literature as to whether growth rings are deposited with an annual periodicity and the factors influencing their deposition (refer to Chapter 1). Similarly, there has been discussion within the literature as to the factors influencing striae abundance (i.e. number of striae deposited per mm), number of striae per day and striae width. In particular there have been two schools of thought that have considered striae to be deposited i) with a certain, for example daily, periodicity ii) as a function of growth rate, with no rhythmicity.

Macro and micro growth patterns can provide valuable environmental information in addition to the isotopic record once the factors governing their deposition are known. The field study in the Menai Strait presented an opportunity to investigate these factors.

4.3. Apparatus and Methods

4.3.1. *Pecten* shell $\delta^{18}O$ / shell $\delta^{13}C$, shell accretionary rate and shell growth patterns

During the year October 1994 - September 1995 juvenile (<1 year) scallops, *Pecten maximus*, were placed in the Menai Strait for a) periods of approximately one month over the year and b) for the whole annual period. This allowed comparison of monthly - derived data with the annual record contained within the shells of individuals placed in the field for the entire year.

Scallops were supplied by C.E.F.A.S., Conwy from the spawning of the same, conditioned, brood stock. Scallops not initially used were kept in running sea water at ambient temperature in the laboratory. The traditional methods of growing scallops in the field (i.e. within nets or 'ear-hanging') were considered to be unacceptable due to the high current conditions experienced in the Menai Strait. A box for growing the scallops was designed for suspension 1m below a raft moored in the Menai Strait (Plate 4.1a). The box was designed such that current conditions within it were reduced. Scallops were glued to each of three vertical plates of a perspex unit that fitted within the central compartment of the box (Plate 4.1b). The compartment opened to the outside at both ends of the box via a series of baffles that reduced current flow through the box. A suitable distance was kept between the perspex plates and the central compartment wall and floor to permit water flow and keep the attached scallops clear from any accumulated sediment. The box was designed to allow the unit to be quickly placed and secured into, or removed from, the central compartment. Plastic meshing was affixed over both the openings to the outside and the immediate exit and entrance to the central compartment to prevent access of predators. Several boxes were constructed and used in rotation each month to minimise the build up of sediment and fouling organisms in and on the box.

Plate 4.1a Box, with perspex inner unit, for placing scallops beneath the raft moored in the Menai Strait.

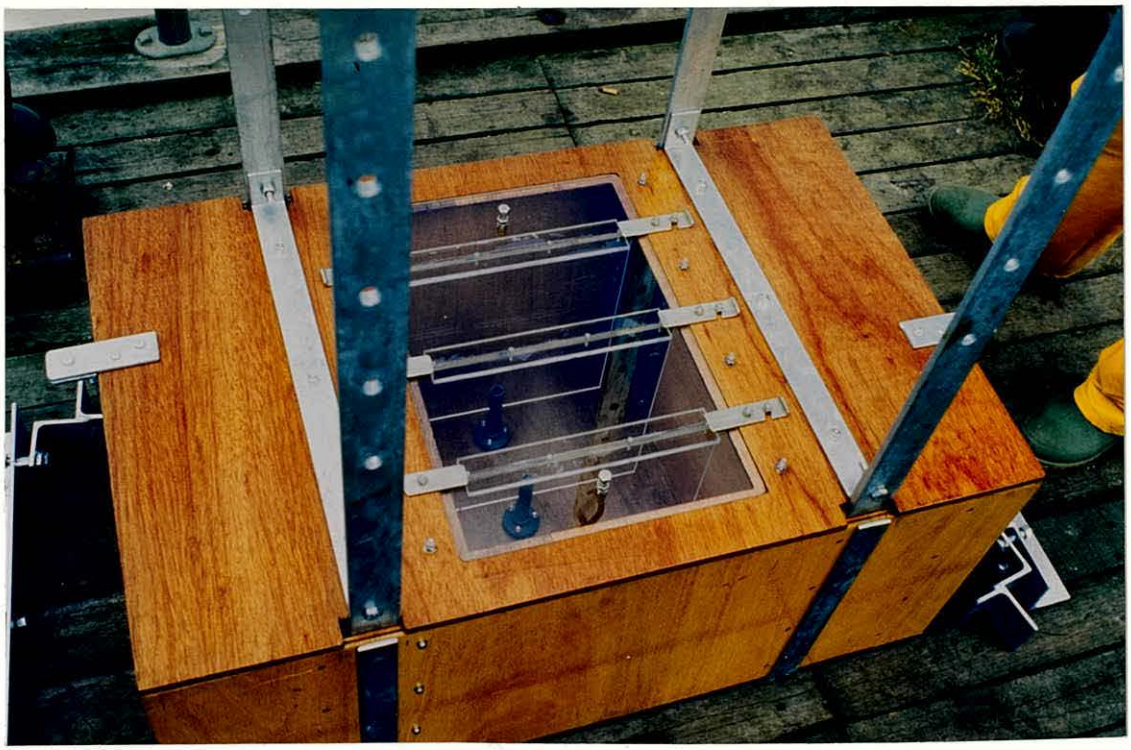

Plate 4.1b Perspex inner unit, with attatched, numbered juvenile scallops, prior to transfer to the raft box in the Menai Strait.

The day prior to placement in the field scallops were measured for shell height (umbo to valve margin) using a binocular microscope fitted with an eyepiece graticule and a small numbered tag glued to the upper shell valve. Scallops were then glued to one of the three vertical plates of the perspex unit, which was subsequently placed in running sea water overnight to allow the scallops to recover before transfer to the raft the next day. Scallops were kept immersed in sea water during boat transfer. Richardson (1991) has shown that a clearly visible growth check is formed in the shells of bivalves exposed to this type of handling, to which all subsequent growth can be related. This procedure was carefully followed during each monthly transfer of scallops to the field. After the assigned period in the field scallops were returned to the laboratory, removed from the perspex unit and immediately deep - frozen.

The following protocol was used for analysis of scallops after monthly or annual periods in the field.

a) scallops placed for monthly periods in the field

Nearly all retrieved scallops displayed a clear disturbance-related growth check in the shell (Plate 4.2). To confirm that the observed growth check was associated with the start of the period in the field, the shell height to the disturbance mark was measured and cross checked with initial shell height data.The increment of shell deposited over the month therefore corresponded to the shell deposited between the growth check and valve margin. In the very few cases where the growth check was not at the initial shell height or there was no observed check, individuals were excluded from analysis. Individuals were checked for gonad maturity according to the classification scheme of Mason (1957b) to establish whether gonad development had occurred in any scallops. Since the onset of maturity has been suggested by some authors to influence shell growth and shell isotopic data (Erlenkeuser and Wefer, 1981, Jones *et al.* 1986), in the few cases where this occurred individuals were excluded from the analysis. The increment of shell deposited during the time period in the field was measured using a Leica binocular microscope equipped with an eye piece graticule, at x16 magnification. The increment of shell deposited at the midline, at the second ray in from the lateral shell margin and at the basal ear (see Plate 4.2) were each measured.

Plate 4.2. Shells of juvenile *Pecten maximus* after a period of growth of approximately one month in the Menai Strait. Upper (U) and lower (L) shell valves are indicated. Also indictated are the clear growth check, or disturbance mark (D), associated with the beginning of the period in the field, and increment of shell (I) deposited during the month on the upper shell valve. The various regions dicussed in the text (midline, second ray and basal ear) are shown.

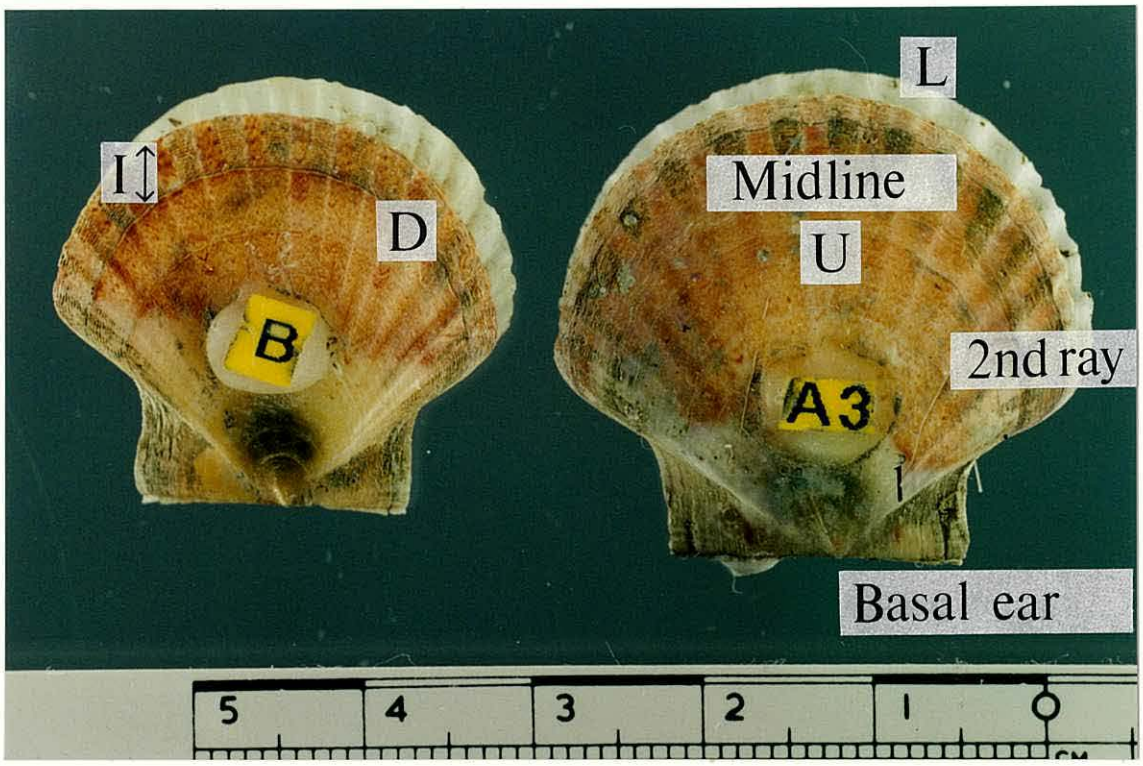

The number of striae deposited within the increment at the midline, second ray and basal ear were then counted at this magnification. Mean stria width (i.e the increment of shell between consecutive striae) was determined by taking the mean value for up to the first five striae width measurements from the valve margin inwards at x40 magnification using the Leica microscope.

Data for shell accretionary growth rate (mm day^{-1}) were calculated by division of the increment in mm by the number of days that the animals were placed in the field. Similarly, the number of striae deposited per mm and per day were calculated by division of the number of striae deposited within the increment by the increment width in mm and the number of days that the animals were placed in the field.

Calcite samples for *Pecten* $\delta^{18}O$ and $\delta^{13}C$ were analysed, after pretreatment in an oxygen plasma to remove organic components, by standard sealed vessel methods (see Chapter 2). Calcite samples were obtained by three sampling protocols (Figure 4.1.) The methodological work undertaken in Chapter 2 had shown that below a threshold of 0.5 to 1mg sample weight isotopic data were unacceptably inaccurate and imprecise. Due to this, it was ensured, by use of one of the following protocols, that sample weights exceeded 1mg.

i) where growth was slow the entire increment secreted by an individual scallop was drilled using a dentists drill fitted with a 0.5mm bit and placed within a Durham tube (Figure 4.1a). Where growth was extremely slow the calcite from several individuals were pooled within the same Durham tube.

ii) where growth was intermediate (i.e. where growth was insufficient to allow profiling but where removal of the entire increment was unnecessary to achieve target weight) a sub-section of the increment from the growth check to the valve margin at the midline was removed (Figure 4.1b)

iii) where growth was fast it was possible to subsample the increment (i.e. profiling). Sequential samples were drilled from the shell surface at 1.5mm intervals in concentric rings from the growth check to the valve margin (Figure 4.1c).

Figure 4.1 Protocols employed when sampling shells of *Pecten maximus* retrieved after monthly periods in the Menai Strait for isotopic analyses.

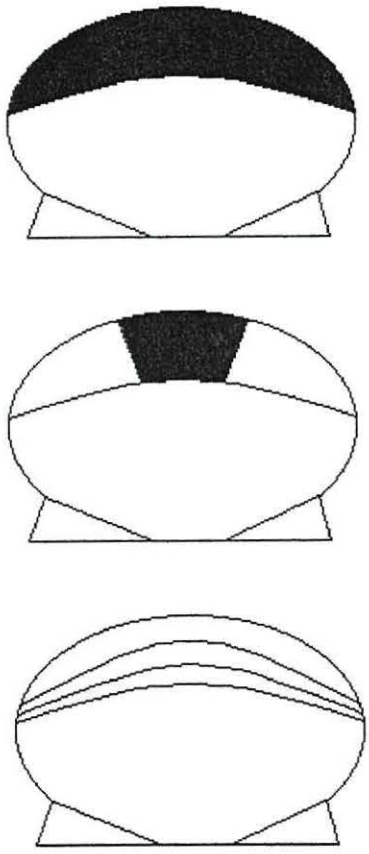

a) entire increment from disturbance mark to valve margin

b) subsample of increment at midline from disturbance mark to valve margin

c) profiling of increment from disturbance mark to valve margin

Two types of data were therefore obtained. Firstly, *mean* data where the whole increment of one or more individuals was analysed (protocols i) and ii)) i.e. where each calcite sample corresponded to the mean data for the monthly time period. Secondly, *profile* data from one individual (protocol iii) where each calcite sample corresponded to the mean data for a smaller time period *within* the month (days to weeks depending upon the number of samples obtained by profiling within the increment). For the first monthly period both increment profiling and sub-section removal were undertaken to allow comparison.

Allometric growth of the scallop shell results in differential growth rates around the valve margin. Growth is fastest at the midline and slowest at the lateral margins. There exists the possibility of variation in metabolic effects (Klein *et al.* 1996b) and / or kinetic effects in faster growing areas of the shell (toward the midline) relative to slower growing regions (toward the lateral margins). The sampling protocols above are associated with either sampling from the midline to the lateral margin or only sampling sections of the increment at the midline. It is therefore important to ensure that there is no trend in isotopic data associated with increased metabolic effects or kinetic effects around the valve margin. To test this two individuals from the first monthly period were analysed by sequential removal of sub-sections of the increment, from the initial growth check to the valve margin, around the valve from the midline to the lateral margin.

b) animals placed out for the period of one year.

Animals placed out in the Menai Strait for a year exhibited considerable fouling (Plate 4.3a). Fouling was noted to be i) confined to a distinct region between the umbo and approximately one third of the distance between the umbo and the valve margin and ii) largely due to settlement of the barnacle *Balanus crenatus* and the calcareous worm *Pomatoceros triqueter*. The extent of the barnacle fouling zone was measured (in terms of shell height from the umbo) for each scallop. Individuals were then carefully cleaned of all fouling organisms. Each individual was assessed for gonad maturity according to the classification scheme of Mason (1957b).

Plate 4.3a Upper shell valves of scallops upon recovery after a period of one year in the Menai Strait. Shells exhibit considerable epifouling within a discreet region of the shell. Epifauna have been partially and completely removed from the bottom two scallops to show zonation of barnacle basal plates.

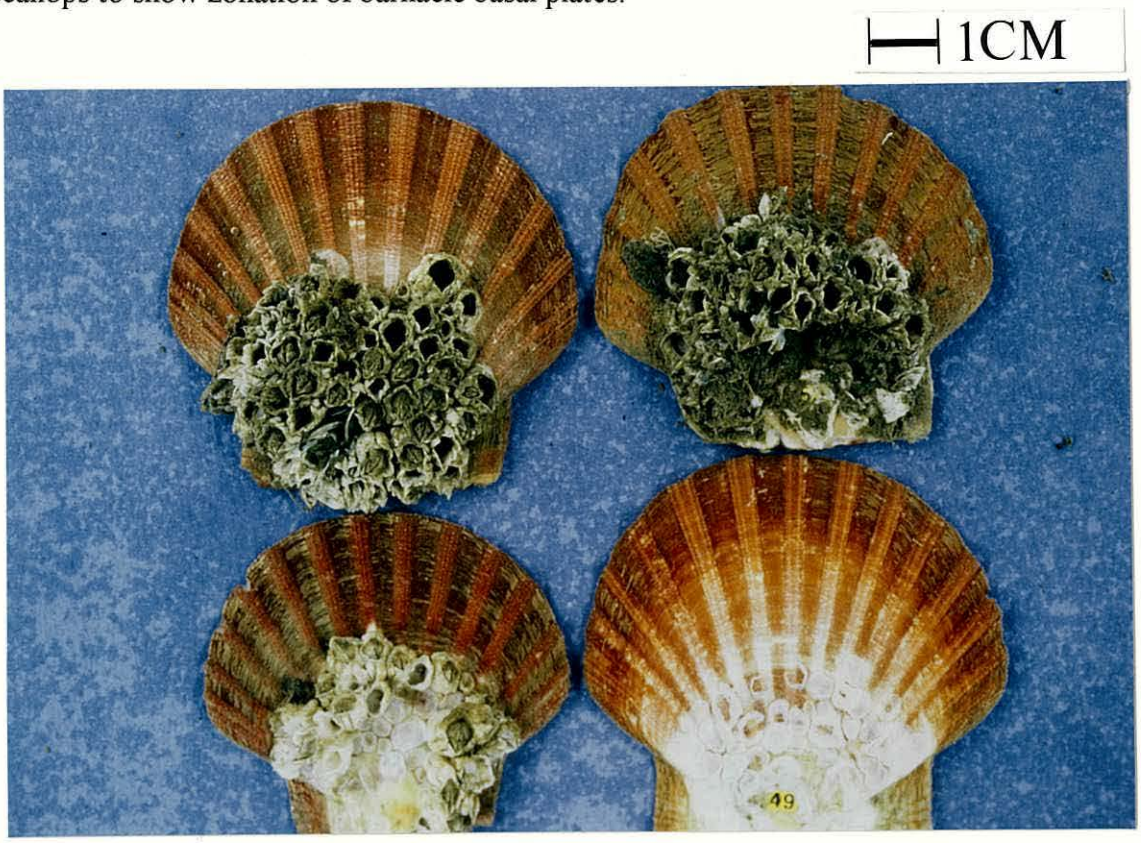

Plate 4.3b Upper shell valve of scallop recovered after a period of one year in the Menai Strait. Indicated are the disturbance mark (D) associated with initial placing in the field, the increment of shell (I) deposited over the year and the growth line (G) associated with the cessation of growth in the Winter

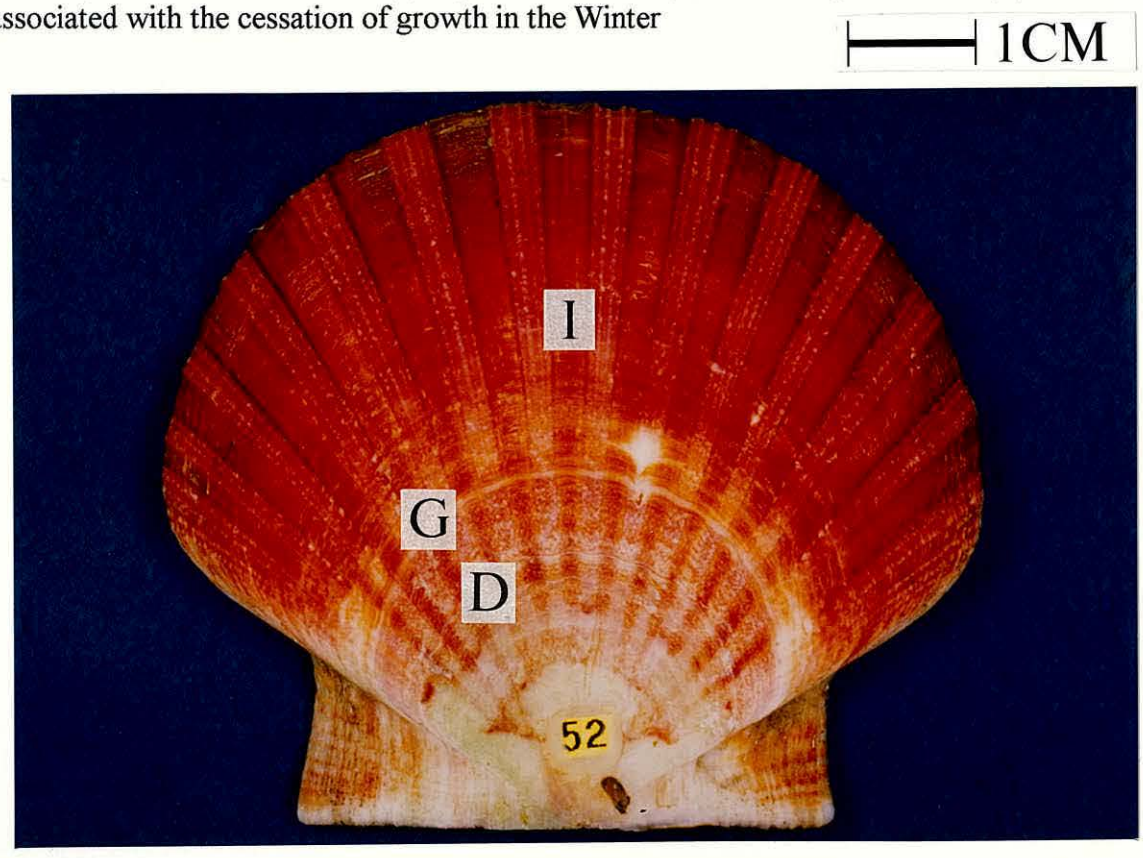

Individuals displaying signs of maturity were excluded from analyses. In some cases gonads were noted to be fully ripe.

As for the monthly scallops, a clear growth check was noted in all individuals in the shell (Plate 4.3b). This was confirmed, using initial shell height data, to be associated with the beginning of the annual time period in the field. The increment of shell between the growth check and valve margin therefore corresponded to the time period of growth in the field (one year). In many individuals a white concentric growth ring was observed approximately 1cm from the growth check (Plate 4.3b.)

The number of striae per mm were measured for each scallop at mm intervals along the shell axis from the growth check to the valve margin. This was done by placing an acetate strip, on to which a ruler with mm interval markings had been photocopied, along the axis of growth at the midline and counting the number of striae per mm at each mm interval using the Leica binocular microscope.The exact distance of the concentric growth ring from the initial growth check was noted. Striae width was measured at each mm interval along the shell axis at x40 magnification. This was done by measuring each increment between consecutive striae within the mm distance interval and taking the mean value.

Two individuals were selected for isotopic profiling. Calcite samples for *Pecten* $\delta^{18}O$ and $\delta^{13}C$ analysis were sequentially drilled from the shell surface in concentric rings from the growth check to the valve margin. It was ensured that sample weight exceeded 1mg in all cases. Calcite samples were analysed, after pretreatment in an oxygen plasma to remove organic components, by standard sealed vessel methods (see Chapter 2).

4.3.2. Measurement of biogeochemical parameters in the Menai Strait.

Measurements were taken at Menai Bridge pier, located near to the raft, at high water every 1 - 2 weeks. Temperature was first measured. An aspirator was rinsed and then filled using a bilge pump which had a 200μm mesh covering an inlet pipe weighted such that sampling was from 1m depth. It was ensured that the outlet pipe from the pump was placed at the bottom of the aspirator and at least twice the aspirator volume was replaced with pumped sea water before cap replacement.

The aspirator was covered with a black bag and immediately returned to the laboratory for processing. Water from the aspirator was subsampled via Nalgene tubing for all parameters except temperature, ensuring it was well shaken immediately before each subsampling.

The following biogeochemical parameters were measured :

a) Water temperature.

Water temperature was measured directly at Menai Bridge pier at each sampling date using a hand held digital thermometer. A data logger (Tiny Talk Temperature Logger, Orion Components, Chichester) was mounted in the raft box during several monthly periods to allow comparison of temperature data within the box and at the Pier.

b) Isotopic composition and concentration of dissolved inorganic carbon ($\delta^{13}C$- ΣCO_2 , $[\Sigma CO_2]$)

Subsampling of the aspirator for $\delta^{13}C$- ΣCO_2 and $[\Sigma CO_2]$ measurement was done immediately upon return to the laboratory. A small volume of water was allowed to run through the Nalgene tubing from the aspirator before clipping off. The tubing end was placed at the base of a TCO_2 (i.e. glass stoppered) bottle and at least twice the bottle volume allowed to be replaced before removal of the Nalgene tubing. The water within the bottle was then poisoned with saturated $HgCl_2$ at 1µl ml^{-1} to halt biological activity and cold - stored in the dark (Kroopnick, 1980). Within 2 hrs a $10cm^3$ sub-sample was filtered from this bottle through a 0.4µm Nucleopore filter into a numbered, pre-weighed, nitrogen - flushed glass ampoule (Adelphi Tubes, U.K.) and flame - sealed for extended storage after re-weighing. Extraction of CO_2 from the sub-sample in the ampoule for determination of $\delta^{13}C$- ΣCO_2 and $[\Sigma CO_2]$ was performed as outlined in Chapter 2.

c) Concentration of aqueous carbon species in sea water $[CO_{2\,(aq)}]$, $[HCO_3^-]$, $[CO_3^{2-}{}_{(aq)}]$

A 10cm spectrophotometer cell was flushed through with sample from the aspirator and then filled, excluding air bubbles.

Concentration of aqueous carbon species in sea water was determined from pH, [ΣCO_2], salinity and temperature measurements as outlined in Chapters 2 and 3.

d) Isotopic composition of sea water relative to VSMOW ($\delta^{18}O$-H_2O)

Water was siphoned from the aspirator into a 150cm^3 glass Winchester bottle, with a screw - top lid containing a rubber insert to prevent evaporation / condensation. These were cold - stored in the dark. $\delta^{18}O$-H_2O was determined as outlined in Chapters 2 and 3.

e) Salinity

Water samples were siphoned from the aspirator into a standard salinity bottle and analysed on an AutoSal 8400A Autosalinometer calibrated with I.A.P.S.O. standard sea water.

f) Chlorophyll and Phaeopigment concentration

Water was filtered, using a filter rig attached to a diaphragm pump, onto a 47mm GFC filter which was placed onto a petri slide and covered before being frozen for extended storage. A policy of filtering to set colour was employed, with volumes between 250cm^3 and 1000cm^3 filtered depending upon the phytoplankton abundance in the water. Analysis was according to the methods outlined in Chapter 2.

g) Dissolved Nitrite , Nitrate, Silicate and Phosphate concentrations

The aspirator filtrate (i.e. filtered through GFC / GFF filter) was used to fill two 120 cm^3 polyethylene bottles for each of the above parameters, which were frozen for subsequent analysis. Analysis was according to the methods outlined in Chapter 2.

h) Total Suspended Solids

Water was filtered through a preweighed 47mm GFC filter, placed inside petri slides and frozen for storage. Filters were defrosted and dried overnight at 40°C. Filters were allowed to come to room temperature and reweighed. Volumes filtered were between 250cm^3 and 1000cm^3, dependent upon the particulate loading in the water.

k) Particulate Organic Carbon and Nitrogen Concentrations ([P.O.C. / P.O.N.])

Between 150cm^3 and 500cm^3 of water (dependent upon the particulate loading in the water) was filtered through a 25mm GFF filter , precombusted for 3 hours at 500°C. Filters were placed inside petri slides and frozen for storage. After defrosting, filters were fumed overnight using concentrated HCl to remove inorganic carbonates and dried at 40°C. After drying, filters were scrunched within 30mm diameter aluminium discs, precombusted for 3 hours at 500°C, to form small balls. Subsequent analysis was performed on a Roboprep CN analyser as outlined in Chapter 2.

l) Algal speciation

150cm^3 glass bottles were filled with water siphoned from the aspirator. For storage purposes 4 drops of acidified Lugols Iodine were added to the bottle. During the period March - September bottles were additionally filled directly when sampling at the Pier to assess the phytoplankton community with size fraction >200µm. For analysis, the bottles were allowed to stand overnight to allow the phytoplankton to settle out. The sea water was then carefully decanted to leave approximately 10cm^3 in the bottle. This volume was transfered to a settling chamber. Distilled water was used to wash the bottle out into the settling chamber. Settling chambers were allowed to stand for one hour and then observed at x4 and x40 magnification in an inverted microscope. Algal counts along two transects at x40 magnification were made. The field of view was calibrated at this magnification to obtain the algal counts for the entire chamber bottom area. These counts were added to counts for larger algae made at x4 magnification (in this instance counting all observable algae on the chamber bottom) Counts were converted to algal numbers per dm^3 using initial bottle volume data.

4.4. Results

4.4.1. Seasonal Variation in Biogeochemical Parameters in the Menai Strait.

a) Temperature, salinity and $\delta^{18}O\text{-}H_2O$

Seasonal temperature, salinity and $\delta^{18}O\text{-}H_2O$ variation at Menai Bridge Pier for the period October 1994 - September 1995 are shown in Figure 4.2a and b and tabulated in Appendix 8 .

Water temperature minimum and maximum values were 6.3°C and 18.9°C respectively i.e. a total range of 12.6°C. The seasonal cycle of water temperature showed the expected sinusoidal pattern with maximum temperatures in August and minimum temperatures during mid February to mid March. Data collected from the TinyTalk datalogger, positioned for several monthly periods within the raft box, showed that temperatures within the box were comparable to those taken at Menai Bridge Pier (Appendix 9).

Salinity minimum and maximum values were 32.30S and 33.93S respectively i.e. a total range of 1.63S. Salinity variation was low over the year and showed no distinct seasonal pattern. $\delta^{18}O\text{-}H_2O$ minimum and maximum values were -0.306°/oo and +0.022°/oo respectively i.e. a total range of 0.328°/oo. $\delta^{18}O\text{-}H_2O$ showed no distinct seasonal pattern. Salinity and $\delta^{18}O\text{-}H_2O$ were well correlated throughout the year (Figure 4.2 b and c). A regression plot of $\delta^{18}O\text{-}H_2O$ against salinity (Figure 4.2c) gave the following relationship:

$$\delta^{18}O\text{-}H_2O = -7.419 + 0.220S \quad (R^2 = 0.90,\ n = 35)$$

b) Pigment concentrations, nutrient concentrations and algal abundance.

The seasonal variation in concentration of chlorophyll for the less than 200μm size fraction and dissolved nutrients are shown in Figure 4.3a, b and c, and tabulated in Appendix 10.

Chlorophyll concentrations fell from an initial value of 2.30μg dm^{-3} in late September 1994 to low values (0.46μg dm^{-3} , 1σ = 0.12μg dm^{-3}) during the winter period (November 1994 to mid March 1995).

Figure 4.2a Annual temperature variation at Menai Bridge Pier 1994 -1995.

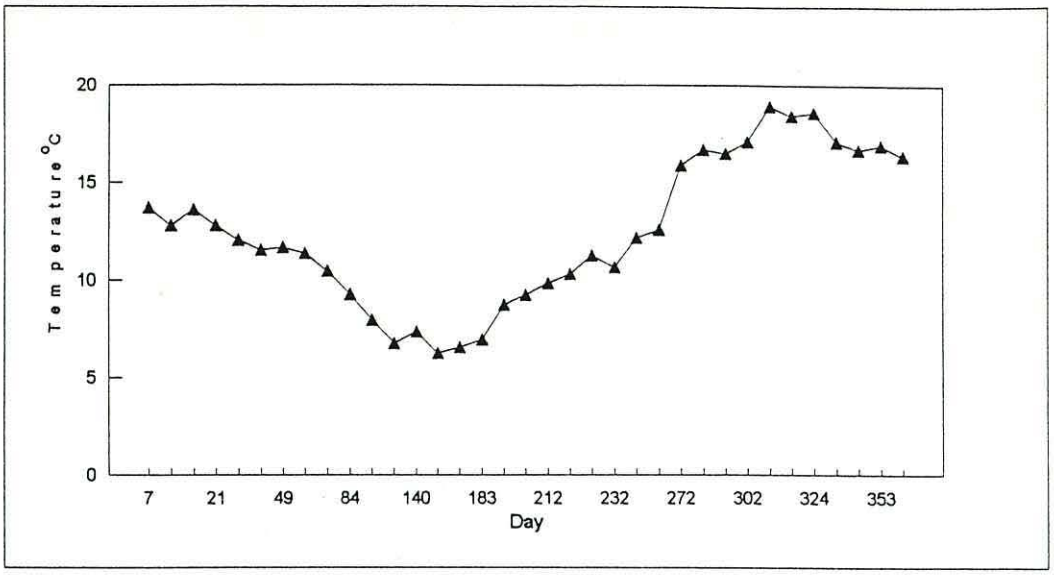

Figure 4.2b Annual salinity and $\delta^{18}O$-H_2O variation at Menai Bridge Pier 1994 -1995.

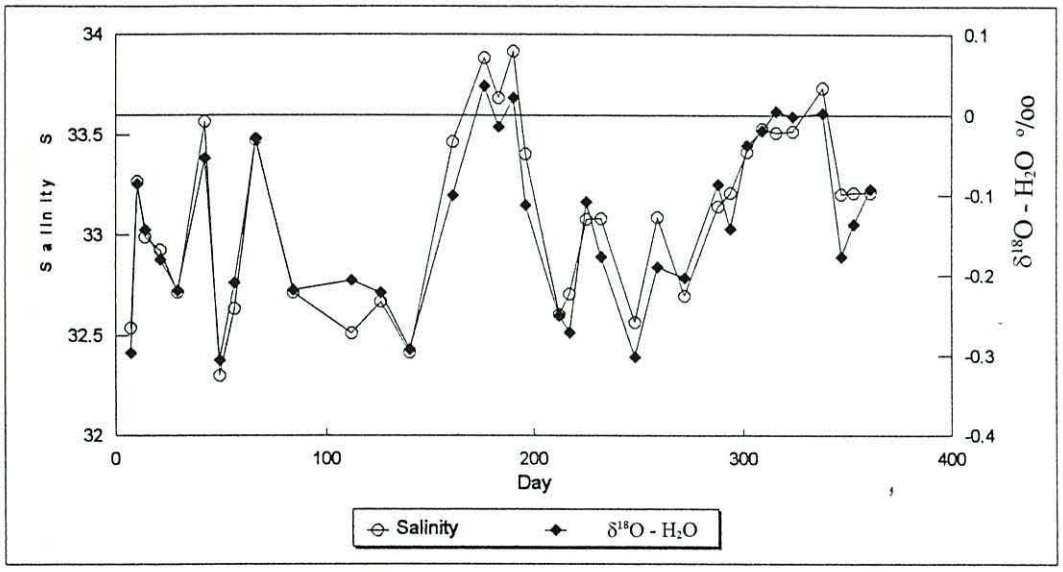

Figure 4.2c Salinity - $\delta^{18}O$-H_2O plot for data collected at Menai Bridge Pier 1994 - 1995.

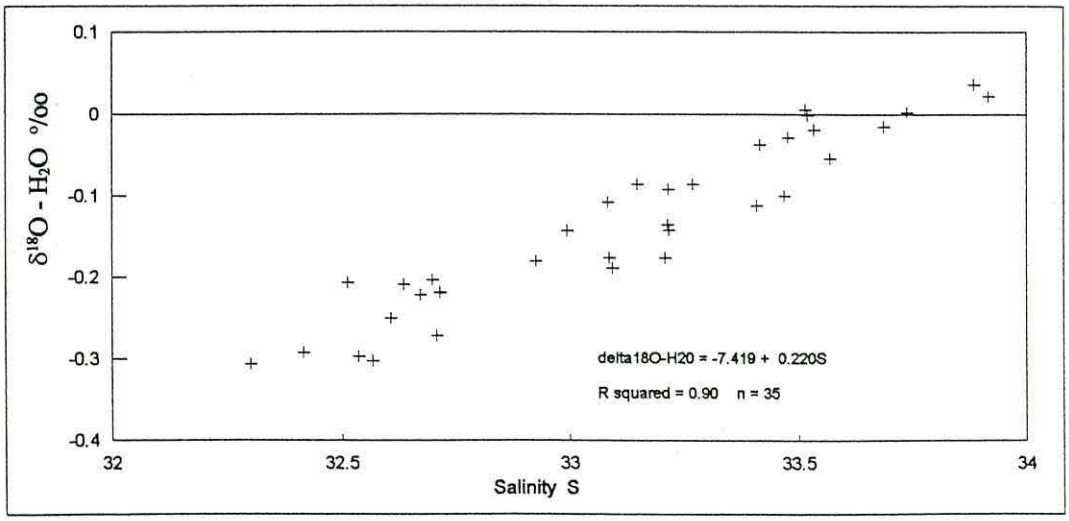

Figure 4.3a Seasonal variation in Chlorophyll concentration at Menai Bridge Pier. Seasonal changes in the dominant members of the algal community are shown.

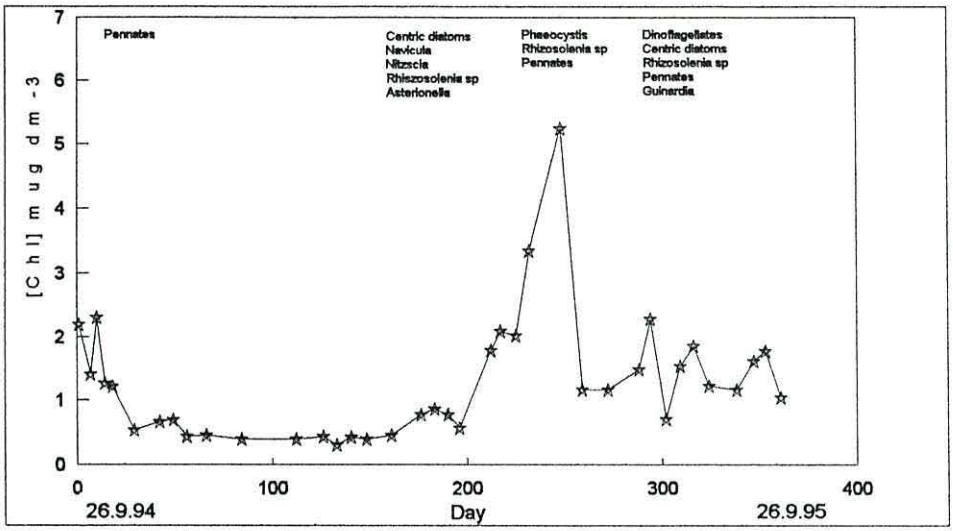

Figure 4.3b Seasonal variation in Silicate and Nitrate concentration at Menai Bridge Pier.

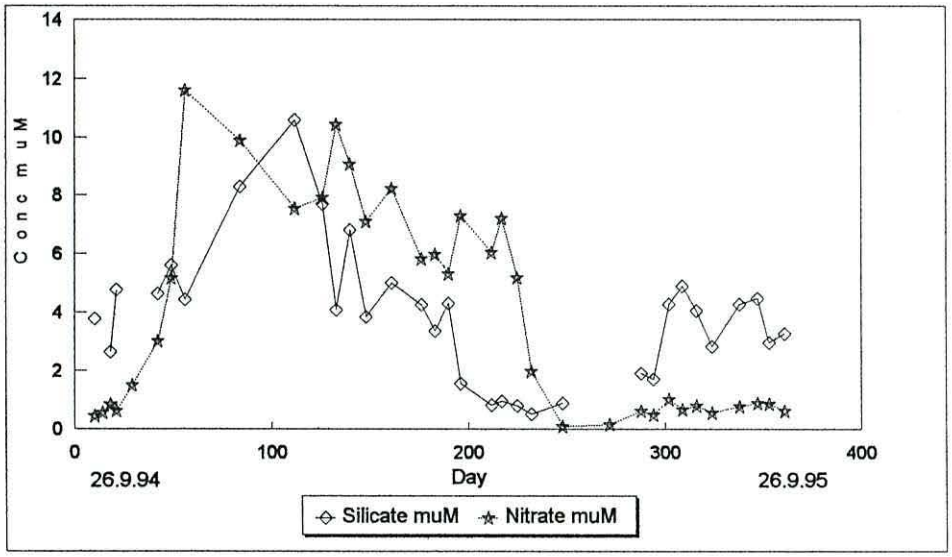

Figure 4.3c Seasonal variation in Phosphate and Nitrite concentration at Menai Bridge Pier

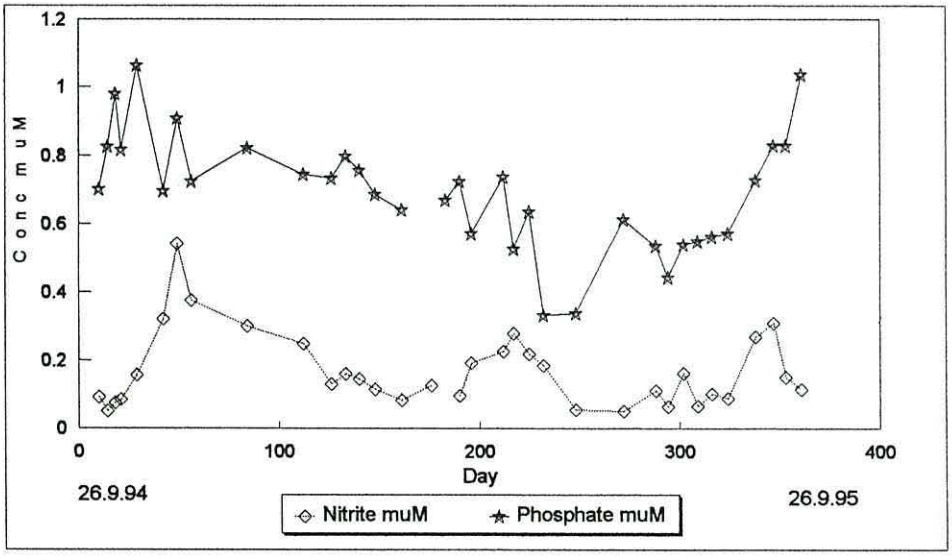

A small rise in chlorophyll concentration occurred at the end of March (i.e. days 176 - 190) , rising to 0.86μg dm^{-3} and falling again. After day 200 (mid April) chlorophyll concentration rose dramatically to an initial value of 2.10μg dm^{-3} at the beginning of May (day 217) and then to a maximum value of 5.25μg dm^{-3} at the beginning of June (day 248). A dramatic and rapid fall in chlorophyll concentration to 1.16μg dm^{-3} had occurred by mid June (day 259). Between this date and the end of September 1995 intermediate chlorophyll levels were observed (1.47μg dm^{-3}, $1\sigma = 0.45$μg dm^{-3}) with three minor peaks in concentration during this period (mid July i.e.day 294, mid August i.e. day 316 and mid September i.e. day 353).

Silicate concentrations were fairly constant at 4.43 μM ($1\ \sigma = 1.04$ μM) between October 1994 and the beginning of April 1995, bar the period mid December 1994 to the end of January 1995 when concentrations rose to 10.57μM and fell again. After the beginning of April (day 190) silicate concentrations fell rapidly (by mid May (day 232)) to a concentration of 0.82μM. Concentrations remained low until the end of July (day 302) when concentrations were rapidly restored to pre April levels. Silicate concentration remained at 3.89μM ($1\ \sigma = 0.76$ μM) from the end of July until October.

Nitrate concentrations showed a gradual rise from initially low values (0.43μM) at the beginning of October 1994 to a peak value of 11.59μM at the end of November (day 56). Concentrations remained high until the end of March 1995 (8.97μM $1\ \sigma = 1.56$μM). A small dip in nitrate concentrations (to 5.72μM ($1\sigma = 0.34$μM)) occurred at the end of March 1995 (day 176). A rapid drop in nitrate concentration occurred in mid May (day 232), falling by the beginning of June (day 248) to 0.094 μM, within the limits of analytical error. Concentrations recovered only marginally in mid July (day 288) to 0.62μM and remained low until the end of October 1995 (0.74μM) ($1\sigma = 0.17$μM).

Seasonal changes in phosphate and nitrite concentration were less pronounced. After an initial rise to high values, phosphate concentrations remained stable at 0.72μM ($1\sigma =$ 0.10μM) from the beginning of November 1994 (day 42) to mid May 1995 (day 225). A small fall in concentration to 0.33μM was observed in mid May (day 232), lasting until mid June (day 259). Concentrations then rapidly returned to pre May levels, rising again gradually at the end of August (day 338) to October 1994 levels.

Nitrite concentrations rose from initially low values (0.076μM , $1\sigma = 0.018\mu M$) to a peak of 0.541μM in mid November 1994 (day 49). Concentrations gradually fell to 0.13μM at the end of January 1995 (day 126) and remained stable at this level until mid May (day 232). A small fall in nitrite concentration occurred at this point (to 0.05μM). By mid July (day 288) a small recovery in nitrite concentration had begun, but concentrations remained low until the end of August (day 338), when concentrations rose and then fell to October 1994 levels.

Seasonal changes in chlorophyll and dissolved nutrient concentrations were tightly coupled with the processes of primary production and bacterial - mediated remineralisation. Chlorophyll concentrations fell during October 1994, at which point nitrate and nitrite concentrations were low, whilst silicate and phosphate concentrations were high. During this period small pennate diatoms, some centric diatoms *(Coscinodiscus sp)* and diatoms of the genus *Rhizosolenia* dominated the algal community (see Appendix 11 and Figure 4.3a). Immediately after the autumn decrease in chlorophyll concentration, rapid remineralisation of nitrate and nitrite occurred. The winter period was associated with low algal abundance (and therefore chlorophyll concentrations) and high nutrient concentrations. Between the end of March (day 183) and mid April (day 200) small blooms of centric diatoms (*Coscinodiscus sp*) and diatoms of the genera *Paralia, Nitzchia* and *Navicula* occurred, associated with a small increase in chlorophyll concentrations. Between mid April and the end of May (day 248) large blooms of the diatoms *Rhizosolenia delicatula, Asterionella gracialis* and later *Rhizosolenia shrubsolei* occurred, associated with large increases in chlorophyll concentration. This period was associated with large falls in silicate concentration accompanying the diatom bloom. The diatom bloom tailed into an intense bloom of the prymnesiophyte *Phaeocystis pouchetti* during the latter half of May (days 232 - 248). The period of the main diatom and *Phaeocystis* blooms was accompanied by a rapid fall in nitrate and nitrite concentrations, and a small drop in phosphate concentration. The rapid drop in these nutrients was followed by a crash of the *Phaeocystis* bloom in mid June (day 259) and nutrient limitation of the *Phaeocystis* bloom seems likely. The period after the *Phaeocystis* bloom until the end of September was associated with intermediate chlorophyll concentrations which showed some cyclical nature.

Increases in dinoflagellate abundance occurred at the end of June (day 272), increases in diatoms of the genera *Rhizosolenia* and *Guinardia*, centric and pennate diatoms occurred in mid August (day 326) and finally increases diatoms of the genera *Rhizosolenia*, *Chaetoceros* and *Coscinodiscus* occurred in mid September (day 353). During this summer period phosphate remineralisation occurred rapidly in mid June, silicate remineralisation occurred at the end of July 1995, whilst nitrate and nitrite concentrations remained low.

c) Seasonal changes in the TCO_2 system and $\delta^{13}C$-ΣCO_2.

Seasonal changes in the TCO_2 system and $\delta^{13}C$- ΣCO_2 are shown in Figure 4.4 and tabulated in Appendix 12. The initial fall in chlorophyll concentration during October 1994 was associated with a rise to winter values in [ΣCO_2] (2069.5μmol kg^{-1},1σ = 23.5 μmol kg^{1}), [$CO_{2(aq)}$] (16.8 μmol kg^{-1}, 1σ = 0.7 μmol kg^{-1}), and [HCO_3^-] (1917.9 μmol kg^{-1}, 1σ = 23.1 μmol kg^{-1}). There was a simultaneous fall to winter values in pH (8.08 μmol kg^{-1}, 1σ = 0.02 μmol kg^{-1}), [CO_3^{2-}] (134.9 μmol kg^{-1} , 1σ = 9.2 μmol kg^{-1}) and $\delta^{13}C$- ΣCO_2 (+0.07 °/oo, 1σ = 0.12 °/oo). A rise in $\delta^{13}C$-ΣCO_2 to + 0.42°/oo occurred during mid March (day 161) and a dip in [ΣCO_2], [HCO_3^-] and [$CO_{2(aq)}$], with accompanying rise in [CO_3^{2-}], occurred at the beginning of April (day 196). However the overiding feature of the seasonal change in the TCO_2 system occurred in mid May (day 225) during the main diatom and *Phaeocystis* blooms. The associated dramatic rise in chlorophyll concentration was accompanied by a sharp fall in [ΣCO_2] (to 1931.2 μmol kg^{-1}), [$CO_{2(aq)}$] (to 7.0 μmol kg^{-1}) and [HCO_3^-] (to 1667.8 μmol kg^{-1}) and sharp rise in [CO_3^{2-}] (to 256.4 μmol kg^{-1}). A simultaneous sharp rise in pH (to 8.36 μmol kg^{-1}) and $\delta^{13}C$-ΣCO_2 (to +1.23 °/oo) was observed at this time. The crash in the *Phaeocystis* bloom in mid June (day 259) was accompanied by a simultaneous return to pre May values of all parameters of the TCO_2 system and $\delta^{13}C$-ΣCO_2.

The seasonal variation in parameters of the TCO_2 system and $\delta^{13}C$-ΣCO_2 in the Menai Strait was tightly coupled to the processes of dissolved inorganic carbon uptake by phytoplankton and the associated fractionation of carbon isotopes during such uptake, and water column remineralisation.

Figure 4.4a Seasonal variation in $\delta^{13}C$-ΣCO_2 and chlorophyll concentration at Menai Bridge Pier.

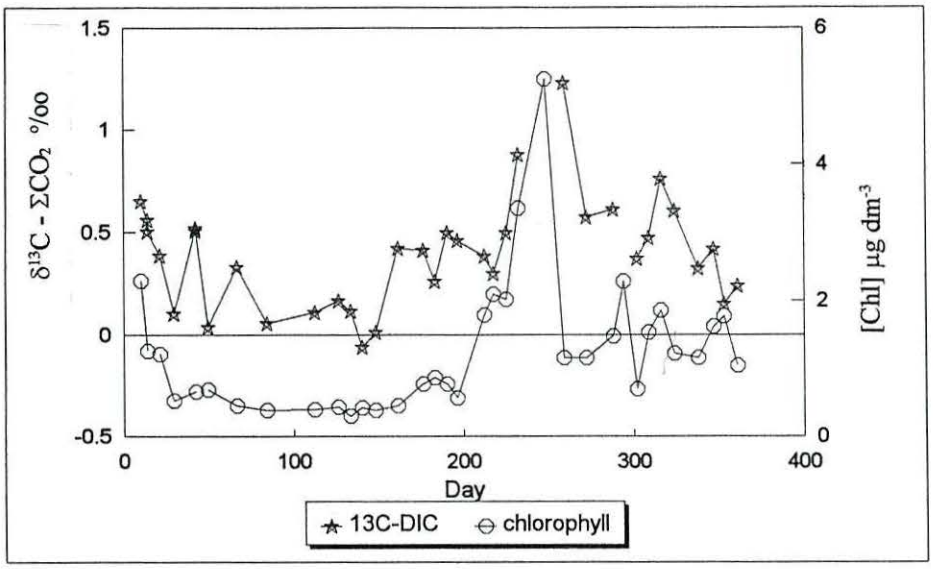

Figure 4.4b Seasonal variation in [ΣCO_2] and pH at Menai Bridge Pier.

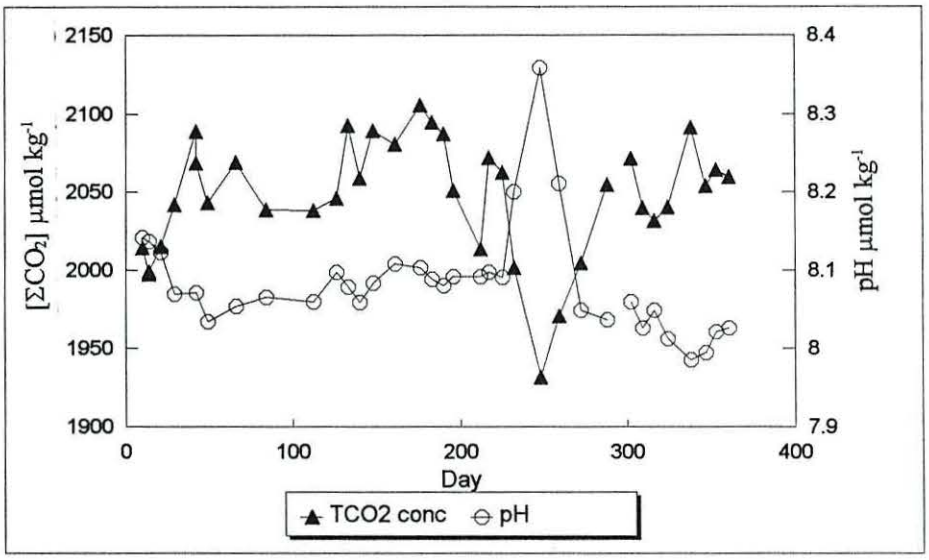

Figure 4.4c Seasonal variation in dissolved inorganic carbon spieces at Menai Bridge Pier.

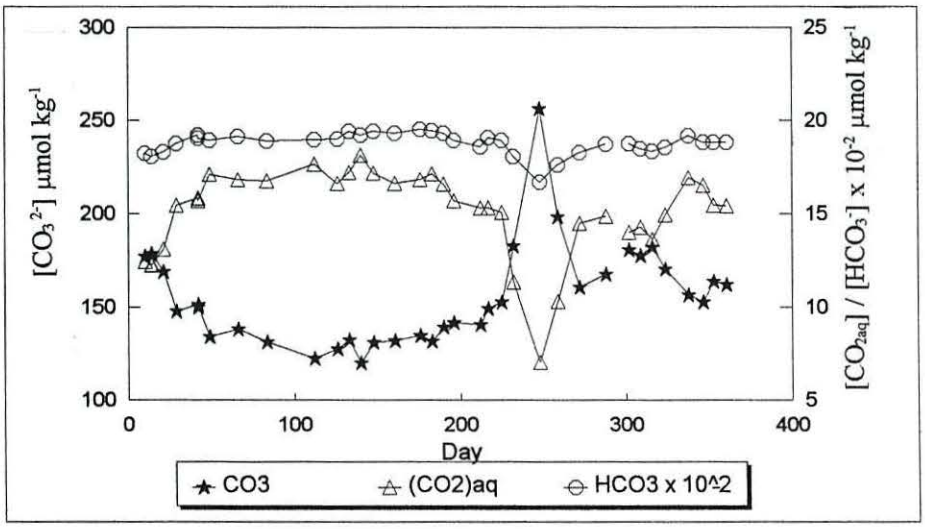

Uptake of $CO_{2\,(aq)}$ and HCO_3^- by phytoplankton results in the observed drops in values for both of these parameters and accompanying rise in pH during the diatom and *Phaeocystis* blooms. Fractionation of carbon isotopes occurs during uptake, fractionation potentially occurring both during diffusion of $CO_{2\,(aq)}$ across the algal cell membrane and during enzymatic carbon fixation (O'Leary, 1981). Preferential uptake of ^{12}C during these fractionating steps results in organic carbon within phytoplankton being isotopically depleted with respect to dissolved inorganic carbon and results in isotopic enrichments in the latter. Dissolved inorganic carbon then becomes progressively isotopically enriched as the bloom progresses according to a Rayleigh distillation model as described in Chapter 1. Conversely, bacterial remineralisation in late summer causes a return to pre bloom values of $CO_{2\,(aq)}$, HCO_3^-, pH and $\delta^{13}C\text{-}\Sigma CO_2$.

d) Seasonal changes in Total Suspended Solids, P.O.C./ N. concentration and C:N ratios.

Seasonal changes in P.O.C. / N. concentration for the less than 200μm size fraction are shown in Figure 4.5 (a) and (b) and tabulated in Appendix 13. In certain cases the amount of filtered organic material was insufficient to obtain detectable levels of organic nitrogen.

It can be seen in Figure 4.5a that whilst P.O.C. concentrations in the less than 200μm size fraction increased at certain times of the year in association with primary productivity increases (for example during the *Phaeocystis* bloom at day 248) concentrations of P.O.C. were generally high throughout the year (195 - 774μg C dm^{-3}), even in winter in the absence of significant productivity within the water column.This is reflected in the poor correlation between [P.O.C.] and chlorophyll concentrations (slope = 0.001, R^2 = 0.03). Such concentrations of P.O.C. are much higher than the seasonal range reported by Wainwright and Fry (1994) for a similar coastal system with low salinity variation and strong tidal mixing. These workers found P.O.C. concentrations for total P.O.M. in the range 8-60 μgC dm^{-3}. Data in Figure 4.5b show concentrations of P.O.N. also to be high thoughout the year (29 -101μg N dm^{-3}), mirroring the temporal changes in concentrations of P.O.C.. These concentrations are again much higher than those reported by Wainwright and Fry (1994), who found seasonal range in particulate nitrogen concentrations to be between 1 and 7 μg dm^{-3}.

C:N ratios are shown in Figure 4.5c and tabulated in Appendix 13 .

Figure 4.5a Seasonal variation in P.O.C. concentration (< 200μm) at Menai Bridge Pier.

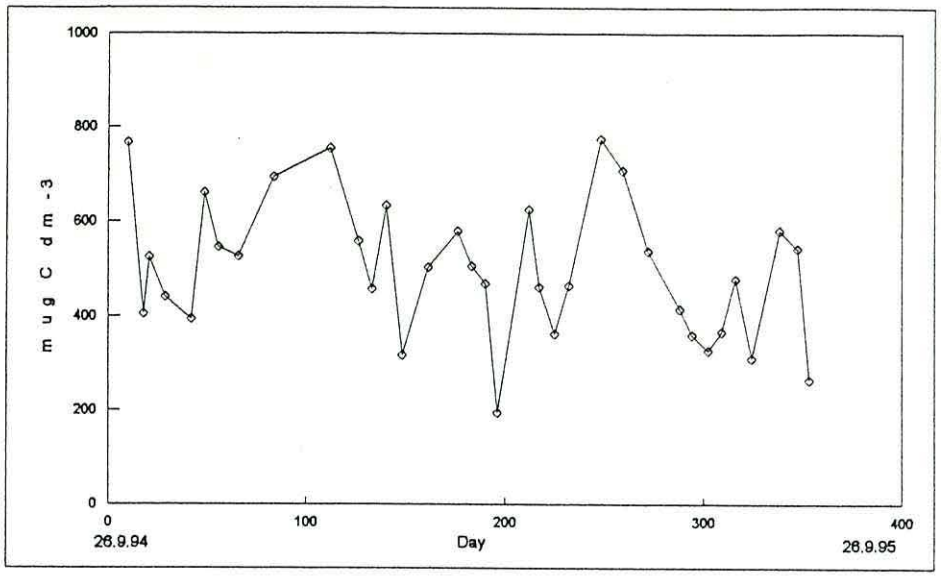

Figure 4.5b Seasonal variation in P.O.N. concentration (< 200μm) at Menai Bridge Pier.

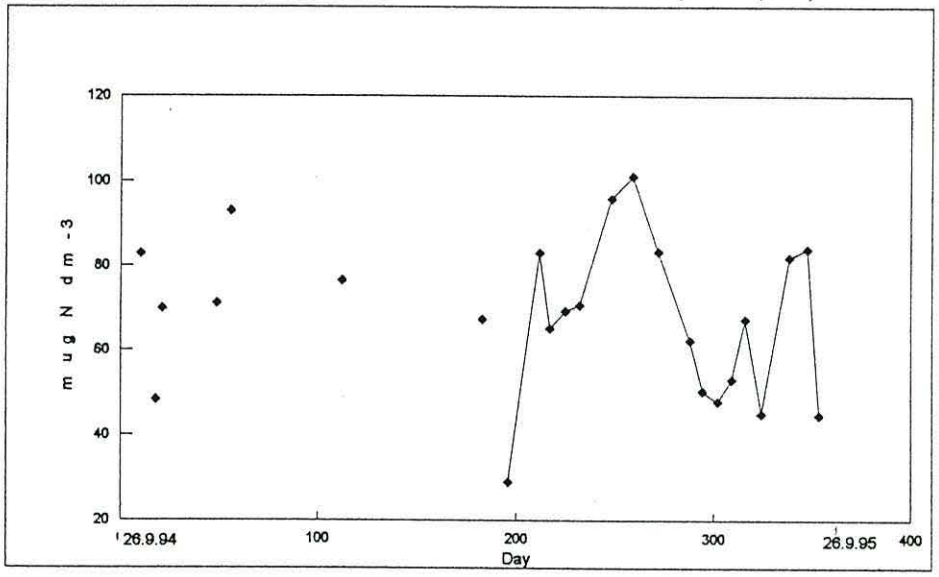

Figure 4.5c Seasonal variation in C:N at Menai Bridge Pier.

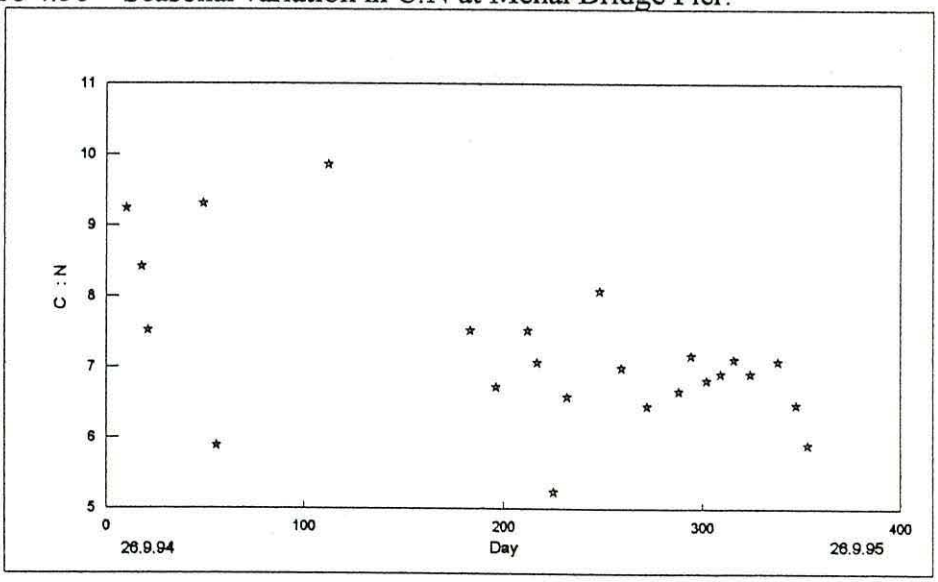

Between April and September (days 196 -353) C:N ratios were in the range 6 -8, with a low value at the peak of the *Phaeocystis* bloom of 5.2. This range is typical for phytoplankton (Cifuentes *et al.* 1988). Although data are limited for the winter period C:N ratios appeared to be slightly higher during this time (5.9 - 9.9).

Cifuentes *et al.* (1988) have suggested that P.O.C.:Chlorophyll ratios in excess of 200 were indicators of two types of organic matter in an estuary in the Delaware river (terrestrial / detrital and planktonic). Parsons *et al.* (1977) report a range in the weight to weight ratio of P.O.C:Chlorophyll a of 20-200 for phytoplankton. At most dates, except during the main diatom and *Phaeocystis* blooms, ratios of P.O.C.:Chlorophyll were considerably higher than 200 (see Appendix 13).

Figure 4.6 shows that concentrations of total suspended solids were also high throughout the year (20 -64mg dm^{-3}) with periodic rises and falls in concentration during the summer period (days 217-324). These data are tabulated in Appendix 13.

Summarising, the annual cycle of [P.O.C./ P.O.N.], C:N, P.O.C.:Chlorophyll, and total suspended solids show the Menai Strait to be a regime that is well mixed throughout the year by strong tidal mixing, with high organic loading throughout the year. The data appear to show that whilst phytoplankton are a significant component of the particulate organic material in the water column during the spring and summer, other sources of organic matter are prevalent throughout the year and make up a significant component of the P.O.M. outside the spring and summer periods.

4.4.2. Seasonal variation in *Pecten* shell growth and microgrowth patterns

a) Seasonal variation in shell accretionary rate.

Shell accretionary rate data for juvenile *Pecten maximus* placed in the Menai Strait for periods of approximately one month during the year October 1994 - September 1995 are shown in Figure 4.7 and tabulated in Appendix 14. Shell accretionary data (mm per day) for individual scallops during each time period are presented for different regions of the shell i.e. at the midline, the second ray in from the lateral margin and at the basal ear.

Figure 4.6 Seasonal variation in Total Suspended Solids (<200μm) at Menai Bridge Pier October 1994 - September 1995.

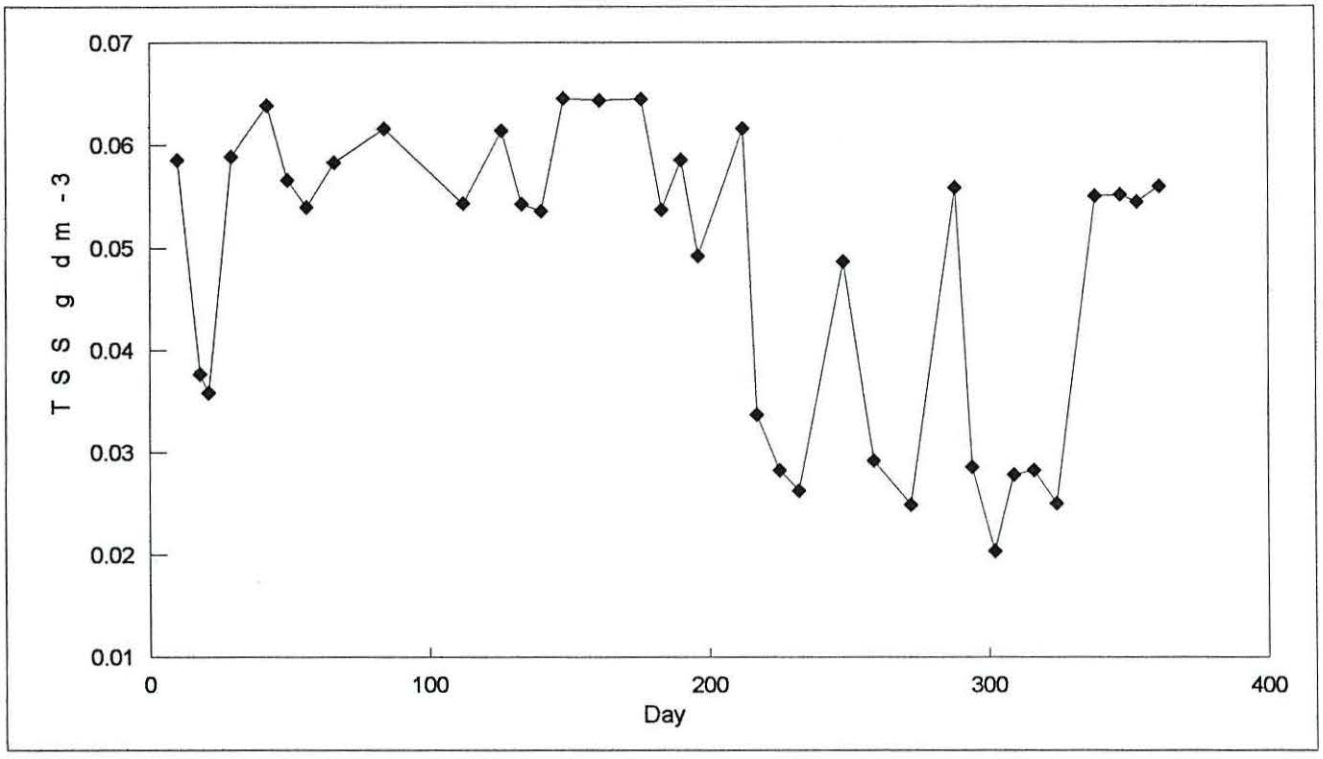

Figure 4.7. Seasonal variation in juvenile *Pecten maximus* shell growth in the Menai Strait
a) Variation in accretionary rate at the midline.

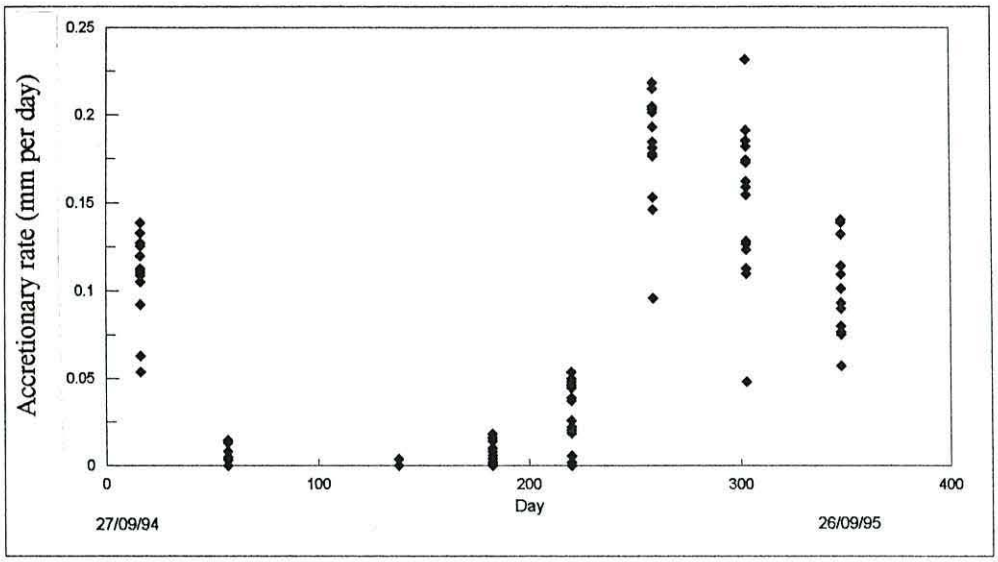

b) Variation in accretionary rate in the second ray.

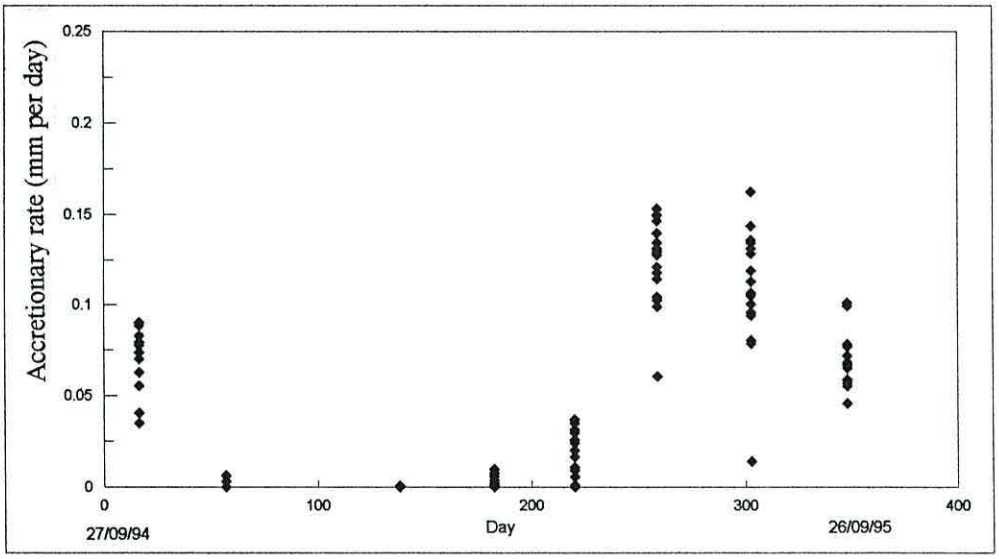

c) Variation in accretionary rate in the basal ear.

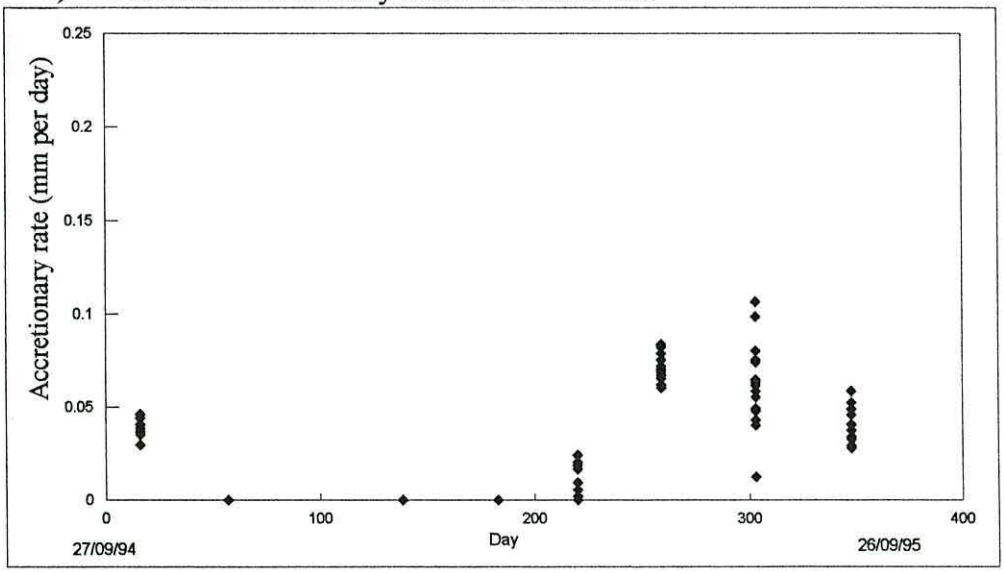

Pecten maximus shell growth exhibited a distinct seasonal pattern. Accretionary rates at the midline decreased during the autumn of 1994 to a minimum during January - February 1995 (days 121-154) when shell deposition was zero in nearly all individuals (Figure 4.7a). Accretionary rates began to increase during the period mid March - mid April (days 168 - 197) and continued to rise through May to a maximum in the period spanning the beginning of June to mid August (days 242-325). During June accretionary rates were of the order 0.186 mm day^{-1} ($1\sigma = 0.04$) and during mid July - mid August accretionary rates were of the order 0.153 mm day^{-1} ($1\sigma = 0.03$) Shell growth rates then decreased during September (days 330-364).

This pattern exhibited at the midline, (where accretionary rates decreased during the autumn to a minimum in the winter (January - February), then began to rise again at the end of March to a maximum during June-August) was also found in the second ray and basal ear (Figure 4.7 b and c). Due to allometric growth accretionary rates were however proportionately lower in these regions of the shell when compared to the midline. Shell growth in the second ray was linearly related to growth at the midline but proportionately reduced by 31% ;

Increment $day^{-1}_{\{2nd\ ray\}} = 0.69$ increment $day^{-1}_{\{midline\}}$ -0.001, $R^2 = 0.98$, n = 116).

Shell growth in the basal ear was also linearly related to growth at the midline but proportionately reduced by 61%;

Increment $day^{-1}_{\{basal\ ear\}} = 0.39$ increment $day^{-1}_{\{midline\}}$ -0.009, $R^2 = 0.96$, n = 110).

Seasonal variation in shell accretionary rate is compared with seasonal variations in water temperature, chlorophyll concentrations and P.O.C. concentrations in Figure 4.8 a - c. Seasonal changes in shell growth rate were independent of P.O.C. concentration. Changes in shell growth rate during the autumn and spring coincided with synchronous decreases or increases in both water temperature and chlorophyll concentration. Low temperatures and low chlorophyll concentrations during the winter were coincident with low growth rates and the period of growth cessation occurred when water temperatures and chlorophyll concentrations were at their lowest. Highest shell growth rates occurred in June, during and after the *Phaeocystis* bloom, when chlorophyll levels were at a maximum but 2 months before water temperatures reached a maximum. Shell growth rates at this point were higher than during the preceding autumn when water temperatures were comparable.

Figure 4.8. Seasonal variation in juvenile *Pecten maximus* shell growth and environmental variables in the Menai Strait a)Variation in accretionary rate at the midline and water temperature.

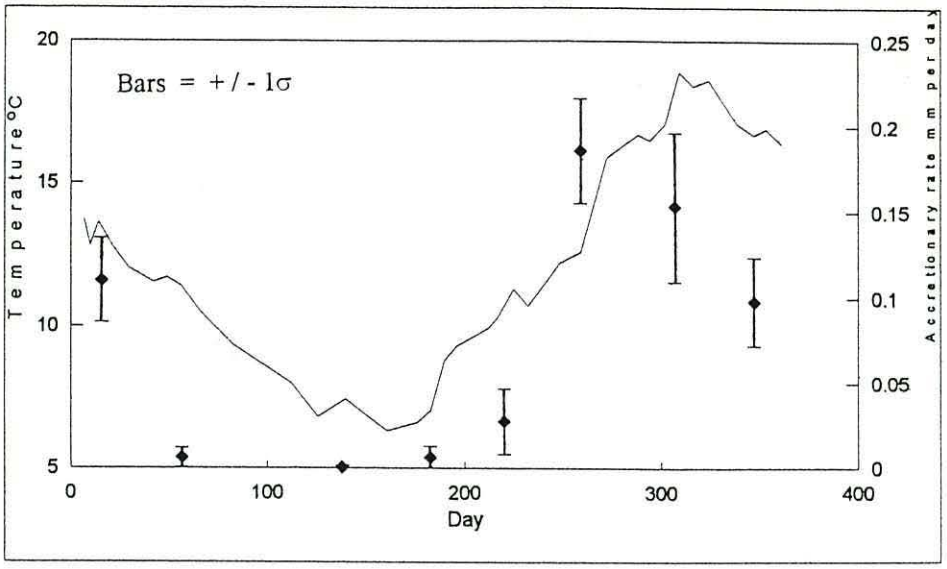

b) Variation in accretionary rate at the midline and chlorophyll concentration.

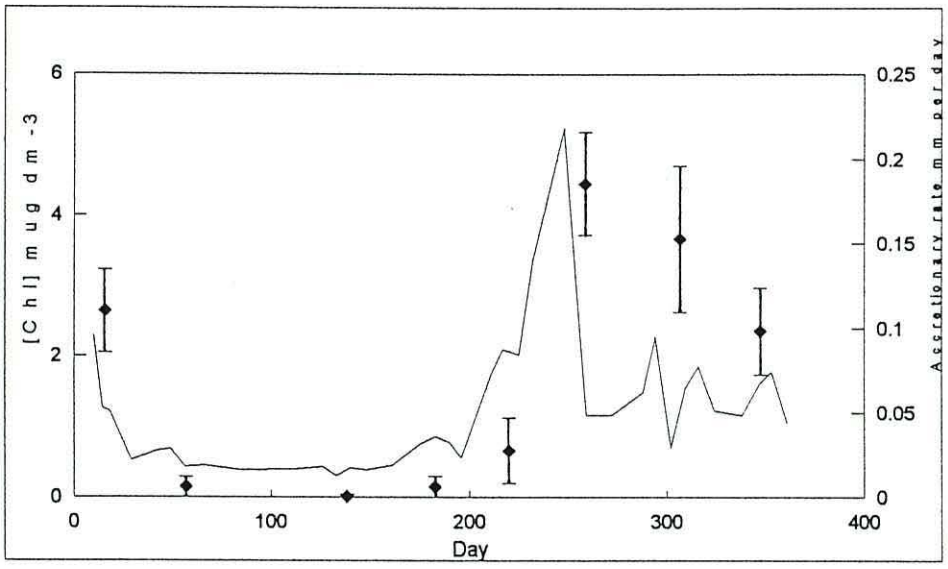

c) Variation in accretionary rate at the midline and P.O.C. concentration.

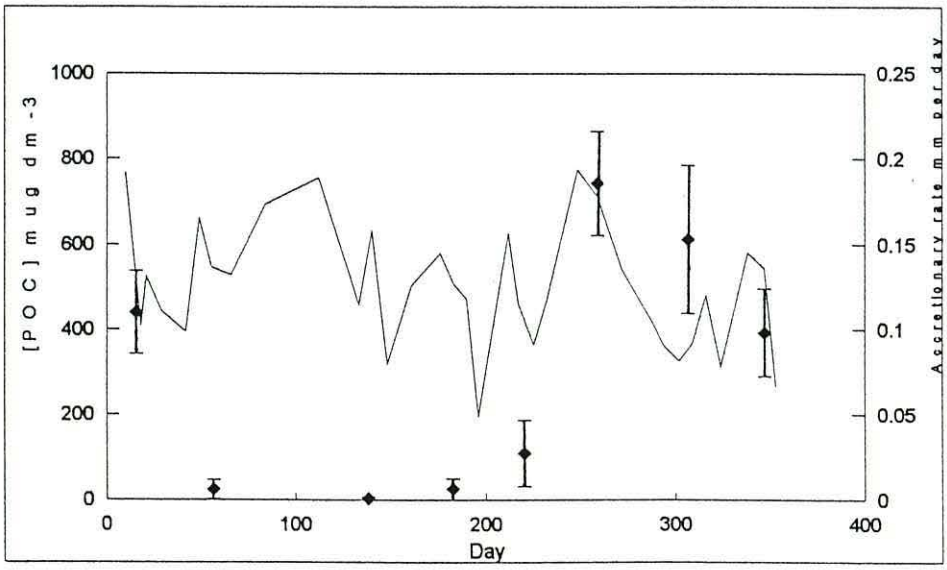

Growth rates remained high during the period of maximum water temperature, chlorophyll levels at this time being comparable or higher than in early spring. The decrease in growth rate in September however occurred when both water temperatures and chlorophyll concentrations remained high and growth rates at the midline were consequently found overall to display only a weak correlation with temperature ($R^2 = 0.60$) see Figure 4.9)

In summary, either water temperature, chlorophyll concentration or both of these environmental variables may have influenced seasonal shell growth rate in *Pecten maximus* within this study. It is not possible however to identify whether one or both of these variables was a determining factor from the available data. A further factor (other than water temperature and concentrations of chlorophyll and P.O.C. concentration) must also have influenced shell growth rate in the autumn periods.

The shell growth rate data obtained within the field study allow an assessment to be made of the variation in time integrated for a given shell sampling protocol associated with different growth rates exhibited by *Pecten maximus* during the year. Variation in time integrated for a sampling protocol in which samples of width 1.5mm are drilled along the midline shell axis for isotopic analysis are shown in Table 4.1. Time integration was lowest during periods of maximal shell growth rate in the summer, averaging between 8 and 10 days per carbonate sample. Integration was slightly higher during the autumn at between 13 and 15 days, reflecting the decreases in shell growth rate at this time. Between late autumn and early spring, time integration was markedly higher, averaging 245 days and 241 days in the periods mid November - mid December and mid March - mid April, with maximum integration occurring during the period of growth cessation in February. Integration time remained high throughout the spring, averaging 55 days per carbonate sample. Between late autumn and spring the percentage of animals not exhibiting shell growth also increased from 29% to a maximum of 87% in February, then decreased to 13% in May. Only during the summer and early autumn was significant shell growth exhibited by all individuals.

b) Seasonal variation in shell microgrowth patterns

Figure 4.9. The relationship between shell growth rate at the midline and water temperature for *Pecten maximus* placed in the Menai Strait

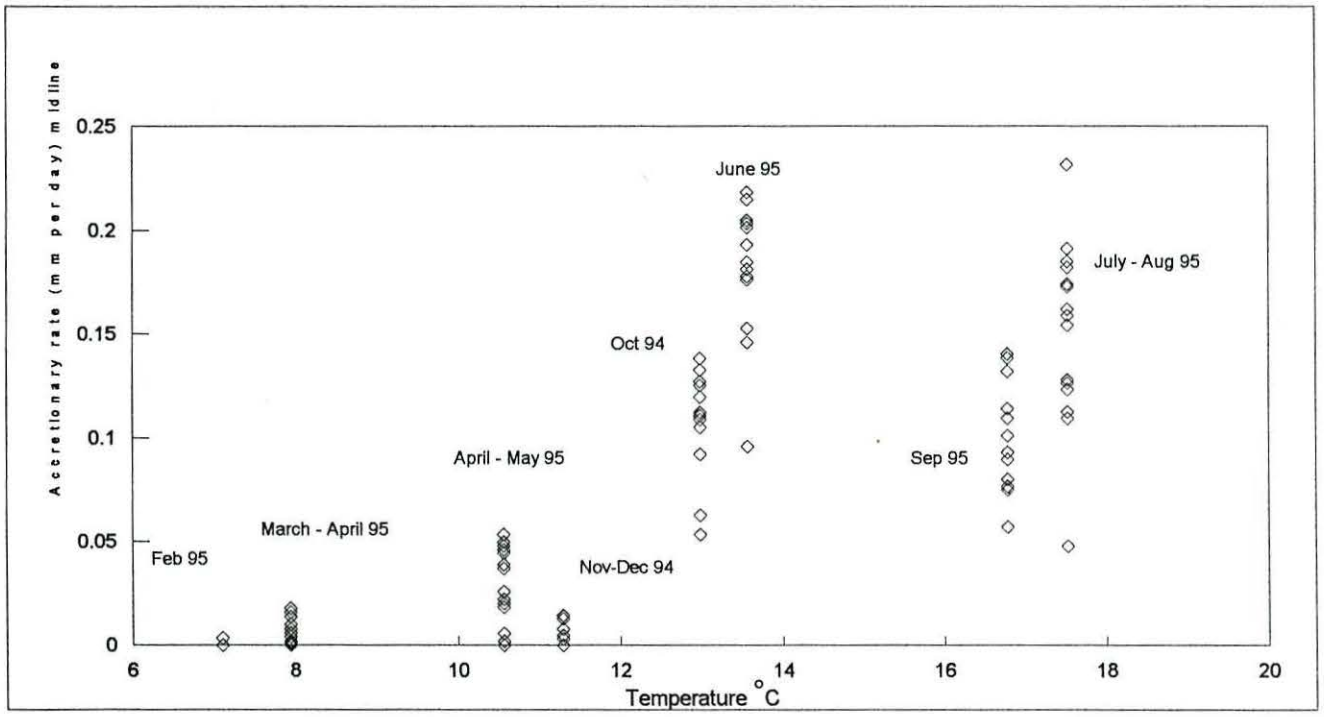

Table 4.1. Seasonal variation in a) percentage of individuals not exhibiting shell growth and b) time integration per carbonate sample drilled along the midline axis of the shell (employing a 1.5mm sampling protocol).

Period	Mean Shell growth rate at Midline mm day^{-1}	Mean Time Integrated per sample (Days)	% non - growers
October 1994	0.110	13.7	0
November-December 1994	0.006	245.0	29
February 1995	< 0.000	3346.9	87
March-April 1995	0.006	241.2	25
April - May 1995	0.027	54.7	13
June 1995	0.186	8.1	0
July -August 1995	0.153	9.8	0
September 1995	0.098	15.3	0

Apart from the first group of scallops placed in the Menai Strait during October 1994, all individuals deposited well - defined striae at the midline, second ray and basal ear on the surface of the upper valve, as shown in Plate 4.4. Only a few individuals deposited striae in the October 1994 period in the midline. However, all individuals within this group deposited well - defined striae at the second ray and basal ear. Figure 4.10. shows that seasonal variation in the number of striae deposited per day at the midline exhibited a distinct seasonal pattern, increasing during the spring to an average of 1.03 - 1.06 striae per day in June - July, then decreasing in the autumn to minimum values during the winter. The number of striae per day and shell growth rate at the midline were well-correlated. (Figure 4.11 a)

Figure 4.10 shows that the patterns of seasonal variation in the number of striae per day deposited at the second ray and the basal ear were identical to that found at the midline, but proportionately lower by a factor of 10% and 51% respectively i.e.;

striae no. per day $_{\{2nd\ ray\}}$ = 0.90 striae no. per day $_{\{midline\}}$ -0.02, $R^2 = 0.98$, n = 98.

striae no. per day $_{\{basal\ ear\}}$ = 0.49 striae no. per day $_{\{midline\}}$ -0.01, $R^2 = 0.95$, n = 94.

Again, striae number per day at the second ray and basal ear were well - correlated with shell growth rates in these regions of the shell (Figure 4.11 b, c).

The seasonal variation in striae width in the midline and second ray are shown in Figure 4.12 a,b. It was not possible to measure striae widths within the basal ear accurately using the binocular microscope at high magnification. Striae widths at the midline showed a distinct seasonal pattern. During late autumn and early spring striae widths were narrow, averaging 0.05mm. In the period covering mid April to mid May striae widths then increased (averaging 0.13mm). Striae widths were at a maximum throughout the period June - September , averaging 0.19 - 0.21mm. The seasonal pattern exhibited in the second ray was identical to that found at the midline, but proportionately lower by 38%, although data exhibited a high level of variability i.e.;

striae width mm $_{\{2nd\ ray\}}$ = 0.62 striae width mm $_{\{midline\}}$ + 0.018 $R^2 = 0.73$.

Figure 4.12 shows that striae widths were not only at a maximum during the summer and autumn of 1995, but also were maximal in the preceding autumn (October 1994). Striae widths were correlated with shell growth rates at both the midline and second ray.

Plate 4.4. Surface microgrowth patterns on the upper shell valve of *Pecten maximus* placed for approximately one month in the Menai Strait. The clear disturbance mark associated with the beginning of the period in the field is indictated (D)
a) surface striae at the midline.

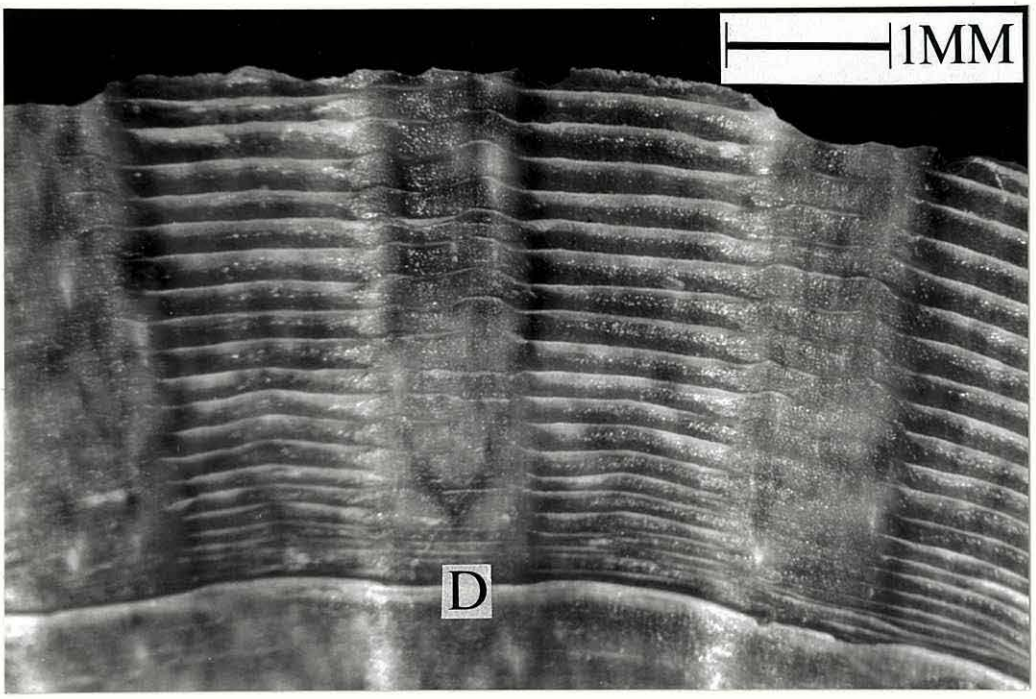

b) surface striae within the basal ear

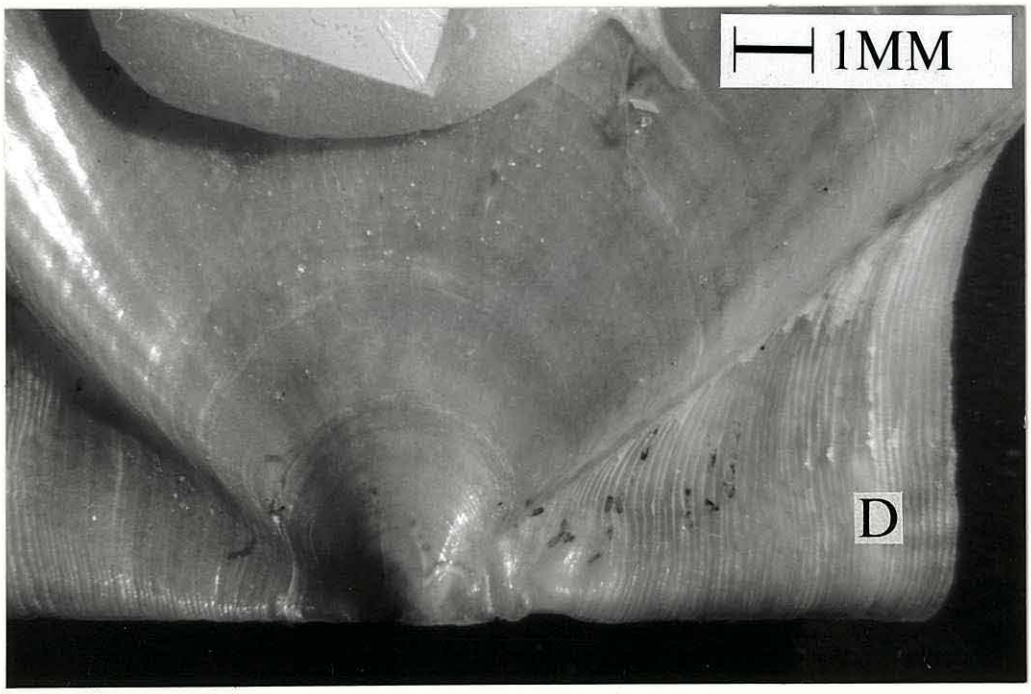

Figure 4.10. Seasonal variation in striae number of *Pecten maximus* grown in the Menai Strait.

a) Number of striae per day at the midline.

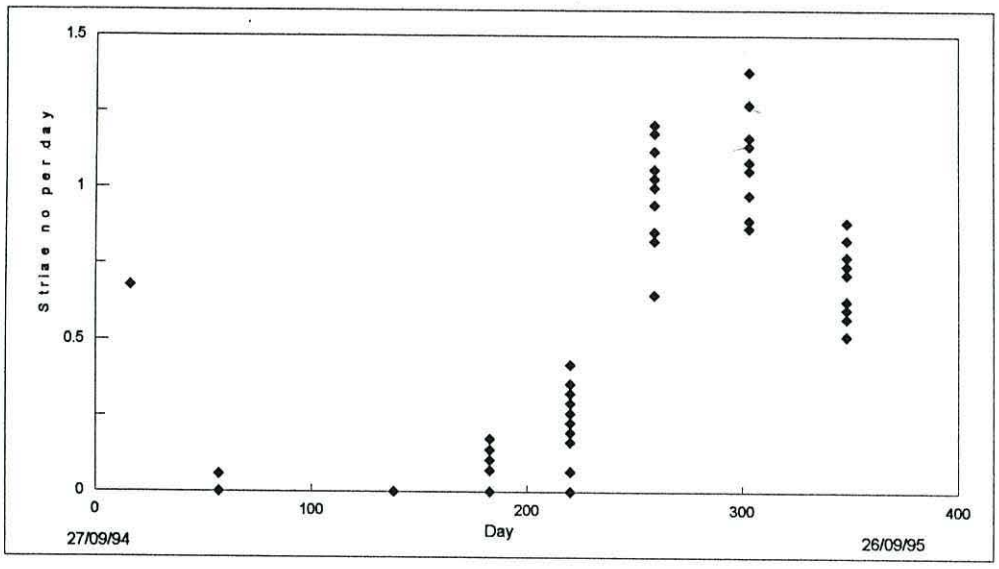

b) Number of striae per day in the second ray.

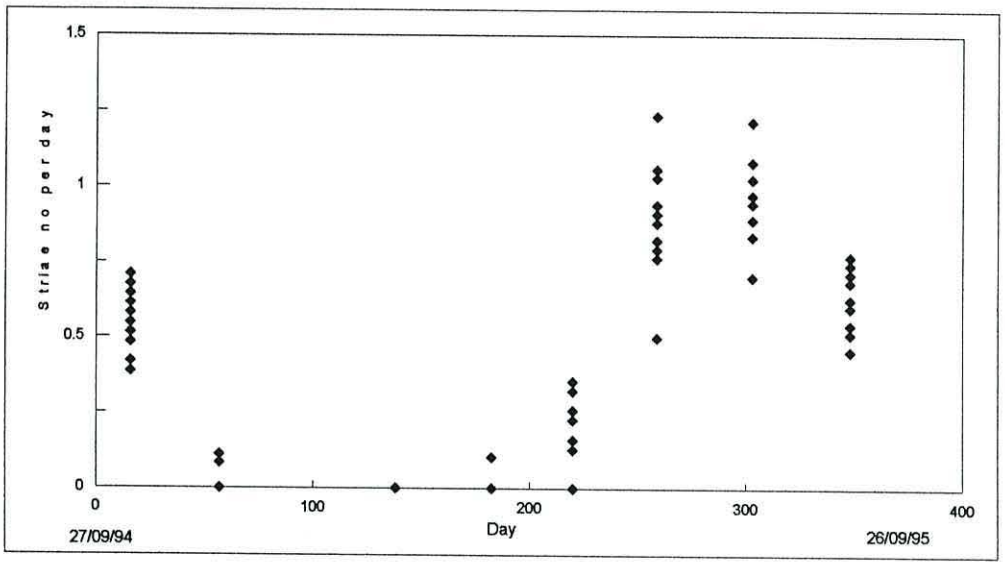

c) Number of striae per day in the basal ear.

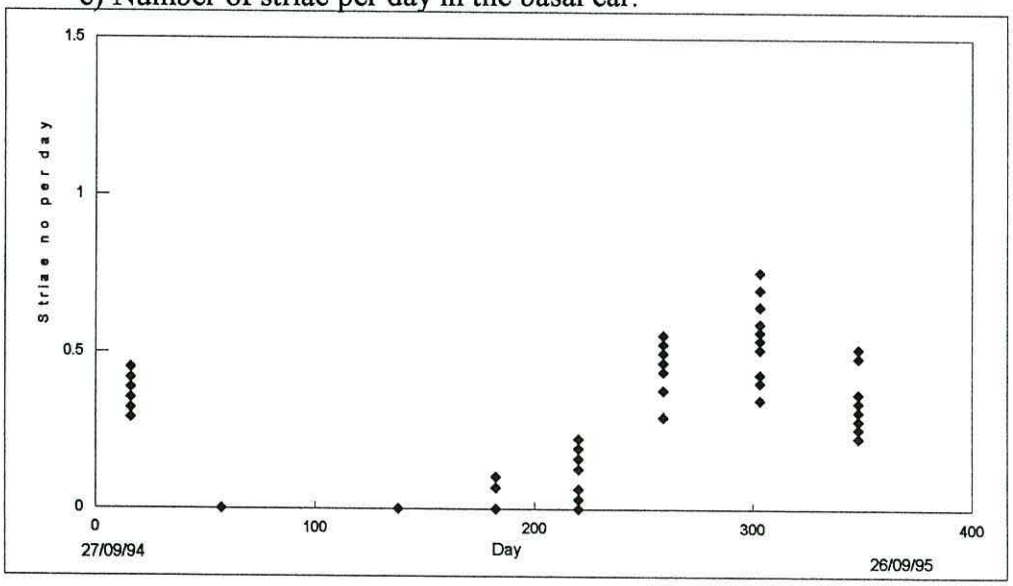

Figure 4.11.The relationship between number of striae deposited per day and shell growth rate for *Pecten maximus* grown in the Menai Strait. a) midline.

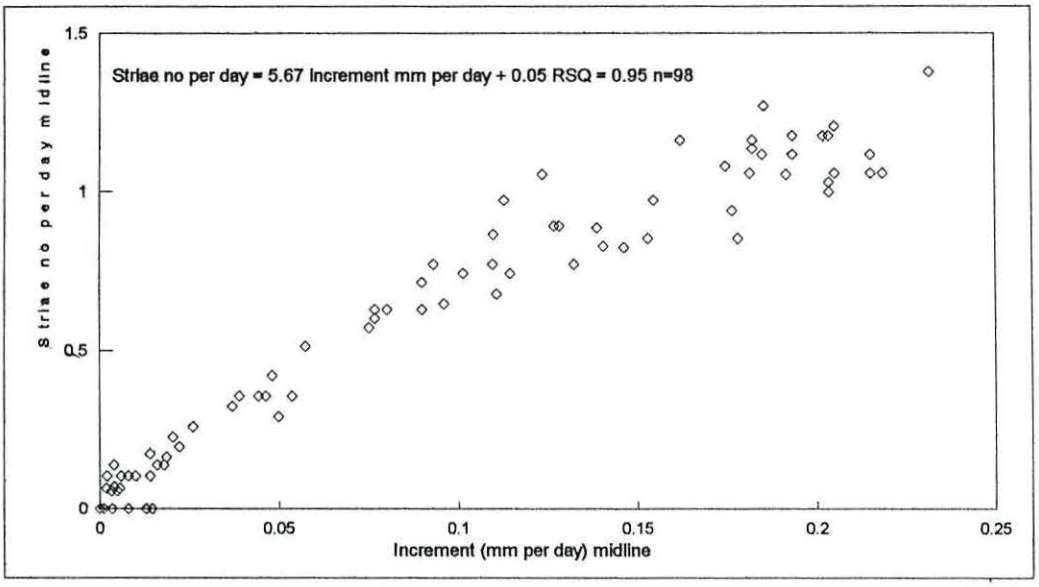

b) Second ray.

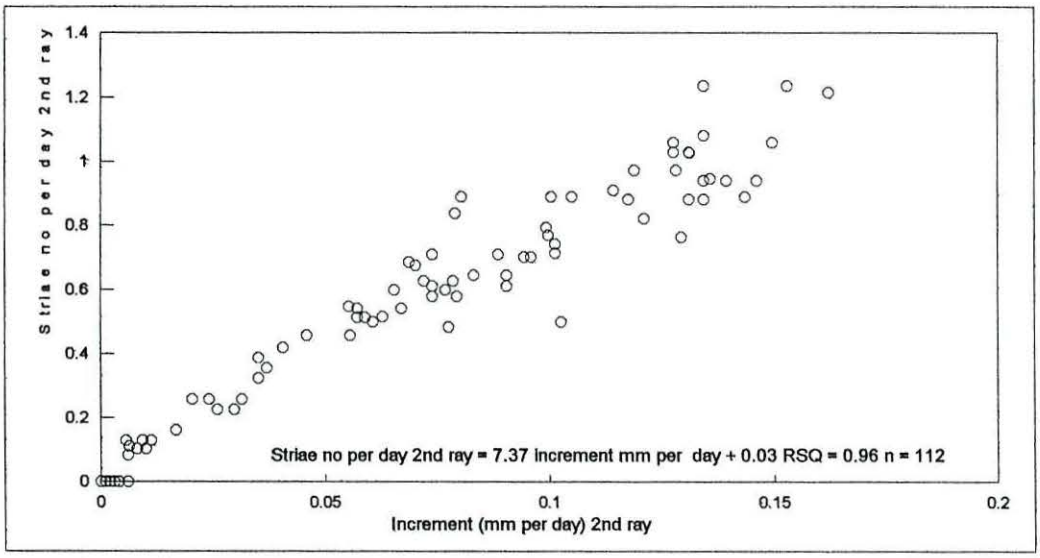

c) Basal ear.

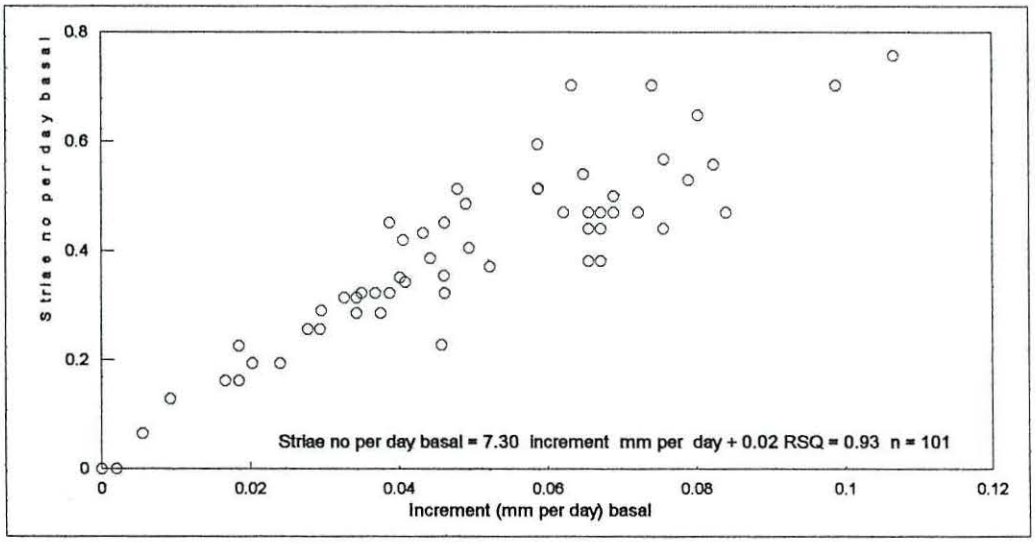

Figure 4.12. Seasonal variation in striae width of *Pecten maximus* grown in the Menai Strait.
a) midline

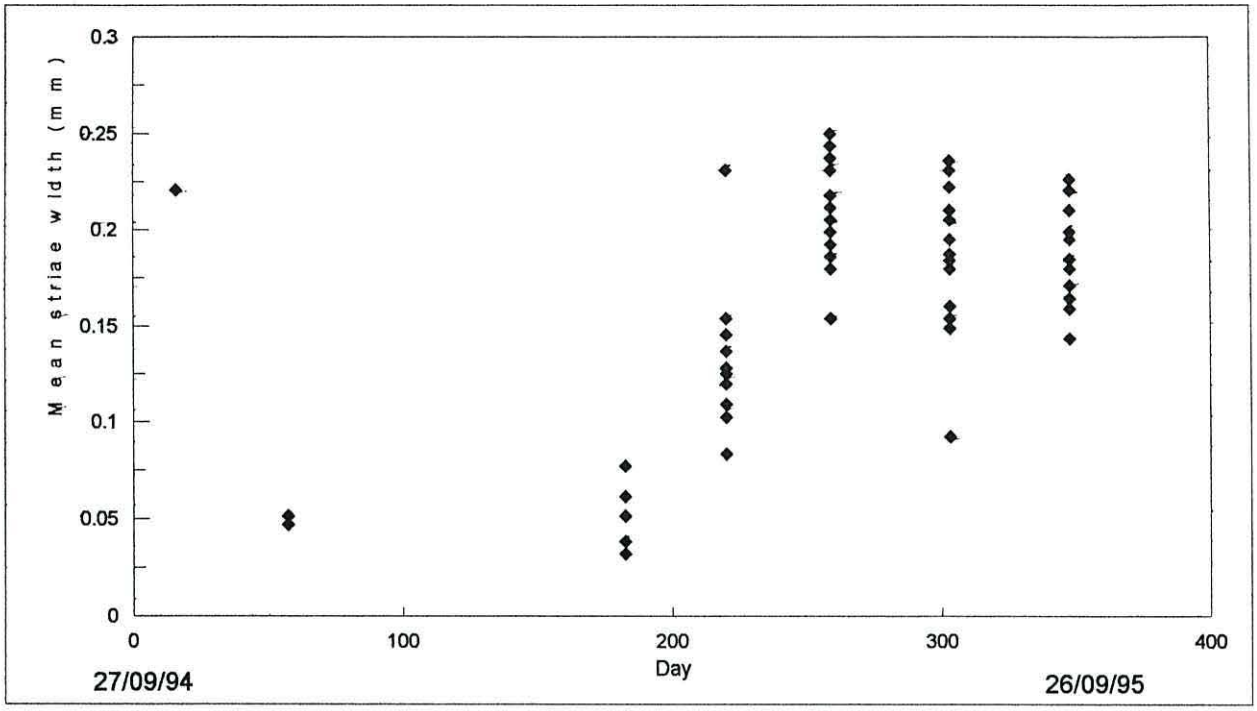

b) Second Ray

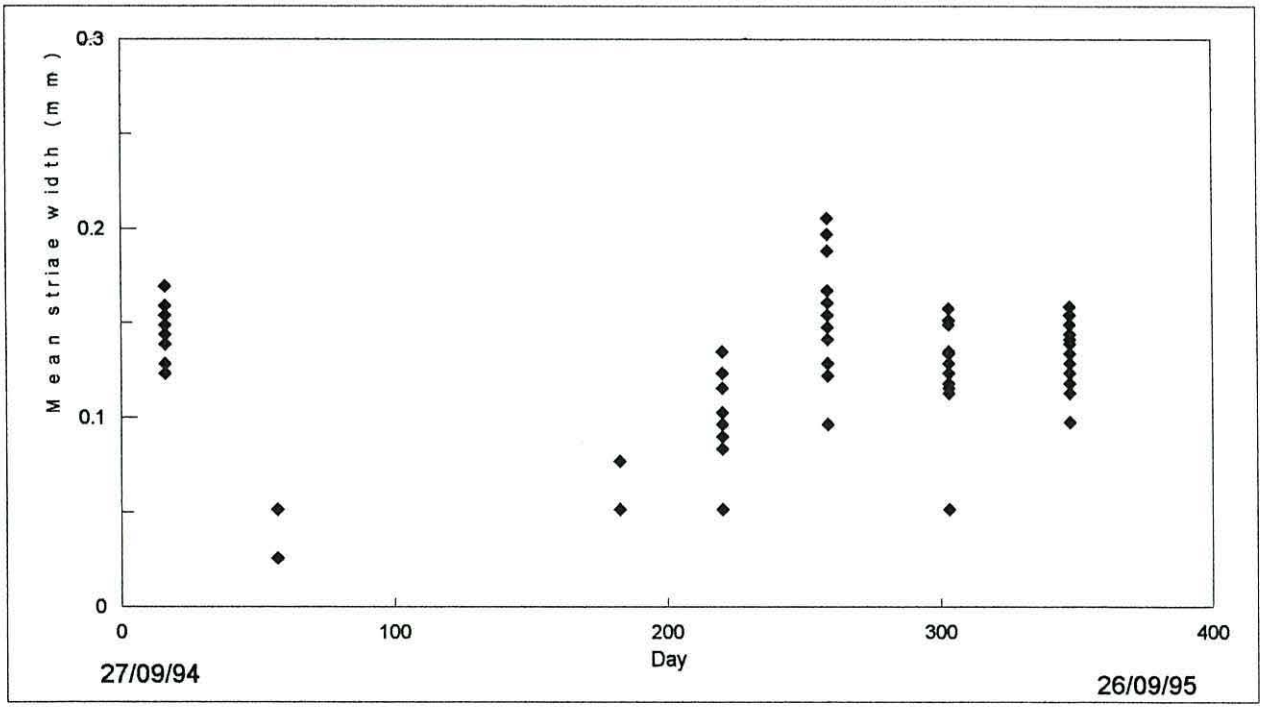

Unlike the linear relationships found between number of striae deposited per day and shell growth rate in all regions of the shell, the relationship between striae width and growth rate appeared to be curvilinear (Figure 4.13). Striae widths at the midline appeared to increase with increasing shell growth rate up to growth rates of approximately 0.1 mm day^{-1} at which point striae widths reached a maximum value of between 0.2 and 0.25mm. Similarly, striae widths at the second ray appeared to reach a maximum of between 0.1 and 0.15mm at growth rates above 0.05mm day^{-1}.

Figure 4.14.a) shows the seasonal pattern of striae abundance (i.e. number of striae per mm) at the midline. High striae abundances (i.e. high numbers of striae per mm) were observed during the late autumn and winter. During March - April striae abundances decreased, with consistently low values during June - October. During this period striae abundances averaged between 5.8 striae per mm in June to 7.3 striae per mm in September.The pattern of striae abundances found at the midline was also found at the second ray (Figure 4.14 b.), but proportionately lower by 39%, although data exhibited a high level of variability i.e.;

striae per mm $_{\{2nd\ ray\}}$ = 0.61 striae per mm $_{\{midline\}}$ + 4.16, $R^2 = 0.50$, n = 61.

An inverse relationship between striae abundance and shell growth rate existed at both the midline and second ray and, as in the case of striae widths, appeared to be curvilinear (Figure 4.15 a, b) Minimum striae abundances of between 6 - 8 striae per mm were found at the midline at growth rates in excess of 0.025mm day^{-1}.

Changes in striae abundance and width between the disturbance mark and valve margin for scallops placed in the Menai Strait for the entire year October 1994-September 1995 are presented in Figure 4.16. All individuals showed a distinct peak in striae abundance at between 5 and 10mm from the disturbance mark, abundances rising sharply to between 12 and 13 striae per mm and then falling sharply again. Either side of this peak abundances were fairly constant at between 4 and 7 striae per mm. Striae widths also showed a distinct drop to below 0.1mm at between 5 and 10mm from the disturbance mark in all individuals. This drop to narrow striae widths always coincided with the peak in striae abundance and often coincided with the deposition of a white growth ring. After this drop, striae widths rose steadily to values consistently between 0.2 and 0.25mm.

Figure 4.13 a The relationship between striae width and shell growth rate at the midline.

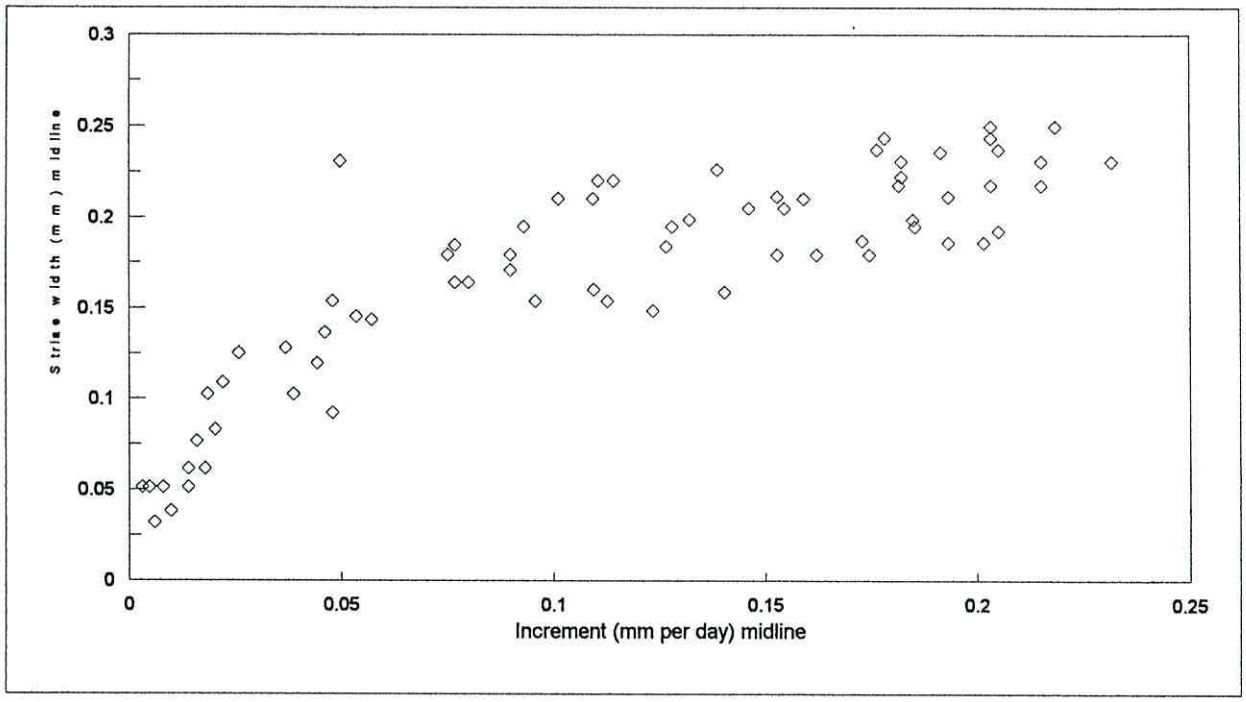

Figure 4.13 b The relationship between striae width and shell growth rate at the second ray.

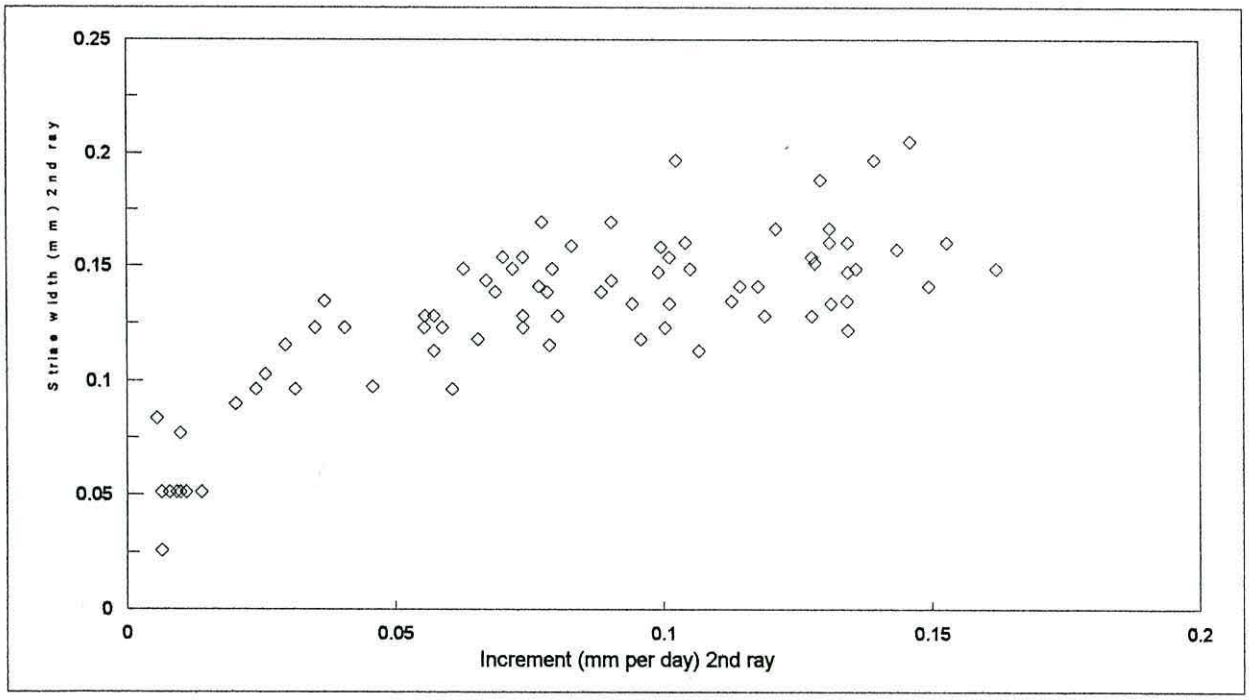

Figure 4.14. Seasonal variation in striae abundance of *Pecten maximus* grown in the Menai Strait.
a) midline

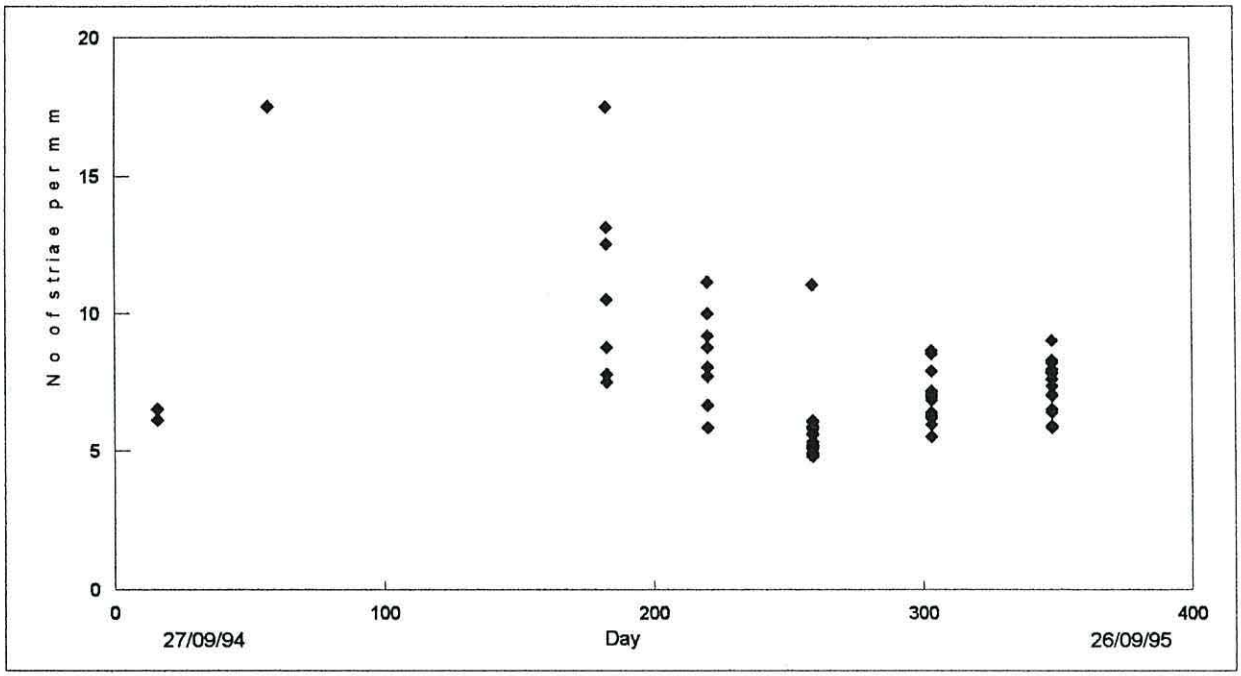

b) Second Ray

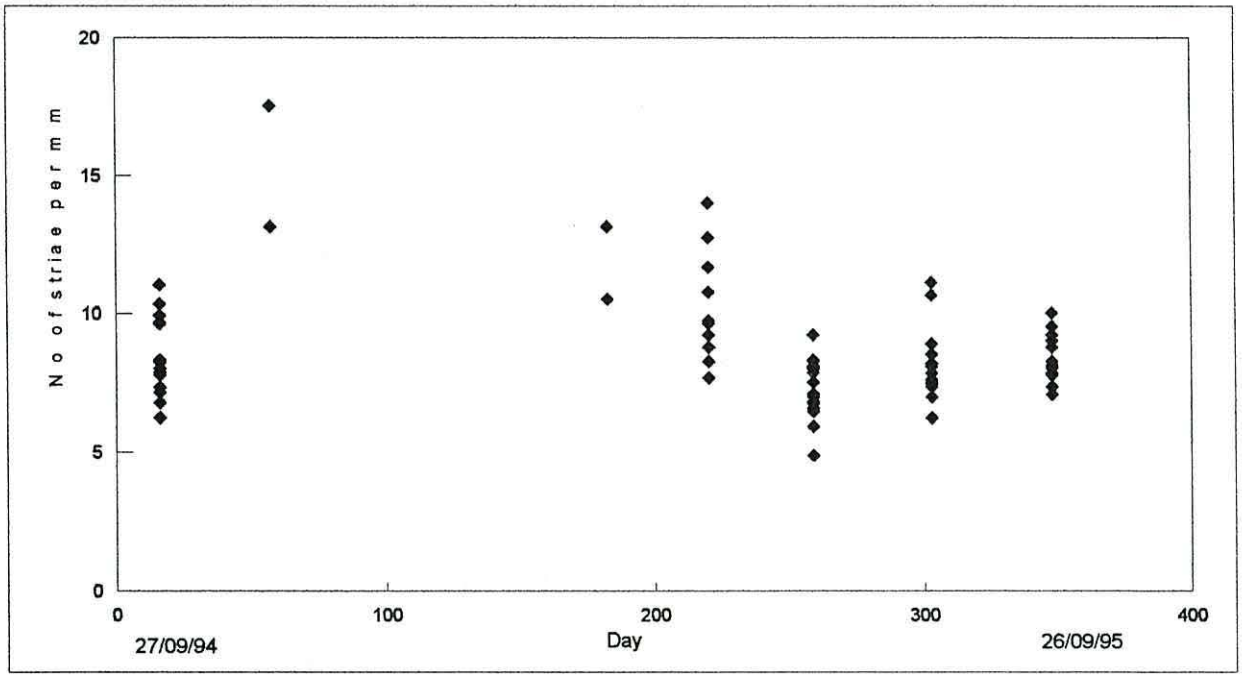

Figure 4.15 a The relationship between striae abundance and shell growth rate at the midline

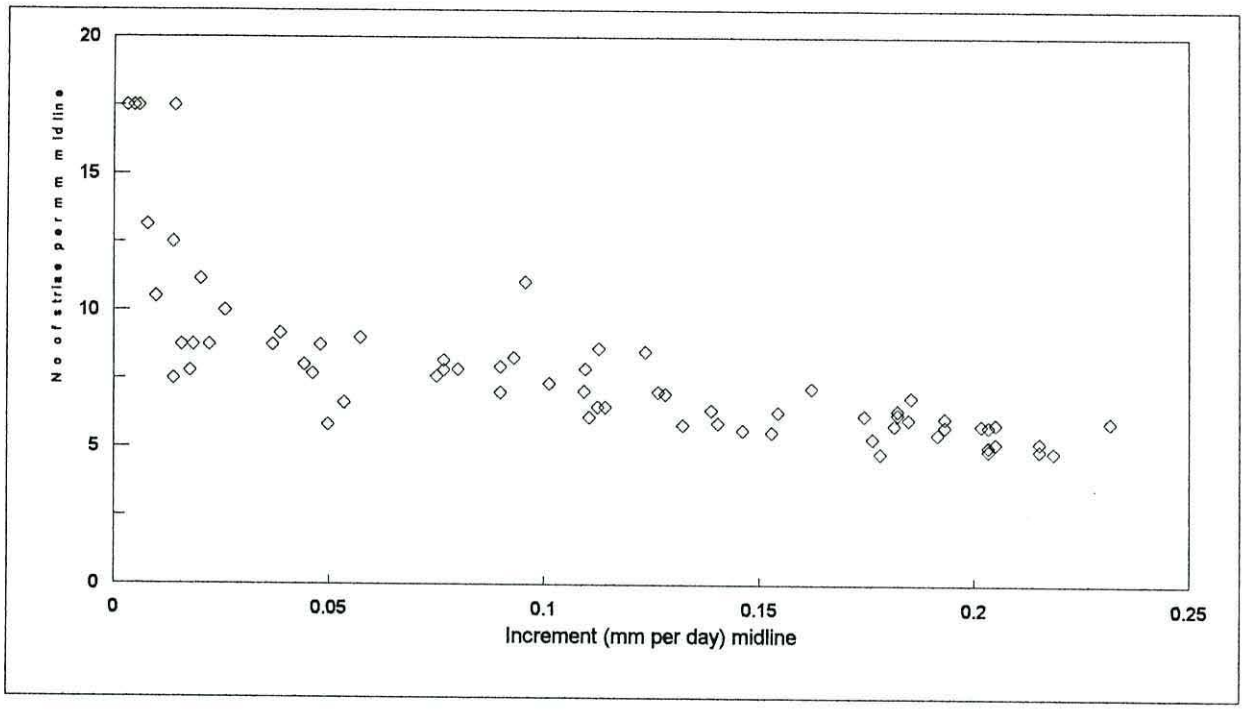

Figure 4.15 bThe relationship between striae abundance and shell growth rate at the second ray

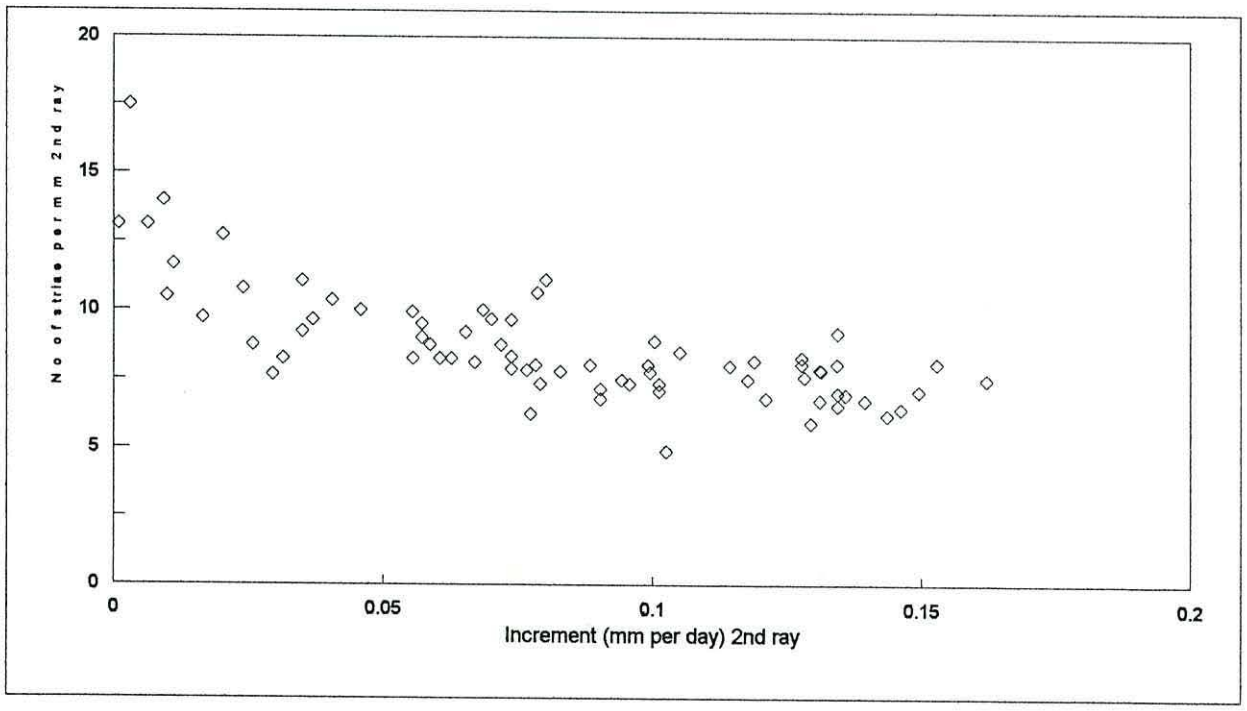

Figure 4.16. Profiles of striae abundance and striae width between disturbance mark and valve margin for *Pecten maximus* placed in the Menai Strait for the entire year October 1994 - September 1995.

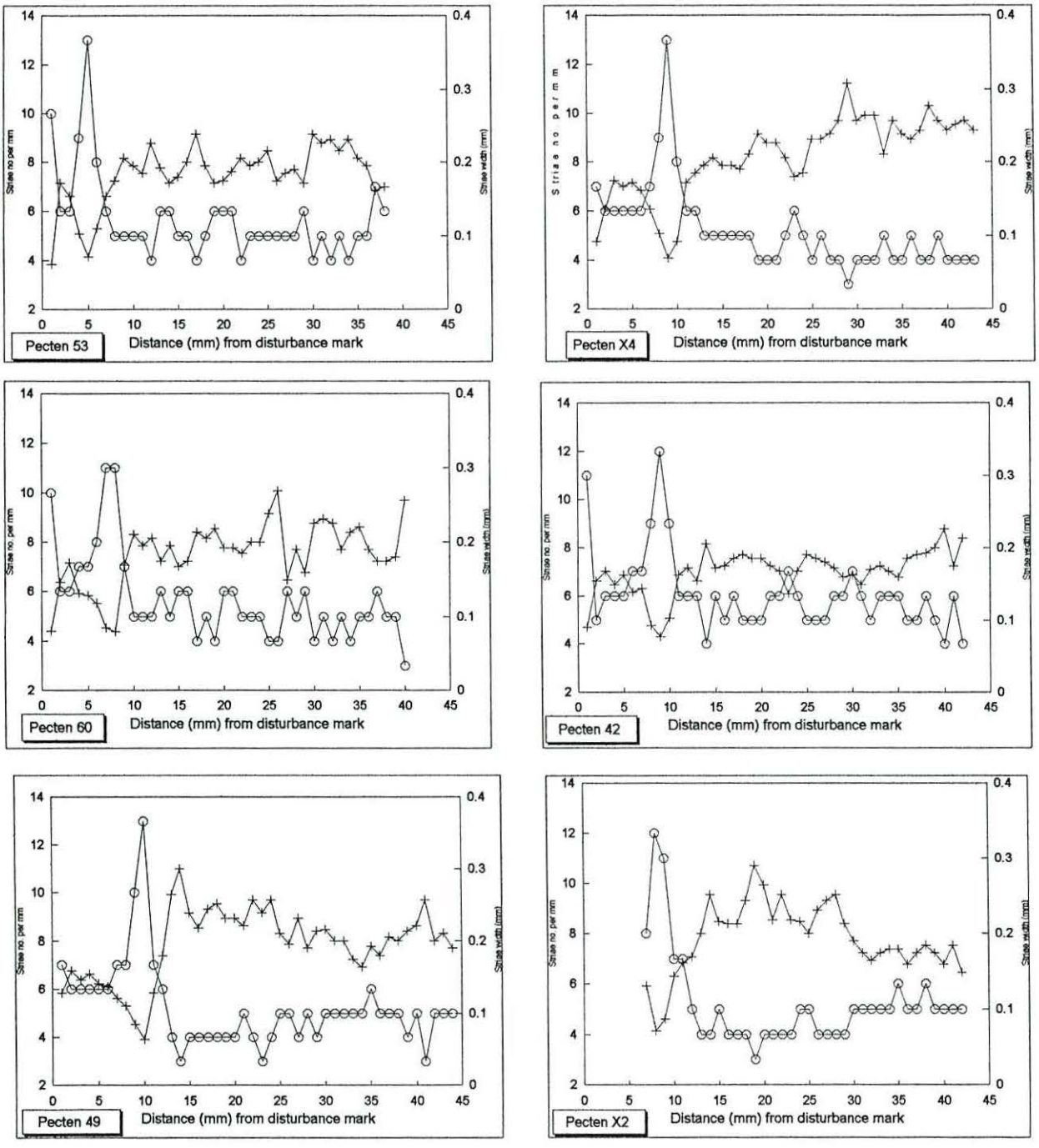

Isotopic data presented later within this chapter showed that the peaks in striae abundance and troughs in striae width coincided with the lowest water temperatures in late February -March.

The observed changes in striae abundance and width displayed within the profiles of scallops placed in the Menai Strait for one year were consistent with the seasonal patterns of abundance and width observed in scallops placed in the field for monthly periods over the year both in form and the range of values.

The relationship between striae width and abundance for pooled data obtained from scallops placed in the field for a year;

Striae width (mm) = - 0.023 striae per mm + 0.316 ($R^2 = 0.78$)

was comparable to that for pooled data obtained from scallops placed at monthly intervals over the year;

Striae width (mm) = - 0.017 striae per mm + 0.303 ($R^2 = 0.78$)

In summary, growth rate was found to be a primary controlling factor influencing striae deposition in all regions of the upper shell valve in *Pecten maximus*. Shell growth rates decreased in the autumn, with complete cessation of growth in winter. This was accompanied by a drop in the number of striae deposited per day and striae width, and a rise in striae abundance (number of striae per mm). A peak in striae abundance was observed in shell microgrowth pattern profiles when growth rates were at their lowest, coincident with a drop to narrowest striae widths. The resumption of growth in April was accompanied by a rise in the number of striae per day and increase in striae width. Striae abundances decreased at this time. The increase in shell growth rates to a maximum in June - August was coincident with maximum number of striae deposited per day ; the tail off in growth rates in September was similarly accompanied by a drop in striae deposited per day. Whilst number of striae per day closely mirrored changes in accretionary rate, striae widths were consistently high and the number of striae deposited per mm consistently low throughout the summer and early autumn, irrespective of the fall in growth rate in September. This is consistent with a linear relationship between number of striae deposited per day and growth rate, and a curvilinear relationship between striae width /striae abundance and growth rate.

This implies that whilst the number of striae deposited per day rises linearly with growth rate, there is a growth rate threshold above which both striae width and abundance reach a plateau. i.e. whilst a larger increment of shell and numerically more striae are secreted at higher growth rate there appears to be a limit to the width of individual striae.

c) Seasonal variation in *Pecten* $\delta^{18}O$ and $\delta^{13}C$ data

i) variation in isotopic data around the shell valve

As discussed previously, allometric growth of the scallop shell results in differential growth rates around the valve margin. Such variations in growth rate around the shell valve may potentially be associated with variation in any metabolic or kinetic isotope effects. Additionally, the sampling protocols employed in isotopic analysis of animals placed out for monthly intervals involved either sampling from the midline to the lateral margin or only sampling sections of the increment at the midline, and it is therefore important to ensure homogeneity of data around the valve margin. Figure 4.17. shows the results of tests whereby two scallops from the first monthly period were analysed by sequential removal of sub-sections of the increment, from the initial growth check to the valve margin, around the valve from the midline to the lateral margin. The data show that for both individuals analysed, there was no systematic variation in $\delta^{13}C$ or $\delta^{18}O$ around the valve margin. $\delta^{13}C$ data were associated with variability (1σ) of 0.052 °/oo and 0.047 °/oo for the two individuals, whilst $\delta^{18}O$ data were associated with variability of 0.120 °/oo and 0.123 °/oo for the two individuals. This variability in isotopic data around the shell valve is only marginally higher than the methodological variability.

ii) seasonal variation in *Pecten* $\delta^{18}O$ and $\delta^{13}C$ data placed in the field for approximately monthly intervals during October 1994 - September 1995.

Figures 4.18 a) and b) show isotopic data for scallops placed in the field for approximately monthly periods over the year October 1994 - September 1995. These data are also tabulated in Appendix 15.

Figure 4.17. Variation in $\delta^{13}C$ and $\delta^{18}O$ around the shell valve margin of Juvenile *Pecten maximus*

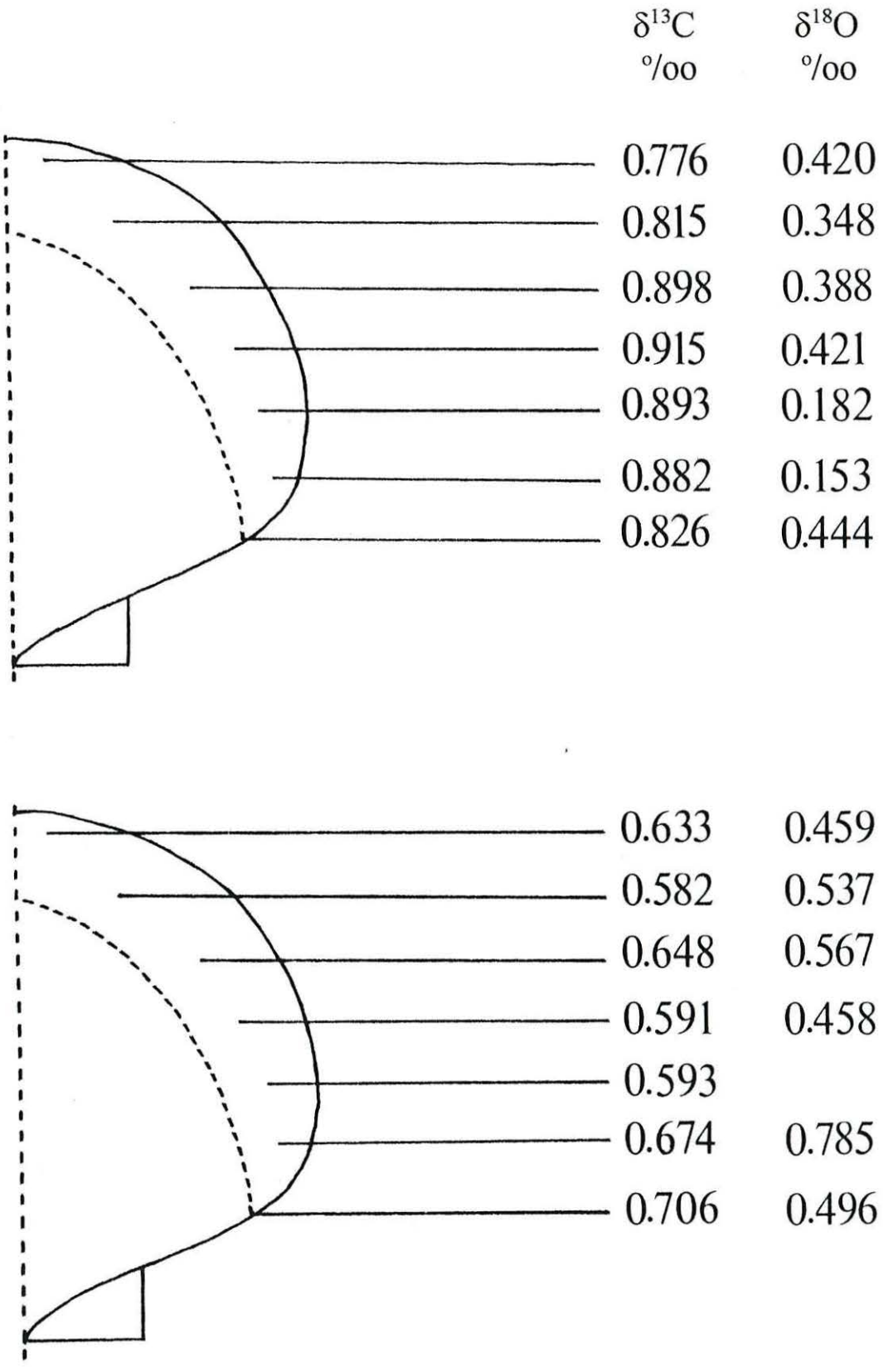

Figure 4.18. a) Seasonal variation in Predicted $\delta^{18}O$ and *Pecten* $\delta^{18}O$ for scallops placed in the Menai Strait for monthly periods October 1994 -September 1995.

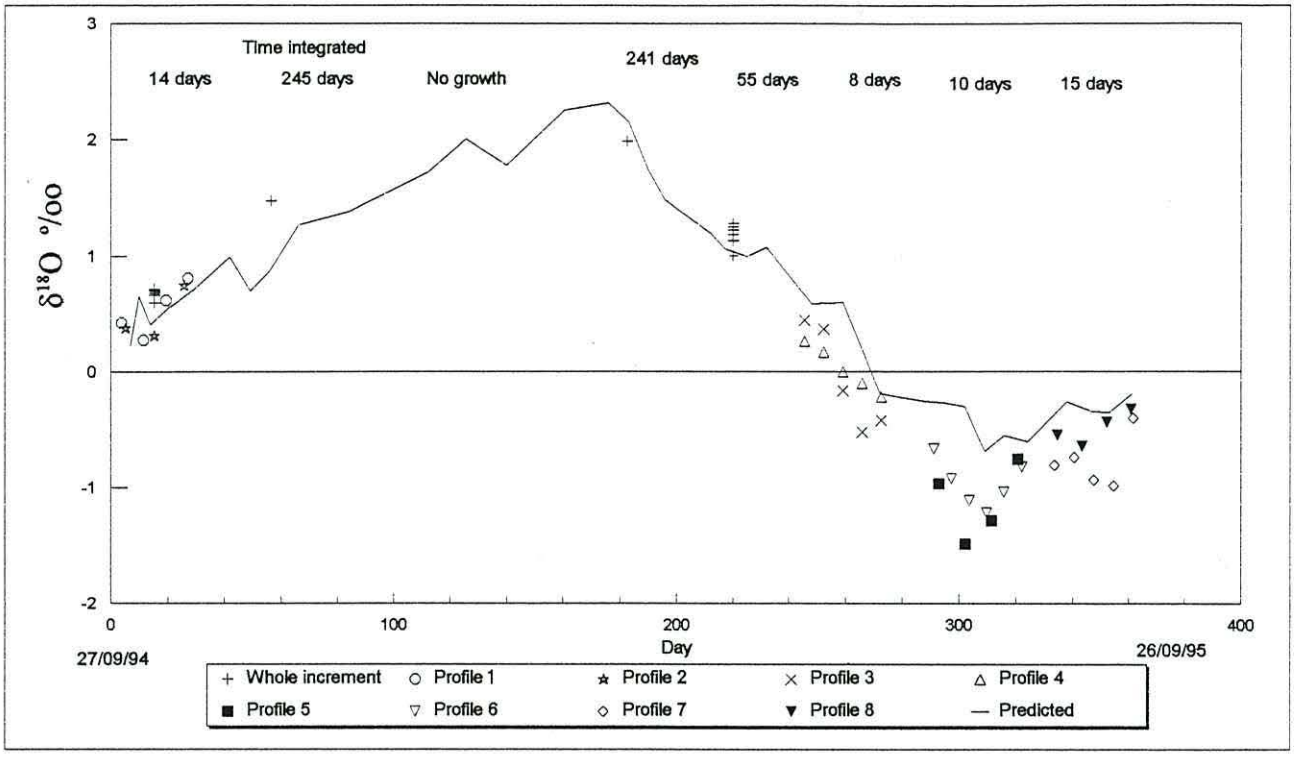

Figure 4.18. b) Seasonal variation in Predicted $\delta^{13}C$, $\delta^{13}C$ - ΣCO_2 and *Pecten* $\delta^{13}C$ for scallops placed in the Menai Strait for monthly periods October 1994 -September 1995.

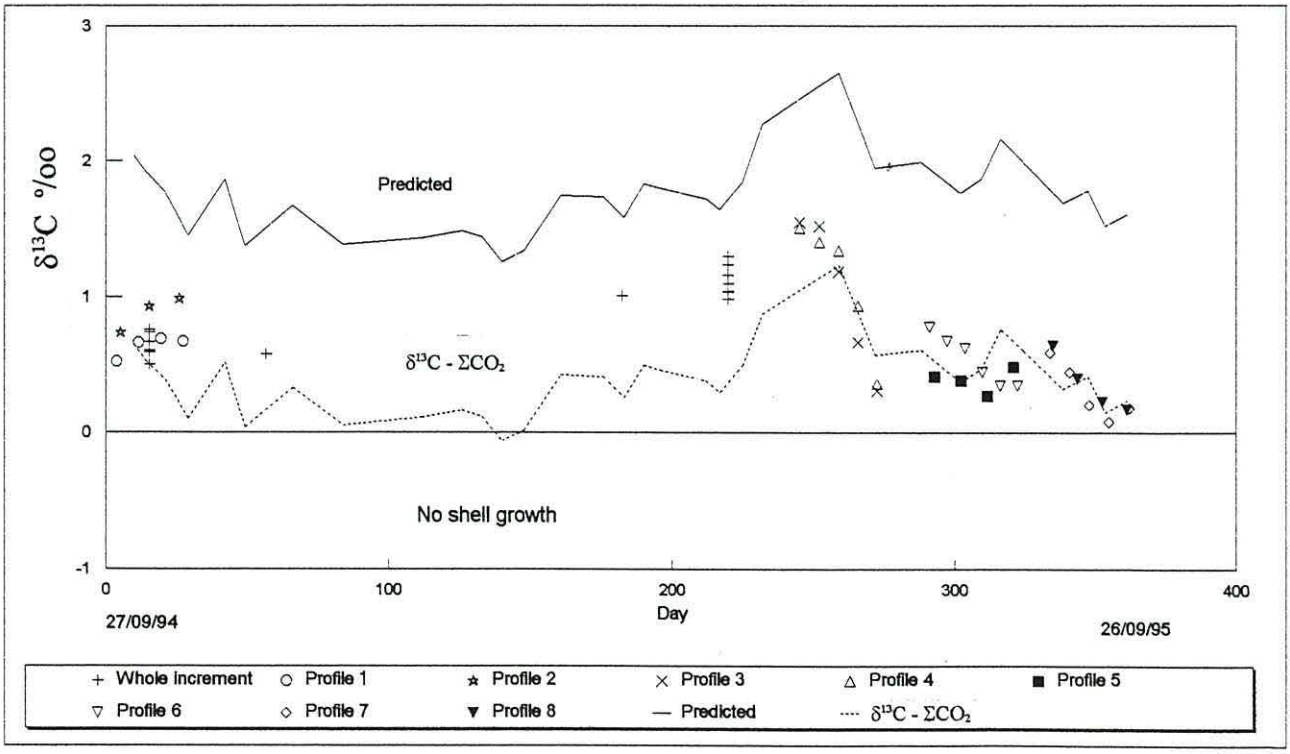

As outlined in section 4.3.1. above, three sampling protocols were employed to obtain isotopic data, dependent upon the amount of shell secreted during the time period (i) the entire increment deposited from one individual or pooled from several individuals, (ii) a subsample of shell at the midline from the disturbance mark to the valve margin or (iii) profiling at the midline, from disturbance mark to valve margin.) Two types of data are therefore shown in Figure 4.18: mean data for a specific time period ((i) and (ii)) and time series data over a specific time period (iii). For analysis, each mean increment data point was assigned to the median day for that time period. For profile data, it was assumed that within the time period shell growth rate was uniform. Each data point within the profile was assigned to a day by interpolation e.g if there were 4 data points within the profile associated with a time period of 28 days, each data point was assigned a day at 3.5, 10.5, 17.5 and 24.5 days within the period. There is therefore potential for some error when assigning isotopic data to specific days associated with any changes in growth rate between weeks within a particular time period.

Also shown in Figure 4.18 a) are predicted $\delta^{18}O$ data for calcite precipitated in isotopic equilibrium with sea water, as calculated from temperature and $\delta^{18}O$ - H_2O data collected at each sampling interval during each time period and using the rearranged O'Neil *et al.* (1969) expression as outlined in Chapter 3. Predicted $\delta^{13}C$ data for calcite precipitated in isotopic equilibrium with sea water are also shown in Figure 4.18 b). These data were calculated from $\delta^{13}C$ -ΣCO_2, pH, salinity, temperature and [ΣCO_2] data and using the equations outlined in Chapter 3. For these calculations, the enrichment factors reported by Zhang *et al.* (1995) for partitioning of carbon isotopes within the TCO_2 system were employed.

The data in Figure 4.18 (a) show that, between October (day 0) and May (day 225) predicted and *Pecten* oxygen isotopic data were in agreement, with *Pecten* shell oxygen isotopic data closely tracking changes in temperature / $\delta^{18}O$-H_2O i.e. shell oxygen isotopes were precipitated in isotopic equilibrium with sea water during this period.

After the end of May (day 242) *Pecten* oxygen isotopic data began to deviate from predicted data, being isotopically depleted. This depletion with respect to isotopic equilibrium was pronounced in July-August (days 295 - 326) and implies that shell oxygen isotopes were precipitated out of isotopic equilibrium with sea water during this period.

Pecten oxygen isotopes appeared to approach isotopic equilibrium (i.e. approximated predicted data) toward the end of September (day 365).

Deviations from isotopic equilibrium during the year are readily visualised in a plot of the difference between *Pecten* and predicted oxygen isotopic data ($\Delta_{Pecten\ -\ Predicted}$) over time (Figure 4.19 a).This again shows that shell oxygen isotopes were precipitated in isotopic equilibrium with sea water during the period autumn to early summer, but were isotopically depleted with respect to equilibrium between June and September. *Pecten* oxygen isotopes differed from predicted data by an average of +0.11°/oo (1σ = 0.15°/oo) for the period October to May. During June to September depletions with respect to isotopic equilibrium averaged - 0.45°/oo (1σ = 0.27°/oo). Figure 4.19b shows a plot of the difference between *Pecten* and predicted oxygen isotopic data ($\Delta_{Pecten\ -\ Predicted}$) and shell growth rate .This shows that depletions in oxygen isotope data with respect to isotopic equilibrium occurred above a threshold in shell growth rate of approximately 0.125mm day^{-1}, such growth rates being exceeded in the summer, between June and September (see a) above) .

Figure 4.18b shows the seasonal variation in predicted and *Pecten* $\delta^{13}C$ data. Seasonal variation in $\delta^{13}C$ - ΣCO_2 data are also shown. Figure 4.18b shows that, unlike oxygen isotopic data, *Pecten* $\delta^{13}C$ were always isotopically depleted with respect to predicted data. i.e. *Pecten* carbon isotopes were always precipitated out of isotopic equilibrium with dissolved inorganic carbon. Figure 4.20a shows a plot of the difference between *Pecten* and predicted carbon isotopic data ($\Delta_{Pecten\ -\ Predicted}$) over the year. During autumn and early summer (days 0 - 225) *Pecten* $\delta^{13}C$ data were isotopically depleted with respect to predicted data and offset by an average of -0.96°/oo (1σ = 0.24°/oo) for that period. Changes in *Pecten* $\delta^{13}C$ tracked the changes in $\delta^{13}C$ - ΣCO_2 during this period, with a peak in shell $\delta^{13}C$ associated with the *Phaeocystis* bloom. The peak in $\delta^{13}C$ therefore occurred in the profile after *Pecten* $\delta^{18}O$ had begun falling due to the rise in water temperature in April - May. After day 225, and coincident with the start of the period of deviation of oxygen isotopes from isotopic equilibrium, shell $\delta^{13}C$ data were further depleted with respect to isotopic equilibrium. Shell $\delta^{13}C$ data were offset by an average of -1.36°/oo (1σ = 0.22°/oo) for the period June -September.

Figure 4.19 a) Seasonal variation in the deviation of *Pecten* shell oxygen isotopes from isotopic equilibrium.

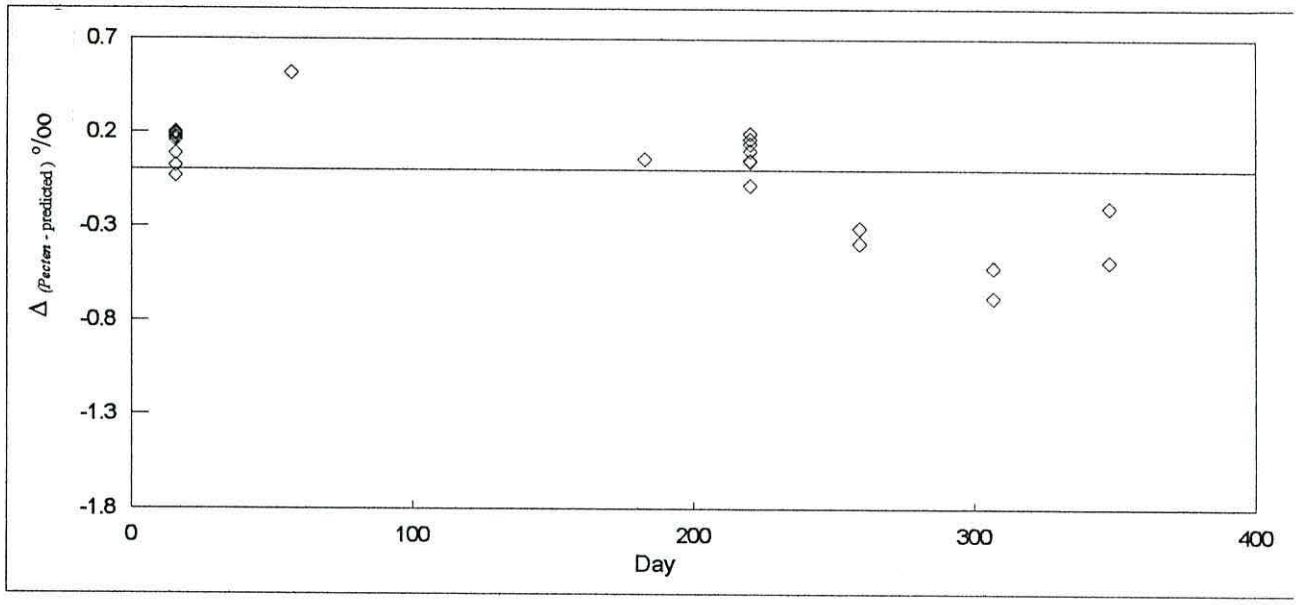

Figure 4.19 b) The relationship between the deviation of *Pecten* shell oxygen isotopes from isotopic equilibrium and shell growth rate.

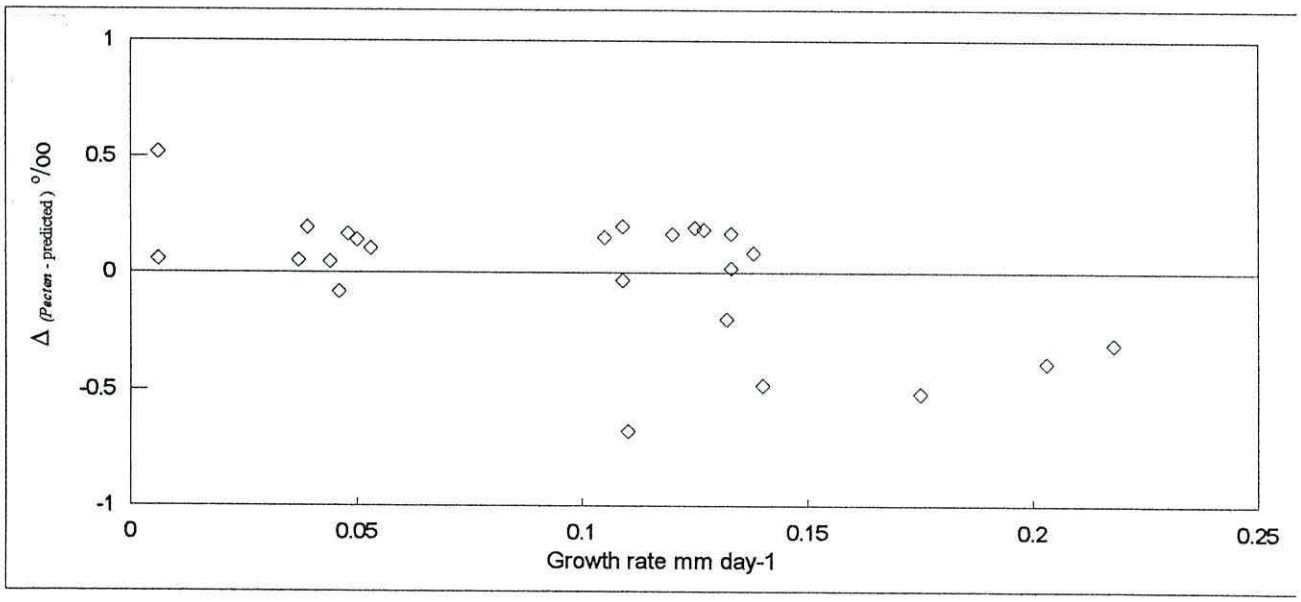

Figure 4.20 a) Seasonal variation in the deviation of *Pecten* shell carbon isotopes from isotopic equilibrium.

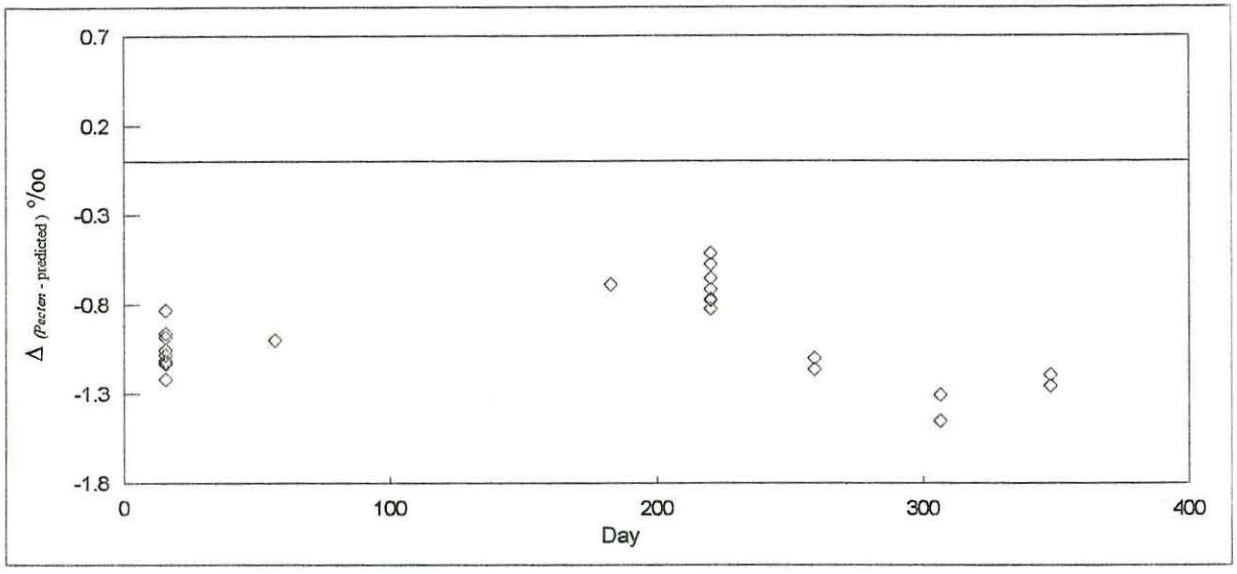

Figure 4.20 b) The relationship between the deviation of *Pecten* shell carbon isotopes from isotopic equilibrium and shell growth rate.

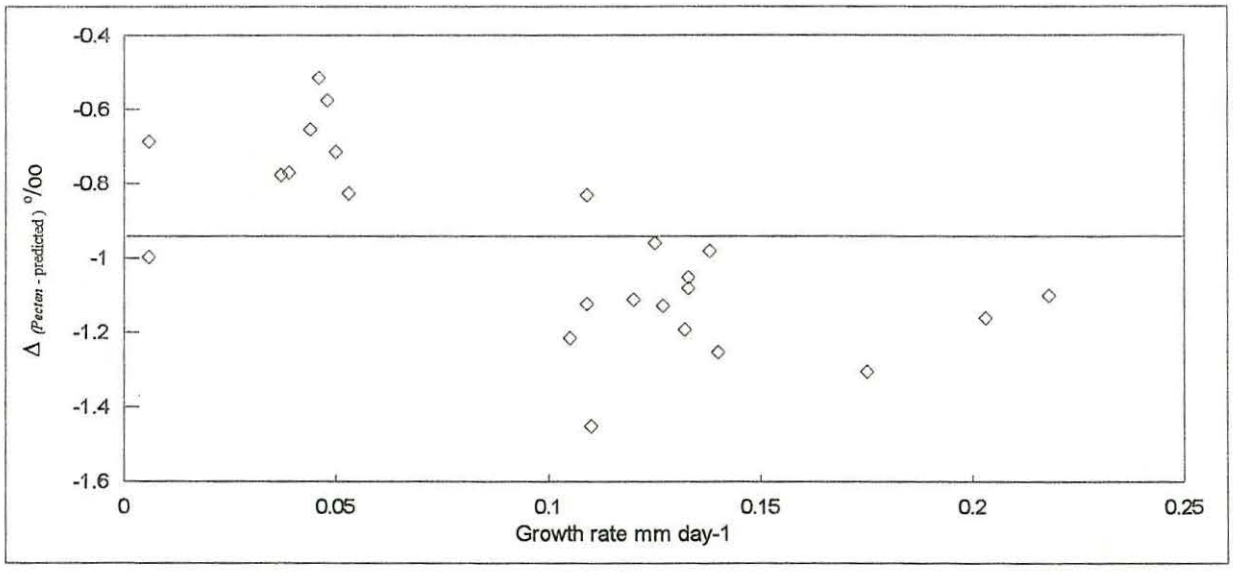

As in the case of shell oxygen isotopes, Figure 4.20b shows that deviations of shell $\delta^{13}C$ from isotopic equilibrium showed a change above a threshold in growth rate (approximately 0.125mm day^{-1}, as for oxygen isotopes).

A useful plot summarising the above isotopic results is one where $\delta^{18}O$ is plotted against $\delta^{13}C$, as shown in Figure 4.21a. This plot allows comparison of predicted $\delta^{13}C$ / $\delta^{18}O$ x - y distributions, or range (i.e. for calcite precipitated in isotopic equilibrium with sea water), with the range in *Pecten* $\delta^{13}C$ / $\delta^{18}O$ data. The plot shows that predicted isotopic data, excepting a few data points associated with the period of the short but intense *Phaeocystis* bloom, occupied a well-defined $\delta^{13}C$ / $\delta^{18}O$ x - y distribution ($\delta^{13}C$ +2.20 to +1.22°/oo, $\delta^{18}O$ + 2.3 to -0.69°/oo). Data for the short period associated with the *Phaeocystis* bloom were within the overall range in $\delta^{18}O$ but were associated with more enriched $\delta^{13}C$ values.

Pecten isotopic data were clearly divided into two distinct $\delta^{13}C$ / $\delta^{18}O$ x - y distributions.
a) isotopic data for the period October 1994 - May 1995 (i.e. pre June 1995) were within the predicted $\delta^{18}O$ range but occupied a range in $\delta^{13}C$ that was offset (isotopically depleted by an average of -1°/oo) from the range of equilibrium $\delta^{13}C$ data.
b) during the summer period (June -September 1995, i.e. post June 1995) *Pecten* $\delta^{18}O$ were isotopically depleted with respect to equilibrium (predicted $\delta^{18}O$) by an average of -0.45°/oo and were associated with *Pecten* $\delta^{13}C$ data that were further depleted (by an average of - 1.36°/oo) with respect to equilibrium (predicted $\delta^{18}C$), as compared to $\delta^{13}C$ data in a) above.

Pecten $\delta^{18}O$ data for the period associated with the *Phaeocystis* bloom were within the range in equilibrium $\delta^{18}O$ data ; *Pecten* $\delta^{13}C$ data were isotopically enriched as compared to the distribution in a) above, reflecting the large enrichments in $\delta^{13}C$ - ΣCO_2 during that period. A summary diagram of the $\delta^{13}C$ / $\delta^{18}O$ x - y distributions reported above is shown in Figure 4.21b.

Figure 4.22 shows the relationship between δ_c - δ_w and temperature using oxygen isotopic data obtained from scallops grown in the Menai Strait during the period autumn to early summer (i.e.exhibiting low growth rates). This was well described by the following linear relationship

$\delta_{c\ Pecten}$ - δ_w = 3.96 - 0.220 t°C (R^2 = 0.89, n = 16)

Figure 4.21 a) Predicted $\delta^{18}O$ / $\delta^{13}C$ distributions and $\delta^{18}O$ / $\delta^{13}C$ distributions for *Pecten* individuals placed in the Menai Strait for monthly periods 1994 -1995.

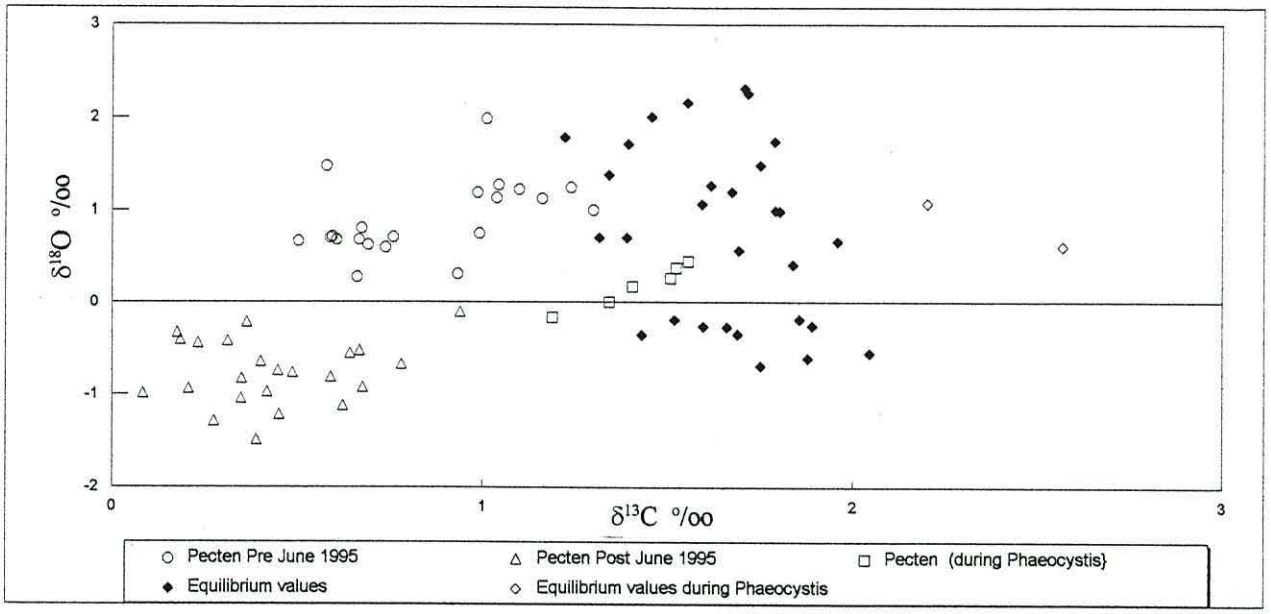

Figure 4.21 b) Model summarising the above $\delta^{18}O$ / $\delta^{13}C$ distributions.

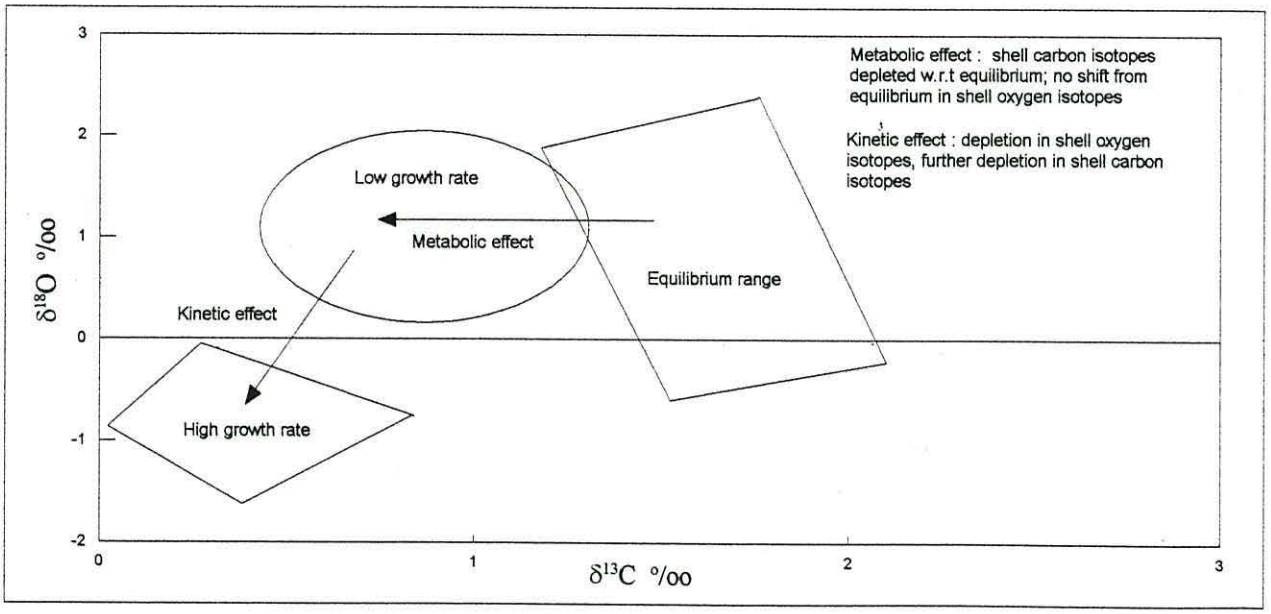

Figure 4.22. $\delta_c - \delta_w$ / temperature plots for *Pecten* individuals placed in the field for monthly periods between October 1994 and May 1995. Also shown are plots of the experimentally derived $\delta_c - \delta_w$ / temperature relationship and the equilibrium expression of O'Neil *et al.* (1969).

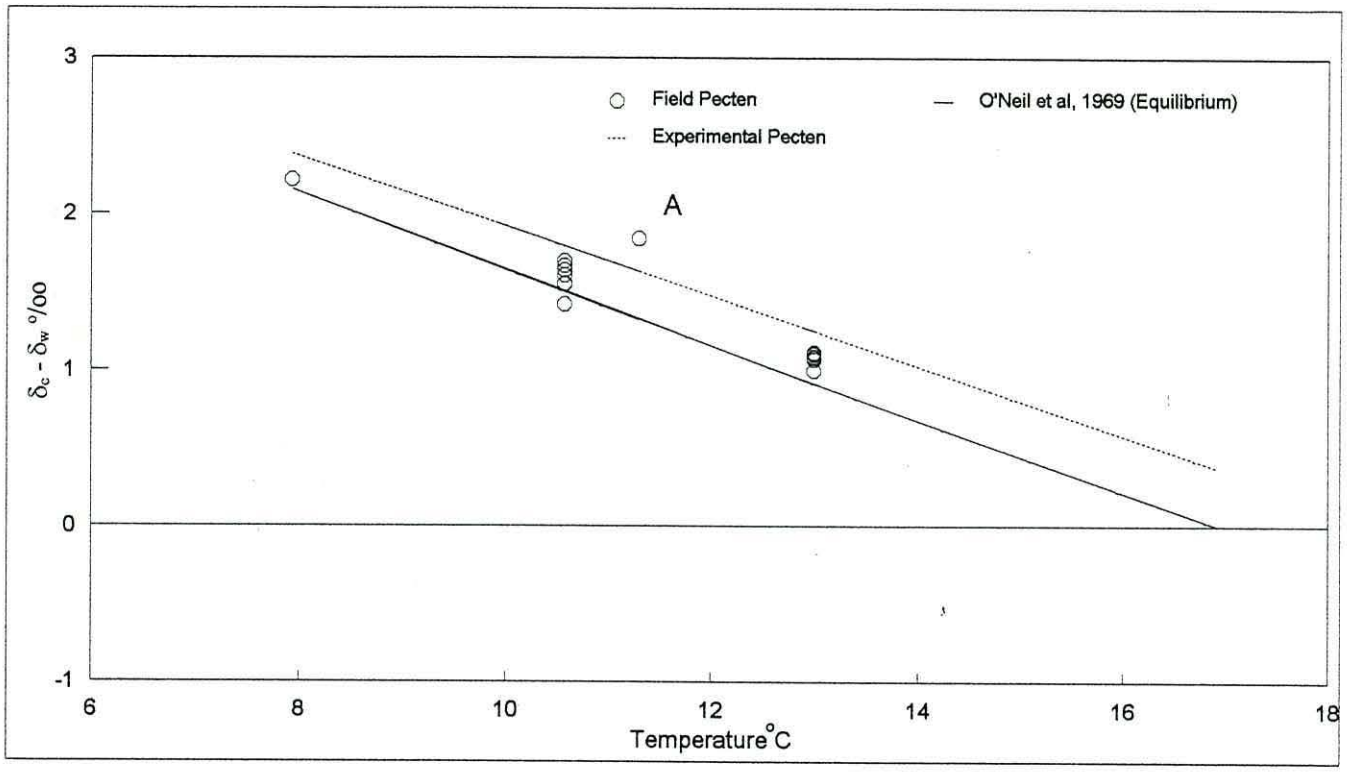

Removing the one marginally anomalous point (A, Figure 4.22) produced the relationship

$\delta_{c\ Pecten} - \delta_w = 3.90 - 0.218\ t^oC$ ($R^2 = 0.96$, $n = 15$)

Also shown are regression plots for the relationship between $\delta_c - \delta_w$ and temperature for oxygen isotopic data obtained during the growth experiment outlined in Chapter 3 and for calcite precipitated in isotopic equilibrium with sea water (O'Neil *et al.* 1969). Figure 4.22 shows that the above relationships are in close agreement with the relationship calculated from the experimental data ($\delta_{c\ Pecten} - \delta_w = 4.20 - 0.228\ t^oC$).

iii) isotopic data for scallops placed in the Menai Strait for a period of one year.

Plates 4.5 and 4.6 show isotopic profile data (i.e. sequential sampling along the shell midline between the disturbance mark and valve margin) for two scallops placed in the Menai Strait for one year between October 1994 and September 1995. Isotopic data are tabulated in Appendix 16. Also shown in Plates 4.5 and 4.6 are photographic montages of the corresponding surface shell microgrowth patterns between the disturbance mark and valve margin for both scallops. In the case of both individuals placed out for the period of one year a clear disturbance mark was observed in the shell associated with the initial placement in the field.

$\delta^{18}O$ and $\delta^{13}C$ profiles were extremely similar for both individuals analysed. In both scallops $\delta^{18}O$ data rose to a maximum at approximately 7mm from the disturbance mark and then decreased again. A sharp decrease in $\delta^{18}O$ occurred in both individuals at approximately 19mm from the disturbance mark. $\delta^{18}O$ data then reached a minimum at approximately 30 -33mm from the disturbance mark before increasing gradually toward the valve margin. $\delta^{13}C$ data in both scallops showed three peaks and troughs between the disturbance mark and a position approximately 19mm from the disturbance mark. The second of these peaks occurred in both of these individuals at approximately 10mm from the disturbance mark, immediately after the $\delta^{18}O$ maximum. The third peak occurred at approximately 16mm from the disturbance mark in both individuals and was particularly pronounced for *Pecten* 60. After the position 19mm from the disturbance mark $\delta^{13}C$ data in both scallops fell dramatically.

This sharp fall was coincident in both individuals with the sharp fall in $\delta^{18}O$ data. $\delta^{13}C$ data then fell very gradually to a minimum at approximately 37mm from the disturbance mark before rising at the valve margin.

The isotopic profiles shown in Plates 4.5 and 4.6 are remarkably similar in form to the seasonal variation in isotopic data for scallops placed in the Menai Strait for approximately monthly periods, as shown in Figure 4.18. Isotopic profiles for the scallops placed out for the entire year differ from the profiles shown in Figure 4.18 only in that much of the isotopic record is telescoped around the period of the $\delta^{18}O$ maximum and enlarged in the latter half of the shell. This is entirely consistent with the fact that isotopic data for scallops placed in the field for monthly periods are 'real time' data whilst data for the two scallops placed in the field for a year reflect the varying time integrated per calcite sample as a result of seasonal changes in shell growth rate as discussed previously.

It is not possible to calculate predicted $\delta^{18}O$ and $\delta^{13}C$ data for each data point shown in Plates 4.5 and 4.6, to allow comparison of data. However, the consistency between the isotopic profiles for the year October 1994 -September 1995 in Figure 4.18 and Plates 4.5 and 4.6 along with interpretation of the corresponding shell microgrowth patterns allow an interpretation of the data for the two individuals placed in the field for the year to be made with a high degree of certainty. Shell $\delta^{18}O$ rose initially as water temperatures fell in the autumn and were associated with a drop in $\delta^{13}C$ in response to remineralisation within the water column at this time with corresponding drop in $\delta^{13}C$ - ΣCO_2. The water temperature minimum in winter (February) was associated with a maximum in $\delta^{18}O$. This corresponded to the period of maximum striae abundance and narrowest striae widths and the deposition of the annual growth ring in both individuals. Striae analysis of scallops placed in the field for monthly periods had previously shown that the period of maximum striae abundance and narrowest width occurred in winter between December and March. The rise in water temperatures in March was associated with the start of the gradual decrease in $\delta^{18}O$. This was associated with a rise in striae width and fall in striae abundance (shown previously to occur during March). The second peak in $\delta^{13}C$ in the shell occurred soon after the initiation of the decrease in $\delta^{18}O$ and striae abundance after deposition of the growth ring and very likely reflected the increase in $\delta^{13}C$ - ΣCO_2 associated with the spring diatom bloom in April.

Plate 4.5 Shell surface microgrowth patterns and isotopic profiles for *Pecten maximus* placed in the Menai Strait October 1994 - September 1995 Pecten 60 , Bars = 1σ.

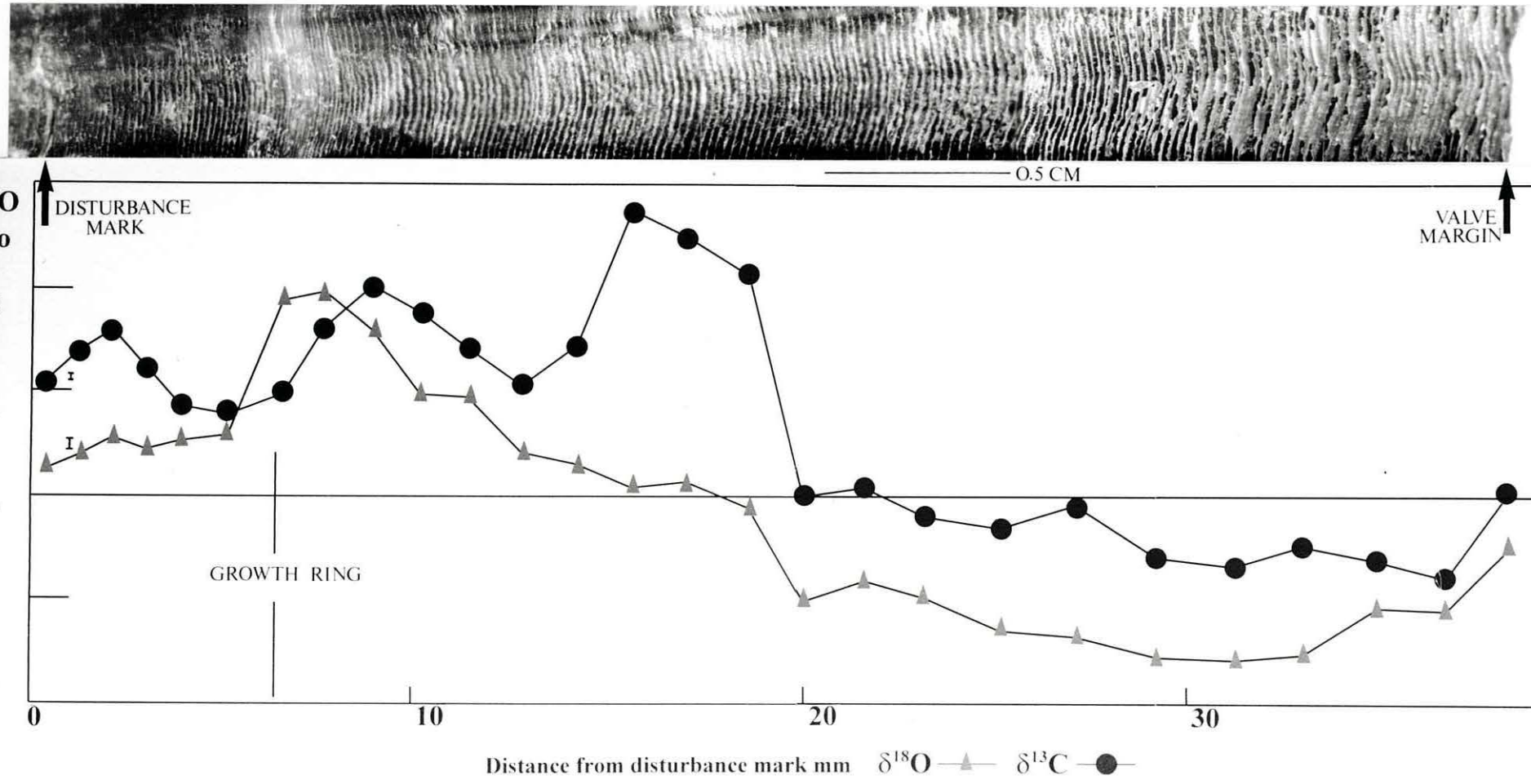

Plate 4.6 Shell surface microgrowth patterns and isotopic profiles for *Pecten maximus* placed in the Menai Strait October 1994 - September 1995
Pecten 52 , Bars = 1σ.

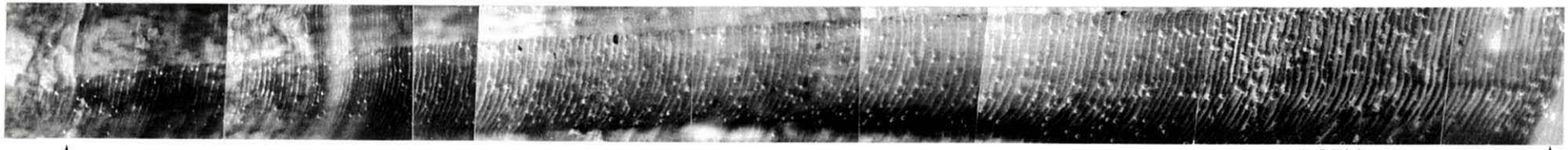

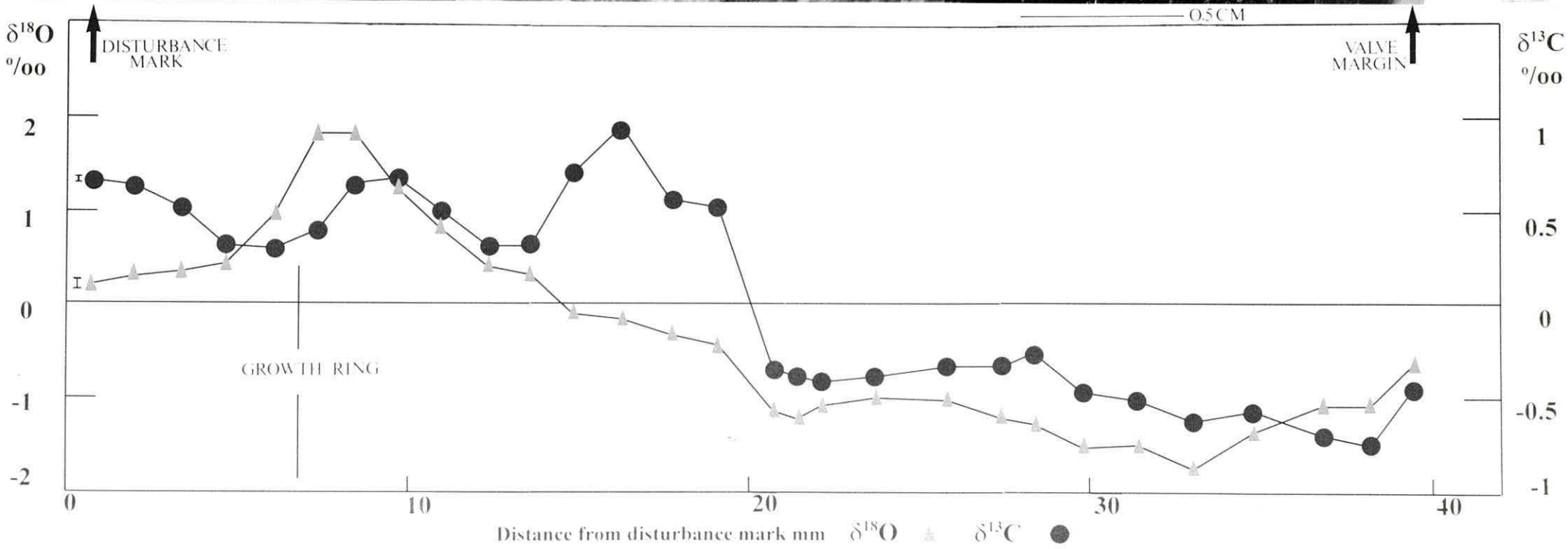

As water temperatures continued to rise, and $\delta^{18}O$ to decrease, $\delta^{13}C$ fell to the second trough and then rose to the third peak at approximately 19mm from the disturbance mark. This very likely reflected the fall in $\delta^{13}C$ - ΣCO_2 during late April - May and rise associated with the *Phaeocystis* bloom in early June. The second trough in $\delta^{13}C$ seen in the annual profiles was absent in the data for monthly individuals and this may be due to the fact that only mean increment and not profile data were available for the monthly *Pecten* data for this period . Striae abundances and widths remained constant in the shell after the second trough in $\delta^{13}C$, soon after the start of the decrease in $\delta^{18}O$. Analysis of microgrowth patterns previously had shown that both striae abundance and width reached a plateau during May and this confirms the above interpretation. Soon after the third peak in shell $\delta^{13}C$, at approximately 19mm from the disturbance mark, both $\delta^{13}C$ and $\delta^{18}O$ fell sharply. This is consistent with the influence of a kinetic effect at higher growth rates during the summer. Such a kinetic effect was shown to occur in the scallops placed in the field for monthly intervals during June - July, soon after the *Phaeocystis* bloom and this is consistent with the drop in shell $\delta^{13}C$ soon after the third $\delta^{13}C$ peak. Kinetic effect influenced both $\delta^{13}C$ and $\delta^{18}O$ during the summer until September, when a slow down in growth rate ocurred. This may explain the final rise in isotopic data in the profiles at the valve margin seen in Plates 4.5. and 4.6.

Indirect evidence for the above interpretation may be gained from two additional observations. Firstly, using monthly shell growth rates as determined in a) above, it is possible to calculate the approximate increment of shell that would have been deposited between June and September 1995, when the annual scallops were removed from the Menai Strait. Measuring back from the valve margin placed the June 1st time marker (coincident with the *Phaeocystis* bloom) at just after the third $\delta^{13}C$ peak (interpreted as being associated with the *Phaeocystis* bloom). Secondly, scallops removed at the end of the year time period were noticed to exhibit considerable fouling by barnacles and tube worms in a discrete region of the shell (see Plate 4.3a.) Barnacles were found to be almost exclusively of one settlement cohort of the species *Balanus crenatus* and occupied a region between the disturbance mark and a radius of approximately 16 mm from the disturbance mark. Data for larval abundance of *Balanus* cyprids within the water column in the Menai Strait presented by Hidayat (1995) show that cyprids were effectively absent from the water column after June 1995. i.e. the end of that settlement period.

The main settlement period for *Balanus crenatus* in British waters is May - July (OECD, 1963). This allows an approximate May - June time marker to be placed at 16mm from the disturbance mark. This time marker coincides with the peak in shell $\delta^{13}C$ interpreted as being associated with the early June bloom of *Phaeocystis* some time after the $\delta^{18}O$ maximum associated with the coldest water temperatures in February.

The similarity in $\delta^{13}C$ and $\delta^{18}O$ profiles for monthly and annual scallop data is also seen when comparing $\delta^{18}O$ / $\delta^{13}C$ x y plots in Figures 4.21 and 4.23. As with the data for the monthly scallops, *Pecten* isotopic data shown in Figure 4.23 occupied two discreet $\delta^{18}O$ / $\delta^{13}C$ x y distributions. $\delta^{18}O$ data upto a position 21mm from the disturbance mark occupied a similar range as the equilibrium $\delta^{18}O$ data, whilst $\delta^{13}C$ data were offset from isotopic equilibrium by approximately -1 to -1.2 °/oo. The 21mm marker in the shell profile occurred soon after the third $\delta^{13}C$ peak, interpreted as being associated with the *Phaeocystis* bloom. After the 21mm location marker $\delta^{18}O$ and $\delta^{13}C$ data occupied a second discreet x y distribution whereby $\delta^{18}O$ data were offset from isotopic equilibrium by an average of - 0.45°/oo and $\delta^{13}C$ data were further offset from isotopic equilibrium, in total by an average of between -1.9 and -2.2 °/oo.

The 21mm location marker in the shell associated with the change in $\delta^{18}O$ / $\delta^{13}C$ x y distribution corresponds approximately to the period in late June soon after the *Phaeocystis* bloom. Figure 4.21 shows that the change in $\delta^{18}O$ / $\delta^{13}C$ x y distribution exhibited by scallops placed in the field for monthly periods occurred at the same time in late June, soon after the peak in $\delta^{13}C$.

The $\delta^{18}O$ / $\delta^{13}C$ plot shown in Figure 4.23 for annual individuals fits well to the generalised model explaining $\delta^{18}O$ / $\delta^{13}C$ distributions shown in Figure 4.21b and allows a similar interpretation to be made. At slow growth rates (i.e. before the 21mm location marker), oxygen isotopes are precipitated in isotopic equilibrium with sea water. Carbon isotopes are precipitated out of isotopic equilibrium with sea water. This implies a metabolic effect, probably reflecting the incorporation of isotopically depleted respiratory CO_2. $\delta^{13}C$ data are however offset by a constant value (-1°/oo) and therefore changes in $\delta^{13}C$ - ΣCO_2 (for example associated with the diatom and *Phaeocystis* blooms) are reflected in the shell $\delta^{13}C$ profile.

Figure 4.23. Predicted $\delta^{18}O$ / $\delta^{13}C$ distributions and $\delta^{18}O$ / $\delta^{13}C$ distributions for *Pecten* individuals placed in the Menai Strait for the entire year 1994 -1995.

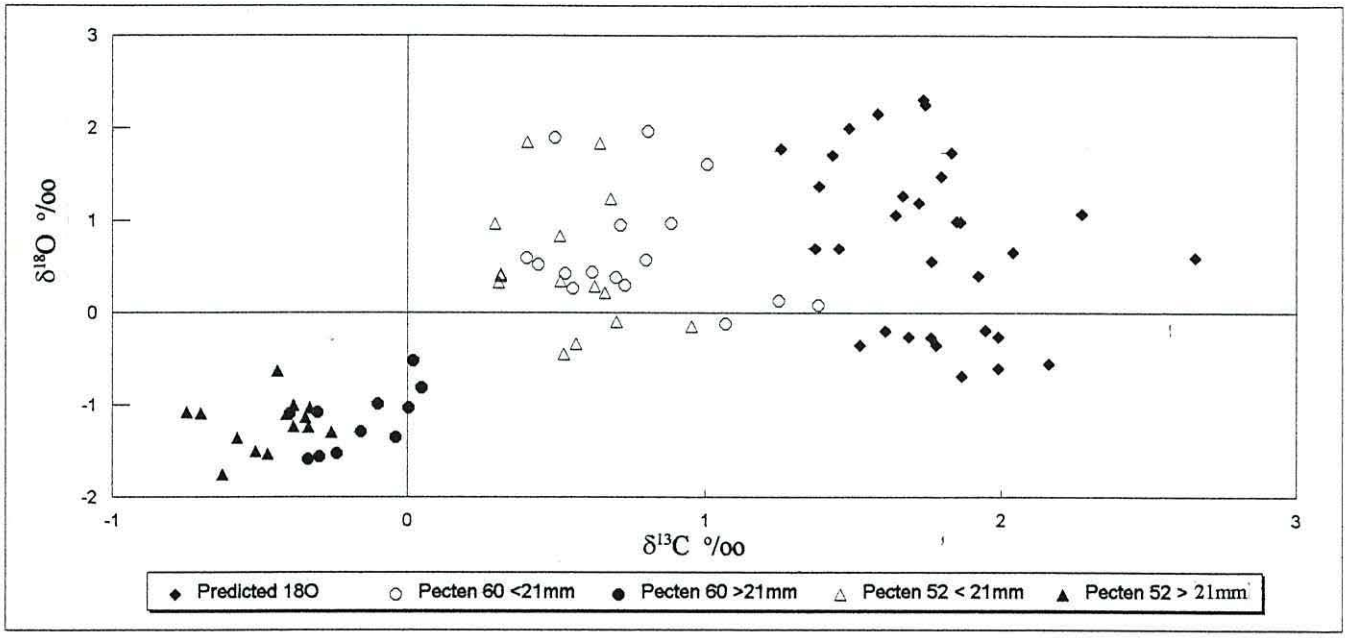

After the 21mm location marker, higher shell growth rates (in the summer) are associated with a kinetic effect, causing oxygen isotopes to be precipitated out of isotopic equilibrium with sea water and further deviation in carbon isotopes from isotopic equilibrium. The level of oxygen isotopic depletion due to this kinetic effect was found to be - 0.45 °/oo i.e. identical to the depletion exhibited by monthly individuals. Carbon isotopic depletion during this period was between -1.9 and -2.2 °/oo.This is considerably more than the depletion in carbon isotopes associated with the period of kinetic influence exhibited by the monthly scallops (-1.4°/oo). Since the magnitude of oxygen isotopic disequilibrium at these higher growth rates was the same for both monthly and annual scallops, this 'excess' isotopic depletion in $\delta^{13}C$ exhibited at the higher growth rates by annual scallops (-0.5°/oo to -0.8°/oo) may reflect an increased metabolic effect.

Table 4.2 a,b shows maximum, minimum, median and annual range data for both predicted and shell $\delta^{18}O$ and $\delta^{13}C$ determined from scallops placed out for monthly intervals and for the entire year. When considering the difference between predicted and *Pecten* maximum $\delta^{18}O$ data (shown in Table 4.3a) it can be seen that predicted maximum $\delta^{18}O$ data exceed *Pecten* maximum $\delta^{18}O$ data by an average of 0.38°/oo (1σ = 0.08°/oo) i.e. an average temperature equivalence of 1.9°C. This reflects the cessation of growth by *Pecten* individuals below approximately 8°C, resulting in the coldest water temperatures (6-8°C) not being recorded in the shell.Table 4.3a shows that *Pecten* minimum $\delta^{18}O$ data are more negative when compared to predicted minimum $\delta^{18}O$ data by an average of -0.92°/oo (1σ = 0.14°/oo). This reflects a kinetic effect which becomes significant in the summer at higher growth rates and results in negative deviations in *Pecten* $\delta^{18}O$ from isotopic equilibrium. This kinetic effect would result in erroneously high shell-derived maximum water temperatures of approximately 4.6°C. Such a kinetic effect causes an increase in isotopic range by an average of +0.54°/oo (1σ = 0.07°/oo), equivalent to approximately 2.7°C, as compared to the predicted range. The combined influences of seasonal growth cessation and kinetic effect result in median $\delta^{18}O$ data that are offset from the predicted median by -0.65°/oo (1σ = 0.11°/oo), i.e. equivalent to approximately -3.3°C. Similarly, Table 4.3b shows that the combined influences of metabolic and kinetic effects result in median $\delta^{13}C$ data offset from the predicted median by -1.42°/oo (1σ = 0.36°/oo) and cause an increase in isotopic range of 0.32 °/oo (1σ = 0.16°/oo) as compared to the predicted range.

Table 4.2a Comparison of predicted median, maximum, minimum and range of $\delta^{18}O$ data for the year September 1994 - October 1995 with *Pecten* $\delta^{18}O$ data.

	Median °/oo	Maximum °/oo	Minimum °/oo	Range °/oo
Predicted	0.812	2.312	-0.689	3.001
Monthly *Pecten*	0.248	1.982	-1.486	3.468
Pecten 52	0.045	1.845	-1.756	3.601
Pecten 60	0.190	1.969	-1.590	3.559

Table 4.2b Comparison of predicted median, maximum, minimum and range of $\delta^{13}C$ data for the year September 1994 - October 1995 with *Pecten* $\delta^{13}C$ data.

	Median °/oo	Maximum °/oo	Minimum °/oo	Range °/oo
Predicted	1.894	2.566	1.221	1.345
Monthly *Pecten*	0.818	1.552	0.083	1.469
Pecten 52	0.103	0.955	-0.749	1.704
Pecten 60	0.491	1.382	-0.401	1.783

Table 4.3a Differences between predicted and *Pecten* median, maximum, minimum and range of $\delta^{18}O$ data.

	Δ Median °/oo	Δ Maximum °/oo	Δ Minimum °/oo	Δ Range °/oo
Monthly *Pecten*	-0.564	-0.330	-0.797	0.467
Pecten 52	-0.767	-0.467	-0.901	0.600
Pecten 60	-0.622	-0.343	-1.067	0.558

Table 4.3b Differences between predicted and *Pecten* median, maximum, minimum and range of $\delta^{13}C$ data.

	Δ Median °/oo	Δ Maximum °/oo	Δ Minimum °/oo	Δ Range °/oo
Monthly *Pecten*	-1.071	-1.014	-1.138	0.124
Pecten 52	-1.786	-1.611	-1.970	0.359
Pecten 60	-1.398	-1.184	-1.622	0.438

4.5. Discussion

a) shell growth

In a field study in which samples of *Pecten maximus* were obtained at weekly to fortnightly intervals over a two year period in the Irish Sea, Mason (1957a) found a pattern whereby shell growth commenced in March - April, reached a maximum in June - July and decreased in the autumn to reach a minimum in February. The seasonal pattern of shell growth described was identical to the findings in this study. Shell accretionary rates were reported by Mason (1957a) as being of the order of 0.16mm per day in June and 0.2mm per day in July for juveniles aged 2 years. These growth rates are comparable to the growth rates found in this study.

In another similar study Richardson *et al.* (1982) investigated growth of queen scallops, *Chlamys opercularis* in the Irish Sea. Scallops were marked, suspended in cages and recovered after one month at intervals over a year. They reported a gradual reduction in shell growth rate in winter, with little or no growth between January and March. Shell growth then rose again in the spring to a maximum in June -August. The seasonal pattern of growth reported in their study was also identical to the findings in this work for *Pecten maximus* in the Menai Strait.

A number of possible factors may determine the seasonal pattern of shell growth. Whilst Richardson *et al.* (1982) found shell growth rate to be significantly correlated with sea water temperature, minimum growth rates were reported 1 -2 months before sea water temperatures were at their lowest. Similarly, maximum growth rates were recorded several months before maximum sea water temperatures. This was also found to be the case in this study (see Figure 4.8).Broom and Mason (1978) found no significant correlation between shell growth in *Chlamys opercularis* and water temperature. Mason (1957a), suggested that both water temperature and food availability may influence shell growth in *Pecten maximus*.

Concentrations of particulate organic matter (P.O.M.) were found to be relatively high and constant throughout the year in the Menai Strait. Whilst the absolute concentration of P.O.M. was not a factor influencing shell growth , changes in food absorption efficiency or qualitative changes in P.O.M. (i.e. the usefulness of available P.O.M.) may be influential.

Vahl (1980) found that as the contribution made by particulate inorganic matter (P.I.M.) to total seston (P.I.M. + P.O.M.) increased, food absorption efficiency decreased in the scallop *Chlamys islandica.* It was suggested that this may be due to the fact that the scallop's pallial organs do not select P.O.M. in preference to P.I.M.. Dilution of the seston by varying amounts of P.I.M. during the year and its effects on absorption efficiency was thought to result in varying ability of the scallop to utilise available P.O.M, thereby influencing shell growth i.e. the relative contribution of P.I.M. and P.O.M. in the seston was an influential factor controlling shell growth.The Menai Strait is an often turbid, well mixed system with both high particulate organic loading and high levels of total suspended solids. P.I.M. data were not available in this study, but in the dynamic environment of the Menai Strait this dilution effect cannot be ruled out as a possible factor. Alternatively phytoplankton speciation may be an important factor i.e. the quality of P.O.M..

b) surface microgrowth patterns

Most individuals within the study deposited well - defined striae on the shell surface at the midline, second ray and basal ear. However, many individuals placed in the Menai Strait during the first month of the study (October 1994) did not deposit striae at the midline. Striae have also been found to be absent at the midline in the first mm along the axis by Dare (1991). The number of striae deposited per day was found to be well - correlated with shell growth rate, which was the determining factor influencing the rate of striae deposition.

As outlined in Chapter 1, there have been two schools of thought within the literature concerning production of striae in scallops, with striae production being thought to be either a periodic phenomenon (Parsons *et al.* 1993; Clark, 1968; 1975) or deposited as a function of shell growth rate (Gruffydd, 1981) .The results of the field study confirmed the experimental findings of Gruffydd (1981) in which the number of striae was found to be related to growth rate. Striae deposition showed no periodicity; as in the earlier study of Broom and Mason (1978) striae deposition was found to be of the order of one per day only in the summer, decreasing either side of this time period. Earlier reports of a daily periodicity of striae production appear therefore to be coincidental.

Striae width was also correlated with growth rate, confirming the earlier findings of Gruffydd (1981) who also found that striae widths increased at higher growth rates. Changes in striae width and abundance along the midline axis of growth between the disturbance mark and valve margin for animals placed out in the Menai Strait for the year reflected seasonal changes in growth rate i.e. during growth rate reduction and cessation in winter, striae abundance increased and width decreased. Such changes in striae abundance and width have been previously reported in the literature (Dare, 1991), and were thought to be associated with seasonal changes in shell growth rate. The relationship between striae width and growth rate appeared to be curvilinear, with maximum striae widths achieved above growth rates of approximately 0.1mm day^{-1} at the midline. Similarly, a curvilinear relationship appeared to exist between striae abundance and growth rate, with minimum striae abundances at growth rates of above 0.025mm day^{-1} at the midline.

The results of the study therefore implied that increasing growth rate is associated with deposition of more striae but that, above a threshold in growth rate, there was no further increase in striae width or decrease in striae abundance i.e. there is a finite limit to stria width.

c) *Pecten* shell $\delta^{18}O$ and $\delta^{13}C$

The field study showed that at slow shell accretionary rates (below 0.125 mm day^{-1}) i.e. during the period autumn to early summer, *Pecten* shell oxygen isotopes were precipitated in isotopic equilibrium with sea water whilst carbon isotopes were precipitated out of isotopic equilibrium, being depleted by approximately 1 °/oo. The relationship between $\delta_c - \delta_w$ and temperature, using oxygen isotopic data obtained from scallops grown in the Menai Strait during the period autumn to early summer (i.e. when growth rates were low), was in agreement with the experimental data for the relationship between $\delta_c - \delta_w$ and temperature. The inferences made from the experimental data are confirmed by these data ; namely that at slow growth rates a metabolic effect (possibly incorporation of respiratory CO_2) causes depletions in shell $\delta^{13}C$ but does not influence shell $\delta^{18}O$ i.e. shell oxygen isotopes are precipitated in isotopic equilibrium with sea water, but that this is not the case for shell carbon isotopes.

The magnitude of depletion in shell $\delta^{13}C$ was considerably less than that exhibited by individuals exhibiting slow growth during controlled experimental conditions (approximately - 2°/oo) and may have reflected a variation in metabolic effect between these two groups.

At higher shell accretionary rates (above approximately 0.125 mm day^{-1}) a kinetic effect appeared to become significant in addition to the above metabolic effect. Such a kinetic effect resulted in deviation of *Pecten* oxygen isotopic data away from isotopic equilibrium toward depleted values and caused a further depletion in shell $\delta^{13}C$ with respect to isotopic equilibrium (in addition to the isotopic depletion caused by metabolic effect). Whilst the magnitude of deviation in shell $\delta^{18}O$ from isotopic equilibrium was comparable between scallops placed out for monthly and annual periods during periods of high growth rate this was not the case for shell $\delta^{13}C$. There was considerably more variation between individuals in the magnitude of deviation in shell $\delta^{13}C$ from isotopic equilibrium (see Table 4.3) which may have reflected a variation in metabolic effect. In a similar mark and recovery study, Klein *et al.* (1996 a,b) profiled the outer calcitic layer of each increment of shell deposited over a year by two individuals of the mussel *Mytilus trossulus*. Whilst shell $\delta^{18}O$ values were found to be in isotopic equilibrium with sea water, shell $\delta^{13}C$ values were depleted with respect to estimated isotopic equilibrium by approximately -2°/oo. These workers also found significant systematic differences in shell $\delta^{13}C$ in coevally precipitated calcite from different regions of the shell. Shell $\delta^{13}C$ in a single, coevally precipitated growth band were most positive at the axis of maximum growth (i.e.the midline), and decreased toward the slower - growing lateral margins of the shell. Shell $\delta^{18}O$ however showed no systematic variation around the shell, with total variation of the order 0.3°/oo. The authors interpreted the systematic variation in shell $\delta^{13}C$ as resulting from variation in metabolic rate within the mantle region in different regions of the shell. Such differences in mantle metabolic rate, they argued, would be reflected as differences in the proportion of metabolically-derived CO_2 in the E.P.F. dissolved inorganic carbon pool. Shell growth rate has been shown to be inversely proportional to mantle metabolic activity in *Mytilus edulis* (Rosenberg *et al.* 1989, Rosenberg and Hughes, 1991). The contribution of isotopically depleted CO_2 could therefore be expected to be greater in slow growing regions of the shell. This appears to be confirmed by the isotopic data presented by Klein *et al.* (1996 b). Similar influences on $\delta^{13}C$ as a function of metabolic rate have been reported by Kalish (1991) for fish otoliths.

In that study, fish with low metabolic rates or living at low temperatures (e.g. deep water fish) had otolith $\delta^{13}C$ that tended toward estimated isotopic equilbrium, whilst those fish living at higher environmental temperatures exhibited extreme depletions in otolith $\delta^{13}C$.

By comparison, in a study in which samples were analysed from around the valve margin of the scallop *Adamussium colbecki* collected in Antarctica, Barrera *et al.* (1990) found no systematic variations in either $\delta^{18}O$ or $\delta^{13}C$ around the shell margin. The results of this study have also shown no systematic variation in shell $\delta^{13}C$ or $\delta^{18}O$ around the upper shell valve margin in juvenile *Pecten maximus* suggesting no variation in metabolic effect around the shell margin.

A mass balance model proposed by McConnaughey *et al.* (1997) may be used to calculate the percentage of shell carbon derived from respiratory CO_2.

$$\delta^{13}C_{(shell)} - E_b \text{ calcite} = R(\delta_{b\ (respiration)}) + (1 - R)(\delta_{b\ (sea\ water)})$$

where R is the fraction of respired carbon in the shell, $\delta_{b\ (respiration)}$ is the isotopic composition of bicarbonate in the E.P.F.derived from respiratory sources, $\delta_{b\ (seawater)}$ is the isotopic compostion of bicarbonate in the E.P.F.derived from sea water and E_b calcite is the enrichment factor between bicarbonate and calcite. E_b calcite was determined by Romanek *et al.* (1992) as +1°/oo, with no significant temperature dependency (see Chapter 1). Mean values of $\delta^{13}C_{(shell)}$ were determined from scallops placed out for the monthly periods where shell oxygen isotopes were shown to have been precipitated in isotopic equilibrium with sea water i.e. when there was no kinetic effect. Corresponding mean values of $\delta_{b\ (sea\ water)}$ were calculated from pH, temperature, salinity and $\delta^{13}C$ - ΣCO_2 data, as outlined in Chapter 3. McConnaughey *et al.* (1997) have shown that, for the purposes of calculation, $\delta_{b\ (respiration)}$ may be assumed to be 0.5°/oo heavier than the organic material being respired. A mean value of the carbon isotopic composition of tissues of a number of bivalves collected from near shore environments and reported by Tanaka *et al.* (1986) was used within this calculation here. In this way it may be calculated that between 3 and 5% of shell carbon was derived from respiratory CO_2. Paull *et al.* (1989) and McConnaughey *et al.* (1997) calculated that between 5 and 14% of shell carbon was derived from respiratory sources for molluscs from various deep - sea environments and fresh water springs.

Higher respiratory carbon contributions to shell carbonate reported by Tanaka *et al.* (1986) have been shown by McConnaughey *et al.* (1997) to be a consequence of biasing resulting from sampling and calculation procedures. Reviewing the literature, McConnaughey *et al.* (1997) concluded that the contribution of respired carbon to shell carbonate in molluscan shells is less than 10% and typically reduces shell $\delta^{13}C$ by less than 2°/oo. The data presented within this study are in agreement with these findings.

Tables 4.2 and 4.3 show that the reconstruction of historical water temperatures / $\delta^{18}O$-H_2O and $\delta^{13}C$-ΣCO_2 (mean data and annual range) from *Pecten* shell isotopes are precluded by two processes :

a) seasonal reduction / cessation of shell growth during the winter, with absence of associated isotopic data. This occurred during periods of the coldest water temperatures and consequently resulted in underestimation of maximum $\delta^{18}O$.

b) precipitation of shell $\delta^{18}O$ and $\delta^{13}C$ out of isotopic equilibrium with sea water. A metabolic effect influenced shell $\delta^{13}C$ at all growth rates and may have been variable in magnitude. A kinetic effect influenced shell $\delta^{13}C$ and $\delta^{18}O$ at higher growth rates. High growth rates occurred during periods when water temperatures were highest and consequently resulted in anomalously depleted values for minimum shell - derived $\delta^{18}O$. The combined influences of seasonal growth cessation and a kinetic effect at high growth rates result in maximum shell $\delta^{18}O$ data offset from predicted maximum data by an average of -0.38°/oo, and minimum shell $\delta^{18}O$ data offset from predicted minimum data by an average of -0.92°/oo. This has the combined effect of causing an offset of median shell $\delta^{18}O$ data from predicted median data by an average of -0.65°/oo and increases the range of shell $\delta^{18}O$ data by an average of +0.54°/oo as compared to the predicted range.

In an isotopic profiling study of *Pecten maximus* collected from waters around the U.K., Dare and Deith (1991) found that, when sampling during the first 3 years of growth, immature *Pecten maximus* did not record temperatures below 9°C. Scallops from the Western Channel, with annual temperature range 9.2 °C - 13.5°C faithfully recorded winter temperatures, whilst those in the Eastern Channel and Irish Sea, (annual temperature ranges 5.7°C - 16.7°C and 6.9°C - 14°C respectively) did not record winter temperatures. In the Western Channel temperatures remained warm enough to permit accretion to continue throughout the winter.

A similar loss of winter $\delta^{18}O$ values is evident but not discussed by Tan *et al.*(1988) in isotopic profile data reported for the scallop *Placopecten magellanicus.*

The results of the study in the Menai Strait have also shown that the coldest water temperatures (below between 7 and 8°C) were not recorded in the shells of *Pecten maximus*. The present study has shown that seasonal variations in shell gowth rate exhibited by *Pecten maximus* have large influences on the time integrated per calcite sample when sampling along the shell axis. Most of the shell growth occurred during the period May to October, when time integrated per sample averaged between 8 and 15 days. Time integration increased significantly in late autumn, was maximal during the winter and remained relatively high until April. Pooling data from 13 shells collected from the waters around the United Kingdom for which actual temperature and water isotope data were available Dare and Deith (1991) divided each annual increment in *Pecten maximus* shells from the umbo across to the valve margin into warming half - year periods (where 75% of growth occurred) and cooling half - year periods (when growth slowed down suddenly). For a 1mm sampling protocol they found that, during the warming periods in years 2 to 5, integration times averaged 5 -15 days whilst in the cooling half year period integration times roughly doubled, with probable integration times for the coldest months of about 1-1.5 months. These results are in close agreement with the data reported in the present field study (see Table 4.1)

A kinetic effect was found to become significant during the summer at growth rates in excess of approximately 0.125mm day^{-1}. This resulted in minimum shell $\delta^{18}O$ values that were isotopically depleted with respect to equilibrium by up to -0.92°/oo and erroneously higher shell-derived temperatures for the summer period (by up to 4.6°C). A kinetic effect has only been suggested as being the underlying mechanism for observed disparity between observed and predicted ^{18}O values in one or two studies. McConnaughey (1989a) attributed such discrepancies in corals as due to kinetic effects associated with rapid skeletogenesis.

Dudley and Goodney (1979), found that the isotopic composition of Coccolithophorids was influenced by growth rate and that only under constant conditions of growth and environment was there temperature controlled fractionation of oxygen isotopes.

In their study of *Pecten maximus* sampled from U.K.waters Dare and Deith (1991) found that shell-derived summer temperatures were frequently higher than recorded temperatures (i.e. reflecting isotopically light values) and showed positive anomolies with age.

$\delta^{18}O$ data for the scallop *Placopecten magellanicus* between 1-4 years of age reported by Krantz *et al.* (1984) also exhibit similar occasional deviations from isotopic equilibrium toward depleted values during the summer of the order of -0.5 to -0.75 °/oo. This was explained by the authors as being a consequence of averaging of hydrographic data by month. However this would represent deviations of 2-3°C in an overall annual temperature range of 6°C and kinetic effects can not be ruled out. Deviations in both summer and winter shell $\delta^{18}O$ data were always in the lighter direction, which one would not expect with averaging error.

Negative deviations from isotopic equilibrium during the summer were not found in the more northerly population of *Placopecten magellanicus* sampled by Tan *et al.* (1988). However, summer temperatures at the more southerly site sampled by Krantz *et al.* (1984) were higher than at the site sampled by Tan *et al.* (1988) and precipitation of shell $\delta^{18}O$ out of isotopic equilibrium with sea water may have occurred at the higher summer temperatures found at lower latitudes. This would agree with the deviations found toward isotopically lighter values during the highest water temperatures found by Dare and Deith (1991) for *Pecten maximus*.

Unfortunately, shell $\delta^{13}C$ are not available for these three studies. However, the model outlined in Chapter 1 indicates that whilst a kinetic effect is associated with negative deviations in shell $\delta^{18}O$ from isotopic equilibrium, such negative deviations are not present when a metabolic effect alone occurs. This implies that a kinetic effect may have occurred for the scallops within these studies during periods of warmest water temperatures in the summer, leading to erroneously high shell-derived summer water temperatures. These conclusions are entirely consistent with the conclusions reported within the present study.

Microgrowth pattern data on the surface of the *Pecten* shell upper valve are restricted to striae abundance (striae per mm) and striae width for fossil shells. The results of the field study have shown that higher growth rates were associated with both a decrease in striae abundance and increase in striae width. However, the relationships between striae abundance / width and growth rate were found to be curvilinear, with asymptotes for both striae width (0.1mm day^{-1}) and abundance (0.025mm day^{-1}) occurring well below the 0.125mm day^{-1} threshold in growth rate at which kinetic effects occurred. This prohibits the identification of those parts of the shell valve associated with high growth rates (and associated kinetic effects).

Chapter 5 Analysis of *Pecten maximus* stable isotopic profiles and surface microgrowth patterns for scallops from offshore, seasonally - stratifying waters.

5.1. Introduction

There is great potential for using isotopic records contained within fossil scallop shells to establish historical records of water temperature / $\delta^{18}O\text{-}H_2O$ and $\delta^{13}C\text{-}\Sigma CO_2$ for palaeo-oceans, once the underlying assumptions of the technique have been satisfied (namely that precipitation occurs in isotopic equilibrium with sea water and that growth occurs over an entire annual cycle). This is of particular relevance given the large number of fossil scallops within the sedimentary record, e.g. Quaternary deposits in Scotland (Scourse, *pers.comm*), within deposits as old as the early Pleistocene in the Antarctic (Barrerra *et al.* 1990), within low latitude Tertiary deposits (Smith, 1991) and Arctic Paleocene deposits (Bice *et al.* 1996).

The calibration work on *Pecten maximus* undertaken in Chapters 3 and 4 and earlier work undertaken by Gruffydd (1981), Dare and Deith (1989) and Dare (1991), have shown that a) when shell growth rates are slow, precipitation of oxygen isotopes occurs in isotopic equilibrium with sea water and carbon isotopes are depleted with respect to isotopic equilibrium by the order of -1 to -2°/oo. At higher growth rates kinetic effects become significant and result in deviations of oxygen isotopic ratios from equilibrium of the order of -0.45 °/oo and further depletions in carbon isotopic ratios from isotopic equilibrium of the order of -0.36°/oo b) shell deposition apparently ceases below 8-9°C c) surface microgrowth patterns are deposited as a function of growth rate. Given such contraints on the isotopic and microgrowth pattern record, an analysis of isotopic and striae profiles was undertaken for scallops collected from an offshore site which exhibits seasonal stratification during the summer (Melville Knoll, south west of the U.K.,49 04 °N 08 48°W). Previous work by Dare and Deith (1989) and Dare (1991) had been undertaken in shallow waters within the principal U.K scallop fishery areas (The English Channel and Irish Sea), regions in which the seasonal temperature range is large (between 6°C and 17°C), usually associated with well-mixed waters, and where seasonally growth rates were often found to be relatively high.

In contrast, limited data for the deeper Melville Knoll site reported by Li and Elliott (1990) show the overall bottom temperature range to be considerably lower (10.2 -11.4°C), exhibiting limited seasonal variation associated with seasonal stratification in the summer and downwelling of warm surface waters during the autumn overturn with a return to well-mixed conditions (Figure 5.1). There are no available $\delta^{13}C$-ΣCO_2 data for the Melville Knoll site. Changes in bottom water $\delta^{13}C$-ΣCO_2 over annual cycles in such offshore, seasonally - stratifying waters are likely to be influenced by isotopic fractionations associated with the biologically mediated processes of inorganic carbon uptake by phytoplankton in surface waters and bacterial mineralisation at depth and the physical processes of seasonal thermocline development and destruction. Kroopnick (1985) reported depth profiles for open ocean sites showing $\delta^{13}C$-ΣCO_2 to be enriched within surface waters and depleted at depth. A possible scenario is one which involves a seasonal cycle where bottom waters become isotopically enriched with respect to carbon, as surface water becomes entrained over the depth profile upon destruction of the seasonal thermocline and then return to isotopically depleted values with remineralisation. Isotopic profiling of a shell of *Pecten maximus* collected from the Melville Knoll site was conducted in the light of the calibration work undertaken earlier to assess whether such changes in water temperature and $\delta^{13}C$-ΣCO_2 were recorded in the shell. Earlier work undertaken within the field study in Chapter 4 had shown striae abundance to be related to shell growth rate in *Pecten maximus*. Upon initial examination, shells collected from the Melville Knoll site were observed to exhibit cycles of striae abundance that suggested seasonal changes in growth rate. Many studies (Krantz *et al.* 1984; Margosian *et al.* 1987; Tan *et al.* 1988; Dare and Deith ,1989; Dare, 1991) have related shell micro and macro growth patterns to profiles of $\delta^{18}O$ to determine the periodicity of formation of such growth patterns e.g. whether shell growth rings are deposited with an annual periodicity. Using such approaches Dare and Deith (1989) and Dare (1991) showed that growth rings on the surface of the *Pecten maximus* shell were not always deposited with an annual periodicity and were therefore unreliable for routine age determination of scallops within the fishery. However, gradual increases and then decreases in striae abundance were found to coincide with periods of enriched $\delta^{18}O$ (i.e. cold water temperatures in the winter). Striae abundance could therefore be used to place location markers of successive winters on the shell surface and allow growth rate determination.

Figure 5.1. Seasonal variation in bottom water temperature at Melville Knoll (data reproduced from Li and Elliott, 1990)

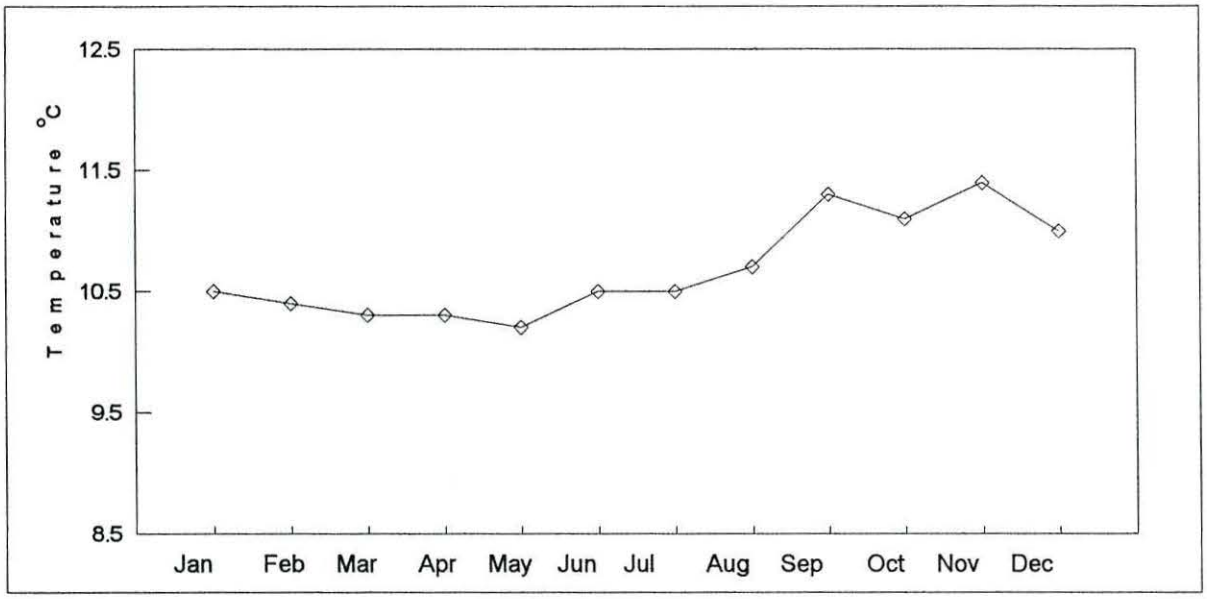

Figure 5.2. Shell - derived and actual annual water temperatures at the Melville Knoll site.

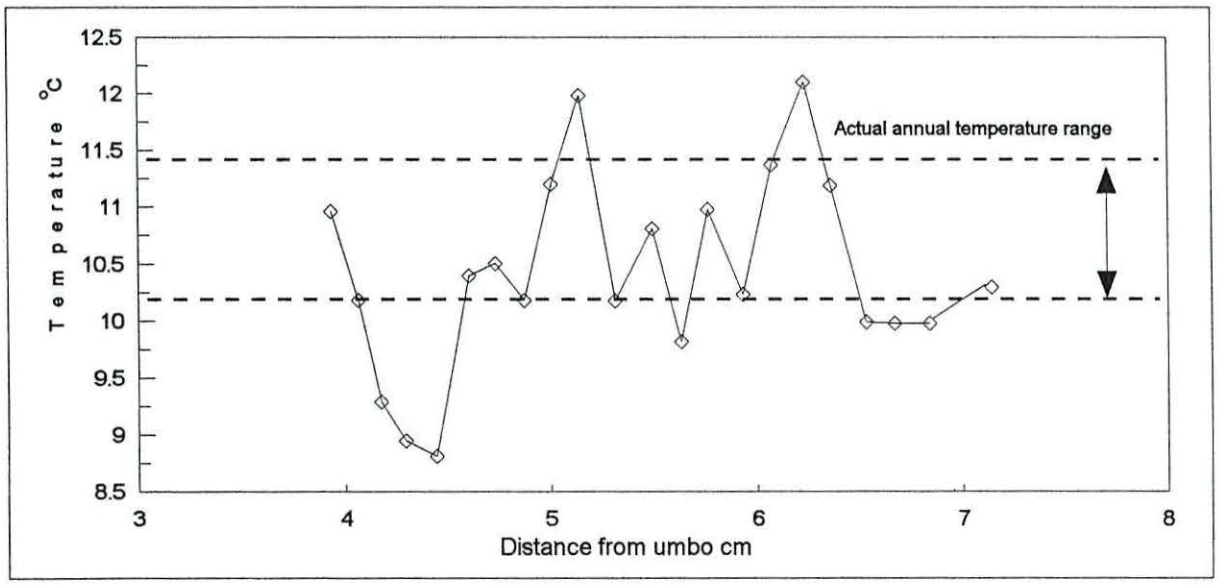

The work undertaken in Chapter 4 has shown that this is a direct result of the relationship between shell growth rate and striae abundance. Such gradual changes in striae abundance could be distinguished from short term disturbances in the striae abundance record that may result in the deposition of a growth line in the shell. An isotopic profiling study of *Pecten maximus* from the Melville Knoll site could provide valuable information allowing an assessment of whether similar observed changes in striae abundance were a result of annual growth reduction. This could then permit determination of growth rates, of particular importance since little is known about the growth rate of this species in these offshore sites. Unlike shallow water locations the annual range in water temperature is very small (1.2°C) and is unlikely to be a factor influencing such changes in shell growth rate. Relating isotopic records to the striae abundance record may additionally provide important information as to factors governing shell growth in offshore waters with little seasonal variation in water temperature.

5.2 Methods

The upper shell valves of *Pecten maximus* dredged from an offshore site (Melville Knoll, 49 04°N 08 48°W), south west of the Isles of Scilly in the British Isles were supplied from archive material by P.Dare (M.A.F.F., Lowestoft). The upper shell valve of one individual was embedded in epoxy resin (Buehler, U.K.), sectioned along the axis at the midline and then ground and polished to reveal the inner and outer shell layers. Calcite samples were drilled sequentially from the outer shell layer from a distance 3.8 cm from the umbo to a distance 7.3 cm from the umbo (i.e. isotopic profiling). Surface striae were then related to the drill holes in the outer shell layer. Calcite samples were typically of the order of 0.1mg (i.e. considerably below the 1mg threshold at which isotopic data has been shown to become significantly inaccurate and imprecise using conventional sealed vessel acidification techniques.) Due to this, the modified sealed vessel method in which the volume of phosphoric acid was considerably reduced was employed. Additionally, the surface microgrowth patterns of 5 individuals were analysed. An acetate strip, onto which a ruler had been photocopied, was placed along the midline between the umbo and valve margin. Striae abundance (no. of striae per mm) was measured at mm intervals between the umbo and valve margin as outlined in Chapter 4.

5.3. Results

Isotopic profile data are presented in Appendix 17 and Plate 5.1. The dashed line within the $\delta^{18}O$ profile indicates data were derived from repeat sampling of the same drill holes. A photomontage of the corresponding microgrowth patterns associated with the sampling region is shown above the isotopic profile in Plate 5.1. Plate 5.1 shows that there were two distinct cycles of $\delta^{13}C$, with maximum values of 1.45°/oo at 5.1mm and 1.47°/oo at 6.2mm from the umbo. $\delta^{18}O$ values also showed two cycles within the profile, with minimum values of 1.55 °/oo and 1.53 °/oo coinciding with the $\delta^{13}C$ maxima. There were three distinct periods of high striae abundance / low striae width within the surface microgrowth pattern profile. $\delta^{13}C$ maxima / $\delta^{18}O$ minima were coincident with periods of low striae abundance (typically of the order of 4-5 striae per mm) and high striae width. Conversely, heavier $\delta^{18}O$ values were associated with periods of higher striae abundance and low striae width in the microgrowth pattern profile. These cycles of striae abundance along the axis of the shell at the midline were also seen in the five scallops sampled for striae abundance, with striae abundances again of the order of 4 -5 striae per mm between the peaks of high striae abundance (Figure 5.3). Periods of high striae abundance often, but not always, coincided with the deposition of a white growth ring. Values for median annual $\delta^{18}O$ and $\delta^{18}O$ range for the scallop shown in Plate 5.1 were 1.88 °/oo and 0.77 °/oo respectively, equivalent to water temperatures of 10.3°C and 3.3°C. Values for median annual $\delta^{13}C$ and $\delta^{13}C$ range were 1.26 °/oo and 0.40 °/oo respectively.

5.4. Discussion

An initial interpretation of the isotopic and striae abundance profiles shown in Plate 5.1 is one in which $\delta^{18}O$ minima / $\delta^{13}C$ maxima are associated with periods of warmest bottom water temperatures (shown in Figure 5.1 to occur between September and November) and heaviest values of $\delta^{13}C$ - ΣCO_2. This would occur during the autumn, coinciding with downwelling of warm, ^{13}C-enriched surface water as the water column returned to well-mixed conditions.

Plate 5.1 Shell surface microgrowth patterns and isotopic profiles for *Pecten maximus* collected at Melville Knoll
Bars = 1σ. + = High striae abundance 0.5cm = ————

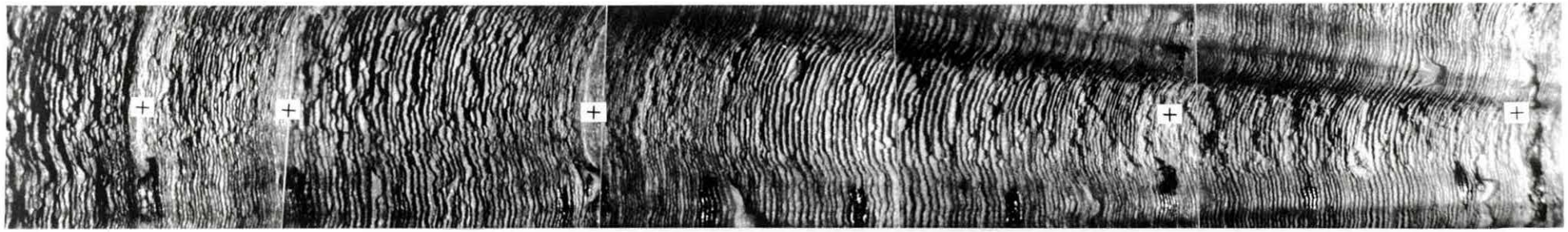

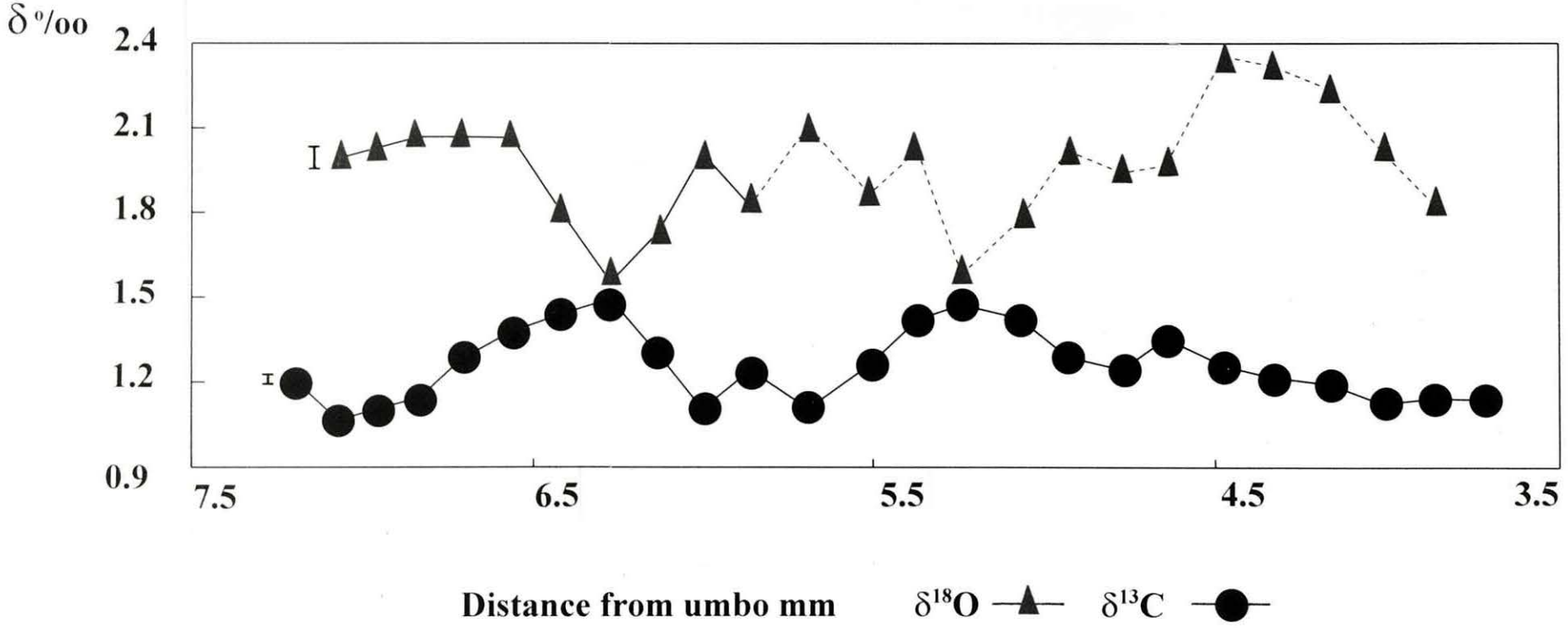

Figure 5.3 Profiles of striae abundance for five *Pecten maximus* collected from Melville Knoll. Downward arrows indicate position of growth rings

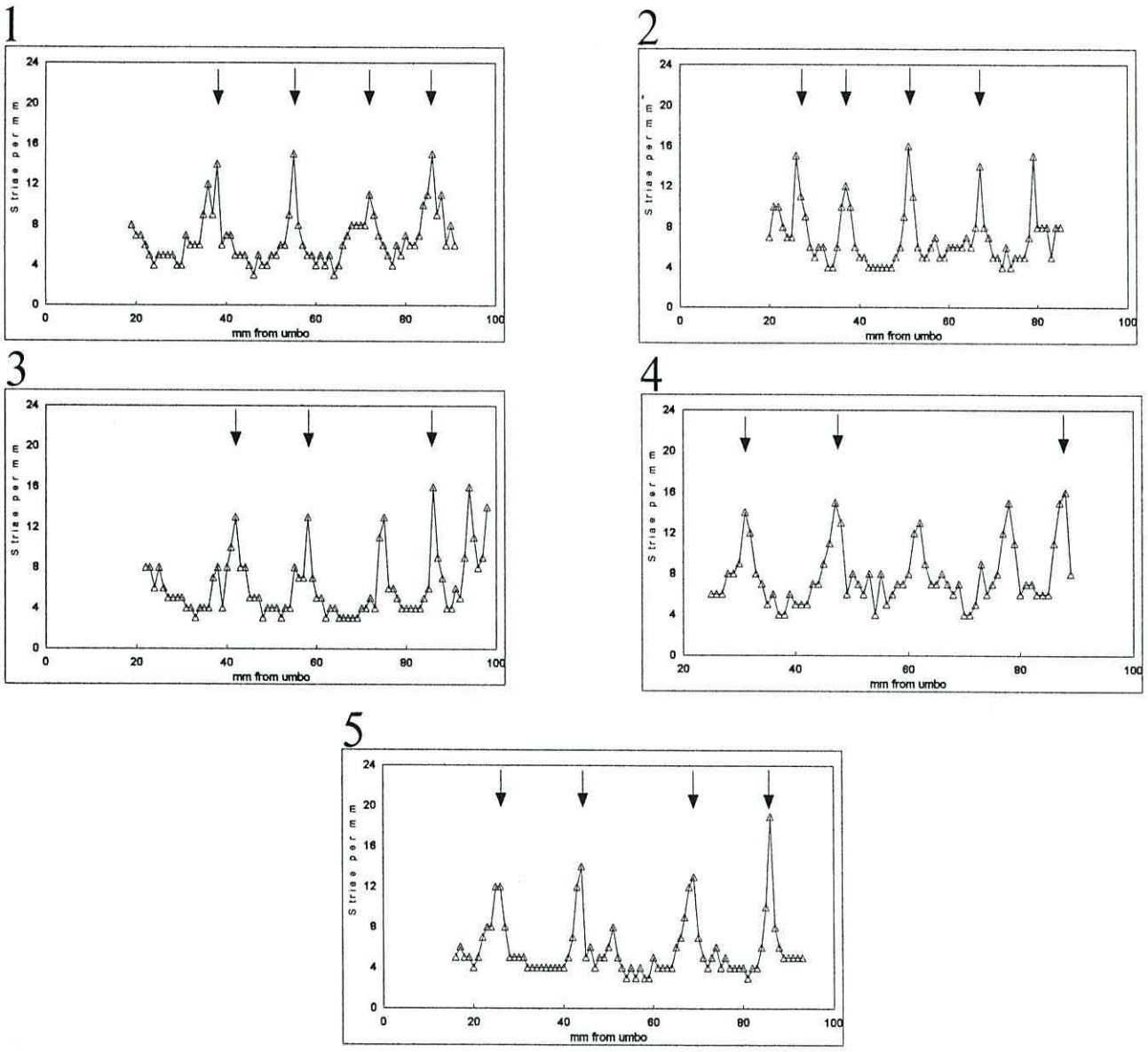

Striae abundances were found to be lowest immediately before and during these periods, reflecting relatively higher shell growth rates. Water temperature is unlikely to be a factor governing shell growth at this site (since the overall range is only 1.2°C).

All five scallops analysed for striae abundance exhibited periods of high abundance, often associated with the deposition of a growth ring, indicative of extreme reduction or cessation in shell growth at certain times of the year (Figure 5.3). Whilst water temperature at this site never falls below 10°C, the threshold for shell growth cessation has been shown in Chapter 4 to be 8 - 9°C. A factor(s) other than water temperature must influence shell growth at this offshore location. One possible factor influencing shell growth is the export of particulate organic material from the surface mixed layer during the summer, and downwelling of organic material during the autumn. This may stimulate relatively high shell growth during the summer and autumn. Such an interpretation is in accordance with the interpretation of the accompanying isotopic profiles for that period, whereby periods of lowest striae abundance coincided with depleted $\delta^{18}O$ and enriched $\delta^{13}C$ data in the shell isotopic record. High striae abundances outside this period were associated with enriched $\delta^{18}O$ and depleted $\delta^{13}C$ data in the shell isotopic record and may be interpreted as reflecting slow shell growth during the winter and spring i.e. periods of marginally cooler water temperatures, low productivity and diminished export of particulate organic matter to the benthos.

No $\delta^{18}O$ - H_2O data are available for the site. A value of +0.6 °/oo was determined by Dare and Deith (1991) for near bottom water sampled in the Western English Channel. Annual salinity variation at this site was found to be low (0.4S). This value may be used, after conversion to δ_w (see Chapter 1, Isotopic Standards), with the mean annual temperature of 10.68°C for the site (Li and Elliott 1990) within the O'Neil *et al.* (1969) expression for inorganic calcite precipitated in isotopic equilibrium with sea water to calculate a predicted $\delta^{18}O$ value of 1.85°/oo. Similarly, the annual range in predicted $\delta^{18}O$ may be calculated as being 0.29 °/oo (1.68 °/oo to 1.97 °/oo). The mean predicted $\delta^{18}O$ value of 1.85°/oo (which equates to a water temperature of 10.7°C) compares well with the median shell derived $\delta^{18}O$ value of 1.88°/oo (which equates to a water temperature of 10.3°C). However the range of shell derived $\delta^{18}O$ is much larger than the predicted range (0.77 °/oo or 3.3°C as compared to 0.29°/oo or 1.2°C). This is shown in Figure 5.2.

If one excludes the heaviest $\delta^{18}O$ values associated with the beginning of the profile in Figure 5.2 (at 4.5mm from the umbo), which appear anomalously isotopically heavy as compared to the rest of the profile, the median and range of shell $\delta^{18}O$ become 1.76 °/oo and 0.53 °/oo respectively. This equates to water temperatures of 11.1°C and 2.2°C respectively. These are more comparable to the mean and range in predicted $\delta^{18}O$ / water temperature.

There are no $\delta^{13}C$ - ΣCO_2 data available for the Melville Knoll site. Data presented for open ocean systems by Kroopnick (1985) show $\delta^{13}C$ - ΣCO_2 to be between +0.5 °/oo and +1.0 °/oo below the permanent thermocline for the Atlantic.Calcite precipitated in isotopic equilibrium with sea water is approximately +1.3 °/oo enriched with respect to $\delta^{13}C$ - ΣCO_2 (see Chapters 3 and 4). This would result in $\delta^{13}C$ values for calcite precipitated in isotopic equilibrium with dissolved inorganic carbon of between +1.8 °/oo and 2.3 °/oo. If these values are compared with the median *Pecten* $\delta^{13}C$ value (1.26°/oo), this would imply that *Pecten* shell $\delta^{13}C$ are depleted with respect to isotopic equilibrium by between 0.5 °/oo and 1 °/oo. The results of the experimental and field work undertaken in Chapters 3 and 4 showed that at low growth rates, oxygen isotopes were precipitated in isotopic equilibrium with sea water but shell $\delta^{13}C$ were depleted with respect to isotopic equilibrium, (as a result of a metabolic effect) by between 1 and 2 °/oo. It is possible, if growth rates were low at the Melville Knoll site throughout the year, that this may also be the case for scallops growing at this location. If shell $\delta^{13}C$ data were constantly offset from predicted data (i.e. a constant metabolic effect) any changes in $\delta^{13}C$ - ΣCO_2 would be recorded in the shell. If shell oxygen isotopes were precipitated in isotopic equilibrium with sea water then changes in water temperature would also be recorded in the shell. This interpretation implies that growth rates at the site were not high enough to exceed the threshold at which a kinetic effect became significant. Striae abundances for scallops at the Melville Knoll site were of the order or 4-5 striae per mm during the growing period (see Figure 5.3.) The field work undertaken in Chapter 4 has shown that, due to the curvilinear relationship between shell growth rate and striae abundance, growth rates both above and below the threshold at which a kinetic effect became significant were associated with similar striae abundances (see Chapter 4, Figure 4.15a) i.e. it is possible to infer from the microgrowth pattern record that growth rates may have been sufficiently low that a kinetic effect did not occur.

It should be noted that depleted shell $\delta^{18}O$ data were not associated with depleted shell $\delta^{13}C$ data (a kinetic effect is associated with simultaneous depletions in both skeletal $\delta^{18}O$ and $\delta^{13}C$). These arguments would support an interpretation of the shell isotope record whereby shell oxygen isotopes were precipitated in isotopic equilibrium with sea water and shell carbon isotopes were depleted with respect to isotopic equilibrium by a constant value. Changes in shell $\delta^{18}O$ and $\delta^{13}C$ could then be explained in terms of changes in water temperature and $\delta^{13}C$ - ΣCO_2 as made above.

Given this interpretation, it may be suggested from the limited data presented that periods of high striae abundance might occur with an annual periodicity, associated with slow growth outside the productive late summer and autumn periods. By measuring the distance between the umbo and each consecutive region of high striae abundance the growth of each of the five scallops analysed for striae abundance has been estimated. Figure 5.4 shows a growth curve fitted to the striae abundance data for the five scallops presented in Figure 5.3. Also shown are growth curves determined from scallop $\delta^{18}O$ profiles for populations in the main fisheries of the Irish Sea and English Channel by Dare and Deith (1989). Growth rates at the Melville Knoll site determined from the scallops within this study and assuming an annual periodicity of striae abundance are considerably lower when compared to growth rates in the more shallow regions of the main fisheries. This has been been previously suggested by P.Dare (*pers comm*).

The above growth rate determinations are based upon the hypothesis of an annual periodicity of striae abundance within the shell, as inferred from isotopic profiles. However, the interpretation of the isotopic record may not be as straight forward as outlined above. The work undertaken in Chapters 3 and 4 have shown that metabolic effects may not be constant, as assumed above. Additionally, these interpretations are based upon analysis of isotopic profiles from one shell and unpublished data within this laboratory for *Pecten maximus* collected at these offshore locations show the shell isotopic record to be far more complex. In conclusion, a more accurate picture of the seasonal cycle of bottom water $\delta^{13}C$ - ΣCO_2 at the site and detailed analysis of more individuals would allow the above interpretations to be more rigorously evaluated.

Figure 5.4. Growth curve for *Pecten maximus* collected from Melville Knoll calculated from striae abundance patterns. Also shown are growth curves obtained by Dare and Deith (1989) for scallop populations in the Western English Channel and Irish Sea.
Growth curves fitted using Von Bertalanffy growth equation of the form $L_t = L_{max} (1 - e^{-k(t - to)})$
Melville Knoll scallops $L_t = 183.8 (1 - e^{-0.105 (t - 0.331)})$
Irish Sea scallops $L_t = 126.7 (1 - e^{-0.282 (t - 0.510)})$
W.Channel scallops $L_t = 116.5 (1 - e^{-0.340 (t - 0.620)})$

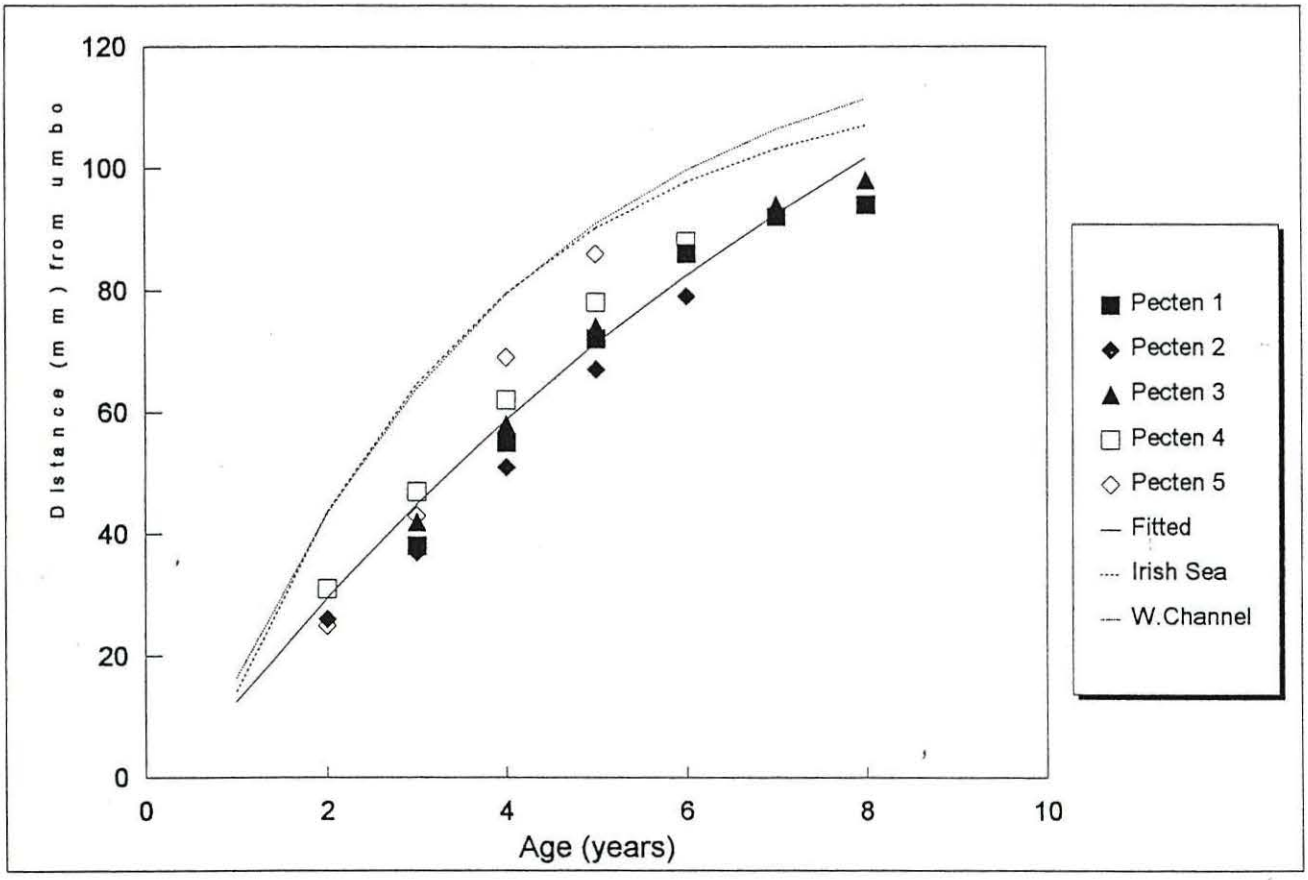

Chapter 6 Summary and Conclusions

When precipitation of carbonates occurs in isotopic equilibrium with sea water the oxygen isotopic composition of the carbonate ($\delta^{18}O$) will be governed by the isotopic composition of sea water ($\delta^{18}O$-H_2O) and water temperature, partitioning of isotopes between the carbonate and sea water occurring as a result of a temperature-dependent equilibrium isotope effect. Similarly, the carbon isotopic composition of the carbonate ($\delta^{13}C$) will be governed by sea water temperature and the isotopic composition of dissolved inorganic carbon ($\delta^{13}C$-ΣCO_2). It was Urey (1947) who first considered the partitioning of oxygen and carbon isotopes between carbonates and sea water from a theoretical viewpoint and who foresaw the potential for utilising $\delta^{18}O$ data to establish historical records of sea water temperature. This initial study prompted further work from the 1950's onwards in which partitioning of oxygen isotopes between inorganically and biologically - precipitated carbonates (foraminifera and molluscs) and sea water was examined by experiment (McCrea, 1950, O'Neil *et al.* 1969, Erez and Luz, 1983, Epstein *et al.* 1953). In open ocean systems changes in $\delta^{13}C$-ΣCO_2 often reflect the biologically-mediated processes of primary production and remineralisation of organic material (Kroopnick, 1985). Since $\delta^{13}C$ is a function of $\delta^{13}C$-ΣCO_2 and water temperature, there exists the potential for the establishment of historical records of $\delta^{13}C$-ΣCO_2 (and thereby productivity cycles) from $\delta^{13}C$ in addition to records of water temperature / $\delta^{18}O$-H_2O from skeletal $\delta^{18}O$.

The molluscan shell represents a time series of carbonate precipitation deposited over the life of the organism. Sequential sampling along the shell axis ('isotopic profiling') allows the establishment of $\delta^{18}O$ and $\delta^{13}C$ profiles. In addition, growth patterns found on the surface and within the shell can potentially provide important information once the factors governing the deposition of these growth patterns have been identified (Richardson, 1991; 1996). A review of the literature had shown that there are two fundamental, yet frequently untested assumptions underlying the utilisation of isotopic profiles derived from biologically-precipitated carbonates to establish historical records of sea water temperature / $\delta^{18}O$-H_2O and $\delta^{13}C$-ΣCO_2. These are a) that the carbonate is continuously precipitated throughout the time period for which the record is being established and b) both oxygen and carbon isotopes are precipitated in isotopic equilibrium with sea water over the range of growth rates exhibited by the organism in question.

The research conducted here tested these assumptions by controlled experiment and a year long field study for the scallop *Pecten maximus*. It also examined factors controlling the deposition of microgrowth patterns ('striae') found on the surface of the scallop shell. In addition to the occurrence of well-defined striae on the shell surface, the scallop is a good case organism for study due to its widespread occurrence within the sedimentary record, in particular within Quaternary deposits. Indeed some workers have attempted to reconstruct palaeowater temperatures from scallop shell $\delta^{18}O$ (Krantz *et al.* 1987; Bice *et al.* 1996). *Pecten maximus* was also chosen for this research since the work built upon existing studies examining partitioning of stable isotopes between *Pecten* shell calcite and sea water using field - collected individuals (Dare and Deith, 1989; Dare and Deith, 1991), and both experimental and field work examining striae deposition (Gruffydd, 1980; Dare ,1991).

Prior to the undertaking of the experimental and field work a study was made assessing some of the underlying methodologies central to the research. A long - established procedure within the analytical method for the determination of the isotopic composition of biologically - precipitated carbonates is the pretreatment of the carbonate to remove organic components prior to sealed - vessel acidification. Shell matrix contains organic components, and a review of the literature had shown that removal of these organic components was associated with depletions in both oxygen and carbon isotopic ratios in carbonates. Experiments undertaken within this study in which homogenised *Pecten* shell was plasma - ashed to remove organic material confirmed this. Ashed shell exhibited isotopic depletions when compared to non-ashed shell of between 0.38 °/oo and 0.9 °/oo for oxygen and between 0.09 °/oo and 0.25°/oo for carbon. Such isotopic depletions were not found when inorganic carbonate was ashed. The possibility that these depletions were an artefact of the organic removal process was explored in a further series of experiments. It is possible that isotopically-depleted CO_2 derived from the organic matrix upon ashing may have exchanged with the carbonate within the asher. This possibility was tested by ashing inorganic carbonate samples in close vicinity to homogenised shell samples. Since the inorganic carbonate samples displayed no significant depletions after ashing it was concluded that the depletions observed in shell isotopic ratios upon ashing were a direct result of organic component removal and were not artefactual, although an underlying mechanism explaining the observed depletions could not be offered.

The relationship between sample size and carbonate isotopic ratios was also investigated in a series of analyses of standard inorganic calcite of varying weight. Below carbonate weights of 1mg, both the precision and accuracy of carbonate isotopic data became significantly compromised. It was suggested that the source of this error lay in the acidification step of the method and may have resulted from dissolution of evolved CO_2 within the acid. It was concluded that the sealed -vessel method as it stood was unacceptable for derivation of water temperature/ $\delta^{18}O\text{-}H_2O$ and $\delta^{13}C\text{-}\Sigma CO_2$ data from carbonate samples below 1mg in weight.

The assumption that precipitation of *Pecten* shell calcite occurs in isotopic equilibrium with sea water was tested in a controlled experiment in which juvenile scallops (<1 year old) were grown at four, constantly - maintained temperatures. Juvenile scallops were chosen since it is the earliest shell growth that is most suitable for isotopic sampling when determining mean and annual ranges in temperature / $\delta^{18}O\text{-}H_2O$ and $\delta^{13}C\text{-}\Sigma CO_2$ from shell isotopic data i.e. when growth is fastest and there are no potential influences of sexual maturity. Water samples were collected from each of the four tanks holding the scallops at regular intervals over the experimental period to allow calculation of predicted $\delta^{18}O$ and $\delta^{13}C$ data for calcite precipitated in isotopic equilibrium with sea water. Predicted $\delta^{18}O$ data were determined from $\delta^{18}O\text{-}H_2O$ and water temperature data, and using the O'Neil *et al.* (1969) expression relating $\delta^{18}O$, $\delta^{18}O\text{-}H_2O$ and water temperature at isotopic equilibrium. Predicted $\delta^{13}C$ data were determined from temperature, salinity, pH and $\delta^{13}C\text{-}\Sigma CO_2$ data, using firstly a mass balance model describing partitioning of carbon isotopes within dissolved inorganic carbon at isotopic equilibrium and published enrichment factors to calculate the isotopic composition of bicarbonate and secondly using the published enrichment factor for partitioning of carbon isotopes between bicarbonate and calcite at isotopic equilibrium. Predicted $\delta^{18}O$ / $\delta^{13}C$ data were compared to shell $\delta^{18}O$ / $\delta^{13}C$ data for the increment of shell grown over the experiment. Over the experimental temperature range shell $\delta^{18}O$ data did not significantly differ from predicted $\delta^{18}O$ data for calcite precipitated in isotopic equilibrium with sea water. Variability associated with shell $\delta^{18}O$ data at each temperature was shown to be largely analytical. Unlike $\delta^{18}O\text{-}H_2O$ and water temperature, $\delta^{13}C\text{-}\Sigma CO_2$ within each of the experimental tanks was not found to be constant.

This may have reflected temporal variations in water residence time within each tank superimposed upon inputs of isotopically depleted respiratory CO_2 to the dissolved inorganic carbon pool from the growing scallops. Despite these variations, shell $\delta^{13}C$ data were found to be significantly different from predicted $\delta^{13}C$ data for calcite precipitated in isotopic equilibrium with sea water, being isotopically depleted with respect to equilibrium by an average of -2°/oo over the experimental temperature range. A review of the literature had shown there to be some uncertainty in the determination of predicted $\delta^{13}C$ data due to uncertainties in the values of the enrichment factor between $CO_3^{2-}{}_{(aq)}$ and gaseous CO_2 (ε_{g} c) for a sea water medium. Correcting for this did not affect the conclusions made from the experiment, with shell $\delta^{13}C$ being depleted with respect to isotopic equilibrium by an average of -1.85°/oo over the experimental temperature range.

McConnaughey (1989b) has postulated a model which may be used to explain the experimental results in terms of a 'metabolic effect' resulting from inclusion of respiratory CO_2 into the extrapallial fluid (E.P.F.) from which the shell precipitates. This causes depletions in skeletal $\delta^{13}C$ which are not accompanied by simultaneous depletions in skeletal $\delta^{18}O$. This is in part because of the large fluxes of water between sea water and the E.P.F. as compared to carbon fluxes between sea water ΣCO_2 and E.P.F. ΣCO_2. It is also due to the action of carbonic anhydr*ase* which is found within the mantle epithelial cells and catalyses oxygen isotope exchange (Silverman , 1973), tending to equilibrate CO_2 with sea water with respect to oxygen isotopes, but has no effect on carbon isotopes. Evidence was reviewed supporting the fact that respiratory CO_2 can comprise a significant proportion of inorganic carbon supply to the E.P.F. in molluscs.

The assumption that precipitation of *Pecten* shell isotopes occurs in isotopic equilibrium with sea water was further investigated in a year long time series field study conducted within the Menai Strait. The annual cycle of productivity in the Menai Strait is associated with a predictable and well-characterised sequence of low algal abundance in the late autumn to early spring, a diatom bloom in the late spring followed by an intense but short-lived bloom of *Phaeocystis pouchetti* and intermediate levels of productivity throughout the late summer and early autumn.

This succession is associated with large changes in $\delta^{13}C$-ΣCO_2. Seasonal variation in water temperature is also large, whilst salinity variations (and therefore $\delta^{18}O$-H_2O variations) are relatively small. A field study in the Menai Strait therefore provided an excellent opportunity to investigate factors influencing shell microgrowth patterns and seasonal variation in shell growth rate (e.g. water temperature, concentration of chlorophyll and P.O.C. and P.O.N). It allowed an assessment to be made of the effects of shell growth rate upon partitioning of isotopes between shell calcite and sea water (further testing the assumption of precipitation of shell calcite in isotopic equilibrium with sea water). It also presented an opportunity to assess the resolution with which changes in water temperature and $\delta^{13}C$-ΣCO_2 may be tracked within the *Pecten* shell given such seasonal variation in growth rate.

The biogeochemistry of the Menai Strait was characterised over the year of the field study, water samples being collected at weekly to fortnightly intervals at Menai Bridge Pier for algal speciation, dissolved nutrients, P.O.C.and P.O.N and chlorophyll concentration, temperature, salinity, pH, $\delta^{13}C$-ΣCO_2 and $\delta^{18}O$-H_2O. Scallops were placed for periods of approximately one month throughout the year in a specially-constructed box attached below a raft in the Menai Strait. The increment of shell grown by each individual during each monthly period was subsequently analysed for $\delta^{18}O$ and $\delta^{13}C$. In addition scallops were placed in the field for the entire year and the increment of shell grown by each individual sampled to establish profiles of $\delta^{18}O$ and $\delta^{13}C$. Shell isotopic data were then compared to predicted isotopic data for calcite precipitated in isotopic equilibrium with sea water, as determined from water samples collected at Menai Bridge Pier. Shell growth rates were determined for each monthly period and related to water temperature, chlorophyll and P.O.C.and P.O.N concentrations. An assessment was made of the variation with growth rate of the time integrated per calcite sample taken from the shell, allowing an appraisal of the resolution with which the shell isotopic record can track changes in water temperature / $\delta^{18}O$-H_2O and $\delta^{13}C$-ΣCO_2. Additionally the number of striae deposited per day, striae width and abundance (number of striae deposited per mm) were determined from the increment of shell grown by each individual during each monthly period.

As expected, seasonal variation in water temperature for the period covering the field study (October 1994 - September 1995) was large, with a minimum water temperature of 6.3°C in March 1995 and maximum water temperature of 18.9°C in August 1995.

Variation in salinity was low and showed no seasonal variation. Both salinity and $\delta^{18}O\text{-}H_2O$ were well correlated and variation in $\delta^{18}O\text{-}H_2O$ was therefore also low and showed no seasonal bias. The seasonal variation in the biogeochemistry of the Menai Strait was primarily influenced by the seasonal productivity cycle. Algal abundance (and therefore chlorophyll concentration) fell in the autumn of 1994 to low values, remaining low throughout the winter. Nutrient concentrations (dissolved nitrate, nitrite, phosphate and silicate) were elevated throughout this period. At the beginning of May 1995 the major spring diatom bloom occurred, with rapid increases in chlorophyll concentration, immediately preceded by a drop in dissolved silicate concentration. The diatom bloom tailed into an intense, but short-lived bloom of *Phaeocystis*, accompanied by rapid and large decreases in nitrate and nitrite concentrations and a peak in chlorophyll concentration. The rapid drop in these nutrients initiated the crash of the *Phaeocystis* bloom in mid June. The bloom period between May and the end of June was associated with large changes within the TCO_2 system and large changes in $\delta^{13}C\text{-}\Sigma CO_2$. In particular, the diatom-*Phaeocystis* bloom period was associated with large falls in $[\Sigma CO_2]$ and $[CO_{2aq}]$, increases in pH and an increase in $\delta^{13}C\text{-}\Sigma CO_2$ from winter values of between 0°/oo and 0.4°/oo to a peak in June of 1.23°/oo. This was a result of inorganic carbon uptake and accompanying fractionation of carbon isotopes associated with primary production. Parameters of the TCO_2 system and $\delta^{13}C\text{-}\Sigma CO_2$ returned to pre - bloom values in late June. Intermediate chlorophyll and low nitrate concentrations were observed between July and September, during which time remineralisation of silicate and phosphate occurred. Despite such changes in primary production, particulate organic loading in the water column was high throughout the year, reflecting the dynamic nature of the Menai Strait. Organic loading appeared to be dominated by phytoplankton in the spring and summer but with other organic matter sources prevalent throughout the year and making up a significant component of P.O.M. oustide the spring and summer.

Pecten shell growth displayed distinct seasonality, with shell accretionary rates decreasing during the autumn of 1994 to a minimum during January -March of 1995 when shell deposition effectively ceased (i.e.at water temperatures below approximately 8 - 9°C).

Shell growth resumed in the spring (mid March - mid April) and rose to a maximum of 0.15 - 0.19mm per day spanning the period between the beginning of June and mid August. Shell growth rate then tailed off in September.

Both water temperature and chlorophyll concentration were identified as possible factors influencing shell growth, with shell growth being independent of concentrations of P.O.C. Striae deposition was found to be governed by shell growth rate. The number of striae deposited per day was found to be linearly related to shell growth rate. Striae width (i.e. the increment of shell between consecutive striae) and striae abundance (number of striae per mm) appeared to exhibit positive and negative curvilinear relationships with shell growth rate respectively. There therefore appeared to be a threshold in shell growth rate above which striae width and abundance reached a plateau. This implies that there is a finite limit to stria width.

Partitioning of isotopes between *Pecten* shell calcite and sea water was also influenced by shell growth rate. At slow growth rates, *Pecten* shell oxygen isotopes were found to be precipitated in isotopic equilibrium with sea water, but shell carbon isotopes were precipitated out of isotopic equilibrium with dissolved inorganic carbon, being depleted by -1 °/oo. These results confirmed the experimental findings, again suggesting inputs of isotopically - depleted respiratory CO_2 to the E.P.F. which cause depletions in shell $\delta^{13}C$, but with no effect on shell $\delta^{18}O$ i.e. a metabolic effect. It was calculated that between 3 and 5% of shell carbon was derived from respiratory CO_2. This is in agreement with the findings of McConnaughey *et al.* (1997) who concluded that, in general, the contribution of respiratory CO_2 to shell carbon is less than 10% for molluscs and typically results in deviations of shell $\delta^{13}C$ from isotopic equilibrium of less than 2°/oo.

At higher shell growth rates (above 0.125 mm day $^{-1}$), during the late spring to early autumn period, deviations in $\delta^{18}O$ from predicted values for calcite precipitated in isotopic equilibrium with sea water of the order of -0.45 °/oo were observed for both scallops placed out for monthly periods and those placed in the field for the entire year, accompanied by further depletions in shell $\delta^{13}C$. These simultaneous deviations in $\delta^{18}O$ and $\delta^{13}C$ from isotopic equilibrium may be interpreted as resulting from a kinetic isotope effect at higher growth rates as postulated by McConnaughey (1989b).

Further depletions in $\delta^{13}C$ from values for calcite precipitated in isotopic equilibrium with sea water of the order of -0.4 °/oo were observed for scallops placed in the field for monthly periods.

Scallops placed in the field for the entire year exhibited further depletions from isotopic equilibrium of -0.9 and -1.2°/oo during this period. This may have reflected an increased metabolic effect within these scallops at this time since the level of oxygen isotopic disequilibrium was the same as for monthly individuals.

In conclusion, the experimental and field work reported in this thesis show *Pecten maximus* shell $\delta^{18}O$ and $\delta^{13}C$ profiles to be of only limited use for establishing historical records of water temperature / $\delta^{18}O$ -H_2O and $\delta^{13}C$ -ΣCO_2.

This is due in part to the fact that it cannot be assumed that shell growth occurs over a complete annual cycle. In the present study seasonal reduction and cessation of shell growth occurred in the winter, with the absence of associated isotopic data. Since this occurred during periods of coldest water temperatures it resulted in an underestimation of the annual $\delta^{18}O$ maximum. It is also due to the fact that the assumption that shell isotopes are precipitated in isotopic equilibrium with sea water cannot be upheld for this species. At low growth rates, whilst shell oxygen isotopes were found to be precipitated in isotopic equilibrium with sea water, this was not the case for shell carbon isotopes. The observed depletions in shell $\delta^{13}C$ with respect to isotopic equilibrium were interpreted as being a result of a metabolic effect, which may be variable. Additionally, periods of high shell growth rates are associated with deviations / further deviations in shell $\delta^{18}O$ / $\delta^{13}C$ from isotopic equilibrium, interpreted as being a result of a kinetic effect. Since striae abundance and width were found to be related to shell growth rate, it should be possible to identify specific striae abundances and widths, in fossil shells for example, associated with shell growth rates at which kinetic effects become significant. However, the relationship between growth rate and striae width / abundance was found to be curvilinear, with asymptotes for maximum widths and minimum abundances occurring well below the 0.125 mm day $^{-1}$ shell growth rate threshold at which a kinetic effect became significant.

The combined influences of seasonal growth cessation and metabolic/kinetic effects resulted in erroneous shell-derived median values and environmental ranges of water temperature / $\delta^{18}O$ -H_2O and $\delta^{13}C$ - ΣCO_2.

The interpretation of isotopic records from field -collected deep water *Pecten* shells must be considered in the light of these findings. Isotopic profiles from the shell of a *Pecten* individual collected from a seasonally-stratifying oceanic site exhibited two cycles, with two $\delta^{13}C$ peaks associated with lightest $\delta^{18}O$ values and lowest striae abundances. An interpretation of the data was made whereby peaks of $\delta^{13}C$ and lightest $\delta^{18}O$ values were explained as reflecting the overturn of productive, warm surface water and were associated with relatively high growth rates and therefore low striae abundances. This interpretation was based on the assumption that growth rates were relatively low throughout the year at this site. It was inferred that, at these low growth rates, oxygen isotopes were precipitated in isotopic equilibrium with sea water and that shell $\delta^{13}C$ was constantly offset from isotopic equilibrium as a result of a metabolic effect, there being no kinetic effect. However, the calibration work undertaken within the field study questions the assumption that any metabolic effect is indeed constant.

The two fundamental assumptions described in Chapter 1 that are central to the use of stable isotopic profiles for establishing historical records of water temperature / $\delta^{18}O$ -H_2O and $\delta^{13}C$ -ΣCO_2 have been shown in this study to not be upheld for *Pecten maximus,* prohibiting the establishment of accurate mean values and ranges for these parameters from the shell record. Stable isotopic profiles may however be useful for certain applications where only broad changes in seasonality need to be identified in the shell record and accuracy is not an important consideration. For example, stable oxygen isotopic profiles may be useful for identifying regions of the shell associated with deposition during periods of warm summer and cold winter water temperatures, allowing the placing of annual location markers in the shell to which macro and micro growth patterns may be related. In this way several workers have tested the assumption of an annual periodicity of growth line formation and calibrated microgrowth patterns for a number of species (scallops (Krantz *et al.* (1984); Tan *et al.* (1988); Dare and Deith (1989); Dare (1991); clams (Weidman *et al.* (1994); mussels (Margosian *et al.* 1987)). This may be of particular importance when such macro and micro growth patterns are used to age commerically - important species.

Reference List

Abelson P.H., Hoering T.C. (1961) Carbon isotope fractionation in formation of amino acids by photosynthetic organisms. Proc. Natl. Acad. Sci. U.S.A. **47**: 623-632.

Antoine L.(1978) La croissance journaliere chez *Pecten maximus*(L.) (Pectinidae, Bivalvia) Haliotis **7**: 117-126.

Arthur M.A., Williams D.F., Jones D.S. (1983). Seasonal temperature - salinity changes and thermocline development in the mid - Atlantic Bight as recorded by the isotopic composition of Bivalves : Geology, **11**: 655-659.

Baertschi P. (1957) Messung und deutung relativer haufigeitsvariationen von ^{18}O und ^{13}C in karbonatgesteinen und mineralien. Schweitz. Mineral. Petrol. Mitt. **37**: 73-152.

Ball J.D., Crowley S.F., Steele D.F. (1996) Carbon and oxygen isotope ratio analysis of small carbonate samples by conventional phosphoric acid digestion - sample preparation and calibration. Rapid Communications in Mass Spectrometry **10** (8): 987-995.

Barrerra E.,Tevesz M.J.S., Carter J.G. (1990) Variations in oxygen and carbon isotopic composition and microstructure of the shell of *Adamussium colbecki* (Bivalvia). Palios **5**: 149-159.

Bice K.L. Arthur M.A., Marincovich, L. (1996) Late Paleocene Arctic Ocean shallow - marine temperatures from mollusc stable isotopes. Paleoceanography **11 (3)** : 241-249.

Bigeleisen J., Mayer M.G. (1947). Calculation of equilibrium constants for isotopic exchange reactions : J. Chem. Phys. , **15**: 261- 267.

Blight S.P. Bentley T.L., Lefevre D., Robinson C., Rodrigues R., Rowlands J., Williams P.J. leB.(1995) Phasing of autotrophic and heterotrophic plankton metabolism in a temperate coastal ecosystem. Mar.Ecol.Prog.Ser. **128**: 61-75.

Boutton T.W. (1991) Stable carbon isotope ratios of natural materials: 1.Sample preparation and mass spectrometric analysis. *In:* Carbon Isotope Techniques, (eds D.C.Coleman, B.Fry) Academic Press, 155-171.

Broom M.J., Mason J. (1978) Growth and spawning in the pectinid *Chlamys opercularis* in relation to temperature and phytoplankton concentration. Mar.Biol. **47**: 277-285.

Cifuentes L.A., Sharp J.H., Fogel M.L. (1988) Stable carbon and nitrogen isotope biogeochemistry in the Delaware Estuary. Limnol. Oceanogr., **33** (5): 1102-1115.

Clark G.R. (1968) Mollusk shell: daily growth lines. Science **161**: 800-802.

Clark G.R. (1975) Periodic growth and biological rhythmns in experimentally grown bivalves. *In* : Growth Rythmns and the history of the Earth's rotation (ed. G.D.Rosenberg, S.K. Runcorn) J.Wiley and Sons, London: 103-117.

CoBabe E.A., Pratt L.M. (1995) Molecular and isotopic compositions of lipids in bivalve shells: A new prospect for molecular paleontology.Geochimica et Cosmochimica Acta **59** (1): 87-95.

Craig H. (1953) The geochemistry of the stable carbon isotopes. Geochimica et Cosmochimica Acta **3**: 53-92.

Craig H. (1957) Isotopic standards for carbon and oxygen and correction factors for mass-spectrometric analysis of carbon dioxide. Geochimica et Cosmochima Acta **12**: 133-149.

Craig H. (1961) Standard for reporting concentrations of deuterium and oxygen-18 in natural waters. Science **133** no 3467: 1833-1834.

Craig H. (1965). The measurement of oxygen isotope paleotemperatures, *in* Stable isotopes in oceanographic studies and paleotemperatures , Spoleto, July 26 - 30, 1965, no 3.(E. Tongiorgi, ed.) pp1 - 24 , Consiglio Nazionale delle Rierche, Laboratorio di Geologica Nucleare, Pisa.

Crenshaw M.A.(1972) The inorganic composition of molluscan extrapallial fluid. Biol. Bull. **143**: 506-512.

Dansgaard W. (1964) Stable isotopes in precipitation. Tellus **16**: 436-468.

Dare P.J. (1991). Use of external shell microgrowth patterns for determining growth and age in the Scallop, *Pecten maximus* : 8th International Pectinid workshop, Cherbourg, France, May, 1991.

Dare P.J., Deith M.R. (1989). Age determination of Scallops, *Pecten maximus*, using stable oxygen isotope analysis, with some implications for fisheries management in British waters. 7th International Pectinid Workshop, Portland, Maine, USA, April 1989.

Dare P.J., Deith,M.R. (1991). Problems with reconstructing sea - water temperature records from stable oxygen isotopic profiles in shells of the Scallop *Pecten maximus* : 8th International Pectinid Workshop , Cherbourg, France, May 1991.

Deuser W.G., Degens E.T. (1967) Carbon isotope fractionation in the system CO_2 (gas) - CO_2 (aqueous) - HCO_3 (aqueous). Nature **215**: 1033-1035.

Dillaman R.M., Ford S.E. (1982) Measurement of calcium carbonate deposition in molluscs by controlled etching of radioactively labeled shells. Mar. Biol **66** :133-143.

Donner J., Nord A.G. (1986) Carbon and oxygen stable isotope values in shells of *Mytilus edulis* and *Modiolus modiolus* from Holocene raised beaches at the outer coast of the Varanger Peninsular, North Norway. Paleogeogr. Paleoclim. Paleoecol. **56**: 35-50.

Dudley W.C., Goodney D.E.(1979) Oxygen isotope content of coccoliths grown in culture. Deep Sea Res. **26A**: 495-503.

Emiliani C. (1955) Pleistocene temperatures. J.Geol. **63**: 538-578.

Emrich K., Ehhalt D.H., Vogel J.C. (1970) Carbon isotope Fractionation during the precipitation of Calcium Carbonate. Earth and Planetary Science Letters. **8**: 363-371.

Epstein S., Lowenstam, H.A. (1953). Temperature - shell growth relations of recent and interglacial Pleistocene shoal - water biota from Bermuda. J. Geol., **61**: 424-438.

Epstein S., Mayeda, T. (1953) Variation of O^{18} content of waters from natural sources. Geochimica et Cosmochimica Acta **4**: 213-224.

Epstein S., Buchsbaum R., Lowenstam H.A.,Urey, H.C. (1951). Carbonate - water isotopic temperature scale : Bull. Geol. Soc. Am., **62**: 417-426.

Epstein S., Buchsbaum R., Lowenstam H.A., Urey, H.C. (1953). Revised carbonate - water temperature scale : Bull. Geol. Soc. Am., **64** : 1315-1326.

Erez J. (1977) Influence of symbiotic algae on the stable isotopic composition of hermatypic corals: A radioactive tracer approach. Proc.3rd Int. Coral Reef Symp. Miami: 563-569.

Erez J. (1978) Vital effect on stable isotope composition seen in foraminiferan and coral skeletons. Nature, **273**: 199-202.

Erez J, Honjo S. (1981) Comparison of isotopic composition of planktonic foraminifera in plankton tows, sediment traps and sediments. Paleogeog. Paleoclim. Paleoecol. **33** : 129-156.

Erez J., Luz B. (1983) Experimental paleotemperature equation for planktonic foraminifera. Geochimica et Cosmochimica Acta **47**: 1025-1031.

Erlenkeuser H., Wefer G. (1981) Seasonal growth of bivalves from Bermuda recorded in their O-18 profiles. Proc.Int.Coral Reef Symp., 4th (Manila), 2: 643-648.

Ewins P.A., Spencer C.P. (1967) The annual cycle of nutrients in the Menai Strait. J.M.B.A.U.K. **47**: 533-542.

Fairbanks R.G. (1982) The origin of Continental Shelf and Slope Water in the New York Bight and Gulf of Maine: Evidence from $H_2{}^{18}O$ / $H_2{}^{16}O$ ratio measurements. J. Geophys. Res. **87**, C8: 5796-5808.

Fastovsky D.E., Arthur M.A., Strater N.H., Foss A. (1993) Freshwater Bivalves (Unionidae), Disequilibrium Isotopic Fractionation, and Temperatures. Palaios, 1993, **v8**: 602-608.

Frew R.D., Heywood K.J., Dennis P.F. (1995) Oxygen isotope study of water masses in the Princess Elizabeth Trough, Antartica. Mar Chem. **49**: 141-153.

Friedman I., O'Neil J.R. (1977) Compilation of stable isotope fractionation factors of geochemical interest. Data of Geochemistry,6th edition (ed M.Fleischer).U.S.Geol. Surv.Prof.Paper **776**: 1-37.

Fritz P., Poplawski S. (1974) ^{18}O and ^{13}C in the shells of freshwater molluscs and their environments. Earth and Planetary Science Letters **24**: 91-98.

Gaffey S.J., Kolak J.J., Bronniman C.E. (1991) Effects of drying, heating, annealing and roasting on carbonate skeletal material, with geochemical and diagentic implications. Geochimica et Cosmochimica Acta **55** (6): 1627-1640.

Goreau T.J. (1977) Carbon metabolism in calcifying and photosynthetic organisms: theoretical models based on stable isotope data. Proc. 3rd Int. Coral Reef Symp. **2**: 395-401.

Grossman E. (1982). Stable isotopes in live benthic foraminifera from the Southern Californian Borderland. PhD Thesis. University of South California, Los Angeles. pp164.

Grossman E., Ku T.L. (1986) Oxygen and carbon isotope fractionation in biogenic aragonite: temperature effects. Chem. Geol. (Isot.Geosci.Sect.) **59**: 59-74.

Grossman E.L., Betzer P.R., Dudley W.C., Dunbar R.B. (1986) Stable isotopic variation in Pteropods and Atlantids from North Pacific Sediment Traps. Marine Micropaleontology **10** : 9-22.

Gruffydd L.D. (1981) Observations on the rate of production of external ridges on the shell of *Pecten maximus* in the laboratory. J.M.B.A. U.K. **61**: 410-411.

Hayes. J.M. (1982) Fractionation, *et al*: An Introduction to Isotopic Measurements and Terminology. Spectra **8** no 4: 3-8.

Hidayat J.W. (1995) Zooplankton composition and seasonal fluctuations in the Menai Strait, Anglesey, North Wales. Msc Thesis, University of Wales.

Horibe S., Oba T. (1972) Temperature scales of aragonite - water and calcite - water systems. Fossils **23/24**: 69-79.

Jones D.S., Williams D.F., Arthur M.A. (1983). Growth history and ecology of the Atlantic Surf Clam *Spissula solidissima* (Dillwyn) as revealed by stable isotopes and annual shell increments : J.Exp.Mar.Biol.Ecol.**73**: 225-242.

Jones D.S., Williams D.F., Romanek,C.S. (1986) Life history of symbiont-bearing Giant Clams from stable isotope profiles: Science **231**: 46-48.

Kahn M.I. (1979) Non-equilibrium oxygen and carbon isotopic fractionation in tests of living planktonic foraminifera. Oceanol. Acta **2**: 195-208.

Kahn M.I., Williams D.F. (1981) Oxygen and carbon isotopic composition of living planktonic foraminifera from the Northeast Pacific Ocean. Palaeogeo.,Paleoclim., Paleoecol. **33**: 47 - 69.

Kalish J.M. (1991). ^{13}C and ^{18}O isotopic disequilibria in fish otoliths: metabolic and kinetic effects : Mar. Ecol. Prog. Ser., **75**: 191-203.

Keith M.L., Parker R.H. (1965) Local variation of ^{13}C and ^{18}O content of mollusc shells and the relatively minor temperature effect in marginal marine environments. Mar. Geol. **3**: 115-129.

Killingley J.S.,Berger, W.H. (1979). Stable isotopes in a Mollusk shell : detection of upwelling events. Science **205**: 186-188.

Klein R.T., Lohmann K.C., Thayer C.W. (1996a). Bivalve skeletons record sea-surface temperature and $\delta^{18}O$ via Mg/Ca and $^{18}O/^{16}O$ ratios. Geology **24**: 415-418.

Klein R.T., Lohmann K.C., Thayer C.W. (1996b). Sr/Ca and $^{13}C/^{12}C$ ratios in skeletal calcite of *Mytilus trossulus*: Covariation with metabolic rate, salinity, and carbon isotopic compostion of seawater : Geochimica et Cosmochimica Acta **60**: 4207-4221.

Krantz D.E. (1990) Mollusk - isotope records of Plio - Pleistocene marine paleoclimate, U.S. middle Atlantic coastal plain. Palaios **5**: 317-335.

Krantz D.E., Jones D.S., Williams D.F. (1984). Growth rates of the Sea Scallop *Placopecten magellanicus*, determined from the ^{18}O / ^{16}O record in shell calcite. Biol. Bull. **167**: 186-199.

Krantz D.E, Williams,D.F., Jones, D.S. (1987). Ecological and paleoenvironmental information using stable isotope profiles from living and fossil Molluscs. Palaeogeog., Palaeoclim., Palaeoecol. **58**: 249-266.

Kroopnick P. (1974) Correlations between ^{13}C and CO_2 in surface waters and atmospheric CO_2. Earth and Planetary Science Letters **22**: 397-403.

Kroopnick P. (1980) The distribution of ^{13}C in the Atlantic Ocean. Earth and Planetary Science Letters **49**: 469-484.

Kroopnick P.M. (1985) The distribution of ^{13}C of ΣCO_2 in the world oceans. Deep Sea Research, **32 (1)** : 57-84.

Land L.S., Lang J.C., Barnes D.J. (1975) Extension rate: A primary control on the isotopic composition of West Indian (Jamaican) scleractinian reef coral skeletons. Mar. Biol **33**: 221-233.

Lesniak P.M., Sakai H. (1989) Carbon isotope fractionation between dissolved carbonate (CO_3^{2-}) and CO_2 (g) at 25°C and 40°C. Earth and Planetary Science Letters **95**: 297-301.

Li Z.,. Elliott A.J. (1990) Tables of monthly surface and bottom temperatures in the U.K. shelf seas. Unit for Coastal and Estuarine Studies report UCES 71, University of Wales.

MacDonald R.W., McLaughlin F.A., Wong C.S. (1986) The storage of reactive silicate samples by freezing. Limnol. Oceanog. **31(5)**: 1139-1142.

Margosian A., Tan F.C., Cai D., Mann, K.H. (1987). Seawater temperature records from stable isotope profiles in the shell of *Modiolus modiolus* : Estuarine, Coastal and Shelf Science **25**: 81-89.

Mason J., (1957a) The age and growth of the scallop *Pecten maximus* in Manx waters. J.M.B.A. U.K. **36**: 473-492.

Mason J., (1957b) The breeding of the scallop, *Pecten maximus* in Manx waters. J.M.B.A. U.K. **37**: 653-671.

McConnaughey T.A. (1988) Biomineralization mechanisms *in* Origin , evolution and modern aspects of biomineralization in plants and animals. (ed Crick, R.E.) Plenum Press, New York: 57-73.

McConnaughey T.A. (1989a) ^{13}C and ^{18}O isotopic disequilibrium in biological carbonates : I. Patterns. Geochimica et Cosmochimica Acta **53**: 151-162.

McConnaughey T.A. (1989b) ^{13}C and ^{18}O isotopic disequilibrium in biological carbonates: II. *In vitro* simulation of kinetic isotope effects. Geochimica et Cosmochimica Acta **53**: 163-171.

McConnaughey T.A., Burdett J., Whelan J.F., Paull C.K. (1997) Carbon isotopes in biological carbonates : Respiration and photosynthesis. Geochimica et Cosmochimica Acta **61** (3): 611-622.

McCorkle D.C. (1987) Stable carbon isotopes in deep sea pore waters: modern geochemistry and paleoceanographic applications. PhD thesis, University of Washington, 209pp.

McCrea J.M. (1950). On the isotopic chemistry of carbonates and a paleotemperature scale. J. Chem. Phys. **18**: 849-857.

McKinney C.R., McCrea J.M., Epstein S., Allen H.A., Urey H.C. (1950) Improvements in mass spectrometers for the measurement of small differences in isotopic ratios. Rev.Sci.Instrum. **21**: 724-730.

Merrill A.S., Posgay J.A., Nichy F.E. (1965) Annual marks on shell and ligament of sea scallop (*Placopecten magellanicus*). Fish.Bull. **65**: 299-311.

Middleton, G. (1997) Variations in the carbon isotope ratio of phytoplankton and dissolved inorganic carbon in the marine environment. PhD thesis, University of Wales.

Mook W.G. (1971) Paleotemperatures and chlorinities from stable carbon and oxygen isotopes in shell carbonate. Paleogeogr. Paleoclim. Paleoecol. **9** : 245-263.

Mook W.G., Bommerson J.C., Staverman W.H. (1974) Carbon isotope fractionation between dissolved bicarbonate and gaseous carbon dioxide. Earth and Planetary Science Letters **22**: 169-176.

Muhs D.R.,Kyser T.K. (1987) Stable isotope compositions of fossil mollusks from southern California: Evidence for a cool last interglacial ocean. Geology **15**: 119-122.

Nier A.O. (1947) A mass spectrometer for isotope and gas analysis. Rev.Sci.Instrum., **18**: 398-411.

Nier A.O. (1950) A redetermination of the relative abundances of the isotopes of carbon, nitrogen, oxygen, argon and potassium. Phys.Rev. **77**: 789-793.

O.E.C.D. (1963) Catalogue of Marine Fouling Organisms. Vol 1. Barnacles.

O'Leary, M.H. (1981) Carbon isotope fractionation in plants. Phytochemistry **20**: 553-567.

O'Neil J.R., Clayton R.N., Mayeda T.K. (1969) Oxygen isotope fractionation in divalent metal carbonates. J.Chem.Phys. **51**: 5547-5558.

Parsons G.J., Robinson S.M.C., Roff J.C., Dadswell M.J. (1993) Daily growth rates as indicated by valve ridges in postlarval giant scallop *Placopecten magellanicus* (Bivalvia : Pectinidae) Can.J.Fish.Aquatic.Sci. **50**: 456-464.

Parsons T.R., Takahashi M., Hargrave B.(1977) Biological Oceanographic Processes. Pergamon Press, Oxford.

Parsons T.R., Muita Y., Lalli C.M. (1984) A manual of chemical and biological methods for sea water analysis. Pergamon Press Oxford.

Paull C.K., Martens C.S., Chanton J.P., Neumann A.C., Coston J., Jull A.J.T., Toolin L.J. (1989) Old carbon in living organisms and young $CaCO_3$ cements from abyssal brine seeps. Nature **342**: 166-168.

Pierce V.B. (1970) Incorporation of metabolic CO_2 into coral skeleton. Nature Lond. **228**: 383.

Popp B.N., Anderson T.F., Sandberg P.A. (1986) Brachiopods as indicators of original isotopic compositions in some Paleozoic limestones. Geol. Soc. Amer.Bull. **97**: 1262-1269.

Qian Y., Engel M.H., Goodfriend G.A., Macko S.A. (1995) Abundance and stable carbon isotope composition of amino acids in molecular weight fractions of fossil and artificially aged mollusk shells. Geochimica et Cosmochimica Acta **59, 6**: 1113-1124.

Richardson C.A. (1991) Bivalve shells: Chronometers of environmental change. Proceedings of the First International Conference on the Marine Biology of Hong Kong and the South China Sea (*ed* B.Morton). Hong Kong University Press: 419-434.

Richardson C.A. (1996) Exogenous or endogenous control of growth band formation in subtidal bivalve shells? Bulletin de l'Insitut oceanographique, Monaco no special **14,4**: 133-141.

Richardson C.A., Taylor A.C., Venn T.J. (1982) Growth of the Queen Scallop *Chlamys opercularis* in suspended cages in the Firth of Clyde. J.M.B.A. U.K. **62**: 157-169.

Romanek C.S., Grossman, E.L. Morse, J.W. (1992) Carbon isotopic fractionation in synthetic aragonite and calcite: Effects of temperature and precipitation rate. Geochimica et Cosmochimica Acta **56**: 419-430.

Rosenberg G.D., Hughes W.W. (1991) A metabolic model for the determination of shell composition in the bivalve mollusc *Mytilus edulis*. Lethaia **24**: 83-96.

Rosenberg G.D., Hughes W.W., Tkachuck R.A. (1989) Shell form and metabolic gradients in the mantle of *Mytilus edulis*. Lethaia **24**: 343-344.

Rye D.M., Sommer, M.A. (1980) . Reconstructing paleotemperature and paleosalinity regimes with oxygen isotopes *in* Rhoads, D.C. and Lutz, R.A. eds., Skeletal growth of aquatic organisms : New York Plenum Press, 169-202.

Shackleton N.J. (1965) The high precision isotopic analysis of oxygen and carbon in carbon dioxide. J. Sci. Instrum. **42**: 689-692.

Shackleton N.J. (1967) Oxygen isotope analysis and Pleistocene temperatures re-assessed. Nature **215**: 15-17.

Sharma T., Clayton R.N. (1965) Measurement of O^{18}/O^{16} ratios of total oxygen of carbonates. Geochimica et Cosmochimica Acta **29**: 1347-1353.

Sharma S.K., Sharma T. (1969) Oxygen isotope fractionation factor between CO_2 and CO_3^{2-}. J. Mass Spectrometry and Ion Phys. **2**: 367-371.

Silverman D.N. (1973) Carbonic anhydrase catalysed oxygen-18 exchange between bicarbonate and water. Archives of Biochemistry and Biophysics **155**: 452-457.

Simkiss K. (1976) Cellular aspects of calcification in Mechanisms of Mineralisation in the Invertebrates and Plants (eds N.Watabe, K.M.Wilbur).South Carolina Press: 1-31.

Smith J.T. (1991) Cenozoic Giant Pectinids from California and the Tertiary Caribbean Province: *Lyropecten*, *' Macrochlamis'*, *Veripecten* and *Nodipecten* species. U.S. Geological Survey Professional Paper 1391:1-7.

Stumm W., Morgan J.J. (1981) Aquatic Chemistry. Wiley.

Swart P.K. (1981) The carbon isotope composition of organic material in coral skeletons and its effect on early diagenisis. Proceedings of the Fourth International Coral Reef Symposium, Manilla **2**: 87-90.

Swart P.K. (1983) Carbon and oxygen isotope fractionation in scleratinian corals: a review. Earth Science Reviews **19**: 51-80.

Swart P.K., Burns S.J.,Leder J.J. (1991) Fractionation of the stable isotopes of oxygen and carbon in carbon dioxide during the reaction of calcite with phosphoric acid as a function of temperature and technique. Chem. Geol. (Isot. Geosci. Sect.) **86**: 89-96.

Tan F.C., Cai D., Roddick D.L. (1988). Oxygen isotope studies on Sea Scallops *Placopecten magellanicus*, from Brown's Bank, Nova Scotia : Canadian. J. Fish. Aquatic. Sci. **45**: 1378-1385.

Tanaka N., Monaghan M.C., Rye, D.M. (1986) Contribution of metabolic carbon to mollusc and barnacle shell carbonate. Nature **320**: 520-523.

Tarutani T., Clayton R.N. Mayeda T.K. (1969) The effect of polymorphism and magnesium substitution on oxygen isotope fractionation between calcium carbonate and water. Geochimica et Cosmochimica Acta **33**: 987-996.

Thode H.G., Shima M,. Rees C.E., Krishnamurty K.V. (1965) Carbon-13 isotope effects in systems containing carbon dioxide, bicarbonate, carbonate and metal ions. Canada J. Chem. **43**: 582-595.

Tourtelot H.A., Rye R.O. (1969). Distribution of oxygen and carbon isotopes in fossils of late Cretaceous age, western interior region of North America : Bull. Geol. Soc. Am. **80:** 1903-1922.

Urey H.C. (1947). The thermodynamic properties of isotopic substances : J. Chem. Soc. **1947** : 562-581.

Urey H.C., Brickwedde F.G., Murphy G.M. (1932) An isotope of mass 2 and its concentration. Phys Rev **40** : 1

Urey H.C., Lowenstam H.A., Epstein S., McKinney C.R. (1951) Measurement of paleotemperatures and temperatures of the Upper Cretaceous of England, Denmark and the Southeastern United States. Bull.Geol.Soc.Am. **62**: 399-416.

Vahl 0. (1980) Seasonal variations in seston and in the growth rate of the Iceland scallop, *Chlamys islandica* (O.F.Muller) from Balsfjord, 70°N. J.Exp.Mar.Biol.Ecol. **48**: 195-204.

Vinot - Bertouille A.C., Duplessey J.C. (1973) Individual isotopic fractionation of carbon and oxygen in benthic foraminifera. Earth and Planetary Science Letters **18**: 247-252.

Vogel J.C., Grootes P.M., Mook, W.G. (1970) Isotope fractionation between gaseous and dissolved carbon dioxide Z.Physik **230**: 225-238.

Wainwright S.C., Fry B. (1994) Seasonal variation of the stable isotopic compositions of coastal marine plankton from Wood's Hole, Massachusetts and Georges Bank. Estuaries **17** (3): 552-560.

Walters L.J., Claypool G.E., Choquette P.W. (1972) Reaction rates and O^{18} variation for the carbonate - phosphoric acid preparation method. Geochimica et Cosmochimica Acta **36**: 129-140.

Watabe N, Kingsley R.J. (1989) Extra-, inter-, and intracellular mineralization in invertebrates and algae. *in* Origin, Evolution and Modern Aspects of Biomineralization in Plants and Animals ed R.Crick . Plenum Press: 209-223.

Weber J.N., Woodhead P.M..J. (1970) Carbon and oxygen isotope fractionation in the skeletal carbonate of reef-building corals. Chem.Geol **6**: 93-117.

Weber J.N., Deines P.D., Weber P.H., Baker P.A. (1976) Depth related changes in the $^{13}C/^{12}C$ ratio of skeletal carbonate deposited by the reef-frame building coral *Montastrea annualris*: further implications of a model for stable isotope fractionation by scleratinian corals. Geochimica et Cosmochimica Acta **40:** 31-39.

Wefer G., Berger W.H.(1991). Isotope paleontology : growth and composition of extant calcareous species. Mar. Geol. **100**: 207-248.

Weidman C.R., Jones G.A., Lohmann K.C. (1994) The long - lived mollusk *Arctica islandica*: A new paleoceanographic tool for the reconstruction of bottom temperatures for the continental shelves of the North Atlantic Ocean. J.Geophysical Research **99**: 18305-18314.

Weil S.M., Buddemeier R.W., Smith S.V. Kroopnick, P.M. (1981) The stable isotopic composition of coral skeletons: Control by environmental variables. Geochimica et Cosmochimica Acta **45**: 1147-1153.

Wheeler A.P. (1992) Mechanisms of molluscan shell formation. *in* Calcification in Biological Systems (ed E.Bonucci). CRC Press: 179-216.

Wheeler A.P., Blackwelder P.L., Wilbur K.M.(1975) Shell growth in the scallop *Argopecten irradians.* I . Isotope incorporation with reference to diurnal growth. Biol. Bull. **148**: 472-482.

Wilbur K.M. (1964) Shell formation and regeneration in Physiology of Mollusca Vol1 (*eds* Wilbur K.M., Yonge C.M.) Academic Press New York.

Zhang, J. Quay P.D., Wilbur D.O. (1995) Carbon isotope fractionation during gas-water exchange and dissolution of CO_2. Geochimica et Cosmochimica Acta **59** (1): 107-114.

Appendix 1. An inter laboratory comparison of $\delta^{18}O$-H_2O of sea water samples supplied by U.E.A. All data are reported relative toVSMOW.

SAMPLE	U.E.A. value °/oo	Menai Bridge value °/oo
12647	-0.471	-0.494
12650	-0.392	-0.393
12645	-0.265	-0.250

Appendix 2. Schematic diagram showing one of the four individual units of the experimental tank system.

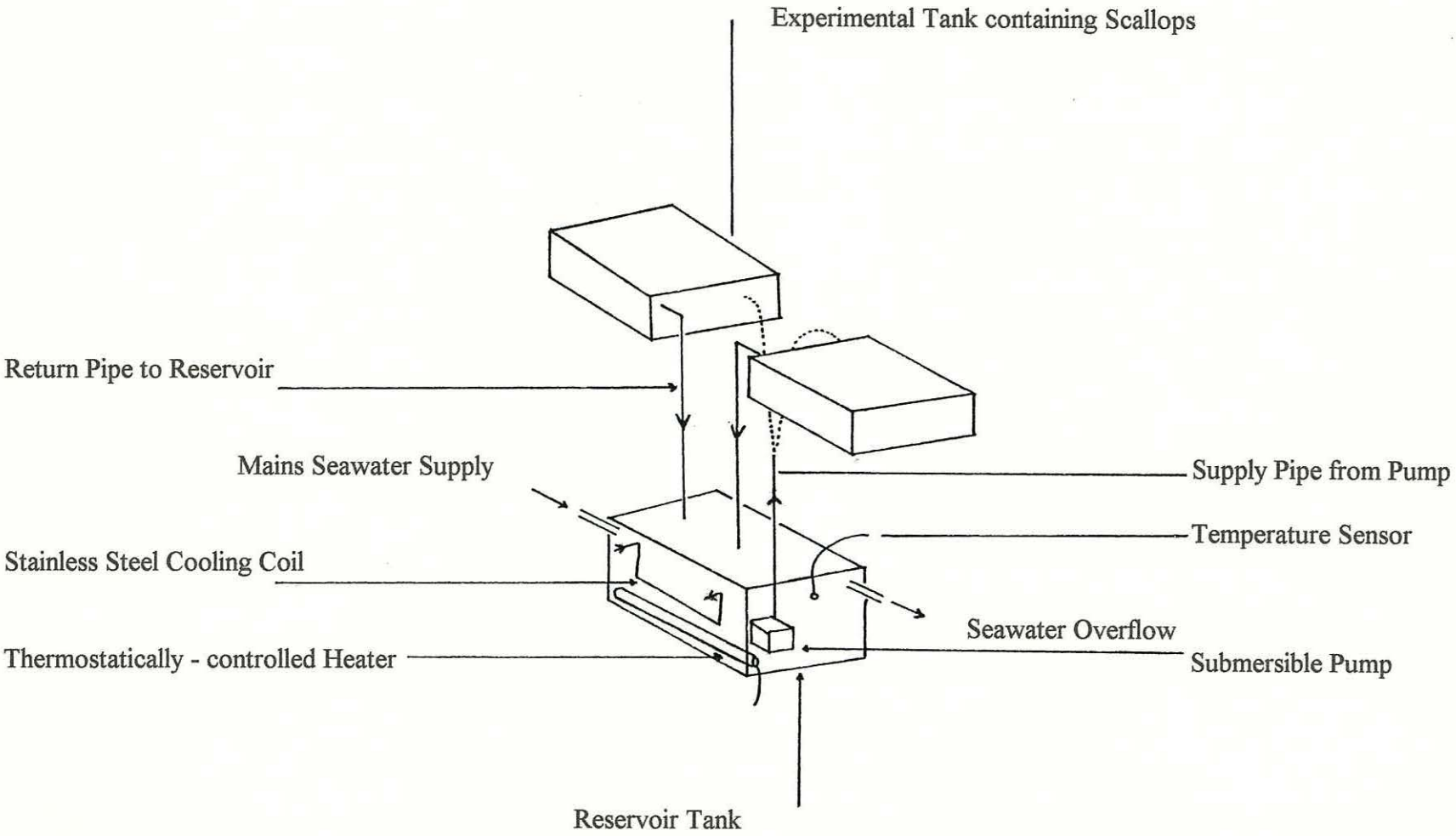

Appendix 3 Continuous water temperature records obtained from the Tinytalk Temperature Datalogger circulated between the four experimental tanks.

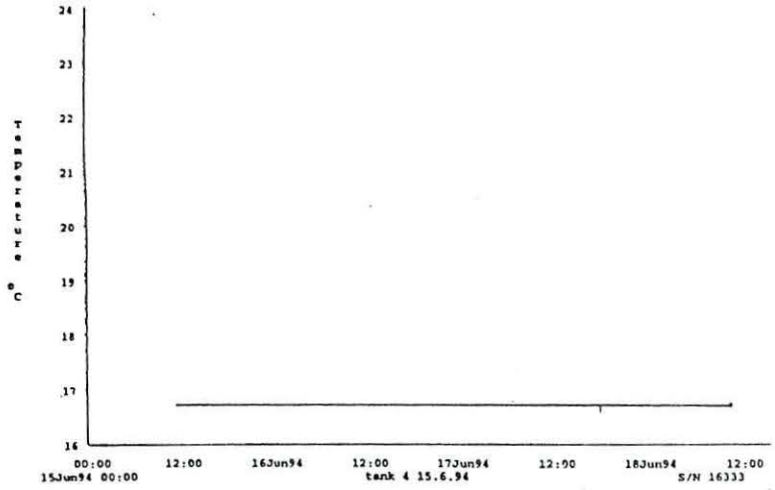

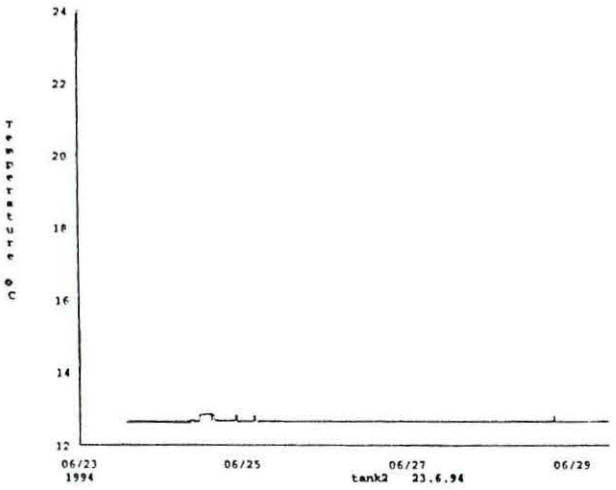

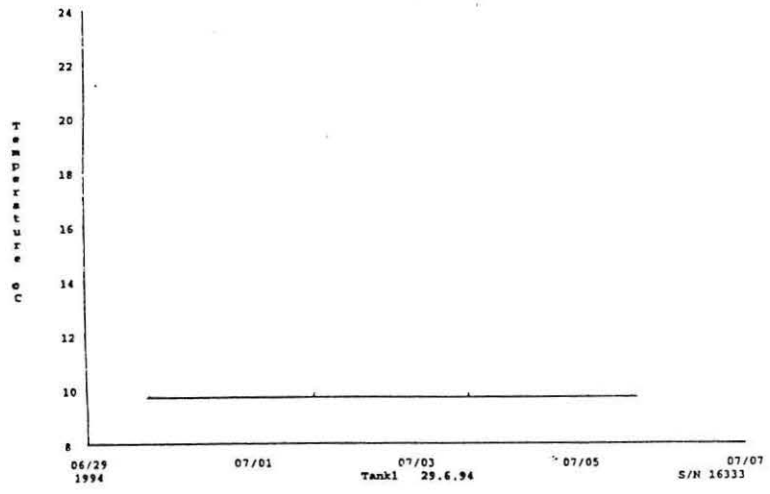

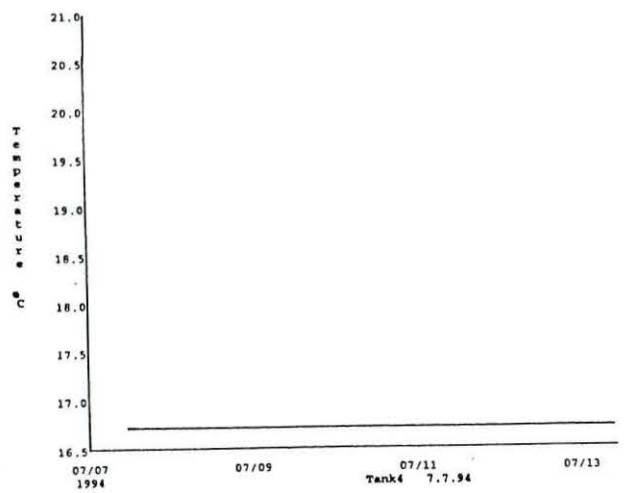

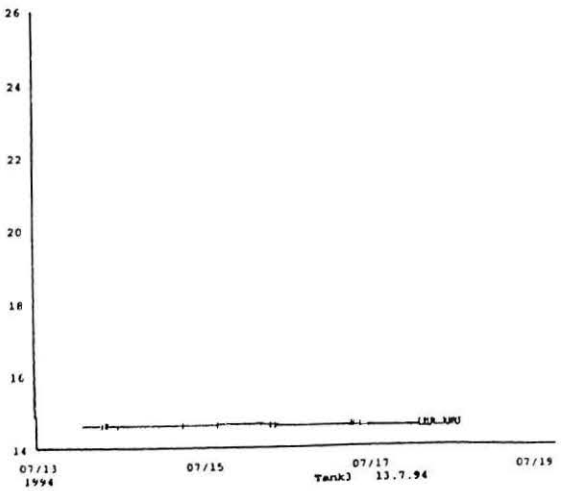

Appendix 4. Experimental $\delta^{18}O$-H_2O and salinity data.

Experimental $\delta^{18}O$-H_2O data. All data are in °/oo referenced to VSMOW

Date (1994)	9.9°C Tank	12.9°C Tank	14.7°C Tank	16.9°C Tank
20th June	0.049	0.025	0.122	0.041
29th June	0.118	0.158	0.079	0.095
7th July	0.085	0.107	0.050	0.066
11th July	-0.049	0.071	-0.003	0.026
18th July	0.047	0.110	0.079	-0.035
Mean	0.050	0.094	0.065	0.039
1σ	0.06	0.05	0.05	0.05

Experimental salinity data. All data are in S.

Date (1994)	9.9°C Tank	12.9°C Tank	14.7°C Tank	16.9°C Tank
20th June	33.816	33.823	33.832	33.839
24th June	33.837	33.842	33.926	33.927
27th June	33.922	33.937	33.922	33.944
29th June	33.954	33.963	33.973	34.002
1st July	33.940	33.944	33.953	33.957
7th July	33.833	33.836	33.852	33.862
11th July	33.809	33.820	33.869	33.913
18th July	33.773	33.774	33.772	33.775
Mean	33.861	33.867	33.887	33.902
1σ	0.068	0.070	0.068	0.073

Appendix 5 Experimental *Pecten* shell, $\delta^{18}O$-H_2O and predicted oxygen isotopic data for calcite precipitated in isotopic equilibrium with sea water.

Temperature °C	*Pecten* $\delta^{18}O$-CO_2 vPDB °/oo	*Pecten* $\delta^{18}O$ vPDB °/oo	*Pecten* $\delta^{13}C$ vPDB °/oo	$\delta^{18}O$-H_2O °/oo vVSMOW	δ_w °/oo	$\delta_{c\ (equilib)}$ * °/oo	δ_c-δ_w *Pecten*	δ_c-δ_w equilib*	δ_c-δ_w Epstein *et al* (1953)
9.9	12.253	1.983	-0.526	0.050	-0.170	1.493	2.153	1.663	1.621
9.9	12.027	1.759	-0.448	0.050	-0.170	1.493	1.929	1.663	1.621
9.9	11.892	1.625	-0.605	0.050	-0.170	1.493	1.795	1.663	1.621
9.9	11.975	1.707	-0.489	0.050	-0.170	1.493	1.878	1.663	1.621
9.9	11.991	1.723	-0.38	0.050	-0.170	1.493	1.893	1.663	1.621
9.9	12.465	2.193	-0.628	0.050	-0.170	1.493	2.363	1.663	1.621
9.9	11.93	1.663	-0.626	0.050	-0.170	1.493	1.833	1.663	1.621
9.9	12.17	1.901	-0.483	0.050	-0.170	1.493	2.071	1.663	1.621
9.9	11.978	1.710	-0.669	0.050	-0.170	1.493	1.880	1.663	1.621
12.9	11.289	1.028	-0.506	0.094	-0.126	0.809	1.154	0.935	0.862
12.9	11.402	1.140	-0.593	0.094	-0.126	0.809	1.266	0.935	0.862
12.9	11.431	1.169	-0.383	0.094	-0.126	0.809	1.295	0.935	0.862
12.9	11.13	0.871	-0.413	0.094	-0.126	0.809	0.997	0.935	0.862
12.9	11.417	1.155	-0.531	0.094	-0.126	0.809	1.281	0.935	0.862
12.9	11.434	1.172	-0.613	0.094	-0.126	0.809	1.298	0.935	0.862
12.9	11.353	1.092	-0.409	0.094	-0.126	0.809	1.218	0.935	0.862
12.9	11.52	1.257	-0.718	0.094	-0.126	0.809	1.383	0.935	0.862
14.7	11.202	0.942	-2.133	0.065	-0.155	0.355	1.097	0.510	0.425
14.7	10.568	0.305	-3.114	0.065	-0.155	0.355	0.460	0.510	0.425
14.7	10.835	0.579	-1.778	0.065	-0.155	0.355	0.734	0.510	0.425
14.7	10.777	0.522	-0.812	0.065	-0.155	0.355	0.677	0.510	0.425
16.9	10.02	-0.228	-2.593	0.039	-0.181	-0.179	-0.047	0.002	-0.093
16.9	10.466	0.214	-3.036	0.039	-0.181	-0.179	0.395	0.002	-0.093
16.9	10.635	0.381	-2.272	0.039	-0.181	-0.179	0.562	0.002	-0.093
16.9	10.664	0.410	-1.97	0.039	-0.181	-0.179	0.591	0.002	-0.093
16.9	10.555	0.302	-2.309	0.039	-0.181	-0.179	0.483	0.002	-0.093
16.9	10.881	0.625	-1.895	0.039	-0.181	-0.179	0.806	0.002	-0.093
16.9	10.774	0.519	Poor trace	0.039	-0.181	-0.179	0.700	0.002	-0.093
16.9	10.015	-0.233	-2.793	0.039	-0.181	-0.179	-0.052	0.002	-0.093
16.9	10.522	0.269	-2.347	0.039	-0.181	-0.179	0.450	0.002	-0.093
16.9	10.362	0.111	-2.921	0.039	-0.181	-0.179	0.292	0.002	-0.093

* Using O'Neil *et al*, (1969) equation for calcite precipitated in isotopic equilibrium with seawater

Appendix 6. Experimental $[\Sigma CO_2]$, $\delta^{13}C-\Sigma CO_2$, pH, $[CO_{2aq}]$, $[HCO_3^-]$, $[CO_3^{2-}]$, δ_a, ,δ_b and δ_c data.

Tank /date	$[\Sigma CO_2]$ µmolkg^{-1}	$\delta^{13}C-\Sigma CO_2$ °/oo	pH µmolkg^{-1}	$[CO_{2aq}]$ µmolkg^{-1}	$[HCO_3^-]$ µmolkg^{-1}	$[CO_3^{2-}]$ µmolkg^{-1}	δ_a °/oo	δ_b °/oo	δ_c °/oo
1/20.6.94	1968.9	-2.008	7.938	21.53	1847.5	99.91	-12.664	-1.739	-4.691
2/20.6.94	2145.2	-4.532	7.931	22.09	2002.1	121.01	-14.835	-4.267	-7.034
3/20.6.94	2093.5	-0.116	8.017	16.68	1923.8	152.98	-10.193	0.161	-2.494
4/20.6.94	2068	0.087	7.924	19.55	1914	134.5	-9.747	0.346	-2.172
1/24.6.94	2075.0	-0.816	7.979	20.52	1938.8	115.7	-11.457	-0.544	-3.490
2/24.6.94	2076.4	-0.677	7.942	20.81	1935.5	120.05	-10.979	-0.411	-3.178
3/24.6.94	2036.2	-3.9	7.951	19.01	1887.6	129.6	-13.977	-3.635	-6.284
4/24.6.94	2032.7	-4.211	7.832	23.95	1900.2	108.52	-14.039	-3.958	-6.470
1/27.6.94	2073.0	0.076	8.001	19.43	1932.1	121.51	-10.562	0.351	-2.595
2/27.6.94	2083.9	0.165	7.976	19.23	1934.7	130	-10.133	0.435	-2.331
3/27.6.94	2033.2	-1.523	7.99	17.31	1875.6	140.26	-11.606	-1.252	-3.906
4/27.6.94	2012.7	-1.697	7.901	20.13	1868	124.56	-11.533	-1.440	-3.959
1/29.6.94	2120.7	-0.346	8.008	19.52	1974.8	126.38	-10.983	-0.070	-3.016
2/29.6.94	2084.7	0.181	7.978	19.14	1934.9	130.71	-10.117	0.451	-2.315
3/29.6.94	2053.0	-1.368	7.988	17.5	1893.7	141.84	-11.439	-1.097	-3.746
4/29.6.94	2042.8	-1.762	7.905	20.18	1894.5	128.16	-11.586	-1.505	-4.017
1/1.7.94	2092.3	0.144	8.012	19.08	1947.5	125.71	-10.492	0.421	-2.526
2/1.7.94	2078.3	0.183	7.976	19.15	1929.3	129.84	-10.115	0.453	-2.313
3/1.7.94	2053.7	-0.003	7.973	18.18	1898.4	137.14	-10.077	0.265	-2.383
4/1.7.94	2075.3	-0.188	7.915	20.01	1922.3	132.99	-10.010	0.070	-2.442
1/7.7.94	2078.3	-0.013	8.015	18.8	1933.9	125.63	-10.649	0.264	-2.683
2/7.7.94	2089.6	0.088	7.978	18.95	1920.6	130.09	-10.198	0.358	-2.402
3/7.7.94	2031.5	-0.442	7.975	17.91	1877.6	135.97	-10.515	-0.173	-2.822
4/7.7.94	2062.7	-0.81	7.887	21.28	1917.2	124.2	-10.635	-0.555	-3.057
1/11.7.94	2071.9	0.372	8.064	16.64	1916	139.26	-10.255	0.658	-2.289
2/11.7.94	2058.3	0.374	8.017	17.16	1900.6	140.59	-9.906	0.650	-2.110
3/11.7.94	1988.1	-2.206	7.984	17.08	1834.6	136.42	-12.266	-1.936	-4.578
3/11.7.94	2006	-2.226	7.984	17.23	1851.1	137.67	-12.286	-1.956	-4.598
4/11.7.94	2015.7	-3.215	7.903	20.07	1870.4	125.23	-13.051	-2.958	-5.476
4/11.7.94	2017.6	-3.244	7.903	20.09	1872.2	125.35	-13.080	-2.987	-5.506
1/18.7.94	2052.6	-0.004	8.025	18.12	1907.5	126.94	-10.627	0.274	-2.666
2/18.7.94	2062.2	0.139	7.995	18.08	1909.3	134.85	-10.133	0.412	-2.342
3/18.7.94	2059.5	0.312	8.003	16.93	1895.8	146.76	-9.745	0.585	-2.057
4/18.7.94	2068.1	0.199	7.954	18.16	1906.2	143.71	-9.618	0.462	-2.050

Appendix 7. Experimental $\delta^{13}C$- ΣCO_2 , $\delta^{13}C_{Pecten}$ and $\delta^{13}C_{(equilib)}$ data. All isotopic data in °/oo.

Delta 13C-Dissolved Inorganic Carbon

Date	Tank 1 9.9oC	Tank 2 12.9oC	Tank 3 14.7oC	Tank 4 16.9oC
20.6.94	-2.008	-4.532	-0.116	0.087
24.6.94	-0.816	-0.677	-3.900	-4.211
27.6.94	0.076	0.165	-1.523	-1.697
29.6.94	-0.346	0.181	-1.368	-1.762
1.7.94	0.144	0.183	-0.003	-0.188
7.7.94	-0.013	0.088	-0.442	-0.810
11.7.94	0.372	0.374	-2.216	-3.230
18.7.94	-0.004	0.139	0.312	0.199
mean	-0.324	-0.510	-1.157	-1.452
stdv	0.769	1.655	1.410	1.605

Delta 13C - (Pecten)

Animal	Tank 1 9.9oC	Tank 2 12.9oC	Tank 3 14.7oC	Tank 4 16.9oC
1	-0.526	-0.506	-2.133	-2.593
2	-0.448	-0.593	-3.114	-3.036
3	-0.605	-0.383	-1.778	-2.272
4	-0.489	-0.413	-0.812	-1.97
5	-0.628	-0.531		-2.309
6	-0.626	-0.613		-1.895
7	-0.483	-0.409		-2.793
8	-0.669	-0.718		-2.347
9	-0.38			-2.921
mean	-0.539	-0.521	-1.959	-2.46
stdv	0.098	0.117	0.951	0.404

Delta 13C-(equilib) using Zhang et al, 1995 enrichment factors)

Date	Tank 1 9.9oC	Tank 2 12.9oC	Tank 3 14.7oC	Tank 4 16.9oC
20.6.94	-0.739	-3.267	1.161	1.346
24.6.94	0.456	0.589	-2.635	-2.958
27.6.94	1.351	1.435	-0.252	-0.44
29.6.94	0.93	1.451	-0.097	-0.505
1.7.94	1.421	1.453	1.265	1.07
7.7.94	1.264	1.358	0.827	0.445
11.7.94	1.658	1.65	-0.946	-1.973
18.7.94	1.274	1.416	1.585	1.462
mean	0.952	0.761	0.114	-0.194
stdv	0.773	1.658	1.412	1.607
median	1.269	1.425	0.365	0.002

Delta 13C-(equilib) using Zhang et al, 1995 enrichment factors with mineral correction)

Date	Tank 1 9.9oC	Tank 2 12.9oC	Tank 3 14.7oC	Tank 4 16.9oC
20.6.94	-0.884	-3.421	0.968	1.181
24.6.94	0.296	0.431	-2.803	-3.093
27.6.94	1.183	1.265	-0.433	-0.597
29.6.94	0.76	1.28	-0.279	-0.664
1.7.94	1.249	1.283	1.09	0.908
7.7.94	1.091	1.187	0.651	0.293
11.7.94	1.465	1.465	-1.126	-2.13
18.7.94	1.098	1.234	1.398	1.287
mean	0.782	0.591	-0.067	-0.352
stdv	0.761	1.650	1.407	1.598
median	1.095	1.250	0.186	-0.152

Delta 13C-(equilib) using Thode et al, 1965 and Zhang et al, 1995 enrichment factors)

Date	Tank 1 9.9oC	Tank 2 12.9oC	Tank 3 14.7oC	Tank 4 16.9oC
20.6.94	-0.863	-3.396	1.002	1.212
24.6.94	0.319	0.457	-2.773	-3.068
27.6.94	1.207	1.293	-0.402	-0.568
29.6.94	0.784	1.308	-0.247	-0.634
1.7.94	1.273	1.311	1.12	0.939
7.7.94	1.116	1.215	0.681	0.322
11.7.94	1.493	1.495	-1.095	-2.1
18.7.94	1.123	1.263	1.431	1.32
mean	0.807	0.618	-0.035	-0.322
stdv	0.763	1.651	1.408	1.600
median	1.120	1.278	0.217	-0.123

Appendix 8. Variation in temperature, salinity, $\delta^{18}O\text{-}H_2O$, δ_w and predicted δ_c at Menai Bridge Pier September 1994 - October 1995.

Date	Day	Temperature °C	Salinity S	$\delta^{18}O\text{-}H_2O$ °/oo v VSMOW	δ_w °/oo	δ_c °/oo
3.10.94	7	13.7	32.54	-0.297	-0.517	0.228
6.10.94	10	12.8	33.27	-0.086	-0.306	0.653
10.10.94	14	13.6	32.99	-0.143	-0.363	0.406
17.10.94	21	12.8	32.93	-0.180	-0.400	0.559
25.10.94	29	12.1	32.72	-0.219	-0.439	0.700
7.11.94	42	11.6	33.57	-0.054	-0.274	0.986
14.11.94	49	11.7	32.30	-0.306	-0.526	0.697
21.11.94	56	11.4	32.63	-0.209	-0.429	0.867
1.12.94	66	10.5	33.48	-0.029	-0.249	1.267
19.12.94	84	9.3	32.71	-0.218	-0.438	1.374
16.1.95	112	8.0	32.51	-0.206	-0.426	1.712
30.1.95	126	6.8	32.67	-0.221	-0.441	2.003
13.2.95	140	7.4	32.41	-0.292	-0.512	1.779
6.3.95	161	6.3	33.47	-0.100	-0.320	2.253
21.3.95	176	6.6	33.88	0.036	-0.184	2.312
28.3.95	183	7.0	33.69	-0.015	-0.235	2.158
4.4.95	190	8.8	33.92	0.022	-0.198	1.739
10.4.95	196	9.3	33.41	-0.112	-0.332	1.480
26.4.95	212	9.9	32.61	-0.250	-0.470	1.193
1.5.95	217	10.4	32.71	-0.271	-0.491	1.061
9.5.95	225	11.3	33.08	-0.108	-0.328	0.992
16.5.95	232	10.7	33.09	-0.176	-0.396	1.071
1.6.95	248	12.2	32.57	-0.302	-0.522	0.581
12.6.95	259	12.6	33.09	-0.189	-0.409	0.598
25.6.95	272	15.9	32.70	-0.203	-0.423	-0.191
11.7.95	288	16.7	33.15	-0.086	-0.306	-0.258
17.7.95	294	16.5	33.21	-0.142	-0.362	-0.268
25.7.95	302	17.1	33.41	-0.038	-0.258	-0.301
1.8.95	309	18.9	33.53	-0.019	-0.239	-0.689
8.8.95	326	18.4	33.51	0.005	-0.215	-0.553
16.8.95	324	18.6	33.52	-0.002	-0.222	-0.605
30.8.95	338	17.1	33.74	0.002	-0.218	-0.261
8.9.95	347	16.7	33.21	-0.176	-0.396	-0.348
14.9.95	353	16.9	33.21	-0.136	-0.356	-0.354
22.9.95	361	16.4	33.21	-0.092	-0.312	-0.195

Appendix 9 Continuous water temperature records obtained from Tinytalk Temperature Datalogger placed within the raft box adjacent to growing scallops for monthly periods over the year October 1994 - September 1995.
Markers indicate simultaneous temperature measurements taken at Menai Bridge Pier using hand-held digital thermometer.

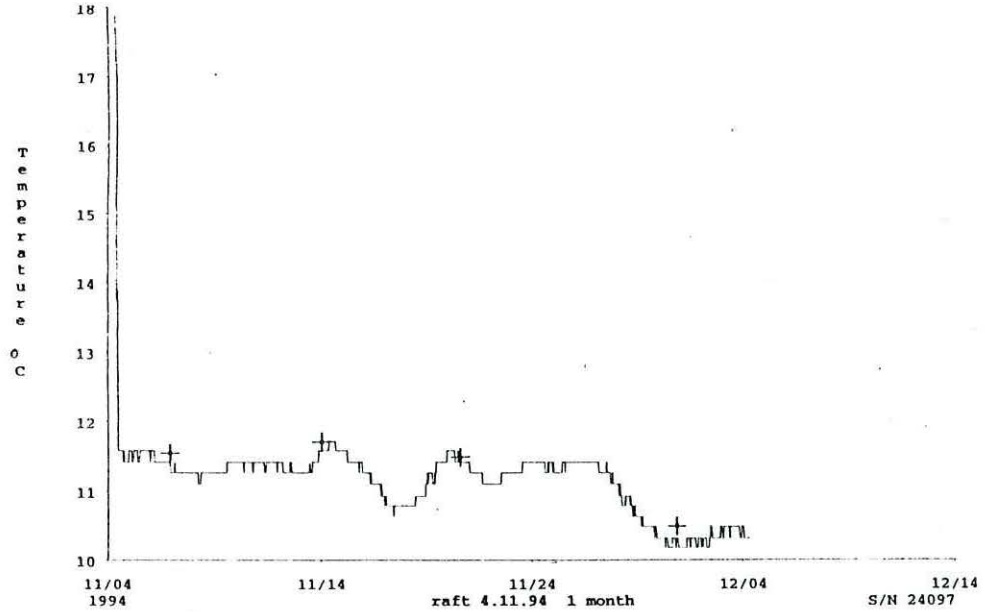

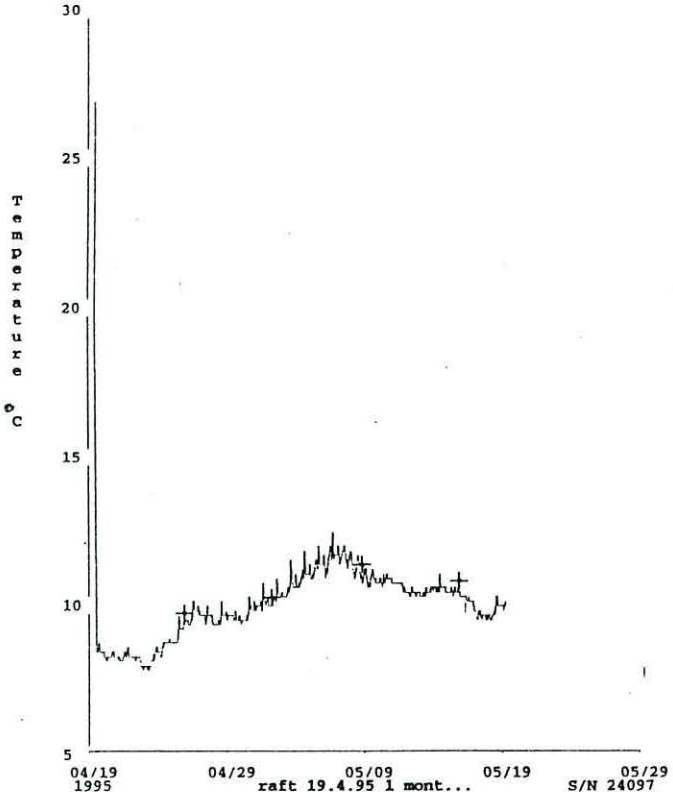

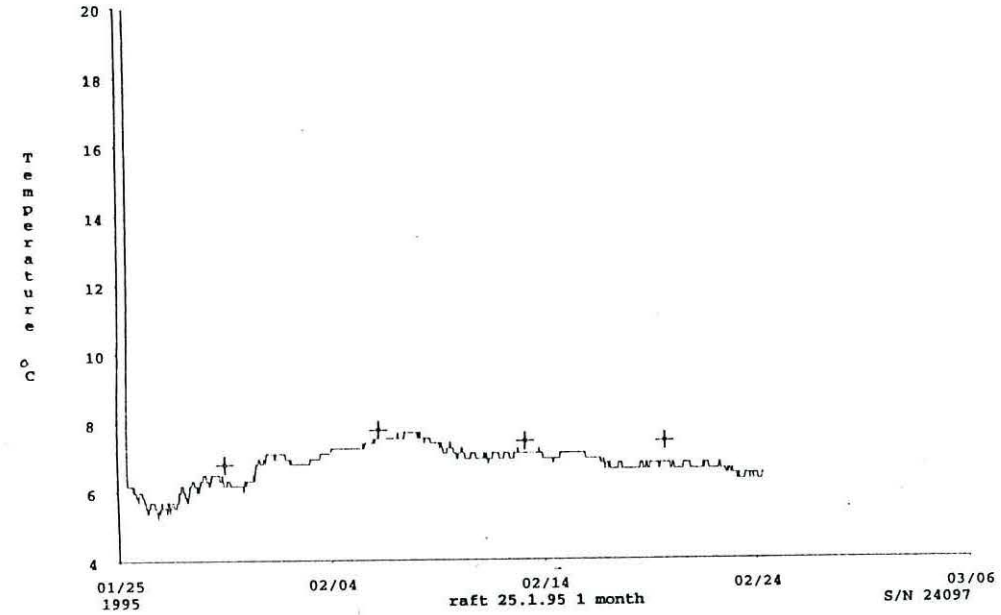

Appendix 9 Continuous water temperature records obtained from Tinytalk Temperature Datalogger placed within the raft box adjacent to growing scallops for monthly periods over the year October 1994 - September 1995. Markers indicate simultaneous temperature measurements taken at Menai Bridge Pier using hand-held digital thermometer.

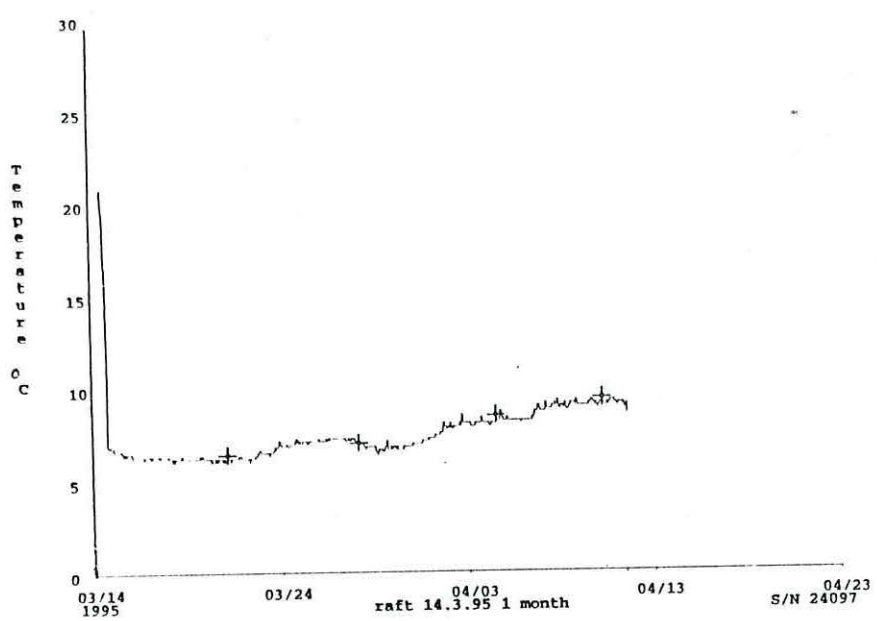

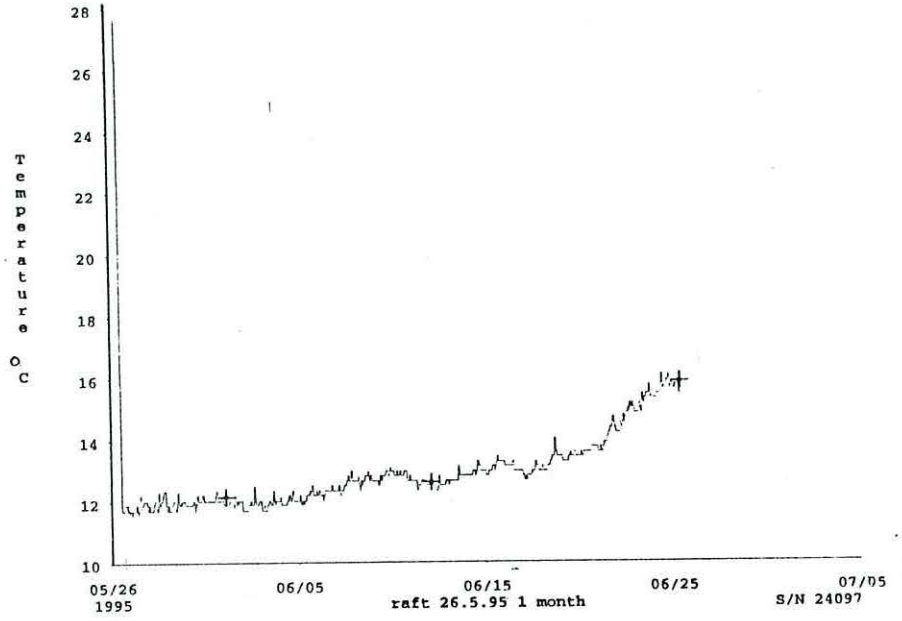

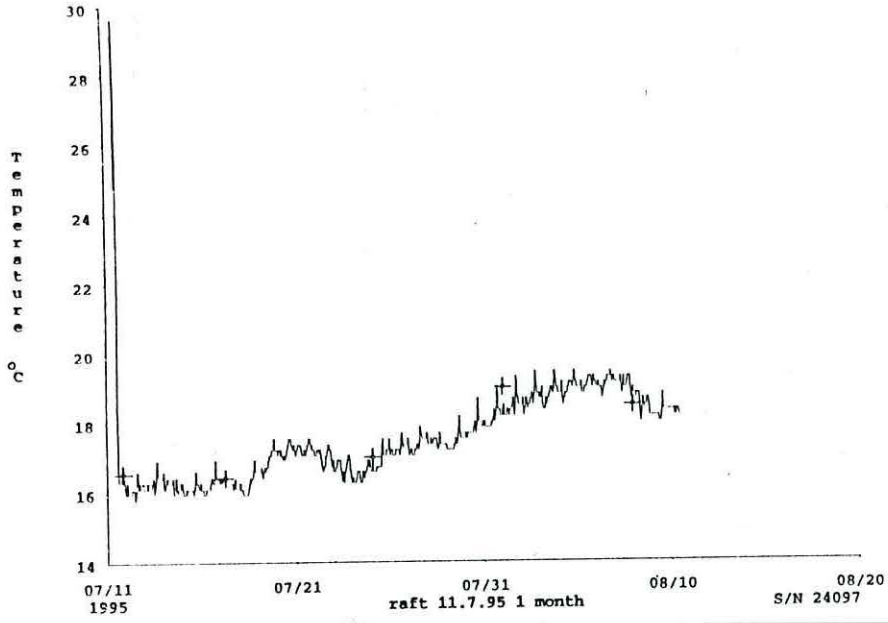

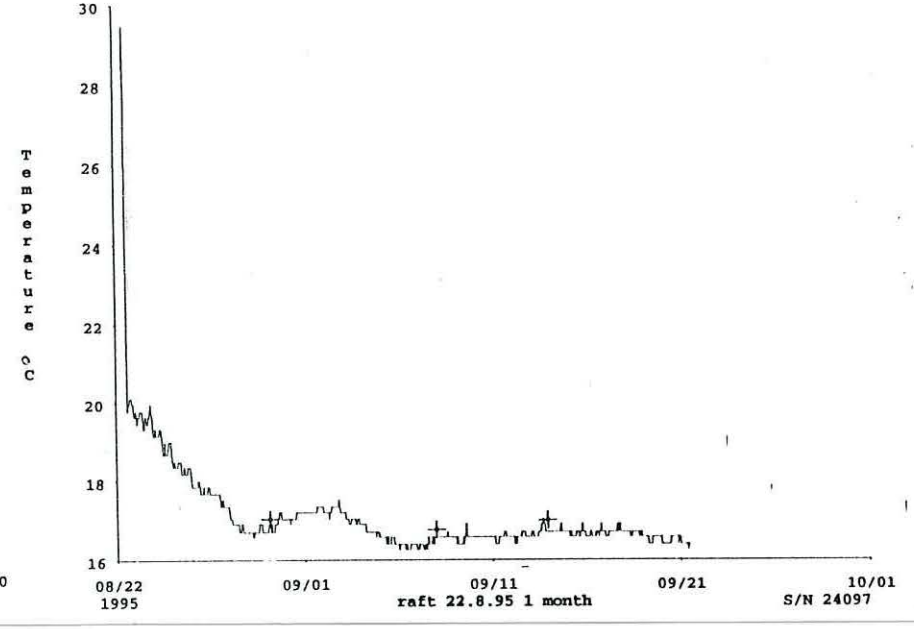

Appendix 10. Chlorophyll and dissolved nutrient concentrations at Menai Bridge Pier, September 1994 - October 1995.

Date	Day	[Chl] $\mu g\ dm^{-3}$	[Silicate] μM	[Nitrate] μM	[Nitrite] μM	[Phosphate] μM
6.10.94	10	2.297	3.791	0.430	0.091	0.700
10.10.94	14	1.261		0.559	0.051	0.826
14.10.94	18	1.214	2.640	0.841	0.075	0.981
17.10.94	21		4.772	0.622	0.085	0.816
25.10.94	29	0.527		1.505	0.156	1.063
7.11.94	42	0.665	4.630	3.015	0.320	0.695
14.11.94	49	0.691	5.612	5.166	0.541	0.908
21.11.94	56	0.428	4.442	11.588	0.375	0.724
1.12.94	66	0.450			0.389	0.884
19.12.94	84	0.389	8.291	9.872	0.300	0.821
16.1.95	112	0.393	10.574	7.552	0.248	0.744
30.1.95	126	0.432	7.706	7.926	0.130	0.734
6.2.95	133	0.301	4.083	10.431	0.160	0.797
13.2.95	140	0.419	6.828	9.074	0.144	0.756
21.2.95	148	0.389	3.847	7.103	0.115	0.687
6.3.95	161	0.449	5.017	8.229	0.082	0.641
21.3.95	176	0.773	4.262	5.836	0.127	
28.3.95	183	0.864	3.357	5.990		0.668
4.4.95	190	0.778	4.319	5.332	0.096	0.724
10.4.95	196	0.562	1.564	7.305	0.193	0.572
26.4.95	212	1.791	0.819	6.062	0.226	0.738
1.5.95	217	2.095	0.951	7.219	0.278	0.526
9.5.95	225	2.020	0.800	5.187	0.218	0.636
16.5.95	232	3.348	0.508	1.987	0.185	0.332
1.6.95	248	5.249	0.876	0.094	0.055	0.337
12.6.95	259	1.162			0.039	0.512
25.6.95	272	1.162		0.144	0.051	0.613
11.7.95	288	1.483	1.923	0.619	0.111	0.535
17.7.95	294	2.281	1.725	0.479	0.065	0.443
25.7.95	302	0.700	4.291	1.010	0.162	0.539
1.8.95	309	1.538	4.895	0.664	0.067	0.549
8.8.95	316	1.859	4.074	0.791	0.102	0.562
16.8.95	324	1.225	2.828	0.549	0.088	0.572
30.8.95	338	1.162	4.281	0.764	0.269	0.728
8.9.95	347	1.620	4.479	0.886	0.309	0.830
14.9.95	353	1.777	2.979	0.859	0.150	0.830
22.9.95	361	1.046	3.291	0.615	0.115	1.037

Appendix 11. Algal abundances in the Menai Strait October 1994 - September 1995. Data are cells per dm^3

Date	10.10.94	25.10.94	14.11.94	1.12.94	19.12.94	16.1.95	30.1.95	13.2.95	6.3.95	28.3.95	10.4.95	26.4.95	9.5.95	16.5.95	1.6.95	12.6.95	25.6.95	11.7.95	17.7.95	1.8.95	8.8.95	16.8.95	30.8.95	14.9.95
Day	14	29	49	66	84	112	126	140	161	183	196	212	225	232	248	259	272	288	294	309	326	324	338	353
Melosira sp								512																
Navicula sp	435	834	889						508	3559	4576	577	1525	1036					805	1520	4358		5423	
Nitszchia sp	870						499	1023	1017	3559	7118	2885	9660	3627			5322	760		760	10168		5423	
Paralia sp							1497	1023		3050	3050	1154	1017				1520			107				
Rhizosolenia delicatula	435	1669	2223	1036								1731	10168	29533	23241		760		1611	3041	63914	14526	10846	18077
Rhizosolenia shrubsolei										508	508			13	10254						17431	2905		
Thalassionema sp													1525	518										
Thallasiosira sp										1525			1017											
Coscinodiscos sp	1305	834	889	1036		1036	1996	3070	2542	7626	2542	2308	3050	1036	684						11621		5423	4519
Biddulphia sp										1525	508			3627										
Chaetoceros sp											508		508	3109		695								7532
Ditylum brightwelli														518										
Guinardia flaccida																				1520	30504			
Eucampia sp																							10846	
Asterionella glacialis												1154	21861											
Skeletonema costatum											1017	577												
Lieptocylindricus sp											508													
Bacillaria paradoxa								512																
Total	3045	3337	4001	2072	0	1036	3992	6139	4067	21353	20336	10384	50332	43017	34179	695	7602	760	2416	6949	137996	17431	37961	30128
Pennates	345825	165610	154244	260615	6217	5699	5989	4604	4067	7626	7626	3461	3050	3627	479867	16686	2281	26608		6082	1339287	1666120	7231	1337673
Phaeocystis pouchetti															yes	yes								
Dinoflagellates		417				2591									2051		17485	760	1611	4561	2905			
(Amphidinium sp, Gyrodinium sp, Ceratium sp.)																								

Appendix 12. TCO_2 system, $\delta^{13}C$-ΣCO_2 and predicted $\delta^{13}C_{calcite}$ data for the Menai Strait, October 1994 - September 1995.

Date	Day	$\delta^{13}C$-ΣCO_2 °/oo	pH µmol Kg^{-1}	$[TCO_2]$ µmol Kg^{-1}	$[CO_{2aq}]$ µmol Kg^{-1}	$[HCO_3^-]$ µmol Kg^{-1}	$[CO_3^{2-}]$ µmol Kg^{-1}	Predicted $\delta^{13}C$ calcite °/oo
6.10.94	10	0.650	8.142	2014.4	12.43	1824.7	177.21	1.959
10.10.94	14	0.559	8.137	1997.4	12.25	1806.9	178.26	1.866
10.10.94	14	0.503	8.137	1999.2	12.26	1808.5	178.43	1.810
17.10.94	21	0.388	8.123	2015.1	13.09	1833	169	1.689
25.10.94	29	0.103	8.07	2041.8	15.44	1878.4	147.99	1.387
7.11.94	42	0.506	8.071	2088.7	15.84	1921.6	151.33	1.793
7.11.94	42	0.520	8.071	2068.5	15.69	1903	149.83	1.807
14.11.94	49	0.037	8.034	2043.2	17.1	1892.2	133.9	1.312
1.12.94	66	0.331	8.054	2069.1	16.85	1914	138.23	1.614
19.12.94	84	0.056	8.066	2038.8	16.76	1890.9	131.13	1.338
16.1.95	112	0.111	8.06	2038.1	17.65	1898.3	122.14	1.391
30.1.95	126	0.165	8.098	2046.0	16.63	1901.9	127.44	1.452
6.2.95	133	0.116	8.079	2092.5	17.21	1942.8	132.47	1.402
13.2.95	140	-0.059	8.059	2058.8	18.16	1920.7	119.94	1.221
21.2.95	148	0.013	8.084	2089.0	17.19	1940.9	130.92	1.299
6.3.95	161	0.422	8.108	2080.8	16.61	1932.3	131.86	1.713
21.3.95	176	0.412	8.103	2105.7	16.83	1954.2	134.64	1.704
28.3.95	183	0.260	8.089	2094.7	17.15	1945.8	131.68	1.549
4.4.95	190	0.498	8.08	2087.1	16.59	1931.3	139.27	1.787
10.4.95	196	0.458	8.092	2050.9	15.7	1893.4	141.78	1.748
26.4.95	212	0.384	8.092	2013.8	15.31	1858.4	140.4	1.671
1.5.95	217	0.298	8.098	2072.0	15.31	1907.6	149.07	1.588
9.5.95	225	0.498	8.091	2062.7	15.08	1894.9	152.77	1.788
16.5.95	232	0.876	8.2	2001.5	11.35	1807.4	182.74	2.202
1.6.95	248		8.359	1931.2	7.03	1667.8	256.38	
12.6.95	259	1.231	8.211	1970.7	10.3	1762.2	198.2	2.566
25.6.95	272	0.574	8.049	2004.5	14.47	1829.3	160.74	1.854
11.7.95	288	0.611	8.037	2054.8	14.86	1872.5	167.43	1.890
25.7.95	302	0.370	8.06	2071.7	14	1877.1	180.55	1.656
1.8.95	309	0.471	8.026	2040.0	14.27	1848.1	177.64	1.748
8.8.95	316	0.761	8.049	2031.8	13.61	1836.1	182.07	2.044
16.8.95	324	0.604	8.012	2040.4	14.92	1855.2	170.22	1.877
30.8.95	338	0.324	7.985	2091.3	16.94	1917.9	156.51	1.593
8.9.95	347	0.417	7.994	2053.7	16.53	1884.6	152.55	1.686
14.9.95	353	0.151	8.021	2064.3	15.46	1885	163.79	1.426
22.9.95	361	0.238	8.026	2059.6	15.43	1882	162.1	1.514

Appendix 13. [POC/N] , C:N , POC:Chl and Total Suspended Solids concentrations ([TSS]) for the Menai Strait, October 1994 - September 1995.

* = data not available

Date	Day	[POC] $\mu g\ dm^{-3}$	[PON] $\mu g\ dm^{-3}$	C:N	POC : Chl	[TSS] $g\ dm^{-3}$
6.10.94	10	767.1	82.9	9.25	334.00	0.0586
14.10.95	18	406.8	48.3	8.42	334.99	0.0377
17.10.94	21	525.3	69.9	7.52		0.0359
25.10.94	29	441.8	*		838.27	0.0589
7.11.94	42	395.3	*		594.19	0.0639
14.11.94	49	661.5	71.1	9.31	957.03	0.0567
21.11.94	56	546.8	92.9	5.89	1278.53	0.0540
1.12.94	66	527.3	*		1171.78	0.0583
19.12.94	84	694.1	*		1785.24	0.0616
16.1.95	112	754.4	76.5	9.86	1919.01	0.0544
30.1.95	126	559	*		1293.98	0.0614
6.2.95	133	458.5	*		1524.47	0.0543
13.2.95	140	632.5	*		1509.40	0.0536
21.2.95	148	317.6	*		816.87	0.0645
6.3.95	161	503.6	*		1120.90	0.0644
21.3.95	176	579.2	*		749.02	0.0645
28.3.95	183	506	67.3	7.52	585.65	0.0537
4.4.95	190	469.6	*		603.91	0.0586
10.4.95	196	194.6	28.9	6.73	346.51	0.0493
26.4.95	212	624.4	83	7.52	348.65	0.0616
1.5.95	217	462.5	65.3	7.08	220.74	0.0337
9.5.95	225	363.6	69.4	5.24	180.04	0.0283
16.5.95	232	465.1	70.7	6.59	138.92	0.0263
1.6.95	248	774.1	95.8	8.08	147.48	0.0487
12.6.95	259	708.1	101.2	7	609.37	0.0292
25.6.95	272	538.1	83.3	6.46	463.07	0.0249
11.7.95	288	416.4	62.4	6.67	280.73	0.0559
17.7.95	294	360.1	50.3	7.18	157.86	0.0286
25.7.95	302	327.1	47.9	6.83	467.05	0.0204
1.8.95	309	367.7	53.1	6.92	239.08	0.0278
8.8.95	316	479.6	67.4	7.12	257.95	0.0283
16.8.95	324	311.4	45	6.92	254.21	0.0250
30.8.95	338	580.8	81.9	7.09	499.82	0.0551
8.9.95	347	543.7	83.9	6.48	335.62	0.0552
14.9.95	353	264	44.7	5.91	148.55	0.0545

Appendix 14. Seasonal variation in shell growth and microgrowth patterns for *Pecten maximus* placed in the Menai Strait October 1994 - September 1995.

Animal No.	Initial Shell Height	Increment mm day^{-1}	Striae no. day^{-1}	Striae width mm	Striae no mm^{-1}	Increment mm d ay^{-1}	Striae no day^{-1}	Striae width mm	Striae no mm^{-1}	Increment mm d ay^{-1}	Striae no day^{-1}
		Midline				Second Ray				Basal	
Month 1											
B	2.14	0.111	0.677	0.221	6.125	0.077	0.484	0.169	6.25	0.037	0.323
C	2.00	0.053				0.035	0.387		11.05		
D	1.76	0.120				0.074	0.613		8.31	0.035	0.323
E	1.92	0.120				0.074	0.581	0.154	7.88		0.323
F	1.92	0.109				0.070	0.677	0.154	9.67	0.039	0.452
G	2.05	0.127				0.079	0.581	0.149	7.33	0.046	0.355
K	2.08	0.063				0.041	0.419	0.123	10.34		
L	1.85	0.109				0.074	0.581	0.123	7.88	0.044	0.387
N	1.89	0.138				0.083	0.645	0.159	7.78	0.046	0.323
P	1.76	0.092				0.055	0.548	0.123	9.92	0.029	0.290
Q	1.95	0.112			6.5	0.074	0.710	0.128	9.63	0.046	0.452
R	1.77	0.105				0.063	0.516	0.149	8.24	0.035	0.323
T	1.80	0.133				0.090	0.613	0.169	6.79	0.039	0.323
U	1.80	0.125				0.090	0.645	0.144	7.14	0.039	0.323
V	1.80	0.133				0.088	0.710	0.138	8.02	0.041	0.419
Month 2											
2A	2.12	0.005	0.056	0.051	17.5	0.000	0.000			0.000	0.000
2E	2.14	0.008	0.000			0.003	0.000			0.000	0.000
2J	2.21	0.013	0.000			0.006	0.111	0.026	17.5	0.000	0.000
2P	2.12	0.003	0.056	0.051	17.5	0.000	0.000			0.000	0.000
2Q	1.97	0.014	0.000		17.5	0.006	0.083	0.051	13.125	0.000	0.000
2L	2.12	0.000	0.000			0.000	0.000			0.000	0.000
2R	2.26	0.000	0.000			0.000	0.000			0.000	0.000
B2	2.70			0.047			0.000				
B8	2.94			0.051			0.000				
B1	3.03						0.000				
B7	2.88						0.000				
Month 3											
3E	2.14	0.003	0.000			0.001	0.000			0.000	0.000
3H	2.15	0.003	0.000			0.000	0.000			0.000	0.000
3A	2.35	0.000	0.000			0.000	0.000			0.000	0.000
3B	2.24	0.000	0.000			0.000	0.000			0.000	0.000
3C	2.39	0.000	0.000			0.000	0.000			0.000	0.000
3D	2.17	0.000	0.000			0.000	0.000			0.000	0.000
3F	2.17	0.000	0.000			0.000	0.000			0.000	0.000
3G	2.36	0.000	0.000			0.000	0.000			0.000	0.000
3J	2.09	0.000	0.000			0.000	0.000			0.000	0.000
3L	2.11	0.000	0.000			0.000	0.000			0.000	0.000
3M	2.20	0.000	0.000			0.000	0.000			0.000	0.000
3Q	2.32	0.000	0.000			0.000	0.000			0.000	0.000
3R	2.29	0.000	0.000			0.000	0.000			0.000	0.000
3S	2.24	0.000	0.000			0.000	0.000			0.000	0.000
3U	2.06	0.000	0.000			0.000	0.000			0.000	0.000
Month 4											
4A	2.30	0.004	0.138			0.001	0.000			0.000	0.000
4C	2.35	0.004				0.001				0.000	0.000
4F	2.12	0.014	0.172	0.062	12.5	0.010	0.103	0.051	10.5	0.000	0.103
4G	2.12	0.014	0.103	0.051	7.5	0.006	0.000			0.000	0.000
4L	2.42	0.002	0.103			0.000	0.000			0.000	0.000
4P	2.08	0.001	0.000			0.000	0.000			0.000	0.000
4R	2.18	0.006	0.103	0.032	17.5	0.000	0.000			0.000	0.000
4T	2.36	0.004	0.069			0.001	0.000			0.000	0.000
4U	2.52	0.018	0.138	0.062	7.78	0.008	0.103	0.051	13.125	0.000	0.069
4V	2.39	0.010	0.103	0.038	10.5	0.004	0.000			0.000	0.000
4W	2.02	0.008	0.103	0.051	13.125	0.002	0.000			0.000	0.000
4X	2.50	0.016	0.138	0.077	8.75	0.010	0.103	0.077	10.5	0.000	0.069
4B	2.42	0.000	0.000			0.000	0.000			0.000	0.000
4H	2.20	0.000	0.000			0.000	0.000			0.000	0.000
4K	2.44	0.000	0.000			0.000	0.000			0.000	0.000
4Q	2.20	0.000	0.000			0.000	0.000			0.000	0.000

Appendix 14. (continued) Seasonal variation in shell growth and microgrowth patterns for *Pecten maximus* placed in the Menai Strait October 1994 - September 1995.

Animal No.	Initial Shell Height	Increment mm day^{-1}	Striae no. day^{-1}	Striae width mm	Striae no mm^{-1}	Increment mm d ay^{-1}	Striae no day^{-1}	Striae width mm	Striae no mm^{-1}	Increment mm d ay^{-1}	Striae no day^{-1}
		Midline				Second Ray				Basal	
Month 5											
5A	2.38	0.022	0.194	0.109	8.75	0.006	0.129	0.083			
5C	2.30	0.048	0.419	0.154	8.75	0.035	0.323	0.123	9.21	0.018	0.226
5D	1.97	0.053	0.355	0.145	6.64	0.031	0.258	0.096	8.24		0.161
5F	2.18	0.037	0.323	0.128	8.75	0.024	0.258	0.096	10.77	0.018	0.161
5G	2.44	0.044	0.355	0.120	8.02	0.029	0.226	0.115	7.66	0.018	0.226
5H	2.24	0.002	0.065			0.001	0.000			0.002	0.000
5L	2.15	0.039	0.355	0.103	9.17	0.020	0.258	0.090	12.73	0.017	0.161
5M	2.17	0.018	0.161	0.103	8.75	0.009	0.129	0.051	14	0.006	0.065
5N	2.32	0.006	0.065			0.001	0.000			0.000	0.032
5T	2.20	0.026	0.258	0.125	10	0.017	0.161		9.72		
5U	2.30	0.046	0.355	0.137	7.7	0.037	0.355	0.135	9.63	0.024	0.194
5W	2.03	0.050	0.290	0.231	5.83	0.026	0.226	0.103	8.75	0.020	0.194
5X	2.06	0.020	0.226	0.083	11.13	0.011	0.129	0.051	11.667	0.009	0.129
5E	2.42	0.000	0.000			0.000	0.000			0.000	0.000
5R	2.42	0.000	0.000			0.000	0.000			0.000	0.000
Month 6											
6L	2.21	0.215	1.118	0.231	5.2	0.139	0.941	0.197	6.75	0.079	0.529
6A	2.06	0.178	0.853	0.244	4.79	0.129	0.765	0.188	5.91	0.069	0.471
6B	2.17	0.218	1.059	0.250	4.85	0.146	0.941	0.205	6.44	0.084	0.471
6C	2.33	0.203	1.000	0.244	4.92	0.134	0.882	0.160	6.56	0.076	0.441
6D	2.11	0.146	0.824	0.205	5.63	0.103	0.500	0.197	4.88	0.066	0.441
6E	3.18	0.096	0.647	0.154	11.05	0.061	0.500	0.096	8.26		0.294
6F	2.48	0.176	0.941	0.237	5.33	0.121	0.824	0.167	6.81	0.076	0.441
6G	2.02	0.215	1.059	0.218	4.92	0.131	0.882	0.167	6.73	0.066	0.471
6H	3.06	0.203	1.029	0.250	5.06	0.118	0.882	0.141	7.5	0.067	0.441
6K	3.03	0.153	0.853	0.179	5.58	0.099	0.794	0.147	8.01	0.066	0.382
6N	2.92	0.205	1.059	0.237	5.16	0.131	1.029	0.160	7.85	0.069	0.500
6P	2.48	0.193	1.176	0.186	6.09	0.150	1.059	0.141	7.08	0.067	0.471
6Q	2.86	0.205	1.206	0.192	5.88	0.134	1.235	0.122	9.19	0.072	0.471
6R	3.11	0.182	1.059	0.218	5.83	0.128	1.029	0.154	8.06	0.062	0.471
6S	2.67	0.185	1.118	0.199	6.05	0.134	0.941	0.147	7	0.071	
6T	3.48	0.202	1.176	0.186	5.83	0.128	1.059	0.128	8.29	0.082	0.559
6U	3.79	0.193	1.118	0.212	5.78	0.114	0.912	0.141	7.98	0.067	0.382
6V	4.17	0.203	1.176	0.218	5.79	0.153	1.235	0.160	8.08	0.076	
6X	3.32	0.153		0.212		0.104		0.160		0.061	
Month 7											
7A	2.83	0.113	0.973	0.154	8.63	0.080	0.892	0.128	11.1	0.040	0.351
7B	2.97	0.048		0.092		0.014		0.051		0.012	
7E	3.58	0.124	1.054	0.149	8.53	0.100	0.892	0.123	8.88	0.059	0.514
7F	2.92	0.182	1.135	0.231	6.23	0.131	1.027	0.133	7.82	0.080	0.649
7G	3.76	0.128	0.892	0.195	6.96	0.094	0.703	0.133	7.46	0.049	0.405
7H	2.94	0.110	0.865	0.160	7.89	0.079	0.838	0.115	10.64	0.043	0.432
7J	3.26	0.127	0.892	0.184	7.04	0.096	0.703	0.118	7.34	0.048	0.514
7L	2.50	0.175	1.081	0.179	6.19	0.134	1.081	0.135	8.05	0.074	0.703
7M	2.38	0.232	1.378	0.231	5.95	0.162	1.216	0.149	7.5	0.107	0.757
7N	2.38	0.185	1.270	0.195	6.85	0.144	0.892	0.157	6.21	0.099	0.703
7P	2.20	0.159		0.210		0.107		0.113		0.056	
7Q	2.88	0.162	1.162	0.179	7.17	0.119	0.973	0.128	8.18	0.063	0.703
7V	2.82	0.173		0.187		0.113		0.135		0.062	
7W	3.61	0.182	1.162	0.222	6.38	0.128	0.973	0.151	7.59	0.065	0.541
7X	3.18	0.154	0.973	0.205	6.3	0.105	0.892	0.149	8.49	0.059	0.595
7U	3.26	0.192	1.054	0.236	5.5	0.136	0.946	0.149	6.96	0.076	0.568
Month 8											
8B	3.77	0.114	0.743	0.221	6.5	0.078	0.629	0.138	8.02	0.041	0.343
8C	3.80	0.077	0.629	0.185	8.19	0.057	0.514	0.128	9	0.034	0.286
8E	3.88	0.057	0.514	0.144	9	0.046	0.457	0.097	10	0.028	0.257
8F	4.18	0.080	0.629	0.164	7.86	0.056	0.457	0.128	8.24	0.046	0.229
8G	4.41	0.090	0.714	0.179	7.95	0.065	0.600	0.118	9.19	0.033	0.314
8J	3.86	0.093	0.771	0.195	8.29	0.069	0.686	0.138	10	0.034	0.314
8N	4.02	0.077	0.600	0.164	7.82	0.057	0.543	0.113	9.5	0.029	0.257
8P	3.45	0.075	0.571	0.179	7.61	0.059	0.514	0.123	8.75	0.029	0.257
8Q	4.44	0.109	0.771	0.210	7.05	0.072	0.629	0.149	8.75	0.041	0.343
8S	3.76	0.101	0.743	0.210	7.34	0.077	0.600	0.141	7.82	0.038	0.286
8T	2.56	0.132	0.771	0.199	5.83	0.100	0.771	0.158	7.75	0.049	0.486
8V	2.71	0.090	0.629	0.171	7	0.067	0.543	0.144	8.11	0.029	0.257
8W	2.65	0.140	0.829	0.159	5.9	0.101	0.714	0.133	7.06	0.052	0.371
8X	2.86	0.139	0.886	0.226	6.38	0.101	0.743	0.154	7.34	0.059	0.514

Appendix 15. Isotopic data for *Pecten maximus* placed in the Menai Strait for monthly periods October 1994 - September 1995.

Scallop no. distances = mm from disturbance mark	$\delta^{18}O$ °/oo	$\delta^{13}C$ °/oo
Month 1		
D	0.677	0.606
G	0.696	0.589
L	0.711	0.594
N	0.595	0.736
R	0.663	0.502
T	0.680	0.666
U	0.704	0.758
Profiles		
V at 0.86mm	0.421	0.522
V at 1.77mm	0.271	0.661
V at 2.63mm	0.620	0.690
V at 4.11mm	0.806	0.673
F at 0.91mm	0.376	0.739
F at 1.77mm	0.309	0.932
F at 3.37mm	0.747	0.990
Month 2		
2E,2J,2Q (pooled samples)	**1.474**	**0.578**
Month 3		
No growth during this month		
Month 4		
4V,4U,4F,4X,4G	**1.982**	**1.01**
Month 5		
5U	0.998	1.297
5G	1.127	1.159
5C	1.246	1.238
5F	1.131	1.036
5D	1.184	0.986
5L	1.275	1.042
5W	1.220	1.098
Month 6 Profiles		
6C at 1.49mm	0.445	1.552
6C at 2.97mm	0.369	1.521
6C at 4.40mm	-0.165	1.187
6C at 5.66mm	-0.521	0.667
6C at 6.91mm	-0.419	0.311
6B at 1.66mm	0.262	1.505
6B at 2.97mm	0.167	1.402
6B at 4.17mm	0.000	1.341
6B at 5.43mm	-0.102	0.938
6B at 7.43mm	-0.217	0.362
Month 7 Profiles		
7H at 0.63mm	-0.968	0.417
7H at 1.43mm	-1.486	0.388
7H at 2.80mm	-1.285	0.274
7H at 4.06mm	-0.757	0.486
7L at 0.86mm	-0.666	0.779
7L at 1.83mm	-0.921	0.677
7L at 2.97mm	-1.114	0.622
7L at 4.06mm	-1.216	0.450
7L at 5.26mm	-1.042	0.348
7L at 6.46mm	-0.820	0.349
Month 8 Profiles		
8W at 0.91mm	-0.807	0.591
8W at 1.71mm	-0.738	0.447
8W at 2.80mm	-0.932	0.205
8W at 3.77mm	-0.984	0.083
8W at 4.91mm	-0.404	0.183
8T at 1.09mm	-0.550	0.642
8T at 2.40mm	-0.642	0.401
8T at 3.60mm	-0.437	0.231
8T at 4.63mm	-0.324	0.174

Appendix 16. Shell Isotopic data for *Pecten maximus* placed in the Menai Strait for the year October 1994 - September 1995.

Pecten 52

mm from disturbance mark along profile	$\delta^{18}O$ °/oo	$\delta^{13}C$ °/oo
0.65	0.212	0.662
2.03	0.285	0.628
3.41	0.341	0.515
4.71	0.419	0.313
6.01	0.960	0.294
7.25	1.845	0.401
8.48	1.837	0.647
9.71	1.237	0.683
10.94	0.830	0.513
12.25	0.396	0.314
13.55	0.327	0.306
14.86	-0.101	0.702
16.23	-0.147	0.955
17.68	-0.338	0.565
19.13	-0.451	0.525
20.65	-1.135	-0.348
21.45	-1.230	-0.390
22.17	-1.101	-0.412
23.77	-0.999	-0.389
25.87	-1.027	-0.332
27.46	-1.235	-0.337
28.48	-1.292	-0.259
29.86	-1.534	-0.474
31.38	-1.507	-0.515
33.04	-1.756	-0.630
34.93	-1.355	-0.578
36.74	-1.089	-0.703
38.19	-1.079	-0.749
39.49	-0.634	-0.444

Pecten 60

mm from disturbance mark along profile	$\delta^{18}O$ °/oo	$\delta^{13}C$ °/oo
0.35	0.261	0.554
1.16	0.381	0.701
2.03	0.572	0.802
2.97	0.439	0.621
3.91	0.525	0.439
5.14	0.593	0.399
6.52	1.898	0.495
7.68	1.969	0.809
8.84	1.609	1.006
10.07	0.971	0.886
11.38	0.948	0.714
12.75	0.427	0.530
14.20	0.298	0.731
15.65	0.078	1.382
17.10	0.128	1.250
18.62	-0.120	1.070
20.14	-1.025	0.001
21.59	-0.815	0.045
23.33	-0.990	-0.101
25.29	-1.290	-0.161
27.25	-1.346	-0.042
29.35	-1.559	-0.300
31.30	-1.590	-0.338
33.04	-1.528	-0.241
35.00	-1.075	-0.306
36.81	-1.089	-0.401
38.33	-0.517	0.017

Appendix 17. Isotopic profile data for *Pecten maximus* collected from Melville Knoll.

cm from umbo	$\delta^{18}O$ °/oo	$\delta^{13}C$ °/oo
3.81		1.130
3.93	1.799	1.134
4.06	1.983	1.116
4.17	2.194	1.181
4.29	2.274	1.205
4.44	2.306	1.244
4.60	1.931	1.338
4.73	1.906	1.232
4.87	1.983	1.275
5.00	1.742	1.407
5.14	1.558	1.454
5.31	1.984	1.404
5.49	1.834	1.248
5.63	2.068	1.099
5.76	1.794	1.230
5.93	1.971	1.098
6.07	1.703	1.285
6.23	1.530	1.474
6.36	1.744	1.428
6.53	2.027	1.364
6.67	2.030	1.268
6.84	2.030	1.137
6.99		1.104
7.14	1.955	1.060
7.29		1.190